Characterising the Role of the Calcium-dependent Citrullinating Enzyme Peptidyl Arginine Deiminase 2 in Ovarian Cancer

Submitted for the Degree of
Doctor of Philosophy
At the University of Northampton

2019

Nermin Ibrahim Albalbeisi

DEDICATION

I dedicate this thesis to my dear father, mother, sisters, brother and my friend G.Hamdan for their support and encouragement in helping me complete this work.

DECLARATION

I declare that this thesis and the results to which it refers to are the outcome of the work composed by myself. This work is entirely my own, except where it stated otherwise by reference or footnotes. This thesis has not been submitted in whole or in part for any other academic degree or professional qualification.

ACKNOWLEDGEMENTS

I am grateful to all of those with whom I have had the pleasure to work with during my PhD. Not only those who directly contributed to my research, but those who have been there as friends and provided support in times of need. I am also enormously grateful to my parents, who supported me with love and understanding.

I would like to acknowledge who played a role in my academic accomplishments. My completion of this thesis could not have been possible without the support of my Supervisory team. I greatly thank my first supervisor Dr Lee Machado, who has guided and supported me throughout my PhD. Lee's guidance and dedication to this research has helped motivate me achieve my goals. I would also like to thank my second supervisor Dr Karen Anthony. Her knowledge with regards to cancer has greatly provided new insights that contributed to my understanding of multiple aspects of my PhD. Thanks also to my third supervisor Dr Roshan Agrawal a consultant medical oncologist specialising in gastro-intestinal/gynaecological malignancies and lead for research Northampton General Hospital (NHS). Thanks also to my director of studies Ian Livingstone who has provided invaluable information with regards to my PhD reviewing and submission processes.

Other important acknowledgments are for the Faculty of Health and Society. The school provided me with great working environment and all the requirement needed to conduct my studies and more. I was also supported by the Faculty of Health and Society and especially Steph Arnold for her help with processing many orders for lab consumables and equipment. More special thanks are dedicated to Valerie Graham, Linda Clapham and Daniel Shaw, for their support and maintenance of the labs and equipment.

STATEMENT OF CONTRIBUTORS

Personnel	Contributions
Dr Lee Machado Associate Professor in Biochemistry Molecular Biosciences Research Group Lead, University of Northampton	Principle PhD supervisor
Dr Karen Anthony Senior Lecturer in Molecular Bioscience Molecular Biosciences Research Group Lead, University of Northampton	Co-supervisor
Dr Roshan Agrawal consultant medical oncologist specialising in gastro-intestinal/gynaecological malignancies and lead for research Northampton General Hospital (NHS).	External supervisor
Dr Ian Livingstone Professor of Physical Geography Programme Leader: PG Cert Research Degree Supervision	Director of studies

CHAPTER 2: MATERIALS AND METHODS

LIST OF FIGURES

LIST OF TABLES

ABBREVIATIONS

ACSL4	Acyl-CoA synthetase long chain family member 4
ACT	Acetate
AKT2	AKT serine/threonine kinase 2
ALDH1A1	Aldehyde dehydrogenase-1A1
APC	Antigen presenting cell
ApoA1	Apolipoprotein A1
ARHGEF10L	Rho guanine nucleotide exchange factor (GEF) 10-like
ARID1A	AT-rich interaction domain 1A
ARID3B	AT-Rich interactive domain 3B
ATG5	Autophagy related 5
ATG12	Autophagy related 12
ATM	Ataxia telangiectasia mutated
ATP	Adenosine triphosphate
ATR	Ataxia telangiectasia and RAD3 related
β-actin	Beta actin
BAA	Benzoyl-l-arginine amide
BARD1	BRCA1-associated RING domain protein 1
BCA	Protein quantification using bicinchoninic acid assay
BMPR1B	Bone morphogenetic protein receptor, type IB
BRAF	B-Raf proto-oncogene, serine-threonine kinase
BRCA1	Breast cancer gene 1
BRCA1	Breast cancer gene 2
BRIP1	BRCA1 interacting protein C-terminal helicase 1
BSA	Protein standard albumin
CA	Calcium
Ca	Calcium binding site
CA125	Cancer antigen 125
CA19-9	Carbohydrate antigen 19-9
Ca^{2+}	Calcium
CA9	Carbonic anhydrase 9
$CaCl_2$	Calcium chloride
Carboplatin	cis-(1,1-cyclobutanedicarboxylato) diammineplatinum(II)
CTNNB1	β-catenin 1
CCNE1	Cyclin E1
CD117	Cluster of differentiation 117
CD144	Cluster of differentiation 144
CD24	Cluster of differentiation 24
CDC42	Cell division cycle 42
CDK	Cyclin dependent kinase
CDK12	Cyclin dependent kinase 12
CDKN2A	Cyclin dependent kinase 2A
cDNA	Complementary DNA
CHEK2	Checkpoint kinase 2

Cisplatin	cis-diamminedichloroplatinum (II)
CNV	Copy number alterations
CRISPR/Cas9	Clustered regularly interspaced short palindromic repeats/Cas9
CSMD3	CUB and sushi multiple domains 3
CT	Computerized tomography
CTL	Cytotoxic T lymphocytes
CTNNB1	Catenin Beta 1
CXCL8	C-X-C motif chemokine ligand 8
DACH1	Dachshund family transcription factor 1
DDR	DNA damage repair
DMEM	Dulbecco's modified eagle medium
DMSO	Dimethyl sulfoxide
DSBs	Double-strand breaks
E[Ca^{2+}]	Extracellular calcium
E2F3	E2F transcription factor 3
E2	Ubiquitin conjugating enzyme
EBSS	Earle's balanced salt solution
ECM	Extracellular matrix
EERC1	Nucleotide excision repair pathway
EGF	Epidermal growth factor
EGFR	Epidermal growth factor receptor
EMT	Epithelial-to-mesenchymal transition
ENO1	α-enolase
EOC(s)	Epithelial ovarian cancer(s)
EPB41L1	Erythrocyte membrane protein band 4.1-like1
EpCAM	Epithelial cell adhesion molecule
EPHA2	EPH receptor A2
ERα	Oestrogen receptor alpha
ERK	Extracellular regulated kinases
FAK	Focal adhesion kinase
FBS	Foetal bovine serum
FGF	Fibroblast growth factors
FIGO	The international federation of gynaecology and oncology
FOXM1	Forkhead box M1
FS	Frameshift mutation
FUS	FUS RNA binding protein
FUT8	Fucosyltransferase 8
FZD5	Frizzled class receptor 5
G1	Growth 1 phase in cell cycle
G2	Growth 2 phase in cell cycle
G3	Growth phase 3
G418	Geneticin
GABRA6	Gamma-aminobutyric acid type A receptor alpha6 subunit
GADD45	Growth arrest and DNA damage inducible alpha
GFP	Green fluorescent plasmid
GRIP1	Glutamate receptor interacting protein 1

GRO1	Growth regulated-α
GSK3β	Glycogen synthase kinase 3 beta
H3	Histone 3
H4	Histone 4
HDAC2	Histone deacetylase 2
HDAC4	Histone deacetylase 4
HDR	Homology-directed repair
HER2/ERBB2	Oestrogen-related receptor B2
HER3/ERBB3	Oestrogen-related receptor B3
HGS	High-grade serous
HNF1	Hepatocyte nuclear factor 1
HR	Homologous recombination
HRR	Homologous recombination repair
i[Ca^{2+}]	Intracellular calcium
IC50	Half maximal inhibitory concentration
Ig	Immunoglobulin
IL-8	Interleukin 8
ING4	Inhibitor of growth family member 4
IP3	Inositol trisphosphate
ITS-G	Insulin transferrin selenium
JAK	Janus kinase
JNK	c-Jun N-terminal kinases
K^+	Potassium
KLK-6	Kallikrein 6
KLK-7	Kallikrein 7
KRAS	Kirsten ras sarcoma viral oncogene proto-oncogene, GTPase
KRT7	Keratin 7, type II
LB agar/broth	LB Broth (Miller) powder microbial growth medium
LC3	Microtubule-associated proteins 1A/1B light chain 3B
LDLRAP1	Low-density lipoprotein receptor adaptor protein 1
LGS	Low-grade serous
LPA	lysophosphatidic acid
mAb	Monoclonal antibody
MAPK	Mitogen-activated protein kinase
MBP	Myelin basic protein
MEGA7	Molecular evolutionary genetics analysis version 7.0
MEK	Mitogen-activated protein (MAP) extracellular signal-related
MHC	Major histocompatibility complex
miR	MicroRNA
ML	Maximum likelihood
MMP-7	Matrix metalloproteinases-7
MMP-9	matrix metalloproteinase-9
MMR	DNA mismatch repair
MPD	(4S)-2-methyl-2,4-pentanediol
mRNA	Messenger RNA
MS	Multiple sclerosis

mTOR	Mechanistic target of rapamycin kinase
MYC	MYC proto-oncogene, BHLH transcription factor
Na^+	Sodium
NADPH	Nicotinamide adenine dinucleotide phosphate
NF1	Nuclear factor 1
NF-$_\kappa$B	Nuclear factor kB
NFS	Non-frame shift mutation
NGS	Next generation sequencing
NHEJ	Non-homologous end joining
NK	Natural killer
NMF	Natural moisturizing factor
NPM1	Nucleophosmin 1
NPTXR	Neuronal pentraxin receptor
nt	Nucleotide
OC	Ovarian cancer
OD	Optical density
Opti-MEM	Antibiotic-free without FBS
OS	Overall survival
P21	Tumour protein 21
p300	Tumour protein 300
P53	Tumour protein 53
p63	Tumour protein 63
PADI(s)	Peptidyl arginine deiminase(s)
PADI1	Peptidyl arginine deiminase 1
PADI2	Peptidyl arginine deiminase 2
PADI3	Peptidyl arginine deiminase 3
PADI4	Peptidyl arginine deiminase 4
PADI6	Peptidyl arginine deiminase 6
PALB2	Partner and localizer of BRCA2
PAM	Protospacer adjacent motif
Par-4	PRKC apoptosis WT1 regulator protein
PBS	Phosphate-buffered saline
PCR	Polymerase chain reaction
PDGF	Platelet derived growth factor
PFKM	Phosphofructokinase
PIK3CA	Phosphatidylinositol-4,5-bisphosphate 3-kinase catalytic subunit
PPI	Protein-protein interaction
PPP2R1A	Protein phosphatase 2 scaffold subunit alpha
P-TEFb	Positive transcription elongation factor b
PTEN	Phosphatase and tensin homolog
PTM(s)	Post-translational modification(s)
qRT-PCR	Quantitative reverse transcription polymerase chain reaction
RA	Rheumatoid arthritis
RAC1	Rac family small GTPase 1
RAD51	RAD51 recombinase

RB1	Retinoblastoma protein 1
RIPA	Radioimmunoprecipitation lysis buffer
RhoA	Ras homolog family member A
RNAP2	RNA polymerase II
ROS	Reactive oxygen species
RPMI	1640 Medium
RPS6KA1	Ribosomal protein S6 kinase
S	Synthesis phase in cell cycle
SD	Standard deviation
SEM(s)	Standard error of the mean(s)
sgRNA	Single guide RNA
SLC7A11	Solute carrier family 7 member 11
SNRPE	Small nuclear ribonucleoprotein polypeptide E
SRC	SRC proto-oncogene, non-receptor tyrosine kinase
STAT1	Acetyl- signal transducer and activator of transcription 1
STIC	Serous tubal intraepithelial carcinoma
STRA6	Stimulated by retinoic acid 6
T7E1	T7 endonuclease 1
TASK-3	Potassium channel subfamily K member 3
TCGA	The cancer genome atlas
TFF1	Trefoil factor 1
TGF-β	Transforming growth factor beta
TIDE	The tracking of indels by decomposition
TKI	Tyrosine kinase inhibitors
TMA	Tissue microarrays arrays
TNF	tumour necrosis factor
TTR	Transthyretin
U133	Microarray
VDAC-1	Voltage-dependent anion-selective channel 1
VCAM1	Vascular cell adhesion molecule 1
VEGF	Vascular endothelial growth factor
VPF	vascular permeability factor
WR	Working reagent
ZNF22	Zinc finger protein 22
ZSCAN12	Zinc finger and scan domain containing 12

ABSTRACT

Epithelial ovarian cancer (EOC) represents the fifth most common cause of cancer mortality among women worldwide and accounts for the highest fatalities amongst gynaecological malignancies. The dysregulation of calcium-dependent peptidyl arginine deiminase 2 (PADI2) plays a key role in the tumorigenesis of several cancers; however, the role of PADI2 in the pathogenesis of EOC is yet to be investigated. Using RNA-seq and microarray data from primary serous ovarian cancers (The Cancer Genome Atlas data set) combined with survival data, the expression of *PADI2* was assessed using each platform (n=262 and n=564). Kaplan-Meier analysis and Log-rank tests showed an association of *PADI2* mRNA expression with overall survival using both platforms (RNA-seq cohort p=0.008 and microarray cohort p=0.0112). Low expression of *PADI2* was associated with improved survival. Expression studies were used to examine the overexpression and knockout (CRISPR/Cas9 editing) of PADI2 expression, respectively, in the human-derived high-grade serous OVCAR-4 and mouse-derived EOC ID8-Luc2 cell lines. In OVCAR-4 cells, PADI2 overexpression reduced proliferation (22%) and cellular aggregation (94%), while increasing apoptosis (34%) and autophagy (38%), in a Ca^{2+}- and citrullination-dependent manner, at 72 hours. PADI2 overexpression also induced cisplatin cytotoxicity by 10% at 72 hours. In ID8-Luc2 cells, PADI2 overexpression significantly decreased cisplatin cytotoxicity by 24%, independently of exogenous Ca^{2+} supplementation or induced citrullination, at 72 hours. In addition, qRT-PCR validation of TCGA gene co-expression data indicated that PADI2 overexpression correlated with expression of a number of genes. This was confirmed in functional studies where there was a 1.69-fold increase in *ARHGEF10L* and 0.75-fold decrease in *FZD5* expression upon PADI2 overexpression. In this thesis, The Cancer Genome Atlas expression studies of *PADI2* showed that higher *PADI2* confers decreased survival of EOC patients. Conversely, *PADI2* overexpression *in vitro*, induced apoptosis/autophagy and decreased proliferation/cellular aggregation possibly via deregulating *FZD5* and *ARHGEF10L*. Collectively, this work suggests that PADI2 may serve as a potential therapeutic target in human EOC. Codon based selection analyses were used to test for evidence of positive selection in PADI2. The phylogenetic maximum likelihood analysis of PADI2 orthologues retrieved from 31 species indicated that there was no evidence of positive selection in PADI2 codons, but numerous residues were under evolutionary constraint.

CHAPTER 1: LITERATURE REVIEW

1.1 INTRODUCTION

Ovarian cancer (OC) is the fifth most common cancer in women worldwide and the leading cause of death among gynaecological malignancies (Rais *et al.*, 2017). The overall difficulty of early detection and diagnosis of OC is due to the ineffective screening methods and low treatment efficacy that contribute to high fatality rate (Rauh-Hain *et al.*, 2011). EOC is the most common type of OC, representing 95% of the cases whereas, the remaining OCs develop from sex cord-stromal tumours and germ cell tumours and account for the remaining 5%-10% (Romanidis *et al.*, 2014). A variety of risk factors are known to influence EOC, including genetic factors that play a prominent role in a patient's susceptibility to EOC. Recent advancements in molecular prognostic factors of EOC have enabled the assessment of suitable treatment strategies for EOC patients. Hence, understanding the key regulators of epigenetics and molecular targets can contribute to developing more effective cancer therapeutics (Sidhu and Capalash, 2017). The epigenetics and post-translational modifications (PTMs) of proteins, including acetylation, phosphorylation, methylation, glycosylation, citrullination and ubiquitination, were found to play key roles in pathogenesis and carcinogenesis (Bettermann *et al.*, 2012; Okudela *et al.*, 2014; Chrun *et al.*, 2017). Peptidyl arginine deiminases (PADIs) are a family of calcium-dependent enzymes that catalyse the post-translational conversion of positively charged arginine residues into neutrally charged citrulline (Horibata *et al.*, 2017). This reaction is referred to as deimination or citrullination, and can result in altered tertiary structures or improper substrate-binding of the target protein (Vossenaar *et al.*, 2003). PADI-mediated protein citrullination is also observed in normal physiological processes. However, aberrant citrullination can lead to different human diseases (Olsen *et al.*, 2018). In fact, there is increasing evidence to suggest that the dysregulation of PADI and mediated citrullination, play crucial roles in cancer, neurodegenerative diseases and inflammatory diseases (Copeland *et al.*, 2009; Bannister and Kouzarides, 2011; Fuhrmann *et al.*, 2015). More recently, citrullinated proteins were used as potential targets for cancer diagnosis and treatment (Cook *et al.*, 2018; Lin Wang *et al.*, 2017).

1.2 Clinical features of EOC

Several factors that could influence EOC may include cancer stage, histological type, early recognition, patient treatment, age and comorbidities (Bristow *et al.*, 2015; O'Malley *et al.*, 2012; Wright *et al.*, 2015; Chang *et al.*, 2018). Currently recommended frontline therapy for malignant EOC comprises of upfront surgery followed by combination chemotherapy using platinum-based and paclitaxel drugs (González-Martín *et al.*, 2014; Chang *et al.*, 2018). For invasive or recurrent EOC, individualised assessments and optimised management are especially required (Rooth, 2013; Jordan *et al.*, 2013; Chang *et al.*, 2018). EOCs are grouped as type I or type II based on clinicopathologic and primary molecular factors that contribute to EOC type-specific genetic instability (Torre *et al.*, 2018). Type I accounts for only 10% of the deaths from EOC. Type I EOCs develop from extraovarian benign lesions and are generally slow growing large unilateral or cystic tumours, and often present in early stages. Type I EOCs do not generally transform to malignant tumours; however, ovarian benign lesions may undergo a series of mutations resulting in malignant transformation (Torre *et al.*, 2018). Type II EOCs are present in advanced stage (>75% of cases) and characterised by genomic instability, rapid development and associated with poor prognosis (Patch *et al.*, 2015). Type II EOCs originate from the fallopian tube intraepithelial carcinoma and includes not only the ovaries, but also extra-ovarian sites, which probably accounts for their clinically aggressive behaviour (Nam and Kim, 2008; Foster, 2008). There is increasing evidence to indicate that type I and II ovarian tumours develop from different molecular pathways (**Table 1.1,** Kurman and Shih, 2010; Kurman and Shih, 2011). Various gene expression signatures for predicting survival in advanced stage EOC were produced by analysing the mRNA expression data obtained from several platforms. Some of these signatures were produced by the cancer genome atlas (TCGA) investigators and has been validated in multiple datasets. However, the performance of these prognostic signatures varies between independent cohorts; some poorly correlate with risk scores between different studies. Therefore, such signatures are yet to be utilised to assist in EOC patient management (Yoshihara *et al.*, 2012).

Table 1.1 Molecular and clinicopathologic features of type I and type II EOCs

Features	Type I	Type II
Stage	Frequently early stage	Almost always advanced stage
Tumour grade	Low grade*y	High grade
Proliferative activity	Generally low	Always high
Ascites	Rare	Common
Response to chemotherapy	Fair	Good (but recur later)
Early detection	Possible	Challenging
Progression	Slow and indolent	Rapid and aggressive
Overall clinical outcome	Good	Poor
Risk factors	Endometriosis	Lifetime ovulation cycles; BRCA-germline mutations
Origin	Ovary benign lesions	Mostly fallopian tube epithelium
Precursors	Atypical proliferative (borderline) tumours	STICs
Chromosomal instability	Low	High
p53 mutation	Infrequent	Almost always
Homologous recombination repair	Rarely defective	Frequently defective

* Clear cell carcinoma is not graded, but many consider the tumour as high-grade.
y Occasional progression to high grade can be observed. BRCA, breast cancer; STIC, serous tubal intraepithelial carcinoma (Kurman and Shih, 2016).

1.3 Gene Expression Profiling Studies of EOC

Since different EOC histological subtypes are associated with different patient prognoses, many transcription profiling studies have focused on the discovery of markers that can discriminate between different subtypes (Schwartz *et al.*, 2002). BRCA1- and BRCA2-positive EOCs are the most common forms, around 20% of these cases are associated with *BRCA1* and/or *BRCA2* germline pathogenic variants (Miyamoto *et al.*, 2013; Cannistra, 2004). Genetic defects were also detected in various double-stranded DNA repair-associated genes in EOC, including *BRIP1*, *PALB2*, *RAD5*1, *CHEK2* and *BARD1* (Cannistra, 2004; King *et al.*, 2003; Walsh *et al.*, 2011; Loveday *et al.*, 2011). Based on histopathology and molecular genetic profiles, type I EOCs are subdivided into four subtypes: endometrioid (10%), clear cell (10%), mucinous (3%), and low-grade serous (LGS, <10%, Prat, 2012). Whereas, type II EOCs are subdivided into high-grade serous (HGS, 70%), high-grade endometrioid, carcinosarcoma and undifferentiated (Prat, 2012). These subtypes represent distinct diseases, as indicated by differences in prognosis, precursor lesions, genetic risk factors, molecular events during oncogenesis and response to chemotherapy (Prat, 2012; Köbel *et al.*, 2010). The genomic instability, as observed by global DNA copy number aberration, is the main molecular feature that differentiates between type I and the marked chromosomal instability present in type II EOC (Kurman and Shih, 2016). In addition, type II EOCs are characterised by ubiquitous *p53* mutations and BRCA-related abnormalities, in contrast to their infrequency in type I EOCs (Garziera *et al.*, 2018). Other notable differences include homologous recombination repair (HRR), retinoblastoma protein, cyclin E1 (*CCNE1*), *NOTCH3* and forkhead box M1 (*FOXM1*). Whereas type I carcinomas are characterised by frequent somatic mutations involved in the phosphatase and tensin homolog (*PTEN*)/phosphatidylinositol-4,5-bisphosphate 3-kinase catalytic subunit a (*PIK3CA*), BRAF proto-oncogene/Kirsten ras sarcoma viral oncogene homolog (*KRAS*), β-catenin 1 (*CTNNB1*), AT-rich interaction domain 1A (*ARID1A*) chromatin remodelling pathways and serine/threonine kinase (*BRAF*)/mitogen-activated protein kinase (*MAPK*) extracellular signal-related kinase (*ERK*, **Figure 1.1**). Although EOC can rarely harbour mixed histologic features (more than one histological type in a given tumour) and is estimated to <1% using the current immunohistochemical staining and diagnostic criteria.

1.3.1 Morphologic and molecular features of type I EOC

Endometrioid, LGS, clear cell and mucinous subtypes representing around 10%, <5%, 10% and <5% of EOC cases, respectively. These subtypes (both clinically and at the molecular level) are less common and represent distinct disease entities, both clinically and at the molecular level, from HGS EOC and from one another. Overall, and conversely to HGS EOC, they harbour activating oncogenic mutations specific to solid tumours but do not show high rates of *p53* mutations (**Figure 1.1**, Sato *et al.*, 2005; Strickland *et al.*, 2016).

1.3.1.1 Endometrioid EOC

Compared to HGS, endometrioid represents the group with the most positive clinical outcome due to their tendency to be diagnosed at earlier stages, and are mostly platinum-sensitive in the first-line setting (Gershenson *et al.*, 2006; Gilks *et al.*, 2008). Endometroid EOC harbour mutations involved in the deregulation of *PIK3CA* pathway, including activating *PIK3CA* mutations that occur in 30% of cases, tumour suppressor genes *PTEN* and *ARID1A;* known to be associated with chromatin-remodelling gene mutations which accounts for 20%-30% of the cases, respectively (Chui *et al.*, 2014; Schwartz *et al.*, 2002; McConechy *et al.*, 2014; Matsumoto *et al.*, 2015; Obata *et al.*, 1998). Activating mutations of KRAS and BRAF display <7% of the endometrioid carcinomas. A few cases of endometrioid EOC also harbour somatic mutations in the *PPP2R1A* gene that encodes a subunit of protein phosphatase 2A (Wiegand *et al.*, 2010). Also, endometrioid frequently harbour mutations in the *CTNNB1* (occurring in around 15%-40% of cases) leading to the activation of Wnt signalling pathway and resulting in the accumulation of β-catenin which was previously shown to associate with well-to-moderately differentiated tumours with small size and good overall prognosis (Chui *et al.*, 2014; Schwartz *et al.*, 2002; Guan *et al.*, 2011).

1.3.1.2 Clear cell EOC

As with endometrioid EOCs, clear cell is associated with endometriosis and can be diagnosed at earlier stages in comparison to HGS. However, advanced stage clear cell EOC correlates with low progression rate and relatively lower overall survival (OS) in patients, due to intrinsic platinum resistance (Zorn *et al.*, 2005; Storey *et al.*, 2008; Aysal *et al.*, 2012). In addition, clear cell carcinomas harbour mutations that contribute in deregulating various genes, including *ARID1A* in around 50% of cases, *PIK3CA* in around 50% of cases and *PTEN* in around 10% of cases (Schwartz *et al.*, 2002; Matsumoto *et al.*, 2015; Shih *et al.*, 2011; Sato *et al.*, 2000). Similarly, few cases of clear cell display somatic mutations in *PPP2R1A* (Wiegand *et al.*, 2010). However, unlike endometrioid, around a third of clear cell tumours (Schwartz *et al.*, 2002) display amplification at chr20q13.2 and do not commonly harbour Wnt-activating CTNNB1 mutations (Schwartz *et al.*, 2002; Campbell *et al.*, 2004). In addition to these genetic changes, a recent genome-wide methylation report suggested that clear cell carcinomas exhibit distinctive methylation profiles in comparison to other EOC histologic subtypes (Yamaguchi *et al.*, 2014). For example, aberrant DNA methylation was observed in multiple genes involved in the Oestrogen receptor alpha (ERα) and hepatocyte nuclear factor 1A (HNF1A). DNA methylation of HNF1A could also play an important role in regulating additional cellular drug metabolism and transporter pathways (Soslow *et al.*, 2012; Bélanger *et al.*, 2010).

1.3.1.3 Mucinous EOC

In comparison to other EOC histological types, mucinous EOCs account for fewer cases (Prat, 2012). Like endometriosis, mucinous EOCs have the propensity for diagnosis at earlier stages compared to HGS (Kuo *et al.*, 2010; Zaino *et al.*, 2011). However, mucinous EOCs often display platinum resistance in the first line setting, and advanced stages are typically associated with poor patient overall survival (OS, Sugiyama *et al.*, 2000; Anglesio *et al.*, 2013). As a result of its low occurrence, mucinous remains relatively poorly understood compared to other histological EOC subtypes, that largely hindered the extensive molecular characterisation of this subtype (Hollis *et al.*, 2016). Common genetic defects representing mucinous tumours, include KRAS mutations, tumour suppressor RNF43 mutation and *HER2* gene amplification, with around 50%, 21% and 20% of cases displaying these defects, respectively (Kuo *et al.*, 2010; Brown and Frumovitz, 2014; Ryland *et al.*, 2013). In mucinous ovarian neoplasia, a mutation screening of the MAPK/ERK pathway showed that MAPK/ERK pathway alterations

and p16 loss are highly recurrent events, detected during early mucinous tumour development (Hunter *et al.*, 2012).

1.3.1.4 LGS EOC

LGS EOCs occur in younger patients and is characterised by prolonged OS compared to HGS even when diagnosed at advanced stage (Schmeler *et al.*, 2008). In contrast to HGS, LGSs typically have wild-type p53. Over 60% of LGS tumours harbour *MAPK* pathway-activating *BRAF* or *KRAS* mutations, but almost none harbour *p53* mutations. Furthermore, it was suggested that LGS EOCs displaying mutation in *KRAS* and *BRAF are* associated with recurrent tumours (approximately 10% recur after surgery) and poor survival in comparison to wild-type *BRAF* and *KRAS*. These tumours are assumed to develop in a step-wise fashion from a subset of serous borderline tumours (SBT, Testa *et al.*, 2018). Hunter and co-workers identified several oncogenes, including MAPK/ERK/oestrogen-related receptor B2 (ERBB2) mutations that were observed in 82% of SBTs, compared to 63% of LGS EOCs. In addition, copy number aberrations were observed in 100% of LGS EOCs, compared to 61% of SBTs. Interestingly, neuroblastoma RAS viral oncogene homolog *(NRAS)* mutations were detected only in LGS EOCs. Some genomic rearrangements resulting in DNA genomic rearrangements resulting in novel copy number alterations (CNV), such as homozygous deletions of Cyclin Dependent Kinase 2A (*CDKN2A)* locus and loss of 9p, are mostly observed in LGS EOCs (Hunter *et al.*, 2015).

1.3.2 Morphologic and molecular features of Type II EOC

1.3.2.1 HGS

Because HGS represents the majority of EOCs and it accounts for approximately all the remaining EOC cases, around 70%, gene expression studies have thus mainly focussed on this subgroup. HGS is characterised by extensive genetic heterogeneity, widespread DNA copy number or morphological aberrations and universal *p53* mutations (Somigliana *et al.*, 2006; Lynch *et al.*, 2009; Seidman *et al.*, 2012; Chan *et al.*, 2008). Almost all of *p53* mutations in HGS patients are missense variants, whereas, variants which result in complete loss of p53 protein commonly referred to as 'p53 nulls', including nonsense, frameshift (FS) or splice junction

account for around 30% (Salani *et al.*, 2008). Additionally, the widespread copy number alterations reflect on the history of genomic instability, including ubiquitous *p53* mutations and low occurrence (>5%) but statistically recurrent somatic mutations in nine further genes, including neurofibromin 1 (*NF1*, 8% deletion, 4% mutation), retinoblastoma protein 1 (*RB*, 8% deletion, 2% mutation), *PTEN* (7% deletion, <1% mutation), cyclin dependent kinase 12 (*CDK12*, 3% mutation, gamma-aminobutyric acid type a receptor alpha6 subunit (*GABRA6*, 2% mutation) and CUB and sushi multiple domains 3 (C*SMD3*, 6% mutation), substantial significant focal DNA copy number aberrations and promoter methylation events. In addition, *FOXM1* and *NOTCH3* signalling pathways were also found to be associated with the pathophysiology of HGS EOC (Bell *et al.*, 2011). However, recent whole genome analysis of HGS cases has identified common targets of previously unknown gene breakage occurrences, including NF1 and RB1, affecting 17.5% and 20% of cases, respectively. Therefore, highlighting the role of large structural-rearrangements leading to the inactivation of EOC tumour suppressors (Yemelyanova *et al.*, 2011). A comprehensive view of the somatic alterations and germline variations in HGS carcinoma cohorts associated with higher cancer risk, led to the identification of various recurrent alteration in large copy number (22 losses and 8 gains) and genes, including BHLH transcription factor (*MYC*) proto-oncogene, MYC and *KRAS* (gain), *PTEN* (loss), *RB1,* and *NF1* (loss). Many of these losses and gains were identified in almost all tumours, emphasising the importance of genomic instability of HGS (Testa *et al.*, 2018). Other common genetic alterations in HGSs include, germline and somatic mutation of *BRCA1/2,* CNAs of *CCNE1* amplification and other alterations affecting the regulatory pathways of HRR-mediated DNA damage repair (Bell *et al.*, 2011). Approximately 50% of HGS have an identifiable somatic, germline or epigenetic defects that occur in HRR pathway, as seen in *BRCA1*/*BRCA2* germline or somatic mutations which together account for around 20% of cases (Vogelstein *et al.*, 2013). Around 4% and 3% of HGS patients harbour somatic *BRCA1* and *BRCA2* defects, respectively, while germline changes in each occur in around 8% and 6% of cases, respectively (Somigliana *et al.*, 2006; Bolton *et al.*, 2012; Patch, *et al.*, 2015). *BRCA1/2*-deficient HGS are characterised by relatively higher DNA copy number alterations, and they typically do not harbour *CCNE1* amplification (Patch *et al.*, 2015).

Four HGS molecular subtypes, termed immunoreactive, proliferative, differentiated and mesenchymal, were initially identified from the gene expression analysis of approximately 300 cases and subsequently validated in TCGA study (Tothill *et al.*, 2008; Cancer Genome Atlas Research Network, 2011). However, the recapitulation of these subgroups in other datasets

has shown distinct clinical outcomes (Helland *et al.*, 2011; Konecny *et al.*, 2014). Zhang et al. (2003) showed that survival differed significantly between the four subtypes and this difference was best illustrated in immunoreactive subtype. Zhang group correspondingly reported similar findings, using histopathological analysis of HGS cases, demonstrating that significant numbers of tumour-infiltrating lymphocytes were associated with good prognosis (Zhang *et al.*, 2003). Moreover, other studies showed that *BRCA1* mutations were also associated with immunoreactive HGS subtype (George *et al.*, 2013). Collectively, these studies suggest that all HGS subtypes may display distinct oncogene activation patterns. In addition, these studies also suggested that the disruptions in DNA repair mechanisms are the leading cause of HGS development, followed by chromosomal instability, copy number changes and leading to the differentiation into molecular subtypes. While the emerging immune stimulation contributes to the improved survival outcome of HGS patients, it is important to successfully utilise these subgrouping methods, including the consensus molecular subgrouping of HGS, that can thereafter be used in a clinical context (Langie *et al.*, 2015).

1.3.2.2 Undifferentiated-carcinoma

Undifferentiated-carcinoma subtype are uncommon (<5%) and show none of the distinctive pathologic features observed in HGS or high-grade endometrioid carcinoma. It remains unclear whether these are variants of poorly differentiated HGSs, distinct tumours or high-grade endometrioid carcinomas. It was suggested that the gene expression patterns of this subtype are similar to the one observed in mesenchymal rather than epithelial cells (Hernández *et al.*, 2012; Kurman and Shih, 2016). However, the molecular background that specifically evaluates this tumour type are currently unavailable; therefore, it remains poorly understood (D'Andrilli *et al.*, 2008).

1.3.2.3 Carcinosarcomas

Carcinosarcoma are also referred to as malignant mixed Müllerian tumour, is a biphasic tumour comprised of sarcoma and carcinoma. Both components are distinct but also display intermixed molecular features. Carcinosarcomas and HGS share numerous molecular genetic abnormalities, including *p53* mutations and *CDKN2A* upregulation (Jin *et al.*, 2003; Kurman and Shih, 2016).

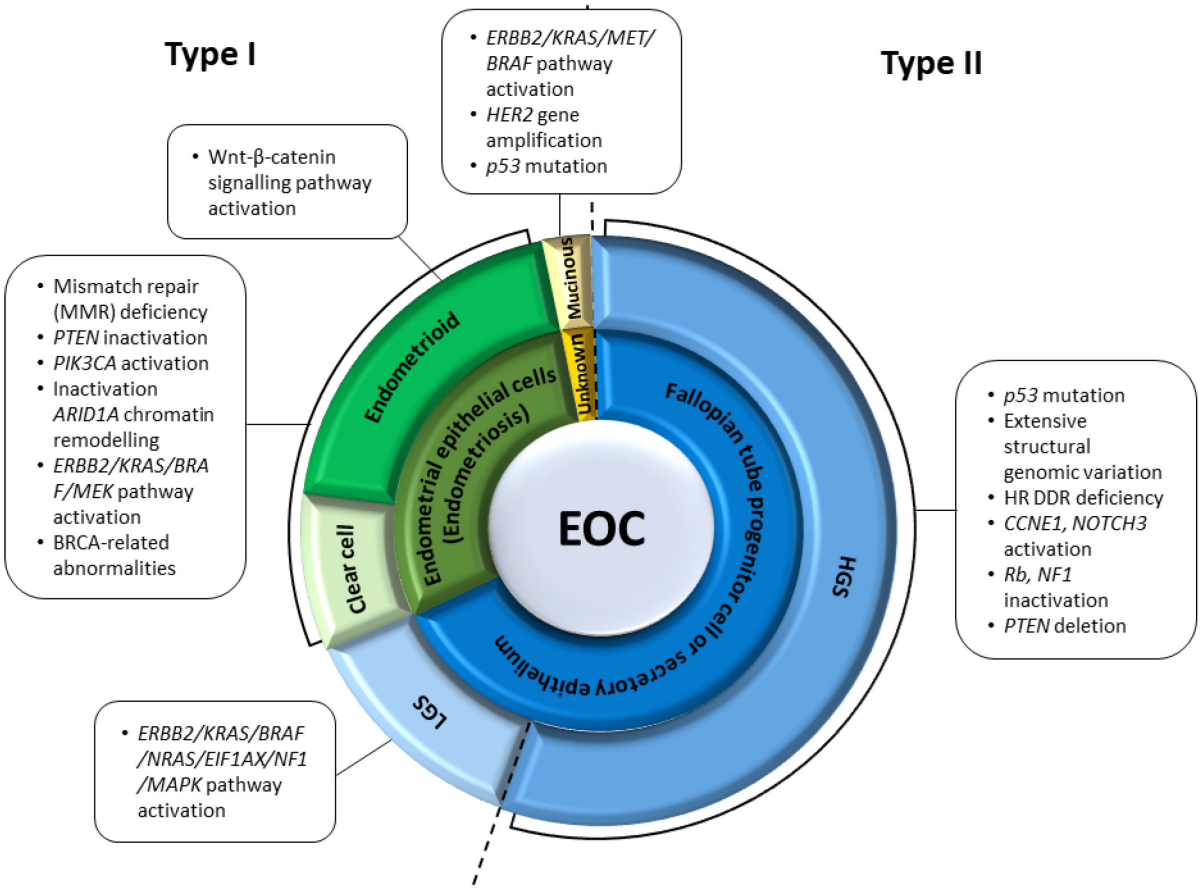

Figure 1.1 A dualistic model representing the pathogenesis of EOC. Type I carcinomas are comprised of clear cell, low-grade serous (LGS), mucinous carcinomas and endometrioid. Type II carcinomas are composed of mainly high-grade serous carcinomas (HGS). Type II carcinomas, including undifferentiated and carcinosarcoma cancers are relatively rare and therefore not included in this figure. The areas of individual histological subtypes represent their relative frequency. The origin of the different type I and type II EOCs is indicated in the inner circles. The cell of origin in mucinous carcinomas is not yet established, therefore, was indicated as unknown. The molecular pathway alterations characterising each tumour subtype are summarised in the square boxes. Abbreviations: RB, retinoblastoma protein; BRAF, B-Raf proto-oncogene; ARID1A, AT-rich interaction domain 1A; MMR, DNA mismatch repair; PI3K, phosphatidylinositol 3- kinase; serine/threonine kinase; ERRB2, oestrogen-related receptor B2; KRAS, Kirsten rat sarcoma viral oncogene homolog; HR DDR, homologous recombination-mediated DNA damage repair; MEK, mitogen-activated protein (MAP) extracellular signal-related kinase (ERK) kinase; PTEN, phosphatase and tensin homolog; cyclin E1, CCNE1; NF1, nuclear factor 1 (Kurman and Shih, 2016).

1.4 Diagnosis of EOC

The high mortality of EOC is largely explained by its asymptomatic/slow course of growth, therefore, two-thirds of all EOC cases are diagnosed at late stages; Stage III or Stage IV (Testa *et al.*, 2018). The lack of effective molecular screening methods, specifically at early disease stages, also contributes to the high mortality of EOC (Yokoi *et al.*, 2018). Early stage EOCs present symptoms that are similar to those of other conditions, including dyspepsia, menstrual irregularities, abdominal pain and other mild digestive disturbances, which may have existed for short periods of time. As the disease advances, discomfort from ascites and abdominal distention increases, and may be accompanied by respiratory symptoms from the fluid transudation into the pleural cavities or from elevated intra-abdominal pressure (Berek *et al.*, 2015). To determine the possible risk factors, a detailed clinical and familial cancer history must be collected. Followed by a comprehensive physical examination, including rectal examination and general pelvic area. Prior to surgery, pleural effusion is screened using chest radiograph and computerised tomography (CT), to outline the extent of intra-abdominal disease (Cameán *et al.*, 2016).

1.5 Cytoreductive (debulking) surgery for advanced stage EOC

Surgical debulking plays an important role in the treatment and early management of advanced EOC. The decision whether a patient is a good candidate for debulking surgery is built according to the surgeons' experience, patient characteristics, complementary tests (serum biomarker levels and CT) and laparotomy or less-invasive imaging techniques, such as ultrasound, that are performed initially to detect metastatic and locally advanced disease (Fischerova *et al.*, 2017; Nick *et al.*, 2015; Rutten *et al.*, 2015; Fotopoulou *et al.*, 2010). For all the disease stages (specifically stages I to III) all visible tumour masses are removed, including total hysterectomy, peritoneal washings, inspection of all abdominal organs/peritoneal surfaces and bilateral salpingo-oophorectomy. In addition, tumour mass removal is coupled with total omentectomy, para-aortic lymphadenectomy and sampling of lymph nodes and adjacent tissues for biopsy from fixed locations throughout the abdominal cavity. There are three types of debulking surgeries: (i) **primary debulking**; complete removal of macroscopic tumour, including diaphragmatic resection, splenectomy, liver resection, intestinal resection or any other abdominal organ affection, before any other treatment (Zapardiel *et al.*, 2011; Peiretti *et al.*, 2012) (ii) **interval debulking**; cytologically confirmed

stage IIIC and IV patients, may not be good candidates for surgical approach, and neoadjuvant taxanes chemotherapy may be used initially in 2 to 3 cycles, followed by interval surgical cytoreduction and additional adjuvant chemotherapy (Bristow and Chi, 2006) (iii) **secondary debulking**; recurred cancer removal surgery (Salani *et al.*, 2007). Around 16% to 35% of the EOCs, that were assessed and initially classified as early stage disease are upstaged later (Colomer *et al.*, 2008). After complete surgical staging for EOC, the new international federation of gynaecology and obstetrics (FIGO) staging system is used to determine patient prognosis and direct management. The new FIGO staging system was recently revised to incorporate ovarian, fallopian tube, and peritoneal cancer, approved since January 2014 as shown in (**Table 1.2**, Mutch and Prat, 2014; Berek *et al.*, 2015). This evaluation system is vital and assists with categorising of patients according to survival rate (short survival and moderate/high-risk of relapse, Testa *et al.*, 2018). However, recent innovations in chemotherapeutic drugs and their administration (i.e. intraperitoneal delivery) have largely eclipsed advances in surgery (Schorge *et al.*, 2010).

Table 1.2 FIGO 2014 EOC staging. The 5-year survival for the various stages is reported. R, rate

Primary EOC FIGO			Tumour Extension	5-year Survival R
Stage I			**Tumour limited to the ovaries (one or both)**	**85–94%**
	IA		Tumour is limited to one ovary; no malignant cells in ascites or peritoneal washings; capsule intact, no tumour on ovarian surface	94%
	IB		Tumour limited to both ovaries; capsule intact, no tumour on ovarian surface; no malignant cells in ascites or peritoneal washings	92%
	IC		Tumour limited to one or both ovaries with any of the following:	85%
		IC1	Surgical spill	
		IC2	capsule ruptures, tumour on ovarian surface	
		IC3	malignant cells in ascites or peritoneal washings	
Stage II			**Tumour includes one or both ovaries with pelvic extension.**	**69–78%**
	IIA		Extension and/or implants in the uterus and/other tube(s); no malignant cells in ascites or peritoneal washings	78%
	IIB		Extension and/or implants in other pelvic tissues; no malignant cells in ascites or peritoneal washings	73%
Stage III			**Tumour includes one or both ovaries with microscopically confirmed peritoneal metastasis outside the pelvis and/or metastasis to the retroperitoneal lymph nodes**	**17–59%**
	IIIA		Microscopic peritoneal metastasis extra pelvic (no macroscopic tumour)	59%
		IIIA1	Positive retroperitoneal lymph nodes only; (i) metastasis ≤ 10 mm and (ii) metastasis > 10 mm	
		IIIA2	Microscopic, extra pelvic (above the brim) peritoneal involvement ± positive retroperitoneal lymph nodes	
	IIIB		Macroscopic peritoneal metastasis extra pelvic, peritoneal metastasis ≤ 2 cm ± positive	39%
	IIIC		Macroscopic peritoneal metastasis extra pelvic >2 cm in greatest dimension and/or regional lymph node metastasis	17%
Stage IV			**Distant metastasis and or metastases to extra-abdominal organs excluding peritoneal metastasis**	**12%**
	IVA		Pleural effusion with positive cytology	
	IVB		Hepatic metastasis, metastasis to extra abdominal organs (including inguinal lymph nodes and lymph nodes outside of the abdominal cavity)	

1.6 Chemotherapy for EOC

The platinum-based combination chemotherapy is the standard and most effective first-line treatment for EOC (specifically EOC advanced stages, Jazaeri *et al.*, 2005). Platinating agent analogues, such as carboplatin (cis-(1,1-cyclobutanedicarboxylato) diammineplatinum(II)) or cisplatin (cis-diamminedichloroplatinum (II)), are commonly used in the treatment of EOC. These agents induce cancer cell death via interfering with DNA replication and transcription by forming cisplatin-DNA crosslinks between the purine bases to form 1,2- or 1,3- interstrand and intrastrand, triggering DNA damage and cell-cycle arrest at the growth 1 (G1) or growth 2 (G2) phases, thereby preventing cell division and growth (Dekou *et al.*, 2001). Other cisplatin-mediated cytotoxicity mechanisms include altered axonal transport, microtubule changes, endoplasmic reticulum integrity alteration, reactive oxygen species (ROS) production, mitochondrial function impairment, activation of calpain and dysfunctions in sodium (Na^+), calcium (Ca^{2+}) and potassium (K^+) channels and Ca^{2+} signalling changes (Kursunluoglu, Taskiran and Kayali, 2018). Cisplatin-induced DNA damage response is regulated by several factors, including protein kinase C that acts as a positive regulator for cisplatin-induced cell death, and transcription factors, such as *p53, p21, p300* and *p63.* These transcription factors also play a critical role in cell apoptosis and pro-apoptotic gene activation (**Figure 1.2**). Other agents, such as taxane-based chemotherapy (e.g. paclitaxel) are also frequently used in the treatment of EOC in combination with other chemotherapeutic drugs, e.g. platinating agents (Chorawala *et al.*, 2012). Taxanes inhibit cell division (mitotic inhibitor) by binding to α-tubulin and stabilising microtubules, consequently, resulting in cell apoptosis (Huizing *et al.*, 1995; Jordan and Wilson, 2004). Chemotherapeutic treatments depend on several factors, including the extent of disease, cancer-specific pathological and molecular characteristics, its location, and patient health status (Chorawala *et al.*, 2012).

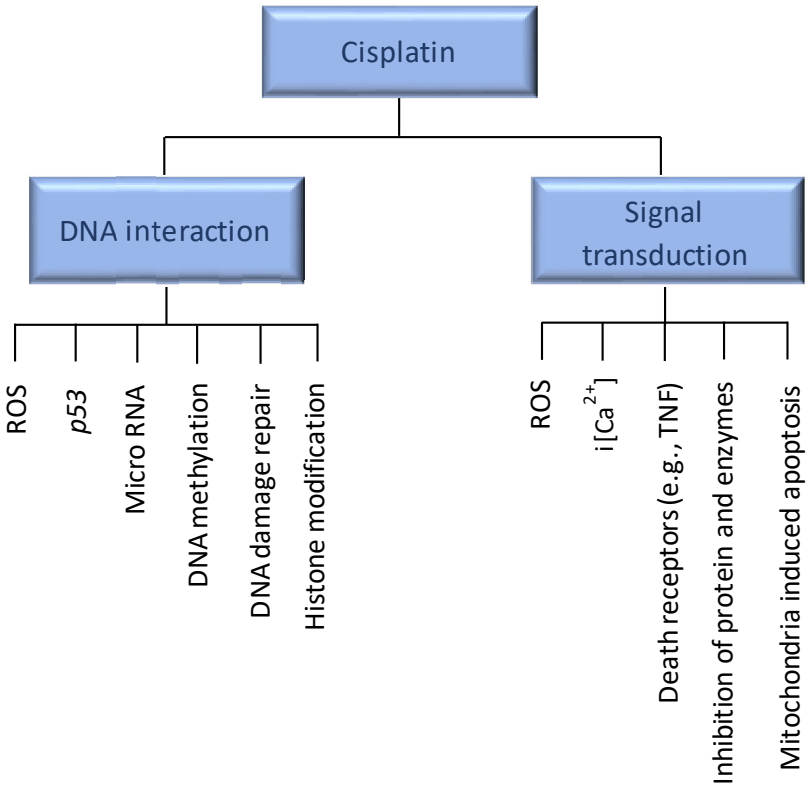

Figure 1.2 The targets of cisplatin. Abbreviations: ROS, Reactive oxygen species; TNF, tumour necrosis factor; i[Ca^{2+}], intracellular calcium.

1.6.1 Gene expression profiles associated with response to chemotherapy in EOC

The integration of newer biologic drugs and molecular targeted therapies can provide enhanced medical management of EOC (Schorge *et al.*, 2010). While platinum-based drugs are commonly used in cancer treatment, many tumours are entirely resistant to these drugs with no clinical response achieved. Around 20% to 30% of patients diagnosed with advanced-stage disease (75%) progress on or rapidly develop resistance to platinum-based drugs and similarly show low rates of response to other second-line agents. The early prognosis of these chemoresistant patient groups can benefit from the ongoing clinical trials or experimental therapeutic interventions. In practice, chemosensitive tumours are classified as such based on patient response to chemotherapy and a platinum-free interval of ≥13 months. In addition, it was suggested that the length of platinum-free interval, dictates the subsequent response rates of this group to additional chemotherapy.

The vast majority of patients that were initially identified as chemosensitive, will eventually relapse and develop chemoresistance. Suggesting that chemoresistance can be acquired during treatment or may pre-exist at the outset of treatment (intrinsic resistance). The pre-clinical assessment of molecular abnormalities in EOCs can help in defining the developing sites of precursor lesions and provided insight into the underlying mechanisms involved in tumour clonal aggregation processes that mediate chemoresistance, including natural evolution and drug-induced clonal selection (Kim *et al.*, 2018; Testa *et al.*, 2018; Murugaesu *et al.*, 2013). In addition, these molecular studies were of profound importance in defining not only the inter-tumour heterogeneity, but also the intra-tumour heterogeneity that can be used to assist with the development of therapeutic treatments for advanced stages. Characterisation of the mechanisms involved in chemoresistance are required for successful treatment of EOC. The key molecular mechanisms involved in this resistance may include reduced intracellular accumulation by uptake/efflux transporters or alteration in platinum inactivation, increased adduct tolerance/repair or inhibition of apoptotic pathways. Several studies have explored clinical drivers that contribute to the acquired resistance to chemotherapic agents, including cisplatin and paclitaxel, in EOC patients. In this context, a recent study, using extensive molecular analysis of chemoresistant patients, showed that the acquired resistance to chemotherapy was linked with gene breakages inactivation at the level of known tumour suppressors, including *RAD51B, NF1, RB1 and PTEN* and resistant tumours are mostly associated with amplifications of *CCNE1* (Patch *et al.*, 2015; Testa *et al.*, 2018).

Interestingly, in some chemoresistant tumours, reversion in *BRCA1* or *BRCA2* mutations or loss of *BRCA1* hypermethylation was also observed. Prieske *et al.*, (2017) correspondingly reported that high *BRCA1* and *BRCA2* mutations are linked to an increased risk of breast cancer; however, they found that BRCA-associated tumours respond better to platinum-based therapy. In another study, advanced ascitic EOC patients were screened to reveal common abnormalities of the *PI3K* signalling pathway that were detected in majority of the chemoresistant patients. These abnormalities include *PI3KCA* mutations found in 5% of samples; amplification of AKT serine/threonine kinase 2 (*AKT2*) and *PI3KCA* and deletion of *PTEN* were found in 10%, 12% and 27% of samples, respectively (Huang *et al.*, 2011). At the protein level, several genetic and biochemical studies *in vitro* have shown that *PTEN*-mediates the downregulation of *PI3K/AKT*- signalling. Therefore, the loss of *PTEN* was associated with increased *AKT* activation and subsequent increased proliferation, migration and progression of various human cancers (Di Cristofano *et al.*, 1998; Carracedo and Pandolfi, 2008; Keniry and Parsons, 2008).

Other studies based on gene profiling analysis used microarray platforms to detect differential gene expression patterns and identify novel genes that correlate with EOC patient's response or resistance following a standard treatment (Macgregor and Squire, 2002; Testa *et al.,* 2018). In one report by Dressman *et al.*, (2007), gene profiling analysis was carried out on a subset of 83 advanced serous OC cases and identified deregulated genes whose expression correlated with patient response or resistance to platinum-based therapy. These deregulated genes, involved in non-receptor tyrosine kinase (SRC) proto-oncogene, MYC and E2F transcription factor 3 (E2F3) pathways, were shown to be associated with cancer growth and proliferation and correlate with a poor patient response to platinum treatment (Dressman *et al.*, 2007; Gatza *et al.*, 2014). Another study by Stronach *et al.*, (2011), compared clinically derived tumour samples collected before and after chemotherapy treatment, which identified molecular signatures associated with the acquired resistance in patients. Further analysis suggested that histone deacetylase 4 (HDAC4) may serve as a molecular signature for OC and its upregulation mediates resistance by activating acetyl-signal transducer and activator of transcription 1 (STAT1) signalling pathways following platinum treatment (Stronach *et al.*, 2011). Furthermore, a number of studies attempted to identify membrane markers that may contribute to the development of serous EOC initiating cells. These studies used various methodologies, including molecular phenotyping and histological analysis, to assess heterogeneous populations of serous EOC cells (i.e. tumour xenografts *in vitro* tumour-

spheres, primary tumours and tumour cell lines). The results obtained from these studies indicated that the deregulation of CD44, CD117 (Zhang *et al.*, 2008), CD24, CD133 (Baba *et al.*, 2009), Aldehyde dehydrogenase-1A1 (ALDH1A1) (Landen *et al.*, 2010) and epithelial cell adhesion molecule (EpCAM) (Alvero *et al.*, 2009), drives the development of serous tumour-initiating cells.

Similar to what was observed in chemoresesistant patients in clinical setup, *in vitro* chemoresesistant EOC cell lines also revealed the underlying molecular mechanisms involved in the emergence of this resistance. A number of studies reported several mechanisms of chemoresistance *in vitro* cell lines, including efflux pumps, DNA repair capacity via nucleotide excision repair pathway (*EERC1*) and deregulation of genes involved in survival pathways *PI3K/AKT, MAPK, EGFR,* mechanistic target of rapamycin kinase (*mTOR*), oestrogen signalling and deficiency in tumour suppressors *p53* and PRKC apoptosis WT1 regulator protein (*Par-4*) (Nicolantonio *et al.*, 2005; Stapf *et al.*, 2016). The biological processes associated with stress responses play a vital role in the normal development and homeostasis. While standard chemotherapy has been effective to some degree; however, the poor bioavailability, adverse side effects, high-dose requirements and development of multiple drug resistance mechanisms are the main drawbacks (Senapati *et al.*, 2018).

1.6.2 Targeted therapies for treatment of platinum-resistant EOC

As with many other types of cancer, resistance to platinum-based therapies is an increasing concern in the treatment of EOC which must be addressed to advance therapeutics (Leamon, Lovejoy and Nguyen, 2013). Assessing the genetic profiling of resistant tumours before and after chemotherapy treatment will provide additional insight into the underlying mechanism mediating drug resistance (Tan *et al.*, 2015; Leamon *et al.*, 2013). The analysis of patient genetic profiles can predict the combination of therapies required for optimal effect and prevention of treatment escape (Leamon, Lovejoy and Nguyen, 2013). Currently developing approaches for EOC targeted therapy can be categorised into different groups, according to therapy-specific mechanisms of action as well as specific advantages. For example, some of these therapies target the Vascular endothelial growth factor (VEGF) pathway (e.g. bevacizumab and aflibercept humanised monoclonal antibody (mAb)), whereas others inhibit DNA repair mechanisms in platinum-resistant patients, specifically those who harbour BRCA mutations (e.g. iniparib, olaparib and veliparib), or the folate pathway (farletuzumab, pemetrexed, and vintafolide) and p53 mutation in platinum-resistant HGS EOC (Pujade-

Lauraine *et al.*, 2014; Kaye *et al.*, 2011; Gray *et al.*, 2018; Birrer *et al.*, 2011; Naumann *et al.*, 2013; Lehmann *et al.*, 2012). An overview of some key clinical trials that are testing the potential combinational therapies and new drugs in platinum-resistant EOC (often in combination with chemotherapy) (Al-Bahlani *et al.*, 2011; Leamon, Lovejoy and Nguyen, 2013). It has been shown that the demonstration of oral supplements, such as Ca^{2+} or folic acid, reduce or avert some of chemotherapy drugs side effects (Leamon, Lovejoy and Nguyen, 2013). Therefore, it appears that elevated calcium levels, via calcium supplementation, may act as another mean of cytoprotection, by competing for binding sites with cisplatin and averting various cisplatin-associated toxicities (Aggarwal, 1998). Cisplatin-mediated disruption of Ca^{2+} homeostasis can affect multiple cellular functions and initiate anti-tumour immunity. It can also induce apoptosis through blocking potassium channel subfamily K member 3 (TASK-3) in EOC (Innamaa *et al.*, 2013; Bose *et al.*, 2015). More recently, PLC-mediated i[Ca^{2+}] signalling has been proposed as a promising target to overcome cisplatin resistance (Wang and Bourguignon, 2006). Cisplatin-induced Ca^{2+} influx damages the cells through depletion of adenosine triphosphate (ATP), inhibition of mitochondrial function and other cofactors. These damages are recognised by cytotoxic T lymphocytes (CTL) and natural killer (NK) cells, leading to cell apoptosis and tissue necrosis (Florea and Büsselberg, 2006; Splettstoesser *et al.*, 2007; Tomaszewski and Büsselberg, 2007). Cisplatin-Ca^{2+} homeostasis is regulated by BRCA1-mediated inositol trisphosphate (IP3) and Voltage-dependent anion-selective channel 1 (VADC-1) ion channels. The activation of IP3-and VADC-1 receptors attenuates cisplatin induced Ca^{2+}-influx activating calpain-mediated cell apoptosis (**Figure 1.3,** Hedgepeth *et al.*, 2015; Thinnes, 2009**)**.

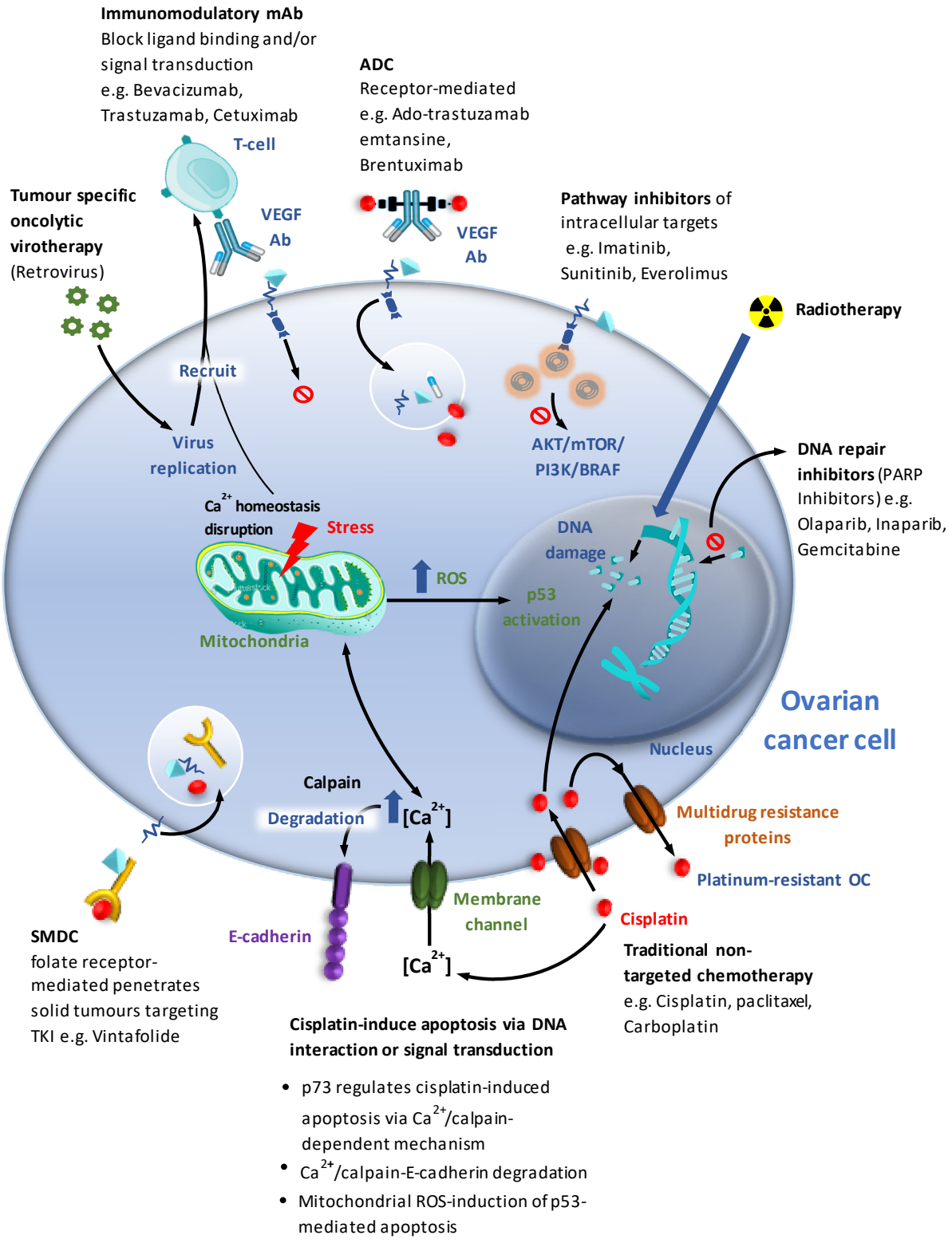
Immunomodulatory mAb
Block ligand binding and/or signal transduction
e.g. Bevacizumab, Trastuzamab, Cetuximab
T-cell
VEGF Ab
ADC
Receptor-mediated
e.g. Ado-trastuzamab emtansine, Brentuximab
VEGF Ab
Pathway inhibitors of intracellular targets
e.g. Imatinib, Sunitinib, Everolimus
Radiotherapy
Tumour specific oncolytic virotherapy
(Retrovirus)
Recruit
Virus replication
AKT/mTOR/ PI3K/BRAF
DNA repair inhibitors (PARP Inhibitors) e.g. Olaparib, Inaparib, Gemcitabine
Ca2+ homeostasis disruption
Stress
ROS
DNA damage
p53 activation
Mitochondria
Ovarian cancer cell
Nucleus
Calpain
Degradation
[Ca2+]
Multidrug resistance proteins
Platinum-resistant OC
Membrane channel
Cisplatin
E-cadherin
[Ca2+]
SMDC
folate receptor-mediated penetrates solid tumours targeting TKI e.g. Vintafolide
Traditional non-targeted chemotherapy
e.g. Cisplatin, paclitaxel, Carboplatin
Cisplatin-induce apoptosis via DNA interaction or signal transduction
p73 regulates cisplatin-induced apoptosis via Ca2+/calpain-dependent mechanism
Ca2+/calpain-E-cadherin degradation
Mitochondrial ROS-induction of p53-mediated apoptosis

Figure 1.3 Schematic presentation of the existent and emerging EOC treatments. Immunotherapy targeting regulatory T cell can be targeted with therapies, such as oncolytic virotherapy or mAB-redirected T-cell–based adoptive immunotherapy, aiming to increase the pre-existing antitumoral immunity effector functions. The PARP inhibitors, block the PARP complex, leading to a disturbance of single stranded DNA repair. Inactivation of cancer inducing pathway by pathway inhibitors, such as *PI3K/Akt/BRAF/mTOR*. SMDC comprising of folic acid linked to vinca alkaloid desacetylvinblastine hydrazide (DAVLBH), a potent microtubule destabilizing agent, induce apoptosis. Radiotherapy and chemotherapy induce DNA damage and apoptosis via *p53, P73,* Ca^{2+}/calpain-dependent mechanism. Simultaneous targeting of BRCA-mutated platinum-resistant with PARP inhibitor olaparib or mAbs or pathway inhibitors in combination with cisplatin can achieve significant antitumoral responses. Abbreviations: NF-κB, nuclear factor κB; PI3K, phosphatidylinositol 3- kinase; miR, microRNA; JAK, Janus kinase; STAT, acetyl- signal transducer and activator of transcription; NADPH, nicotinamide adenine dinucleotide phosphate; p53, tumour protein 53; BRCA, breast cancer gene; AKT, AKT Serine/Threonine Kinase; MAP, mitogen-activated protein; SMDC, small molecule drug conjugate; VEGF, vascular endothelial growth factor; mAB, monoclonal antibody; ADC, antibody–drug conjugate; ERK, extracellular signal-related kinase; EGFR, Epidermal growth factor receptor.

1.7 Prognostic biomarkers and oncogenes in EOC: current options and future promise

Recently, the study of protein expression and genomic alterations involved in breast carcinogenesis has identified a growing number of gene targets for drug development in the setting of EOC, substantially improving the prognosis (Toss *et al.*, 2017). Recently developed drugs (e.g. trastuzamab, etc.) can target these molecular abnormalities, therefore, leading to improved survival outcome in cancer patients (Toss *et al.*, 2017). Accordingly, clinical trials provided emerging evidence that the genetic context of a tumour may dictate its resistance or sensitivity to certain drugs (Toss *et al.*, 2017). In addition, some studies have previously shown that treating tumours with therapies corresponding to their molecular alterations achieved longer survival and higher objective response rates. Predictive molecular biomarkers may optimise patient-specific treatment selection of effective therapies, subsequently reducing treatment cost and side effects (**Figure 1.4,** Toss and Cristofanilli, 2015).

1.7.1 Current Biomarkers for EOC

The most commonly used biomarkers for EOC clinical screening and prognosis are carbohydrate antigen 19-9 (CA19-9), cancer antigen 125 (CA125), human epididymis protein 4 (HE4) and vascular cell adhesion molecule 1 (VCAM1, Montagnana *et al.*, 2011; Antalis and Hodge, 2013). These biomarkers can detect EOC at earlier stages in patients and healthy subjects with 86% sensitivity at 98% specificity (Yurkovetsky *et al.*, 2010). CA125 and CA19-9 antigens are glycoproteins commonly expressed by primary non-mucinous EOC and non-gynaecologic cancers, including those of the pancreas, breast, colon, lung and thyroid (Montagnana *et al.*, 2011). Following cytoreduction, a steep decline in CA125 levels in patient serum indicates optimal surgical outcome, the failure to demonstrate this response is associated with suboptimal surgical outcomes and higher risk of relapse (Nolen and Lokshin, 2014). CA125 serum levels are elevated in 80% of advanced-stage EOC patients but are increased in only 50–60% of patients with early-stage disease (Al-Ibraheemi and Wahed, 2013). Downregulating CA125 promotes epithelial-to-mesenchymal transition (EMT), and re-establishes EGFR signalling through increasing AKT and ERK1/2 phosphorylation (Comamala *et al.*, 2011). Human epididymis 4 (HE4), VCAM1 and CA19-9 are slightly less sensitive than CA-125 in the detection of EOC at early-stages but have greater specificity for distinguishing malignant from benign pelvic masses, particularly in premenopausal women (Antalis and Hodge, 2013).

Recently discovered protein biomarker candidates include mesothelin glycoprotein, osteopontin glycoprotein, apolipoprotein A1 (ApoA1) and kallikreins (KLKs, Rastogi, Gupta, *et al.*, 2016). Similar to CA125 and CA19-9, osteopontin and mesothelin facilitate tumour progression and cell survival by inducing NF-$_{\kappa}$B and the calcium-dependent proteolytic enzyme, matrix metalloproteinases-7 (MMP-7), through MAPK/ERK and C-Jun N-terminal kinases (JNK) pathways. In addition, the upregulation of osteopontin and mesothelin induce drug resistance through PI3K/AKT and MAPK/ERK signalling pathways (Chang *et al.*, 2012; Chang *et al.*, 2009; Ye *et al.*, 2011; Yurchenco and Schittny, 1990). Likewise, KLK-6 and KLK-7 are proteases used in the early detection and diagnosis of serous subtypes and advanced-stage disease in primary human EOC (Tamir *et al.*, 2014). Higher KLK expression levels promote cell proliferation, migration, and invasion by inducing E-cadherin shedding (Klucky *et al.*, 2007; Johnson *et al.*, 2007). Moreover, Transthyretin (TTR) prealbumin is an anti-oncogene and its downregulation serves as an important marker in cancer (Zhang *et al.*, 2004). TTR blocks retinol uptake and cell signalling by stimulating retinoic acid-induced STRA6 (Holo-retinol-binding protein receptor) and janus kinase (JAK)/STAT signalling cascade (Berry *et al.*, 2012). In contrast, higher levels of ApoA1 in serum are associated with increased OS and better prognosis in EOC patients (Marinho *et al.*, 2019). The ApoA1-mediated anti-tumourigenic mechanisms include tumour microenvironment modulation, neoangiogenesis inhibition, regulation of inflammatory signalling (i.e. STAT3 pathway) and decreased pro-invasion factors levels (e.g. matrix metalloproteinase-9 (MMP-9), Marinho *et al.*, 2019). Furthermore, it was demonstrated that ApoA1 and ApoA1-mimetic peptides also mediate anti-tumourigenic and increased platinum drug efficacies in EOC by binding to the pro-inflammatory pro-oncogenic phospholipids, such as lysophosphatidic acid (LPA, Zamanian-Daryoush *et al.*, 2013; Gkouskou *et al.*, 2016; Jia *et al.*, 2017).

1.7.2 Novel biomarker development in EOC

Similar to other cancers, the initiation and development of EOC is characterised by disruption of oncogenes and tumour suppressor genes by both epigenetic and genetic mechanisms (Kobayashi *et al.*, 2012). Recent advances in nucleic proteomics technology and acid–based analyses demonstrated promising discoveries of novel and more valuable serum biomarkers, which cumulatively represents the next generation of EOC screening tool (**Figure 1.4**, Kobayashi *et al.*, 2012).

1.7.2.1 EOC biomarkers with angiogenic features

1.7.2.1.1 Vascular endothelial growth factor (VEGF)

It is well established that angiogenesis (i.e. the formation of new blood vessels) is essential for the growth and metastasis of solid tumours (Folkman, 1990). Tumour angiogenesis is regulated by a complex of angiogenic stimulators, such as fibroblast growth factors (FGF) family members and inhibitors (e.g. endostatin and thrombospondin-1, Rajabi and Mousa, 2017; Hanahan and Weinberg, 2000) The most studied angiogenic stimulator is VEGF or vascular permeability factor (VPF). VEGF levels have been known to be elevated in EOC patients, where it contributes to the accumulation of ascites. A number of groups have since evaluated the prognostic potential of serum VEGF levels in women with EOC. However, its therapeutic effect is largely limited to newly forming tumour vessels and is dependent on complicated interactions with other factors, such as EGF, platelet derived growth factor (PDGF), interleukin 8 (IL-8), EPH receptor A2 (EPHA2), and the matrix metalloproteinases. Meanwhile, there is a lack of effective biomarkers for monitoring response to new antivascular agents (Hurwitz *et al.*, 2004; Jain *et al.*, 2006). The upregulation of VEGF and intracellular signalling in angiogenesis has been correlated with the activation of the JAK-STAT pathway components, PI3K/AKT pathway and MAPK (Zhang *et al.*, 2003; Xu *et al.*, 2004; Chen *et al.*, 2004; Bermudez *et al.*, 2007).

1.7.2.2 Cell aggregation pathway biomarkers

1.7.2.2.1 Claudin family members

In tumour cells, the loss of cell-cell adhesion is essential for metastatic potential and cellular transformation. The claudins are integral components of tight junctions, such as apical cell-cell adhesions, that regulate epithelial paracellular permeability and are critical for epithelial cell polarity (Singh *et al.*, 2010). Certain members of the claudin gene family, such as claudin-3, 4 and 7, are abnormally regulated in several human cancers, including EOC and show increased invasiveness *in vitro*, which is mediated through MMP-2 overexpression (Michl *et al.*, 2003). Claudin-3 is upregulated in 90% of ovarian tumours, including all four major subtypes (i.e. clear cell, mucinous, serous and endometrioid) and is also associated with shorter survival (Gao *et al.*, 2011). Although claudin proteins are known to activate MMPs, they were also shown to regulate migration and cell-cell adhesion, however, the exact roles

of claudin in invasion are controversial (Dahiya *et al.*, 2011). Claudin-3 expression also promotes migration, invasion, and survival of EOC cells. in addition, one study suggested that Claudin-7 upregulation was associated with a net increase in invasion as a result of MMP activation but also a decrease in cellular migration. The reduced expression of Claudin-3 and -4 increased both cell migration and invasion in EOC in vitro assays (English and Santin, 2013; Dahiya *et al.*, 2011).

1.7.2.3 Cell migration and invasion pathway biomarkers

1.7.2.3.1 Focal adhesion kinase (FAK)

Cell motility and migration is a major component of oncogenesis and requires a series of repeated adhesion attachment and detachment events from ECM. These events are mainly regulated by integrins. FAK, an integrin-linked protein tyrosine kinase component of the integrin-signalling pathways, is an important mediator of signalling pathways that occur between cells and their ECM, thereby facilitating migration and invasion (McLean *et al.*, 2005). The calcium-dependent FAK activation is facilitated by an intramolecular autoinhibitory interaction, thereby, disrupting the interactions between its central kinase and amino terminal domains. The activated FAK generates a FAK-Src family kinases complex, therefore, initiating various downstream signalling pathways regulating diverse cellular functions via protein phosphorylation (Zhao and Guan, 2011).

1.7.2.4 Apoptotic and signalling pathway biomarkers

1.7.2.4.1 *p53* mutation

p53 mutation is the most frequent genetic alteration in EOC occurring in 60% - 80% of all sporadic EOCs and correlates highly with high-grade tumours. Subtype-specific mutations in *p53* have been found in 60%-100% of HGS tumours but only in 16% of mucinous tumours, which suggests a prominent role for *p53* mutation in carcinogenesis of HGS but not mucinous EOC. For example, *p53* promotes *p21* expression, thereby, activating *p53*-dependent cell cycle arrest at the G1 phase and senescence. *p21*-induces expression of Puma, Bax or miR-34, which are also critical for the *p53*-dependent apoptosis (Zhang *et al.*, 2016). A recent study showed that as well as inducing apoptosis, *p53* also induces ferroptosis, a special type of cell death

caused by ROS, in lung cancer by activating the expression of solute carrier family 7 member 11 (*SLC7A11*), a key component of the cystine/glutamate antiporter (Jiang *et al.*, 2015).

1.7.2.4.2 BRCA1/2 carriers

The *BRCA1* and *BRCA2* tumour suppressor genes help regulate transcription, chromosomal stability, promote cellular proliferation, DNA repair via Homologous recombination (HR) and control cell cycle checkpoints through *p53*-dependent and independent mechanisms. Females carrying *BRCA1* or *BRCA2* germline mutations have higher lifetime risk of developing EOC by 16%–60% and 16%-27%, respectively (Scully and Livingston, 2000; Piura *et al.*, 2001). Interestingly, recent studies indicate that women with a BRCA1 or 2-related EOC have better survival outcome than non-carriers, particularly if they receive platinum-based therapy (Chetrit *et al.*, 2008; Ben David *et al.*, 2002). BRCA1 regulates DNA damage response during synthesis (S)/G1 phase by mediating HR to maintain replication fidelity and may also play a role in other DNA repair processes, such as non-homologous end joining (NHEJ, Rosen, 2013). BRCA2 is primarily involved in HR, by mediating the phosphorylation of BRCA1 by ataxia telangiectasia and RAD3 related (ATR) or ataxia telangiectasia mutated (ATM) at G1/S-checkpoint, facilitating subsequent phosphorylation of p53, thereby, initiating of the cyclin dependent kinase (CDK) inhibitor P21 and ionizing radiation-induced G1/S checkpoint activation and finally inducing apoptosis (Siliciano *et al.*, 1997; Roy *et al.*, 2012). BRCA1 also recruits RAD51 to DNA damage sites through its interactions with partner and localizer of BRCA2 (*PALB2*) and *BRCA2* (Moynahan *et al.*, 2001). Therefore, deleterious mutations in *BRCA1/2* was shown to increase the risk of breast and EOC in women (Roy *et al.*, 2012).

1.7.2.4.3 EGFR (HER) family members

The human EGF receptor (HER) family mediates crucial cellular processes, including growth, proliferation, and progression. This receptor family consists of four transmembrane receptors: *HER1,* 2, 3, and 4. Each receptor has an extracellular binding domain, an intracellular domain and a transmembrane domain. A range between 60%-98% of EOCs express high levels of HER. In contrast to HER1, 2 and 4 proteins, HER3 do not contain tyrosine kinase activities, but can dimerise with other HER family members leading to the activation of HER pathways (Vaidya *et al.*, 2005). HER family members activate downstream signalling pathways, such as phosphatidylinositol-3 kinase (*PI3K*)/AKT and external signal-regulated kinase (ERK) pathways (Tanaka *et al.*, 2011). The roles of *HER1*/2 have been established in breast cancer and the

combination of cytotoxic chemotherapy and EGFR/HER inhibitors, such as HSP90 blockade and tyrosine kinase inhibitors, yield better clinical response (Amler, 2010). Tyrosine kinase inhibitors (TKI) are biologically targeted antibodies directed towards *ErbB1/EGFR/HER1* (erlotinib, gefitinib and cetuximab) and *ERBB2/HER2* neu in rodents (trastuzumab), and more recently toward *ERBB4/HER4* and *ERBB3/HER3*, are currently being investigated as potential therapy for patients with EGFR/ERBB/HER proto-oncogene-driven malignancies (Baron *et al.*, 2009). Ongoing trials of these agents alone or in combination with traditional chemotherapeutic agents are currently under investigation (Poliaková *et al.*, 2018; Canonici *et al.*, 2018)

1.7.2.5 Biomarkers with immune signatures

1.7.2.5.1 IL-6, IL-7, IL-8

There has been a recent emerging interest in the role of cytokines in the biology of EOC. Interleukins are potent cell chemo-attractants and are closely related to vascular formation and stimulates defective angiogenesis in EOC (Gopinathan *et al.*, 2015). Current investigations have focused on IL-6, -7 and -8 as a prognostic factor in EOC. The elevated levels of IL-6, -7 and -8 in serum correlate with overall poor prognosis. Increased IL-6 and IL-8 expression correlates with poor initial response to paclitaxel chemotherapy and elevated expression of IL-6 also correlates with poor final outcome. The resultant activation of NF-κB by several cytokines (i.e. IL-1 and TNFα) and EGF, upregulates the expression of growth regulatory cytokines; anti-apoptotic genes (CFLAR), angiogenic factors (IL-8), IL-6 or growth regulated-α (GRO1) and antioxidant proteins (e.g. superoxide dismutase or ferritin heavy chain, Bast *et al.*, 2009). Subsequent upregulation of IL-6 activates JAK2, facilitates the phosphorylation and nuclear translocation of STAT3, leading to the inhibition of apoptosis and increased angiogenesis and proliferation (Rosen *et al.*, 2006; Bast *et al.*, 2009). In addition to new STAT3 inhibitors, such as decoy oligodeoxynucleotides, antibodies against IL-6 and inhibitors of JAK2 are currently being developed to target most EOCs (Soldevilla and Pastor, 2018; Burke *et al.*, 2001; Duan *et al.*, 2007; Bast *et al.*, 2009).

1.7.2.5.2 B7-H4

It has been reported that the B7 family, including B7-H1 and B7-H4 are co-stimulatory molecules responsible for inhibiting T-cell activation. High B7-H4 levels in serum correlate with

poor prognosis (Fan *et al.*, 2014). It has also been reported that B7-H4 promote malignant transformation by inhibiting cell cycle progression, cytokine production, and T-cell proliferation (Simon et al., 2006). While, the functional role of B7-H4 in tumour biology and immune evasion was previously established, stand-alone or combinatorial anti-B7-H4 targeted therapies to overcome B7-H4-mediated hypo-function of T cells in the EOC microenvironment are currently under investigation (Smith *et al.*, 2014).

1.7.2.6 Tissue-based microRNAs (miRs) biomarkers

Recently, miRs have been emerging as potential epigenetic markers of EOC. miRs are non-protein-coding single stranded RNA molecules that function as negative regulators for gene expression (Rastogi *et al.*, 2016; Kinose *et al.*, 2014). miRs, as regulatory molecules, are known to act as tumour suppressors or oncogenes. A variety of miR candidates are aberrantly or differentially expressed in EOC. Changes in tumour miR expression prolife are mediated by various mechanisms, including epigenetic regulation, genetic alterations, or altered expression of transcription factors (Soto-Reyes *et al.*, 2012; Kobayashi *et al.*, 2012). Previous analysis of miR expression profiles by Iorio *et al.*, (2007) has indicated that miRs expression was deregulated in EOC tissues/cell lines compared to normal tissues. miR-200a, miR-141, miR-200c, miR-200b and were most significantly upregulated in cancer samples, whereas, miR-140, miR-199a, miR-125b1, and miR-145 were downregulated in cancer samples (Rastogi *et al.*, 2016). In platinum-resistant EOC cell lines, the overexpression of miR-136 was shown to promote cisplatin-induced apoptosis (Kuroda *et al.*, 2013; Testa *et al.*, 2018). Other studies also showed that miR-136 overexpression contributes to lower activity in cancer stem cells and promotes paclitaxel efficacy in chemoresistant EOC cells by regulating *NOTCH3* (Bhattacharya *et al.*, 2009; Testa *et al.*, 2018).

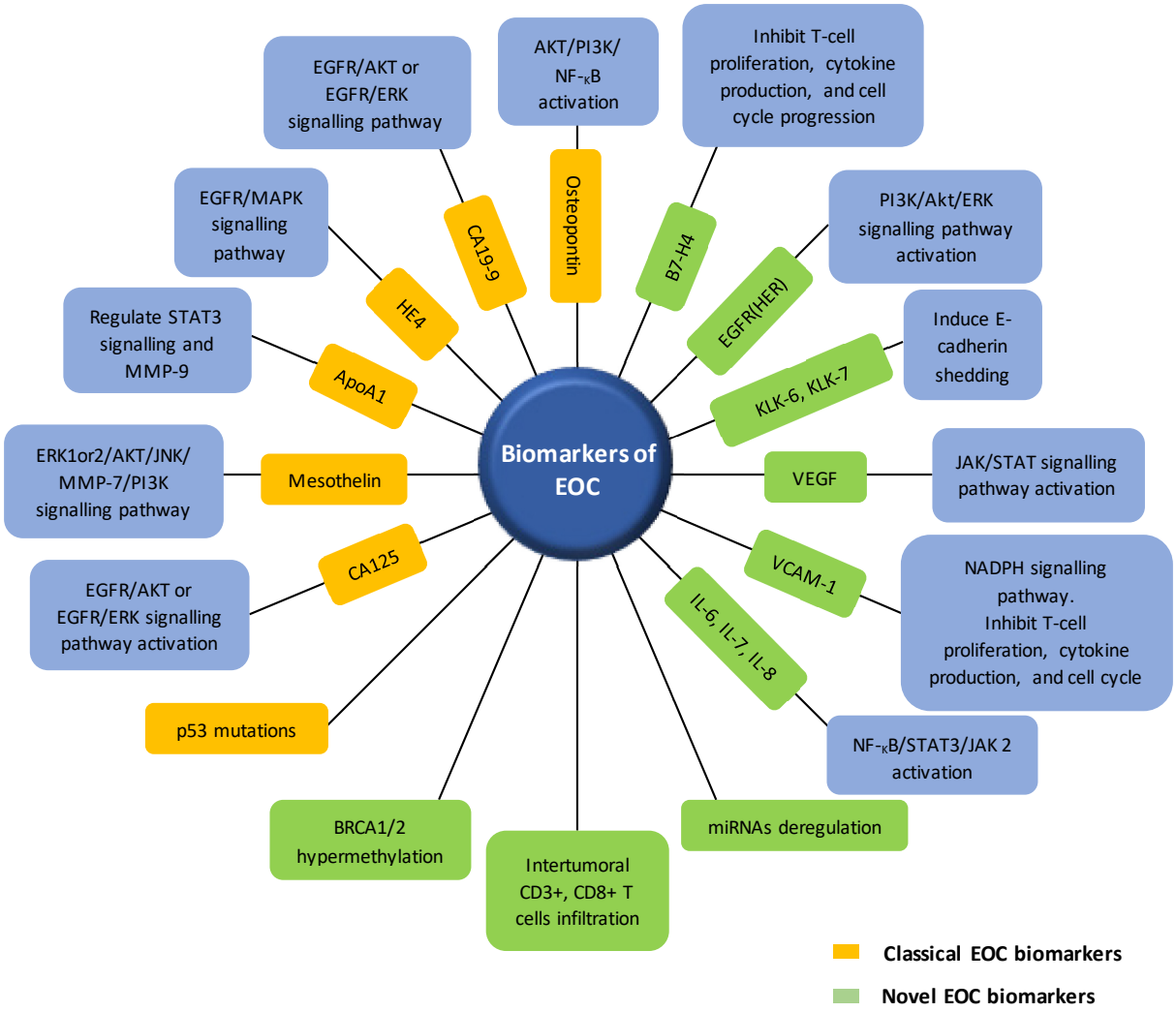

Figure 1.4 Summary of EOC biomarkers. The molecular and protein EOC biomarkers: current options and future promise are summarised in the square boxes. Currently used biomarkers for prognosis and diagnosis of EOC are shown in orange. Novel and newly developed biomarkers for prognosis and diagnosis of EOC are shown in green. Biomarkers with high expression levels were associated with improved patient overall survival. Abbreviations: NF-κB, nuclear factor κB; ERK, extracellular signal-related kinase kinase; PI3K, phosphatidylinositol 3- kinase; miR, microRNA; JAK, Janus kinase; STAT, acetyl- signal transducer and activator of transcription; NADPH, nicotinamide adenine dinucleotide phosphate; p53, tumour protein 53; BRCA, breast cancer gene; AKT, AKT Serine/Threonine Kinase; MAP, mitogen-activated protein; EGFR, Epidermal growth factor receptor.

1.8 The role of PADI-mediated citrullination in disease pathogenesis

Post translational modifications of proteins are crucial as they play an essential role in various cellular processes (Darling and Uversky, 2018; Bürkle, 2001). PTMs modulate various chemical and physical properties, including folding, stability, conformation and activity of proteins by covalently binding small chemical molecules to specific amino acid residues, thus allowing proteins to respond to various environmental stimuli or developmental signals (Audagnotto and Dal Peraro, 2017). These modification also alter target protein interactions with ligands or other proteins, some of which are involved in diseases, such as cancer and neurological disorders (Darling and Uversky, 2018; Bürkle, 2001). One such PTM, citrullination, corresponds to the post-translational deimination or demethylimination of protein-bound arginine to citrulline residues mediated by a family of Ca^{2+}-dependent peptidyl arginine deiminase (PADI) enzymes (Chavanas *et al.*, 2006). Recently, citrullination has become an increasingly investigated type of PTM, as it significantly effects physiological functions of the targeted proteins and may exhibit important roles in cell differentiation, cell apoptosis embryonic development, nerve growth and gene expression regulation (Chavanas *et al.*, 2006; György *et al.*, 2006; Bicker and Thompson, 2013). This modification alters the charge of residues from positive to neutral, resulting in substrate protein loss of conformation, increased aggregation ability, and in some cases, causes denaturation. Beta-sheets and intrinsically disordered proteins are structures most prone to citrullination, and their identified deiminated targets include mitochondrial, cytoplasmic and nuclear proteins (György *et al.*, 2006). Moreover, citrullination is involved in the innate immune response by regulating chemokine activity and development of neutrophil extracellular traps (Mortier *et al.*, 2011; Pingxin Li *et al.*, 2010). Also, citrullinated proteins are recognised as non-self-proteins and can subsequently promote various autoimmune conditions, including rheumatoid arthritis (RA) and multiple sclerosis (MS, Darrah *et al.*, 2012; Klareskog *et al.*, 2014). Increased levels of PADIs and hypercitrullination have been associated with various chronic inflammatory diseases, such as neurodegenerative conditions (e.g. Alzheimer's disease, Anzilotti *et al.*, 2010; Ceuleneer *et al.*, 2012; Chang, 2005; Chang and Han, 2006; Jones *et al.*, 2009). In addition, Jiang *et al.*, (2013) reported that citrullinated proteins were detected in breast, liver, ovarian, lung, kidney, cervical, gastric and pancreatic tumour cell lines.

1.8.1 The PADI family of enzymes structure and Ca^{2+} dependency

Recently, vertebrate PADIs were categorised into five isotypes (PADI1, 2, 3, 4, and 6), based on their amino acid sequences, molecular weights, tissue localisation and substrate specificities. Three PADI isotypes were found in birds (*Gallus gallus*), whereas only one seems to exist in fish species (Takifugu rubripes, Danio rerio*, Oncorhynchus mykiss and* T*etraodon nigroviris*) and amphibians (*Xenopus laevis*, Vossenaar *et al.*, 2003; Ying *et al.*, 2009b; Rebl *et al.*, 2010). In mammals, all five isotypes of PADIs are present in rat (*Rattus norvegicus*), mice (*Mus musculus*) and humans (*Homo sapiens*, Terakawa *et al.*, 1991; Erik R Vossenaar *et al.*, 2003). Mammalian PADI genes are thought to have arisen by gene duplication of an ancestral homologue, *PADI2*, and are all encoded as a cluster of genes on chromosome 1p36.1 (Chavanas *et al.*, 2004). The five mammalian PADI isozymes display highly conserved amino acid sequence with 70-95% homology between human paralogs (Méchin *et al.*, 2007). Although high resolution structures of PADIs 1, 3 and 6 have yet to be reported, significant work has been done to elucidate the structure of PADI4 both with and without Ca^{2+} bound, as well as with PADI4 substrates (i.e. benzoyl-l-arginine amide (BAA), histone 3 (H3), and histone 4 (H4)), and the PADI inhibitor Cl-amidine (Jones *et al.*, 2012; Luo *et al.*, 2006; Causey *et al.*, 2011). More recently, the PADI2 crystal structure has been determined by Slade *et al.*, providing more structural and functional information about this isozyme. This work has indicated that PADI2 contains two distinct domains (i.e. N- domain (1–300 amino acids) and C-terminal domain (301–663 amino acids)) and contains a total of six Ca^{2+} binding sites. Two of these Ca^{2+} binding sites are located in the C-terminal domain and the remaining four binding sites are in the N-terminal domain, which is further divided into two immunoglobulin-like subdomains, one of which (i.e. PAD_M) contains the PADI2-Ca^{2+} activating switch that mediates highly ordered α-helices in the presence of Ca^{2+} (Arita *et al.*, 2004; Slade *et al.*, 2015). It is hypothesised that this Ca^{2+}-regulated conformational change regulates PADI2 protein-protein interactions (Slade *et al.*, 2015). In the C-terminal domain, Ca^{2+} binding induces large conformational shifts, generating the active cleft site allowing substrate binding, thereby activating the enzyme (Arita *et al.*, 2004; Liu *et al.*, 2013; Slade *et al.*, 2015).

1.8.2 PADIs substrate target

PADI family members have broad substrate specificity, therefore, not all arginine residues in a protein are equally likely to be citrullinated by PADIs. PADI specificity is dependent on the structure, location, and abundance of the arginine residues in a protein (Knuckley *et al.*, 2010; Tarcsa *et al.*, 1996). PADI-mediated citrullination can also cause various changes in protein-protein interactions or induce denaturation. Mainly, filaggrin and H3 and H4 are known PADI protein substrates are the most extensively studied. The citrullination sites in these proteins have been identified; thus, the synthetic peptides derived from these proteins were used to determine the sequence specificity of PADI protein substrates (Liu *et al.*, 2017). The main targets of every PADI isozyme are the following: *PADI1* targets keratin and filaggrin (Senshu *et al.*, 1995); *PADI2* targets myelin basic protein (MBP), vimentin, actin, inhibitor of growth family member 4 (ING4), p65, C-X-C motif chemokine ligand 8 (CXCL8), β-catenin, glycogen synthase kinase 3 beta (GSK3β), nucleophosmin 1 (NPM1) and H3 (Lamensa and Moscarello, 1993; Hsu *et al.*, 2014; X. Zhang *et al.*, 2012); *PADI3* targets filaggrin, trichohyalin, apoptosis-inducing factor (AIF), and vimentin (Senshu *et al.*, 1995; U *et al.*, 2014); *PADI4* targets a range of nuclear proteins, such as inhibitor of growth 4 (*ING4), p300, p21, p53*, H3 and H4 and apoptosis (nucleophosmin, nuclear lamin C, Arita *et al.*, 2004; Kan *et al.*, 2012; Guo and Fast, 2011; Lee *et al.*, 2005; Li *et al.*, 2008); *PADI6*; regulates the function of microtubules during early embryo development (Maddirevula *et al.*, 2017; Kan *et al.*, 2011, **Table 1.3**).

Table 1.3 PADI family isozymes-specific target substrates.

Isozyme	Substrates
PADI1	Filaggrin and keratin
PADI2	Myelin basic protein (MBP), vimentin, actin, ING4, P65, CXCL8, β-catenin, GSK3 β, NMP1 and histones (H3 and H4)
PADI3	Filaggrin, trichohyalin, vimentin and apoptosis-inducing factor
PADI4	Inhibitor of growth 4 ING4, p21, p300, nuclear lamin C, nucleophosmin and histones (H3 and H4)
PADI6	Microtubules

1.8.3 PADIs function

Under normal physiological conditions, PADIs exist in an inactive form due to low physiological i[Ca^{2+}] levels (10^{-8} to 10^{-6} M, György *et al.*, 2006; Takahara *et al.*, 2014). PADIs become activated by elevated Ca^{2+} levels (above the normal physiological concentration) that occur during certain events, such as terminal epidermal differentiation and apoptosis (Takahara *et al.*, 2014). Interestingly, PADI-mediated citrullination function in gene regulation and is implicated several cellular processes, such as apoptosis, NETosis and autophagy, at physiological concentrations of Ca^{2+} (György *et al.*, 2006). Ca^{2+} acts as a signalling molecule to coordinate multiple cellular processes, including apoptosis and autophagy; therefore, it is needed at high concentrations within apoptotic cells (Valesini *et al.*, 2015).

1.8.3.1 The role of PADI in structural support

PADIs are also involved in organising structural proteins found in hair follicle and epithelial cells undergoing terminal epidermal differentiation (György *et al.*, 2006; Senshu *et al.*, 1996). This PADI-mediated differentiation is regulated by Ca^{2+}. Higher Ca^{2+} concentrations were shown to activate the PADIs. Within the epidermis, PADIs can citrullinate structural proteins, such as keratin, vimentin, and filaggrin. The epidermal barrier filaggrin protein, known to have a key role in atopic dermatitis, is a 4061 amino acids long, with a relatively high arginine content (10.8%); which provides higher potential target sites for PADIs-mediated citrullination (Pruitt *et al.*, 2014). Upon Ca^{2+}-mediated terminal differentiation of epidermal cells, the PADI-mediated citrullination of these proteins is subsequently activated, causing incomplete protein unfolding, and consequent protein degradation by proteases (Pearton, Dale and Presland, 2002; György *et al.*, 2006). In the epidermis, PADI1, 2 and 3-mediated citrullination of cytokeratin keratin factor 1 and filaggrin, modulates epidermis cornification (Yamamoto *et al.*, 2002). Citrullinated filaggrin also helps maintain healthy skin through its role in the formation of natural moisturising factor (NMF) in the superficial keratinised epidermal cell layers (Senshu *et al.*, 1996; Cau *et al.*, 2017). The cytokeratin citrullination and subsequent loss of charge leads to the disassembly of the cytokeratin-filaggrin complex and proteolytic degradation of these targets (Mohanan *et al.*, 2012). PADI3 expression is only detected in the hair follicle and epithelium. In addition, in the epithelium, PADI3-mediated citrullination of

filaggrin and keratin 1 leads to terminal differentiation of keratinocytes, subsequent alteration of epidermal homeostasis and loss of barrier function (Nachat *et al.*, 2005).

1.8.3.2 PADI regulation of gene expression under normal physiological conditions

In addition to their role in disease, PADI isozymes can regulate gene expression under normal physiological conditions (Wang and Wang, 2013). Most research on PADIs' involvement in gene regulation has been performed on PADI4 and more recently on PADI2 (Mohanan *et al.*, 2012; Guo and Fast, 2011; Cherrington *et al.*, 2012; Cantarino *et al.*, 2016). One of the best studied systems of PADIs' function is their role in histone citrullination and p53 pathway regulation, suggesting the importance of PADI-induced citrullination in apoptosis. PADI4 citrullinates ING4, another tumour suppressor protein known to bind p53, once modified, this protein does not bind to p53, subsequently repressing p53 acetylation, thereby, inhibiting downstream p21 expression (Guo and Fast, 2011). Another mechanism involves the citrullination of methylated arginine on histones. In this mechanism, PADI4 was shown to citrullinate histone 4 arginine 3 (H4R3) and H3R2, R8, and R17 and the modification is associated with gene repression (Kan *et al.*, 2012). For example, PADI4 is involved with the regulatory domain of p53 that targets p21 at the p53-binding sites on the promoter region. PADI4 interaction with these proteins causes citrullination of histones on the p21 promoter region, preventing p21-to-p53 binding and subsequently repressing p21 transcription (Li *et al.*, 2008). This impaired binding occurs due to changes in protein charge that can affect the hydrogen bond formation during protein-protein interactions. Also, citrullination of histones on the promoter region that includes p53-binding sites, may induce conformational changes that sterically hinder p53 binding. Correspondingly, Li *et al.*, (2010) reported similar findings, but they further found that both PADI4 and histone deacetylase 2 (HDAC2) regulate gene expression, by targeting p53 and simultaneously associating with p21 promoter in response to DNA damage (Yuzhalin, 2019). Consistent with these reports, PADI4 overexpression in hematopoietic cancer cell lines was found to be associated with increased p21 and p53 expression leading to apoptosis (Liu *et al.*, 2006; Yuzhalin, 2019). However, the mechanisms regulating PADI4 activation at physiological Ca^{2+} levels and its recruitment to specific promoter sites remain largely unknown (Slack *et al.*, 2011; Denman, 2005). Wang and Wang, (2013) proposed a mechanism by which PADI4 carries out its function by binding to the promoter region of p53 of target genes, such as p21 (CIP1/WAF1), DNA damage inducible

alpha (GADD45) and PUMA. PADI4 represses these target genes expression by histone citrullination during periods where the damage response pathways are not needed. After DNA damage, PADI4 dissociates from the promoter regions, thereby, activating target genes once again. There is also evidence that PADI4 can act as a transcriptional coactivator. In this process, PADI4 mediates the citrullination of methylated arginine2142 in glutamate receptor interacting protein 1 (GRIP1) binding domain of the transcriptional coactivator p300, thereby, enhancing p300-GRIP1 complex modulation of tissue-specific gene expression (Lee *et al.*, 2005). The mechanisms regulating PADI activation is not fully established, but György *et al.*, (2006) hypothesised that at low levels of Ca^{2+}, PADIs might still be active with strict substrate specificity and this could explain PADI involvement in gene regulation. However, this is unlikely to be accurate because different substrates have similar Ca^{2+} dependencies (Slack *et al.*, 2011).

1.8.3.3 The role of PADI-mediated citrullination in cancer pathogenesis

1.8.3.3.1 The role of PADIs in apoptosis and proliferation

PADI isozymes exert a complex regulatory role in numerous cellular activities, including cell death. In particular, the overload or influx of extracellular e[Ca^{2+}] mediates various signalling molecules to coordinate cell apoptosis. Therefore, Ca^{2+} is found at high concentrations within apoptotic cells (Mattson and Chan, 2003). PADIs are activated by these elevated Ca^{2+} concentrations in pro-apoptotic cells. Once activated, PADIs may target proteins that are arginine-rich or have arginine-rich regions within their amino acid sequence. For example, vimentin, is found to be citrullinated during ionomycin-induced macrophage apoptosis (Hsu *et al.*, 2014). Citrullinated vimentin peptides stimulate strong anti-tumour immunity (Durrant *et al.*, 2016). The vimentin protein is 466 amino acids long with 9.2% arginine residues. Inagaki *et al.*, (1989) previously reported that PADIs citrullinate the non-α-helical head domain of the vimentin protein. In this non-α-helical head domain (2–95 amino acids), there are 12 arginines that are citrullinated by PADIs (Pruitt *et al.*, 2014). Citrullination of vimentin impairs the polymerisation of vimentin filaments resulting in filament disassembly and subsequent structural breakdown and further completion of apoptosis (Inagaki *et al.*, 1989; Katsumoto *et al.*, 1990). The increased expression of vimentin has been detected in several epithelial cancers, including breast cancer, gastrointestinal tumours, prostate cancer and other types of cancers (Hsu *et al.*, 2014). Citrullinated vimentin is also expressed on the cell surface of PADI2-overexpressed and Jurkat-activated cancer cells during apoptosis (Hsu *et al.*, 2014). This

presentation induces cytotoxic $CD4^+$ T-cell responses, thus providing evidence for the use of citrullinated peptides as vaccination targets in cancer therapy (Brentville *et al.*, 2016). Like citrullinated vimentin, other citrullinated proteins, such as the ubiquitous glycolytic enzyme α-enolase (ENO1), can be presented on the cell surface as citrullinated peptides or citrullinated epitopes, thus, stimulating potent antitumor responses (Cook *et al.*, 2018). Overall, PADI2 activation (due to amplified Ca^{2+} levels during the early stages of apoptosis) can facilitate apoptotic cell death via citrullinating several nuclear and cytoskeletal proteins that can cause structural changes resulting in the disintegration of secondary and tertiary protein structures or induce citrullinated epitopes presentation on cell surfaces, thereby, activating anti-inflammatory response (**Figure1.5,** Inagaki *et al.*, 1989; Vossenaar *et al.*, 2003; György *et al.*, 2006).

Likewise, histones and nucleophosmin are known targets of PADI2 and PADI4, and their citrullination can cause the nucleosome and nuclear lamina to collapse, triggering apoptosis (Vossenaar *et al.*, 2003; György *et al.*, 2006). The oligomerisation of nucleophosmin is necessary for nucleolar localisation and inhibits the mitochondrial apoptosis pathway in a p53-independent manner (Durbin *et al.*, 2010; Dhar and Clair, 2009). Chang and Fang, (2010) correspondingly reported that *PADI4* overexpression upregulates *p53* and stimulates mitochondrial-associated apoptosis. A recent study in breast cancer, reported that PADI2-mediated citrullination of a key residue (i.e. arginine 1810 (cit1810)) at RNA polymerase II (RNAP2) recruits protein complexes that affect transcription elongation and activate the transcription of thousands of genes (Sharma *et al.*, 2019). The inhibition of (RNAP2 citrullination site) equally reduced cell proliferation via inducing cell-cycle arrest at the G1 phase (Yuzhalin, 2019). Interestingly, in breast cancer cells, other members of the PADI family (PADI3 and PADI4) were unable to catalyse the citrullination of RNAP2 and induce the above-mentioned effects (**Figure1.5,** Yuzhalin *et al.*, 2019; Sharma *et al.*, 2019).

1.8.3.3.2 The role of PADIs in cell migration

Cell migration is involved in various normal and oncogenic biological processes, including immune response and embryonic development, and its dysregulation plays a key role in metastasis and invasion (Cyster, 2005; Luster *et al.*, 2005; Aman and Piotrowski, 2010; Friedl and Wolf, 2003; Yamaguchi *et al.*, 2005). PADI4 suppresses breast cancer cell migration via citrullinating nuclear GSK3β and subsequent activation of transforming growth factor beta

(TGFβ) signalling, thereby, inducing epithelial-to-mesenchymal transition (EMT, Stadler *et al.*, 2013). Another mechanism involves inducing p53 transactivation during DNA damage response. In this mechanism, PADI4 binds to the intronic p53-binding site forming a p53/PADI4 network, thereby, inducing citrullination in histone chaperone protein, nucleophosmin (NPM1). In the nucleoli, NPM1 was shown to be associated with various process, including ribosome subunit assembly, pre-rRNA processing, and rRNA transcription, which are essential for cellular homeostasis (Tanikawa *et al.*, 2009). The PADI4-mediated NPM1 citrullination, resulted in NPM1 translocation from the nucleoli to the nucleoplasm, subsequently inhibiting ribosomal biogenesis leading to inhibition of tumour cell growth (Tanikawa *et al.*, 2009; Matsuda *et al.*, 2002; Zhu *et al.*, 2013). Aside from PADI4, PADI2 was also found in mammary tissues and is deregulated in breast cancer. Unlike PADI4, PADI2 was shown to regulate mammary carcinoma cell migration possibly through epidermal growth factor (EGF) signalling pathway (**Figure 1.5,** Horibata *et al.*, 2017).

1.8.3.3.3 The role of PADIs in autophagy

Autophagy plays a crucial role in physiology and pathophysiology, such as ageing, cancer, infectious diseases and autoimmune diseases (Glick *et al.*, 2010; Nicholas and Bhattacharya, 2014). Autophagy is upregulated in response to intra- or extracellular stress and signals, including growth factor deprivation, starvation, deregulated Ca^{2+} homeostasis, and endoplasmic reticulum stress. It was demonstrated that autophagy was involved in the generation of citrullinated peptides by antigen presenting cells (APCs), which was associated with increased PADI activity detected in purified autophagosomes (Valesini *et al.*, 2015). Processing of proteins in autophagy vesicles of APC generates citrullinated peptides which are presented on cells, such as B cells, and recognised by the MHC-II molecules that stimulate $CD4^+$ T-cell responses (Durrant *et al.*, 2016; Mohamed *et al.*, 2018). The authors suggested that citrullination may represent a "biochemical marker of autophagy" (**Figure 1.5,** Ireland and Unanue, 2012).

1.8.4 The role of PADI2-mediated citrullination in cancer pathogenesis

In recent years, studies have found that citrullination is correlated with tumour progression in majority of human cancers, suggesting that PADIs are potential therapeutic targets for cancer.

While the apparent function of PADIs activity in most diseases are associated with inflammation, the role of PADIs in cancer progression remains unclear. As explained previously in this chapter, *PADI2* is the ancestral homologue of all PADI family isozymes and is widely expressed in mammalian tissues. Recently, PADI enzymes, particularly *PADI2*, have been identified as potential biomarkers and therapeutic targets in many diseases, including cancer (McElwee *et al.*, 2012; N. Cantarino *et al.*, 2016). Wang *et al.*, (2016) reported that PADI2 is associated with increased breast cancer risk, and its expression contributes to tumorigenesis via the deregulation of acyl-CoA synthetase long chain family member 4 (*ACSL4*), *BINC3* and carbonic anhydrase 9 (*CA9*) signalling pathways (Wang *et al.*, 2016). Furthermore, Bhattacharya *et al.*, (2006) detected high *PADI2* expression and citrullination in glaucoma, and McElwee *et al.*, (2014) also reported that overexpressing *PADI2* induces spontaneous skin neoplasia in transgenic mice. McElwee *et al.*, (2012) found that EGF plays an important role in the proliferation of normal mammary epithelium and appears to regulate *PADI2* expression in mammary cancer cells. They also found that *PADI2* mRNA expression significantly correlates with *HER2*, a known biomarker and oncogene in breast cancer. Following oestradiol exposure, it was suggested that ER directly or indirectly induces PADI2-mediated citrullination of histone H3 arginine 26 (H3R26), subsequently inducing Ubiquitin Conjugating Enzyme (E2)-mediated activation of endoplasmic reticulum-target genes. H3R26 citrullination abbreviates core nucleosome particles and shifts its DNA size from 149 to 125 bp. Thus, inducing altered conformation of the nucleosome allows for a more stable interaction between the endoplasmic reticulum and its nucleosomal binding sites (Guertin *et al.*, 2014). Cherrington *et al.*, (2010) correspondingly reported that EGF upregulates *PADI2* transcription and translation in CMT25 canine mammary tumour cells. It was previously shown that PADI2 modulates epithelial-mesenchymal plasticity in mammary carcinoma by deregulating the expression of the cytoskeletal regulatory proteins, including ras homolog family member A (RhoA), rac family small GTPase 1 (Rac1), and cell division cycle 42 (Cdc42), and downregulating intracellular junctions, such as E-cadherin (Horibata *et al.*, 2017). Collectively, these studies suggest that PADI2 potentially function as an ER cofactor, thus regulating the expression of the canonical ER target gene, such as trefoil factor 1 (TFF1, **Figure 1.5**, Zhang *et al.*, 2012).

Whilst high PADI2 expression levels and histone citrullination are known to associate with metastatic features, such as cell proliferation, recently Guertin *et al.*, (2014) identified a strong correlation between H3R26 citrullination and high PADI2 expression with increased survival in oestrogen receptor (EGFR)/HER2+ tumour patients. The authors also suggested that histone

citrullination may be valuable for sub classification of HER+ tumours into clinically relevant subsets. Tanday, (2016) recently reported that inhibiting PADI2 expression may prevent the progression of myeloma. In addition, Cantarino *et al.*, (2016), demonstrated that the downregulation of PADI2 is an early event in colorectal carcinogenesis. These observations further suggest the potential role of PADI2-mediated citrullination as a tumour suppressor or promoter mark in cancer. Therefore, further studies are required to elucidate the comprehensive role of PADI2 during tumour development and to emphasise whether it functions as a tumour suppressors or oncogene. Therefore, the effect of PADI2 on the tumourigenic process and regulatory mechanisms should be comparatively studied among different tumours. The detailed regulatory mechanisms of PADI2 and its function during the tumourigenic process in OC are not fully explored. Preliminary unpublished tissue microarray data (TMA) indicated that high PADI2 expression in tumours is protective and may represent an independent prognostic marker. To gain more insight into the tumourigenic role of PADI2, the present study analysed the expression levels of PADI2 in EOC cells and the effect of PADI2-overexpression on EOC tumorigenesis.

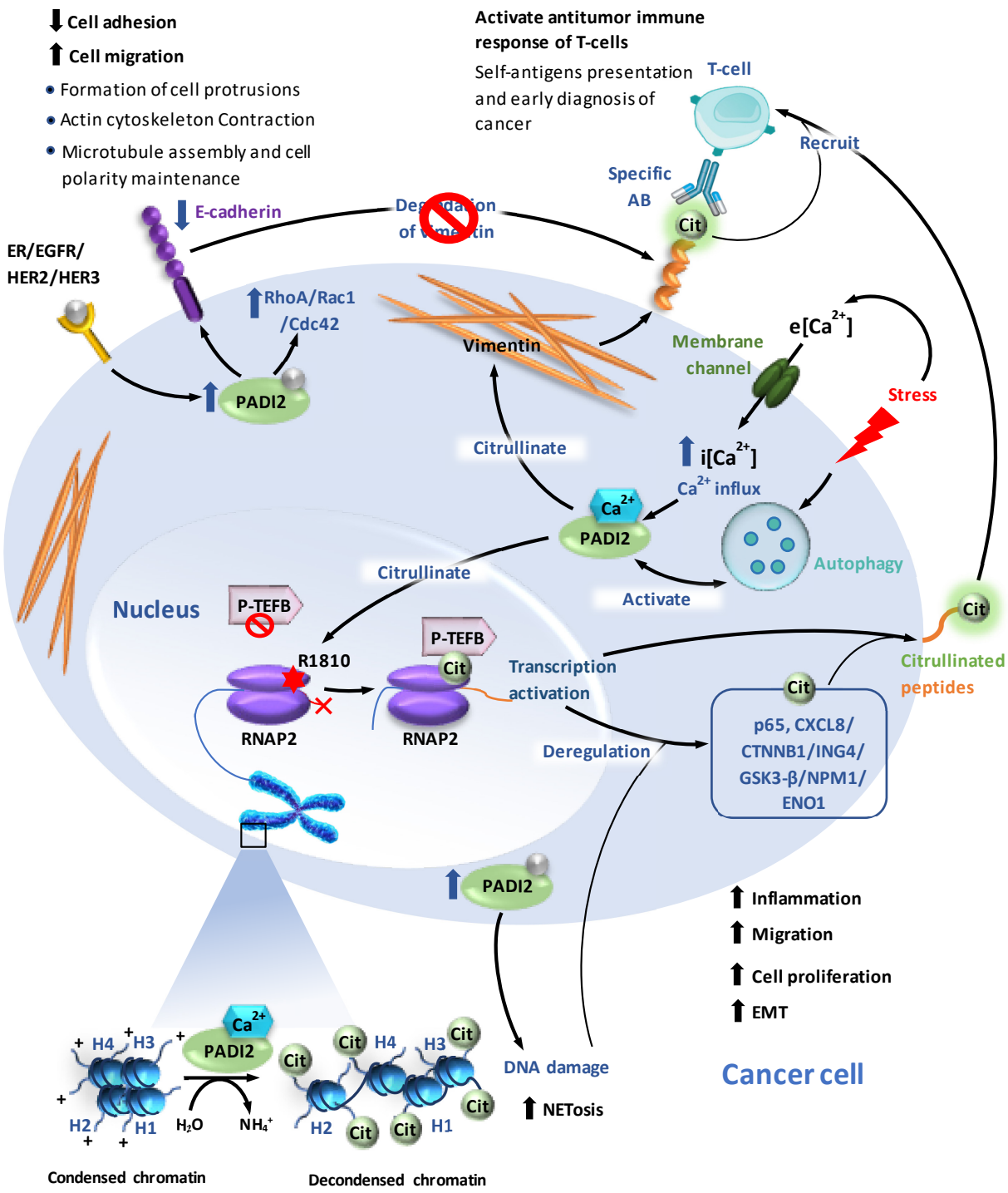
Cell adhesion
Cell migration
Formation of cell protrusions
Actin cytoskeleton Contraction
Microtubule assembly and cell polarity maintenance
Activate antitumor immune response of T-cells
Self-antigens presentation and early diagnosis of cancer
T-cell
Recruit
Specific AB
Cit
E-cadherin
Degradation of vimentin
ER/EGFR/ HER2/HER3
RhoA/Rac1 /Cdc42
Vimentin
Membrane channel
e[Ca2+]
PADI2
Stress
Citrullinate
i[Ca2+]
Ca2+ influx
Ca2+
PADI2
Autophagy
Activate
Citrullinate
Nucleus
P-TEFB
R1810
P-TEFB
Cit
Transcription activation
Cit
Citrullinated peptides
RNAP2
RNAP2
Deregulation
p65, CXCL8/ CTNNB1/ING4/ GSK3-β/NPM1/ ENO1
PADI2
Inflammation
Migration
Cell proliferation
EMT
Cancer cell
Ca2+
PADI2
H4
H3
H2
H1
H2O
NH4+
Cit
DNA damage
NETosis
Condensed chromatin
Decondensed chromatin

Figure 1.5 Schematic presentation of the proposed mechanism of PADI2 function in cancer. PADI2 is activated by various factors, including receptor signalling (i.e. ER, EGFR, HER2, HER3), oxidative stress which leads to membrane disruption and i[Ca^{2+}] influx, and hypoxia, which initiate autophagy and DNA damage. Increased expression and activation of PADI2, catalyses the citrullination of histones and other proteins, subsequently promoting cell proliferation, epithelial-mesenchymal transition, migration and inflammation. PADI2-mediated citrullination of proteins generate citrullinated peptides that stimulate CD4+ T cell responses. In high PAD2 expressing cells, Rho family of small GTPases are upregulated whereas, E-cadherin is downregulated, subsequently promoting cell migration. At the tissue level, this increased cell migrating ability (motility) may lead to increase cell invasion. PADI2-mediated citrullination of R1810 (Cit1810) at repeat 31 of the CTD on RNAP2 recruits P-TEFb kinase complex to chromatin, facilitating RNAP2 pause release resulting in transcription activation of several signalling pathways. Initiating RNAP2-mediated transcription activation, leads to increased gene expression and cancer cell proliferation. Abbreviations: P-TEFb, positive transcription elongation factor b; ER, oestrogen receptor; EGFR, epidermal growth factor receptor; HER2/3, human epidermal growth factor receptor 2/3; RNAP2, RNA polymerase II; AB, antibody; Cit, citrulline; p65, tumour protein 65; CXCL8, C-X-C motif chemokine ligand 8; CTNNB1, β-catenin; ING4, inhibitor of growth family member 4; GSK3-β, Glycogen synthase kinase 3 beta; NPM1, nucleophosmin 1; ENO1, α-enolase; Ca2+, calcium, E[Ca^{2}], extracellular calcium; i[Ca^{2+}], intracellular calcium; HER, Oestrogen-related receptor; CDC42, cell division cycle 42; RAC1, rac family small GTPase 1; RhoA, ras homolog family member A.

1.9 AIMS AND OBJECTIVES

This research focuses on the relationship between PADI2 expression and EOC. More recently, research investigating PADI2-mediated post-translational citrullination has garnered increased attention due to its emerging role in various human and animal cancers. Although the molecular mechanisms are not yet fully understood, PADI2 seem to exhibit a key role in regulating various tumourigenic processes. PADI2 provides a novel biomarker and therapeutic target in breast cancer and research to date has focused on its expression impact on patients' overall survival and on *in vitro* cellular activity. The role of PADI2 and its associated regulatory mechanism in EOC has never been investigated. The preliminary unpublished tissue microarray data indicated that high PADI2 expression in tumours is protective and may represent an independent prognostic marker. Based on this, **the primary aims of this thesis were to:**

1. Assess the relationship between PADI2 expression and overall survival of EOC patients

2. Investigate the interaction of *PADI2* with other genes to provide an improved understanding of the molecular regulatory pathways and novel gene targets by which PADI2 carries out its role in EOC.

3. Elucidate the evolutionary history of *PADI2* by comparing orthologues sequences and detecting evolutionarily conserved amino acid residues to predict functionally important residues for PADI2 function.

4. Explore the role of PADI2 as a potential EOC biomarker and therapeutic target by analysing its expression and function *in vitro*.

5. Develop CRISPR/Cas-sgRNA complex tool to gene edit PADI2 *in vitro*.

The objectives of this thesis were:

1. To determine whether high *PADI2* gene expression confers a survival advantage in EOC patients, *in silico* analyses were employed to assess gene expression data obtained from online cancer databases the cancer genome atlas program (TCGA).

2. To identify the molecular regulatory pathway, co-expression data obtained from TCGA were analysed to identify the highest correlating genes. Candidate genes were further analysed regarding their interaction with *PADI2 in vitro.*

3. To establish the phylogenetic orthology relationships and identify divergence events of *PADI2* across various species, *in silico* analyses were utilised to analyse full length orthologues (obtained from NCBI database) and construct PADI2 3D and 2D structures.

4. To explore the role of PADI2 in EOC, the impact of PADI2 overexpression on downstream effect on cellular activity, including proliferation, apoptosis, autophagy, necrosis and cellular aggregation *in vitro*.

5. To employ CRISPR/Cas9 tools with specific sgRNAs to genetically delete *PADI2* expression *in vitro* human and mouse cells lines.

2.1 TCGA and cBioPortal databases for Cancer Genomics

2.1.1 Collecting and processing the cBioPortal EOC clinical data

Clinical patient and gene expression data retrieved from microarrays and RNA-seq were downloaded from the TCGA cBioPortal OC cohort. The mRNA expression values of the primary tumours from patient samples with serous OC were determined via RNA-seq or agilent microarray analysis (Agilent Technologies, Inc., Santa Clara, CA, USA). These data were downloaded from the cBioPortal (cBioPortal online - accessed April 2015) (http://www.cbioportal.org/). These data sets were used in line with (Gao *et al.*, 2013; Cerami *et al.*, 2012) recommendations. All publicly available TCGA tumour data is compliant with US law protecting patient confidentiality and maintains high ethical standards. These patient datasets were used to investigate the relationship between *PADI2* mRNA expression and EOC patient OS time. Data regarding gene expression determined using Log2 median-cantered intensity in OC and normal controls were analysed using Pearson's correlation coefficients by comparing the gene expression values of *PADI2* with other (11813 genes) deregulated genes in the EOC dataset.

2.1.2 Survival analysis of patients with high or low expression of PADI2mRNA transcript

X-tile software was used to dichotomise samples into high and low expressing groups by providing cut point values using a minimal p-value approach. Vital status (dead/alive), OS time of EOC patients and *PADI2* mRNA gene expression data was used to determine *PADI2* expression cut-points. Followed by the SPSS-Kaplan-Meir curve survival analysis using the cut points obtained from X-tile (Camp *et al.*, 2004). Samples were then recoded into high and low expressing groups and Kaplan Meier plots were generated. The significant difference in survival outcomes between groups was determined using the log-rank test ($p < 0.05$ for statistical significance).

2.2 *PADI2* structure and phylogenetic analysis

2.2.1 *PADI2* sequence alignment and phylogenetic reconstruction

PADI sequences were retrieved from Ensembl (http://www.ensembl.org/index.html) and NCBI (https://www.ncbi.nlm.nih.gov/). The nucleotide sequences of PADI2 orthologues were aligned and translated to protein using the molecular evolutionary genetics analysis version 7.0 (MEGA7) software (Kumar *et al.*, 2016). Phylogenetic relationships of the PADI2 aligned nucleotide sequences in diverse species was inferred using the Phylogenetic Analysis by Maximum Likelihood (PAML) v.1.3.1 in Mega7 (Yang, 2007). Nodal support was assessed using bootstrap analysis with 1000 replicates. The analysis involved 31 PADI2 ortholog sequences from species representing a range of taxa: human primate, non-human primates: Rhesus monkey, Chimpanzee and Olive Baboon; Rodents: Mouse, Rat, Alpine Marmot and Molerat; Chioptera; bats: Rousette, Flying Fox and Opterus Natalensis; Artiodactyla: Wild Camel; ungulates: Horse and Ass; Carnivora: Dog and Giant panda; Aves class birds: Canary, Ruff, Eagle and Chicken; teleost: Bony Tongue, Piranha, Catfish, Molly, Vulus, Rhinocerous, Barramundi Perch and Poecilia Mexicana; Celastrales flowering plants: Japonicus; amphibia: Frog (**Appendix Table S.1**).

2.2.2 3D and 3D visualisation of *PADI2*

The aligned PADI2 amino acid sequence produced from PAML was employed by the molecular visualisation program; PyMOL version 1.8. to generate 3D and 2D structures (Schrödinger., LLC, n.d.). The individual amino acids were colour coded according to the selection status (positive, neutral and conserved selection). The previously determined ligand binding sites and Ca^{2+} binding sites were also mapped on the truncated PADI2 amino acid sequence.

2.3 Cell culture of EOC cell lines

Table 2.1 Ovarian cancer cell lines used in this study

Cell line	Source	Chemotherapy treatment	Histology	Reference	Tissue site
SKOV-3	ECACC	Platinum-resistant	HGS G1/2	(Novetsky *et al.*, 2013; Liang *et al.*, 2012)	Ascites
ID8-Luc2	John B. Liao	N/A	Epithelial EOC	(Hernandez *et al.*, 2016)	Mouse ovary
OVCAR-3	Nottingham Hospital	Platinum-resistant	HGS adenocarcinoma G2	(Mitra *et al.*, 2015; Liang *et al.*, 2012)	Ascites
OVCAR-4	Nottingham Hospital	Platinum-resistant	HGS adenocarcinoma G2	(Mitra *et al.*, 2015; Lengyel *et al.*, 2014)	N/A
OVCAR-5	Nottingham Hospital	N/A	HGS adenocarcinoma G1	(Mitra *et al.*, 2015)	N/A
OVCAR-8	Nottingham Hospital	N/A	HGS adenocarcinoma G3	(Mitra *et al.*, 2015)	N/A
OVCA-433	Nottingham Hospital	N/A	HGS	(Novetsky *et al.*, 2013)	N/A
OAW42	Nottingham Hospital	Platinum-resistant	Serous or HGS	(Beaufort *et al.*, 2014)	N/A
TOV-112D	ATCC	Untreated	Endometrioid G3	(Beaufort *et al.*, 2014)	N/A

Abbreviations: G1, grade 1 (well differentiated); G2, grade 2 (moderately differentiated); G3, grade 3 (poorly differentiated); N/A, not available; HSG, high grade serous; ECACC, The european collection of authenticated cell cultures; ATCC, The global bioresources center.

2.3.1 Recovery of cryopreserved cell lines

Human EOC cell lines: SKOV-3, OVCAR-3, OVCAR-4 OVCAR-5, OVCAR-8, OVCA-433, and OAW42 were kindly provided by professor Lindy Durrant (University of Nottingham). TOV-112D was purchased from the ATCC. The murine EOC cell line ID8-Luc2 was kindly provided by Professor John B. Liao, (University of Washington). All cell lines were received frozen in 1ml cryovials shipped on dry ice. Frozen cells were stored in liquid nitrogen for long term storage or -80^{o}C for short term use. The vials were thawed by gentle agitation in a 37°C water bath (Clifton NE2D, NE2-14D) and removed immediately upon thawing. The content of the vials was diluted with 10ml pre-warmed cell growth medium and harvested by centrifugation at 300g for 5 minutes at 25^{o}C. The cells were then re-suspended in fresh culture medium and transferred to the T25 flask containing 10ml pre-warmed growth medium (described below) and grown at 37°C with 5% CO_2. Medium was replaced after the first 24 hours and then replaced as required (**Table 2.1**).

2.3.2 Growth Medium

All SKOV-3, OVCAR-3, OVCAR-4 OVCAR-5, OVCAR-8, OVC-14433, OAW42 and TOV-112D were cultured in RPMI-1640 (RPMI 1640 Medium, GlutaMAX™ Supplement, Fisher Scientific, USA) growth medium. The RPMI medium was supplemented with 10% FBS (foetal bovine serum (heat inactivated E.U approved South America origins)), 100 IU/ml penicillin and 100 IU/ml streptomycin (Fisher Scientific, USA). ID8-Luc2 were cultured in DMEM medium (Dulbecco's modified eagle medium, GlutaMAX/High glucose, supplement and 25mM HEPES, Fisher Scientific, USA) growth medium supplemented with 4% FBS, 5ml insulin transferrin selenium (ITS-G) 1X (Fisher scientific, USA, 41400045), 100 IU/ml penicillin and 100 IU/ml streptomycin. All cells were grown at 37°C in a humidified atmosphere of 5% CO_2. All cell lines were tested for mycoplasma every 6 months (EZ-PCR mycoplasma test kit, Bioind).

2.3.3 Sub-culturing of cell lines

Upon reaching approximately 70-80% confluence, cells were sub-cultured into T75 and/or T175 flasks at a ratio of 3:10 for SKOV-3, OVCAR-3, OVCAR-4, OVCAR-5, OVCAR-8 OVCA-433, OAW42 and 1:10 TOV-112D and ID8-Luc2. First, cells were detached from the flask by

treatment with 1-2 ml of 0.25% trypsin-EDTA (Fisher Scientific, USA) for approximately 1-3 minutes at 37^{o}C. Trypsin was neutralized by the addition of serum-containing growth medium. Cell-medium suspension was then centrifuged at 300g and supernatant containing trypsin was removed. Cell pellets were then re-suspended in fresh pre-warmed growth medium and seeded into new T75/T175 flasks at the dedicated ratios mentioned above and incubated at 37°C in a humidified atmosphere of 5% CO_2.

2.3.4 Cell counting and viability

After harvesting**,** cell pellets were re-suspended in growth medium, mixed with gentle agitation to avoid cell lysis. 10µl of cell suspension was mixed with 10µl of Trypan blue (VWR, USA), the sample was again mixed gently. 10µl of trypan/cell solution was then added to a haemocytometer cells numbers were then determined by counting the total number of cells from 16 squares and dividing by 16. Cell viability was then measured by dividing the live cell count by total cell count.

2.3.5 Cryopreservation of cell lines

Cells were periodically frozen to maintain a stock of the cell line for future use. Cells were trypsinised and harvested as described above (method section 2.3). Cell pellets were then re-suspended in enough pre-chilled (4^{o}C) recovery cell culture freezing medium; supplemented with 10% (v/v) DMSO (Fisher Scientific, USA) in 1ml pre-chilled (4^{o}C) cryovials (Sarstedt), to create a cell suspension of $1x10^{6}$- $10x10^{10}$ cells per 1ml. Cryovials containing cells were then transferred immediately to freezing container containing isopropanol and cooled in a controlled fashion and then stored at -80^{o}C.

2.4 Plasmids used for transfection studies

2.4.1 CRISPR plasmids

RNA-guided CRISPR/Cas9 plasmids were obtained from Genscript (U7802BD260, pX459-puromycin cassette, USA). These plasmids were used to genetically delete *PADI2* locus in OC cell lines; SKOV-3 and ID8-Luc2, by gene editing. Two sgRNAs were designed to target homologous sequences on both the human and mouse *PADI2* loci in exon one and exon seven

(chr1:17,066,761-17,119,435). The chosen sgRNAs were designed using a CRISPR online tool (open access online, http://crispr.mit.edu) according to their higher on-target percentage and lower number of mismatches (**Table 2.2**).

Table 2.2 Sequences of sgRNA

sgRNA sequence	Chromosome/Exon	Start/End position on chromosome (Hg18)	on-target locus:	On-target score %
sgRNA1: CGTGGAGGCGGTGTACGTGC	1/1	17119311/17119330	Chr1: -17119307	91
sgRNA2: AGGCCTCTGTTTCCCCGACG	1/7	17086577/17086596	Chr1: -17086573	80

2.4.2 Preparation of chemically Competent *E. coli* cells

Frozen glycerol stocks of XL1 Blue (*E. coli*) bacterial cells were streaked onto LB agar (Lysogeny broth 40g/l in 400ml) containing 10µg/ml tetracycline and incubated overnight at 37°C for 24 hours. A single colony of *E. coli* was inoculated into 10 ml starter culture of LB broth (25g/l) containing 10µg/ml tetracycline as selective antibiotic and incubated overnight at 37°C (shaker) for 6-8 hours. 100ml of LB broth (25g/l) was inoculated into 1 ml starter culture containing 10µg/ml Tetracycline and incubated until optical density (OD) of 0.1. After the detection of 0.1 OD, the cell broth was further incubated at 37°C (shaker) until reaching an OD of 0.4-0.6. Cells were then harvested by centrifugation at 800g for 15 minutes at 4°C and re-suspended in 100ml of pre-chilled 50mM calcium chloride ($CaCl_2$) (VWR, USA). After incubation for 45 minutes on ice, cells were then harvested as described above (method section 2.3). For long term storage of competent cells, harvested cells were re-suspended in 1ml of 25% glycerol and 75% 50mM $CaCl_2$ at -80°C.

2.4.3 Transformation of *E. coli* (XL1 Blue) with plasmid DNA and maxi preparation of plasmid DNA

CRISPR/Cas9 sgRNA1, CRISPR/Cas9 sgRNA2, *PADI2* overexpression (pCDNA3.1 *PADI2*-+DYK) and negative control empty vector (pCDNA3.1-+DYK) were purchased from Genscript, USA. Green fluorescent plasmid (GFP) plasmid was purchased from Addgene, USA (pCMV-GFP). To transfer plasmid DNA into competent cells, 1µg of plasmid DNA was mixed with 45µl of competent cells and incubated on ice for 15 minutes. DNA plasmid-transformed *E. coli* LB broth was then streaked on a selective plate of LB agar containing 100µg/ml Ampicillin and incubated at 37°C for 48 hours. A single colony was selected from a freshly streaked selective plate and re-inoculated into a starter culture of 10 ml LB broth (10g/L NaCl, 5 g/L LB-Lennox NaCl, 0.5g/L NaCl LB-Luria) containing 100µg/ml Ampicillin as a selective antibiotic and incubated at 37°C for 12 hours with shaking at 300rpm. 1ml of the starter culture was then diluted in 500ml selective LB broth and incubated at 37°C for 12 hours with shaking at 300rpm. DNA plasmid-transformed *E. coli* cells were harvested by centrifugation at 11,000g for 15 minutes at 4°C. Cell pellets were re-suspended in P1 buffer (50mM Tris-Cl, 10mM EDTA 100µg/ml RNase). Cells were then lysed using P2 lysing buffer (20mM NaOH, 1% SDS (w/v)) and neutralized in P3 buffer (3M potassium acetate pH 5.5). The cell lysate was incubated in a QIAfilter Cartridge for 10 minutes at room temperature, followed by extraction with a liquid

vacuum. After filtering the lysate, the QIAfilter was washed using FWB2 (1M potassium acetate 15–25°C pH 5.0) and 12.5ml ER buffer was added to the filtered lysates. The filtered lysate was applied to the equilibrated QIAGEN-tip 10000 in QBT buffer (750mM NaCl, 50mM MOPS pH 7.0; 15% isopropanol (v/v); 0.15% Triton® X-100 (v/v)). After all the lysates had passed through the filter, the QIAGEN-tip was washed using the QC buffer (1.25M NaCl, 50mM Tris.Cl pH 8.5 and 15% isopropanol) and QN (1.6M NaCl, 50mM MOPS pH 7.0, 15% isopropanol) elution buffer was added to elute the DNA. The DNA pellet was air-dried for 20 minutes after DNA was precipitated and washed from the tip using Isopropanol and 70% ethanol (Endotoxin free). To confirm the success of the extraction and to quantify the total concentration of plasmid DNA, the eluted DNA solution was measured using a Nanodrop 2000 spectrophotometer (Thermo Fisher Scientific, USA).

2.4.4 Restriction digest analysis of CRISPR/Cas9, Empty vector and *PADI2* overexpression plasmids using agarose gel electrophoresis (DNA)

The purified plasmid DNA structure and quality was then determined using restriction digest enzyme method. Plasmid maps were constructed to determine compatible restriction enzymes using Snap gene editor software using primary plasmid sequences provided by Genscript, USA (**Figure 2.1**). Restriction enzymes used for CRISPR/Cas9 was *Sac*I–HF New England Biolabs (NEB), USA at (2,000units/ml) and for empty vector and *PADI2* overexpression plasmids were *HindIII*-HF and *EcoR1*-HF NEB, USA at (2,000units/ml). Plasmid DNA-restriction digest mix was prepared and incubated for 15 minutes at 37°C (**Table 2.3**). Digested DNA was then analysed using gel electrophoresis (1% (w/v) agarose gel in TAE buffer). DNA fragments sizes were estimated using DNA ladder quick-load purple NEB, USA. The numbers and sizes of fragments were then compared to the plasmid maps predicted sizes (**Figure 2.1**).

Table 2.3 Restriction digest analysis using restriction end protocol by NEB

Reagent	Volume (µl)
Restriction enzyme (2,000units/ml)	1
Plasmid DNA	1µg/µl
10X NEBuffer	5
Molecular grade water	43
Total	**50**

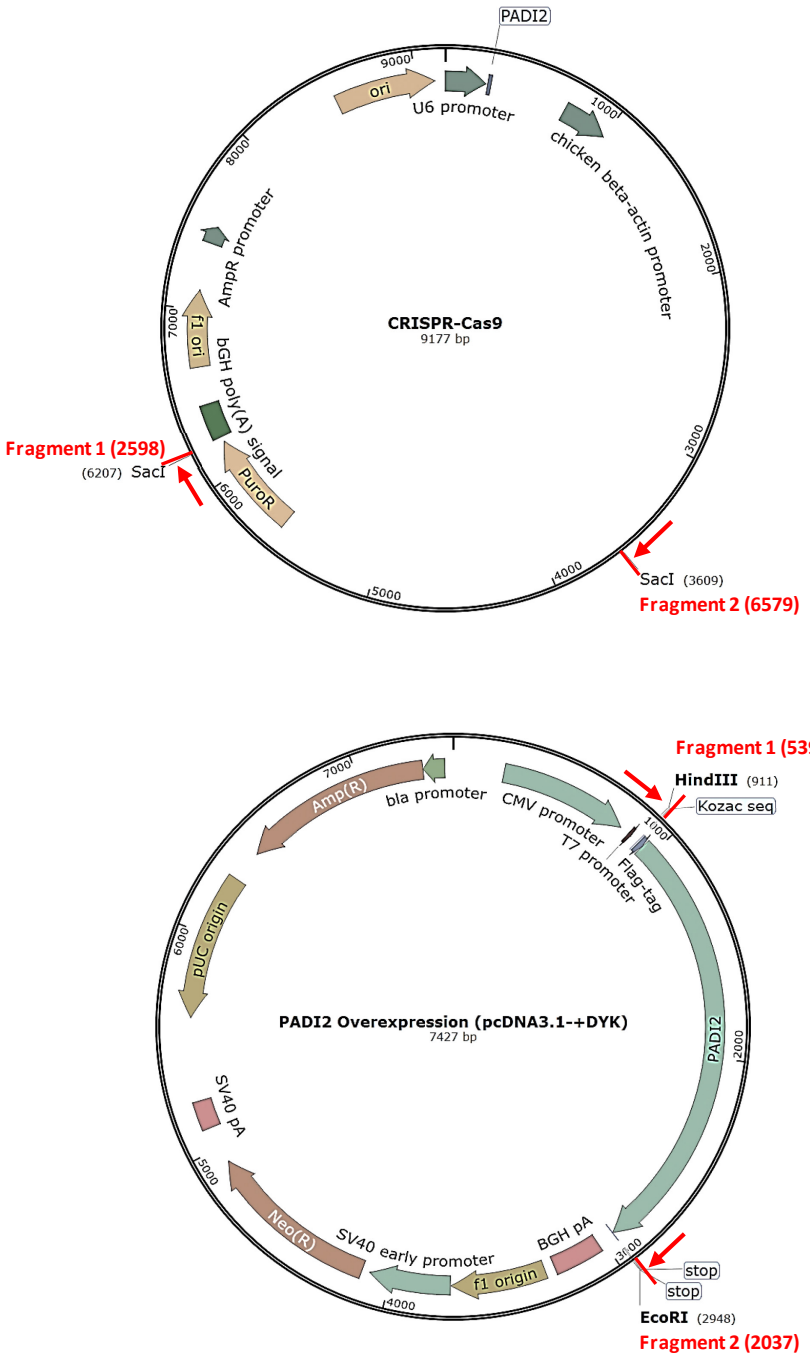

Figure 2.1 Plasmid maps indicating restrictions digest enzyme sites in CRISPR/Cas9 and pcDNA3.1-+DYK Empty vector and *PADI2* overexpression vector. Predicted DNA fragment sizes are represented at every enzyme cutting site.

2.5 Antibiotic kill curves: optimization of mammalian antibiotic selection conditions

The minimum concentration of mammalian antibiotic (i.e. puromycin or G418) required to kill non-transfected (plasmid DNA) cells was determined by generating antibiotic kill curves before transfection. Cells were plated equally at cell density of 0.8–3.0×10^5 cells/ml in 0.2ml of complete growth medium per well in 24-well tissue culture plate 24 hours prior to introducing antibiotic selection. Prior to adding the selection antibiotic, cells were sub-confluent (60-80%). Growth medium was removed and then 0.2ml fresh media was added with varying concentrations of antibiotic G418 (0-1,000µg/ml) and puromycin (0-10µg/ml) and incubated at 37°C in 5% CO_2 for 7-8 days. All samples were then analysed for variability in duplicates. Cell density and viability were counted/calculated using a haemocytometer after having stained cells with trypan blue (VWR, USA).

2.6 Transfection of ovarian cancer cell lines with plasmid DNA

Purified DNA; CRISPR/Cas9 sgRNA1, CRISPR/Cas9 sgRNA2, *PADI2* Overexpression and negative control empty vector were transfected into EOC cell lines; SKOV-3 and ID8-Luc2. *PADI2* overexpression and negative control empty vector were transfected into OVCAR-4 and ID8-Luc2. All transfection/co-transfection studies were performed using Lipofectamine 3000 reagent (Fisher Scientific, USA). Initially, SKOV-3, OVCAR-4 and ID8-LUC2 cell lines, were seeded at cell density of $0.5x10^5$ cells/ml in 6-well tissue culture plates containing 2 ml complete growth medium and incubated for 24 hours at 37°C in a humidified atmosphere of 5% CO_2. Prior to transfection, cell growth medium was replaced with 1ml/well of Opti-MEM medium (antibiotic-free without FBS). Cells were then incubated for 10 minutes at 37°C. Meanwhile, Lipofectamine 3000 reagents were incubated with plasmid DNA at room temperature. Lipofectamine 3000/plasmid DNA mixture was then added to the cells and incubated at 37°C in a humidified atmosphere of 5% CO_2 for 48 hours under. Growth medium was not replaced during the first 48 hours post-transfection. 48 hours post-transfection, CRISPR/Cas9 or expression plasmid-transfected cells were either subjected to 48-72 hours of antibiotic selection with puromycin or G418 respectively. post transfection and selection, cells were then employed in downstream functional assays. Transfected cells were also harvested as explained above (method section 2.3) and re-suspended in 10%FBS phosphate-buffered saline (PBS) to measure transfection efficiency using Flow cytometer analysis (Coulter EPICS Elite ESP, equipped with a water-cooled argon laser emitting at 525 nm). Flow

cytometry results were analysed using Flowing software Ltd in New Zealand. Distinct populations of cells were visible on the flow histograms; therefore, determination of the percentage of transfected cells was based on the inclusion of only cells that had the correct forward and side scatter characteristics (Kovala *et al.*, 2000). To optimise co-transfection efficiency of CRISPR/Cas9 or overexpression plasmids with GFP plasmid, different plasmid concentrations were tested (2.5µg, 3µg and 4µg). All samples were analysed in duplicate to demonstrate statistical measurement of analytical precision as well as comparisons among methods (Colón *et al.*, 2001).

2.7 Cell functional studies

2.7.1 Measurement of cell proliferation

Cell proliferation was detected using a WST-1 assay (Sigma Aldrich). OVCAR-4 and ID8-Luc2 cells were transiently transfected with empty vector and *PADI2* overexpression vector and seeded at a density of 1×10^4 per well and 0.7×10^4 cells per well respectively into 96-well microplates (Sarstedt) containing 200µl medium per well. Cells were allowed to adhere for 24 hours by incubation at 37°C in a humidified atmosphere of 5% CO_2. Cells were then treated with cisplatin (anti-cancer drug dissolved in DMSO, Sigma Aldrich) at a dose range of 0-100µg/ml or $CaCl_2$ at a dose range of 0-2.5mM or cisplatin at a dose range of 0-100µg/ml in the presence of 1mM $CaCl_2$. After further 24 hours incubation, the proliferation of cells was then measured by adding 20µl of WST-1 reagent to each well every 24 hours for 3 days. The absorbance was measured using BioRad (model 680XR) microplate reader at 595nm after 4 hours of incubation at 37°C in a humidified atmosphere of 5% CO_2 and in ID8-Luc2 at 450nm after 1 hour of incubation at 37°C in a humidified atmosphere of 5% CO_2. All experiments were performed three times.

2.7.2 Measurement of cell apoptosis and necrosis

Cell apoptosis and necrosis was detected using apoptosis/necrosis detection kit (blue, green, red, Abcam, UK, ab176749). OVCAR-4 cells were transiently transfected with empty vector and *PADI2* overexpression vector and seeded at a density of 5×10^5 cells/well into 96-well microplates containing 100µl medium per well and allowed to adhere for 24 hours. Cells were

then treated with 50µg/ml cisplatin or 1mM $CaCl_2$ or cisplatin at two different doses 10 µg/ml and 50µg/ml in the presence or absence of 1mM $CaCl_2$. Cells were further incubated at 37°C in a humidified atmosphere of 5% CO_2 for 48 hours and apoptosis was measured every 24 hours for 2 consecutive days. First, growth medium was removed, and cells were washed by assay buffer containing 5% FBS. Cells were then stained by adding 202µl of Apopxin Green dye diluted in assay buffer. Finally, stained cells were washed with assay buffer and analysed by BioRad Fluorescent microplate reader. Excitation and fluorescence emission spectra (490/525nm). All experiments were performed three times.

2.7.3 Measurement of cell Autophagy

Cell autophagy was detected using a florescent autophagy detection kit (Abcam, UK, ab139484). OVCAR-4 cells were transiently transfected with Empty vector and *PADI2* overexpression vector and seeded at a density of 2×10^4 cells/well and $1x10^4$ cells/well respectively into 96-well microplates containing 100µl growth medium per well and allowed to adhere for 24 hours by incubation at 37°C in a humidified atmosphere of 5% CO_2. Cells were then treated with $CaCl_2$ at a dose range of 0-3mM. Earle's balanced salt solution (EBSS) an 100µM chloroquine were used as a positive control treatment in this experiment. EBSS is an autophagy inducer, whereas chloroquine is autophagy inhibitor. The cells were further incubated at 37°C in a humidified atmosphere of 5% CO_2 for 48 hours. Autophagy was measured every 24 hours for 2 consecutive days. first, growth medium was removed, and cells were washed once by 1X assay buffer containing 5% FBS. Cells were then stained by adding 100µl of dual detection buffer. Finally, stained cells were washed with 1X assay buffer and analysed by BioRad fluorescent microplate reader. Excitation and fluorescence emission spectra (463/534nm) for autophagy green detection reagent and (350/461nm) for nuclear stain. All experiments were performed three times.

2.7.4 Measurement of cell aggregation (Spheroid)

OVCAR-4 cells were transiently transfected with empty vector and *PADI2* overexpression vector. Single-cell suspensions were adjusted to $2.5x10^6$ cells/ml in the presence and absence of 1mM $CaCl_2$. Aliquots containing 20µl of the cell suspension were placed as droplets on cell culture plates lids and incubated at 37°C in a humidified atmosphere of 5% CO_2 for 48. (**Figure**

2.2) Cell aggregates were transferred to autoclaved glass bottles containing 5ml complete growth medium in the presence or absence of 1mM $CaCl_2$. Cells were then further incubated in a water bath at 37°C in a humidified atmosphere of 5% CO_2 for 48 hours. Cell aggregates were observed under Olympus inverted microscope. All images of cell aggregates were analysed using ImageJ software. All experiments were performed at least three times.

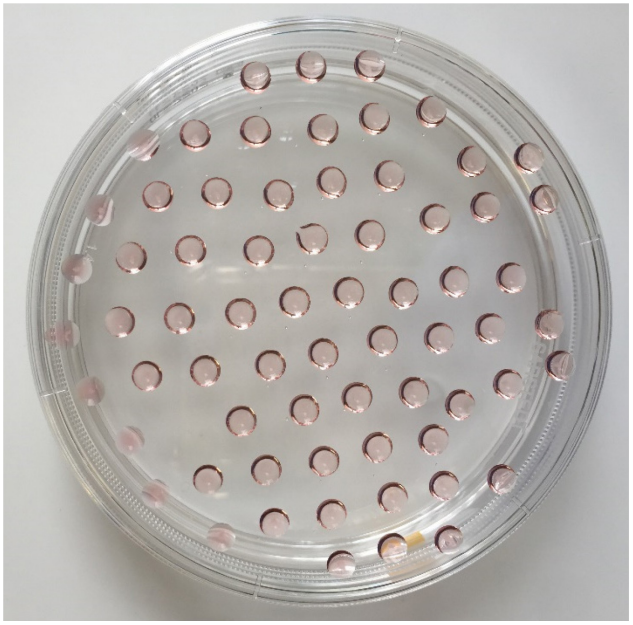

Figure 2.2 Hanging drop assay for creating OVCAR-4 cell aggregates. 10µl drops on the inner side of a 100 mm dish lid. The lid was placed with drops upside down and on top of the plate filled with 10 ml PBS.

2.8 Western blotting analysis

2.8.1 Protein quantification using bicinchoninic acid assay (BCA)

Western blot analysis was carried out using whole-cell extracts. Whole-cell extracts were prepared from cell pellets with cell density of $5x10^6$, harvested as described above (method section 2.3) then washed in 1X PBS and stored at -80°C. Initially, proteins were extracted from cell pellets using 500 µl of pre-chilled cell lysis RIPA buffer (Radioimmunoprecipitation lysis buffer (25mM Tris-HCl pH 7.6, 150mM NaCl, 1% NP-40, 1% sodium deoxycholate, 0.1% SDS), Fisher scientific, USA) containing 1% protease inhibitor cocktail (Fisher scientific, USA). The cell lysate-RIPA mixtures were incubated at -20°C for 60 minutes. Cell lysates were centrifuged for 30 minutes at room temperature at 12,100g. Protein concentration in lysates was then determined by BCA (Pierce Labs, Rockford, IL) test prior to gel loading to ensure equal protein loading. Protein standard Albumin (BSA) dilutions were prepared in a concentration range from 0-10mg/ml. BCA working reagent (WR) was prepared and 200µl were added to every well in 96-well plate to each of standards or unknown sample replicate. After incubation at 37°C for 30 minutes, absorbance was determined at 595nm on a BioRad microplate reader. The protein concentration in cell lysates was calculated by plotting a standard curve (average Blank-corrected 562nm measurement for each BSA standard vs. its concentration in µg/ml).

2.8.2 Polyacrylamide gel electrophoresis

Total amount of protein loaded/well was 30-70µg. The extracted proteins were prepared for loading SDS-PAGE by adding 1XLaemmli reducing buffer. Samples were boiled at 100°C for 5 minutes, followed by brief incubation on ice (samples were kept on ice until use to prevent protein degradation). Samples were then subjected to SDS polyacrylamide gel electrophoresis on a 10% Bis-Tris NuPAGE polyacrylamide gel (Biorad), along with 10µl Magicmark molecular weight ladder (Fisher Scientific, USA) and 5µl Seablue marker (Fisher Scientific, USA). Gel electrophoresis was performed at 100V for the first 15 minutes and then 180V for 30 minutes.

2.8.3 Protein transfer and membrane Immunoblotting

Proteins were transferred from the SDS gel onto a PVDF membrane for 60 minutes at 35V. To prepare the transfer cassette, four pieces of Whatman paper and 2 sponges were pre-socked in pre-chilled transfer buffer. Also, PVDF membrane was activated in 100% methanol for 5 minutes and washed in distilled water for 2 minutes. The transfer cassette was organised in a specific manner (**Figure 2.3**). Transfer tank was filled with pre-chilled 1Xtransfer buffer. Immunoblotting was performed at 35V for 1 hour at room temperature. After incubating the PVDF membrane were incubated in blocking buffer (5% BSA diluted in PBS) for 1 hour at room temperature. PVDF Membranes were then incubated for 1 hour at 4°C with primary antibodies; mAB Beta actin (β-actin, Sigma) 1µg/ml, mAB PADI2 (Santa Cruz, USA) 0.2µg/ml, monoclonal PADI4 (Abcam, UK) and mAB citrulline (Sigma) 1µg/ml, diluted in 5ml blocking buffer. Blots were washed and then incubated with secondary antibodies for 1 or 12 hours at 4°C; Goat anti-Mouse secondary (Dako) 0.26µg/ml and Goat anti-Rabbit secondary (Dako) 0.26µg/ml diluted in 5ml blocking buffer. All membranes were washed for 30 minutes (3×10 minutes) with PBS-Tween after primary and secondary antibody incubation and then visualized by Gnome machine using ECL detection reagent (Fisher Scientific, USA).

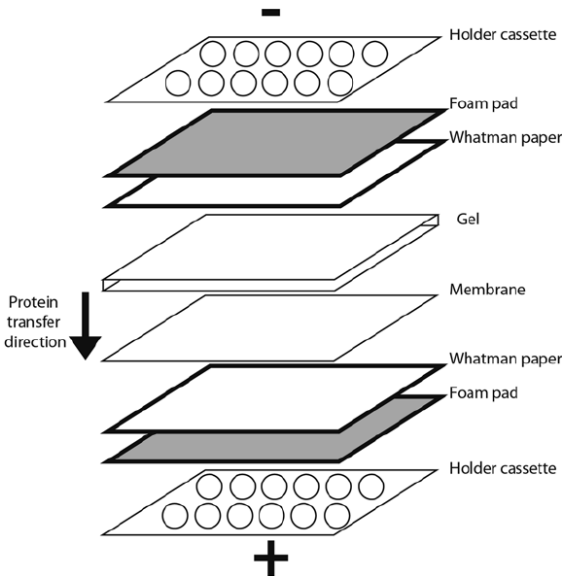

Figure 2.3 The preparation of the gel-membrane sandwich for transfer from SDS-PAGE to PVDF in preparation for an immunoblot

2.9 Detection of *PADI2* locus specific cleavage by CRISPR/Cas9

Locus specific cleavage of *PADI2* gene in EOC cell line genome was detected using GeneArt genomic cleavage detection kit (Fisher Scientific, USA) and Sanger Sequencing (Eurofins TubeSeq services, UK).

2.9.1 Cell lysis and DNA extraction

After transfection, non-transfected and CRISPR/Cas9 sgRNA1/sgRNA2 transfected SKOV-3 and ID8-Luc2 cell pellets were harvested, as described (method section 2.3). Cell pellets were lysed in a solution containing 50µl cell lysis buffer (provided by the kit) and 2µl protein degrader to obtain genomic DNA and incubated in Techne TC0512 thermocycler to provide lysing conditions required (**Table 2.4**).

Table 2.4 Thermal cycling Lysis and extraction conditions

Step/Stage	Step 1	Step 2	Step 3
Temperature	68°C	95°C	4°C
Time (mm:ss)	15:00	10:00	∞

2.9.2 Gradient PCR and primer optimisation

Specific primers were designed using NCBI primer blast and IDT primer quest tools, to target the *PADI2* gene Locus where the CRISPR-induced-double-strand breaks (DSBs) occur. The specific position of the DBS breaks was predicted by the CRISPR design online tool. Two primer pairs were designed for each sgRNA1 and sgRNA2 to amplify around *PADI2* locus in human and mouse genome (**Table 2.5**). The designed oligonucleotide primers were obtained from Sigma Aldrich. All primer sequences were subjected to gradient PCR using AmpliTaq Gold DNA Polymerases (Fisher Scientific, USA, 10156624) to determine the optimum annealing temperature and optimise PCR reaction specificity. PCR amplification was performed on purified human and murine genomic DNA (Promega) using the designed primer oligonucleotides. The PCR amplification was achieved by using the Techne TC0512 thermocycler under conditions recommended by the manufacturer's protocol (**Table 2.6**). The length of the amplified sequences was estimated to 400bp.

Table 2.5 sgRNA1 and sgRNA2 oligonucleotide primer sequences

Target	Sequence 5'-3'	
	Forward primer	Reverse primer
Human sgRNA1	CTGCTGCAGGTGCTCCC	AACTGGAGAGGGCCAGACG
Human sgRNA2	CCAACGCTATATCCACATCCTGG	ACACAGGCGTGGAGTGTGTC
Murine sgRNA1	CTGCAGCAGGTGCTTATTCC	TGAAAGGGGCGTGTTACAGA
Murine sgRNA2	GCGCTATATCCACATCCTGGG	CTGGGCTGGGCAAATGAACT

Table 2.6 Thermal cycling PCR conditions

Stage/Step	Enzyme activation	Thermal Cycling (40 cycles)				
		Denature	Anneal	Extend	Final extension	Hold
Temperature	95°C	95°C	55°C (SKOV-3) 63°C (ID8-Luc2)	72°C	72°C	4°C
Time (mm:ss)	10:00	00:30	00:30	00:30	7:00	∞

GeneArt® Genomic Cleavage Detection Kit by Thermo Fisher scientific (A24372).

2.9.3 Preparation of PCR amplification product for Sanger sequencing

The purified PCR products of non-transfected and CRISPR/Cas9 sgRNA1 and CRISPR/Cas9 sgRNA2 transfected SKOV-3 and ID8-Luc2 cell lines were first quantified by Nanodrop. Samples were then prepared for Sanger sequencing by adding 15µl of purified 5ng/µl DNA and 2µl of 10µM optimised gRNA primer into each sample tubes.

2.9.4 Use of PCR amplification product for GeneArt genomic cleavage assay

The purified PCR product was further analysed using a cleavage assay. Products were run on a 2% agarose gel. The PCR product was denatured and reannealed so that mismatches are generated as strands with n re-annealed indel to strands with a different indel or no indel. The Gene editing tool-induced mismatches are subsequently detected and cleaved by detection enzyme and then the resultant bands are analysed by gel electrophoresis.

2.10 Reverse transcription-qPCR

2.10.1 RNA extraction

Total RNA was extracted from cultured cells at cell density of $1x10^6$ using an RNA extraction kit (RNeasy mini kit, Qiagen). Cell pellets were lysed using 350-600µl of RLT buffer. Cell lysates were homogenised by adding 70% ethanol and transferred into spin columns placed in a 2ml collection tubes and centrifuged for 15 seconds at 8000g. All flow through was discarded and 700µl RW1 Buffer was added to the RNeasy spin column and centrifuged for 15 seconds at 8000g. All flow through was discarded again and 500µl of RPE Buffer was added to the RNeasy spin column and centrifuged for 2 minutes at 8000g. Finally, 30µl RNase-free water was added to the spin column and centrifuged for 60 seconds at 8000g. Flow through was collected in RNase free tube and stored at -80°C. RNA concentration and quality were analysed by Nanodrop.

2.10.2 Reverse transcription and cDNA synthesis

cDNA was synthesized from total RNA using (Applied Biosystems™ TaqMan™ High-Capacity RNA-to-cDNA Kit, Fisher Scientific, USA). The reaction consists of 1µl of 20X enzyme mix (MultiScribe Reverse Transcriptase (50U/µl)), 10µl 2X RT Buffer Mix (includes dNTPs) and 20X random primers ad 1µg/µl RNA (**Table 2.7**). Reverse transcription was performed using Techne TC0512 thermocycler as follows: 37°C for 60 minutes, and 95°C for 5 minutes.

Table 2.7 Reverse transcription and cDNA synthesis protocol

Reagent	Volume (µl)
2X RT Buffer Mix	10
20X RT Enzyme Mix	1
RNA sample	1µg/µl
Nuclease-free H_2O	Up to 20
Total per reaction	**20**

2.10.3 RT-qPCR

The expression of *PADI2* mRNA levels were measured by qRT-PCR TaqMan gene expression assays (Fisher Scientific, USA, 11967021) using the comparative Ct (2−ΔΔCt) method. RT-qPCR was performed on wild type and *PADI2* overexpression and empty vector transfected EOC cell lines. Reaction was prepared by adding 10µl of master mix TaqMan (Universal PCR Master mix, Fisher Scientific, USA), 1µl TaqMan *PADI2* primer (Human Hs01042505_m1 and Murine Mm01341648_m1) or eukaryotic *18S* reference gene primer (Hs03003631_ g1). qRT-PCR was also used to detect the mRNA expression of PADI-possible target genes that are deregulated in EOC. Target genes TaqMan primers are, *KRTZ* (Hs00559840_m1); *ARHGEF10L* (Hs00737842_m1); *FZD5* (Hs00258278_s1); *RPS6KA1* (Hs01546657_m1). The qPCR reaction was done using applied Biosystems StepOnePlus RT PCR system, reaction conditions (**Table 2.8**).

Table 2.8 Thermal cycling PCR conditions

Stage/Step	Enzyme activation	Thermal Cycling (40 cycles)			
		Denature	Extend	Final extension	Hold
Temperature	50°C	95°C	95°C	60°C	4°C
Time (mm:ss)	02:00	10:00	00:15	1:00	∞

Statistical analysis

All statistical analyses were performed using Microsoft Excel, SPSS 24 software (SPSS Inc., Chicago, IL), X-tile 3.6.1 software (Yale University School of Medicine, New Haven, CT, USA) and GraphPad Prism (GraphPad Software Inc., San Diego, CA, USA). The cut-point for gene expression scores was obtained using X-tile 3.6.1 software. X-tile plots were conducted for assessment of gene expression scores; this was expressed as optimisation of cut points based on survival outcome. Categorical data were analysed using Chi-square test or Fisher's exact test, and continuous variables were analysed using the analysis of variance test (ANOVA). Gene expression cut-points generated by X-tile were modelled using the Kaplan-Meier method using univariable Cox regression to compare cumulative event rates between groups using SPSS 24 software. Gene expression association with overall survival was reported as means and clinical characteristics and variant burden were compared using log-rank test. The Pearson correlation analysis was used to determine the correlations coefficients between two variables using Microsoft Excel. $P<0.05$ was considered statistically significant in all cases.

CHAPTER 3: Gene expression analysis of PADI2 mRNA expression from The Cancer Genome Atlas (TCGA) and cBioPortal for serous EOC.

3.1 INTRODUCTION

PADI2 function has been reported in different biological contexts, such as H3 citrullination during breast cancer oncogenesis, the oestrus cycle in the uterus or in gonadotropic cells, as well as citrullination during colon cancer oncogenesis and induction of T-cell apoptosis (i.e. Jurkat cells, Hosokawa *et al.*, 2018; Hsu *et al.*, 2014). One of the major functions of *PADI2*, is its role in H3 citrullination, first proposed upon the discovery of exposed chromatin architecture around ERE regions at the promoters of a subset of 17 β-E2-induced genes; known to promote global citrullination of H3R26 on chromatin (Cherrington *et al.*, 2010; Zhang *et al.*, 2012). There is also *in vitro* evidence to suggest that *PADI2* can citrullinate arginine residues on histone H4 (Cherrington *et al.*, 2010). These histone modifications deregulate the transcription of thousands of genes under the control of the oestrogen receptor (Cherrington *et al.*, 2010; Sharma *et al.*, 2019). Taken together these studies highlight the important role for *PADI2* in the tumourigenic process of some tumours and suggest that *PADI2* plays a key role in gene transcriptional regulation in models of human disease (Slade *et al.*, 2014). However, the role of *PADI2* in EOC has not been described.

Whilst gene mutation and DNA alterations are important in cancer pathogenesis, deregulated gene expression may represent important cancer driving events (López-Cortés *et al.*, 2018). To better understand the impacts of the genetic composition of tumours on clinical prognosis, gene expression profiling has been increasingly incorporated with and accepted for clinical diagnosis (Aldape *et al.*, 2015; Chin and Meyerson, 2008). Herein, a combination of comprehensive genome-wide gene expression collections such as The Cancer Genome Atlas (TCGA) has been used to provide a genome-wide overview of the association of *PADI2* expression with survival of EOC patients and the identification of functionally related gene sets. Such analysis identifies associated or co-expressed genes based on their correlating expression profiles obtained from high-throughput gene expression profiling data analysed using microarray (U133) and RNA-seq experiments. While similar in purpose, there are fundamental differences between the two technologies. U133 methods measure the intensity of fluorescence of hybridised samples, which reflects the corresponding gene expression

levels, whereas RNA-seq methods measure sequence read depth which is used to calculate gene expression levels (Guo *et al.*, 2013).

3.2 AIMS AND OBJECTIVES

In this chapter, the relationship between *PADI2* expression and EOC tumorigenesis was investigated. Preliminary data (generated by Dr Lee Machado) indicates that *PADI2* high expression in tumours is protective and may represent an independent prognostic marker. To explore the mechanistic basis underpinning this, *in silico* analysis will be employed to determine the association of *PADI2* mRNA expression with survival in EOC patient. *PADI2* interaction with other genes will be explored to provide new *understanding* of *PADI2* regulatory pathways and *novel* gene targets by which it carries out its role in EOC. Candidate genes will be further analysed regarding their interaction with *PADI2* in the tumour cell.

1. Employ *in silico* analysis of gene expression data from TCGA cBioPortal, to determine whether high *PADI2* gene expression confers a survival advantage in EOC patients.

2. Determine the genes that are co-expressed with *PADI2* expression and reassess their association with PADI2 expression in PADI2 overexpressing EOC cell line.

3.3 RESULTS

3.3.1 *PADI2* expression levels are associated with serous EOC patient overall survival

To explore the association of *PADI2* mRNA expression levels with clinical outcomes in EOC patients of serous subtype, TCGA was used to extract data with the aid of cBioPortal. RNA-seq (262 EOC patients) and U133 (564 EOC patients) data cohorts allowed the assessment of *PADI2* expression association with OS of EOC patients. When performing survival analysis, the acquired patient's clinical data (i.e. survival status, *PADI2* expression levels and overall patient survival time) were analysed using X-tile software to determine *PADI2* expression cut-point values (i.e. high and low expression). These cut-point values were used to define high or low expression groups for survival analysis. Using SPSS, Kaplan-Meier curves were then constructed to demonstrate the effect of *PADI2* high or low expression on the cumulative survival of EOC patients. The mean OS was 52.3 and 41 months for RNA-seq and U133, respectively. Although the prediction did not show statistically significant results in the mean expression, the high *PADI2* expression was significantly associated with poor OS in both RNA-seq and U133 cohorts, with p-values of 0.008 and 0.0112, respectively (**Figure 3.1**).

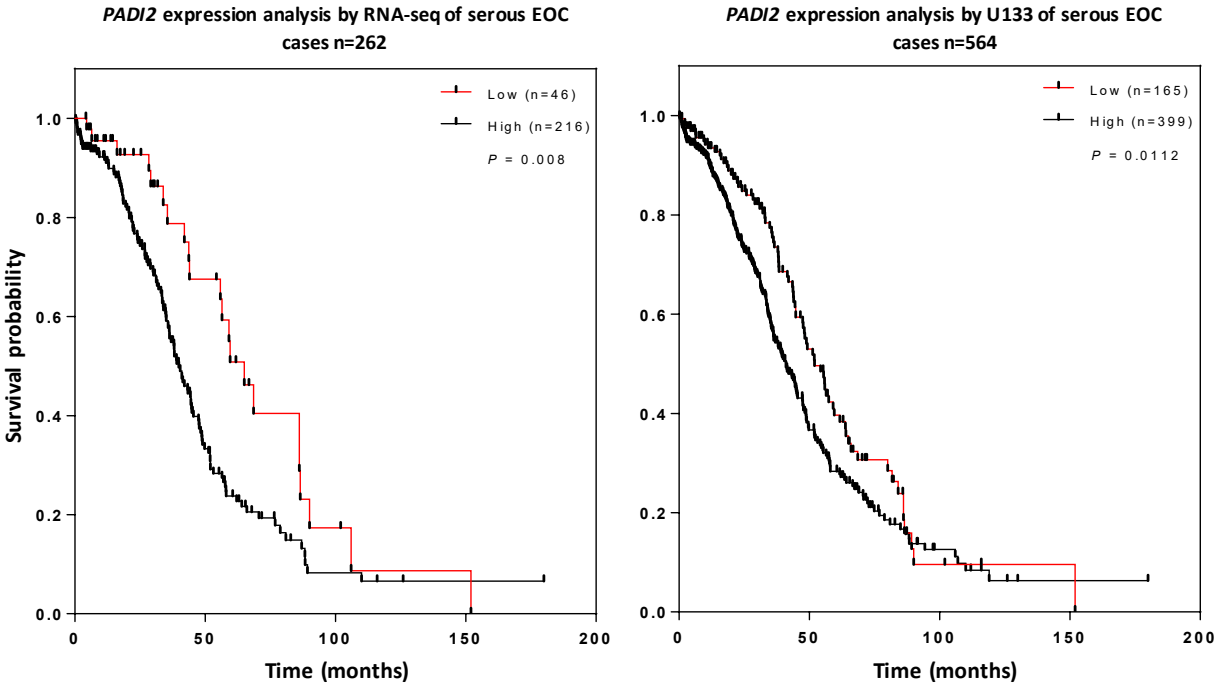

PADI2 expression	Mean overall survival (OS Months)			
	Estimate	Std. Error	95% Confidence Lower	95% Confidence Upper
Low	61.1	4.6	52.1	70.2
High	52.3	3.3	45.1	58.7
Overall	54.5	2.7	49.3	59.8

PADI2 expression	Mean overall survival (OS Months)			
	Estimate	Std. Error	95% Confidence Lower	95% Confidence Upper
Low	52.0	3.6	44.9	59.1
High	41.0	2.5	36.2	45.8
Overall	44.5	1.8	40.9	48.1

Figure 3.1. High *PADI2* expression is associated with poor survival in serous EOC patients. Kaplan-Meier survival analysis was used to estimate the association between *PADI2* expression and OS of serous EOC patients. The RNA-seq and U133 patient data were retrieved from TCGA cBioPortal. X-tile was used initially to determine the high and low expression cut-point values of *PADI2*. Kaplan-Meier curves were then constructed using SPSS to demonstrate the effect of PADI2 high or low expression on the cumulative survival of EOC patients. Number of EOC patients at risk with higher *PADI2* expression (red) and lower *PADI2* expression (black). Data were analysed using the log-rank test. OS: overall survival; U133: microarray.

3.3.2 The correlation between *PADI2* expression and other co-expressed genes in EOC

To identify the correlation between *PADI2* expression and co-expressed genes in EOC, correlation analysis was conducted using the TCGA (i.e. U133 and RNA-Seq gene expression data collected 182 primary tumour samples). Around 16,000 genes common to both platforms were used for correlation analysis. Gene-wise comparison of U133 and RNA-Seq data revealed that 82% had a Pearson's correlation coefficient greater than 0.2. Further analysis indicated high correlation between U133 and RNA-Seq with the highest Pearson's correlation coefficients in only 15 genes. These genes are either positively or negatively correlated with *PADI2* expression. The correlation was measured as the absolute value of Pearson's correlation coefficient. The range of expression values was between -0.2and 0.44 (**Table 3.1**).

Table 3.1. The correlation between *PADI2* expression and other co-expressed genes in EOC. The correlation was measured as the absolute value of Pearson's correlation coefficient. RNA-seq (green) and microarray (U133) (blue).

Gene abbreviation	Gene name	Gene accession number	Pearson correlation	*P*-values
ARHGEF10L	Rho guanine nucleotide exchange factor (GEF) 10-like	NC_000001.11 NT_032977.10 NC_018912.2	0.37 0.42	2.29e-11 2.59e-10
BMPR1B	Bone morphogenetic protein receptor, type IB	NC_000004.12 NT_016354.20 NC_018915.2	-0.26 -0.28	8.24e-4 1.65e-5
DACH1	Dachshund family transcription factor 1	NC_000013.11 NT_024524.15 NC_018924.2	-0.23 -0.25	1.14e-3 1.12e-4
EPB41L1	Erythrocyte membrane protein band 4.1-like1	NC_000020.11 NT_011362.11 NC_018931.2	0.35 0.42	3.12e-8 8.06e-7
FUS	FUS RNA binding protein	NC_000016.10 NT_187260.1 NC_018927.2	-0.23 -0.30	1.33e-6 1.11e-6
FUT8	Fucosyltransferase 8	NC_000014.9 NT_026437.13 NC_018925.2	-0.24 -0.26	2.84e-4 1.65e-6
FZD5	Frizzled class receptor 5	NC_000002.12 NC_018913.2 NT_005403.18	-0.31 -0.37	8.47e-8 1.11e-4
KRT7	Keratin 7, type II	NC_000012.12 NT_029419.13 NC_018923.2	0.42 0.43	1.32e-10 1.48e-4
LDLRAP1	Low-density lipoprotein receptor adaptor protein 1	NC_000001.11 NT_032977.10 NC_018912.2	0.36 0.35	5.42e-6 6.54e-7
NPTXR	Neuronal pentraxin receptor	NC_000022.11 NC_018933.2 NT_011520.13	0.40 0.33	2.91e-7 3.45e-7
PFKM	Phosphofructokinase	NC_000012.12 NT_029419.13 NC_018923.2	-0.26 -0.28	3.95e-3 4.76e-4
RPS6KA1	Ribosomal protein s6 kinase	NC_000001.11 NT_032977.10 NC_018912.2	0.38 0.42	5.33e-8 4.30e-7
SNRPE	Small nuclear ribonucleoprotein polypeptide E		-0.24 -0.35	9.17e-7 3.56e-7
ZNF22	Zinc finger protein 22	NC_000010.11 NC_018921.2 NT_030059.14	-0.24 -0.27	2.62e-5 1.33e-6
ZSCAN12	Zinc finger and scan domain containing 12	NC_000006.12 NT_007592.16 NC_018917.2	-0.21 -0.29	1.80e-5 3.59e-4

3.3.3 The association between PADI2 mRNA level in EOC cell lines and other co-expressed genes

The human derived OVCAR-4 EOC cells were transfected with the *PADI2* expression plasmid. OVCAR-4 cells transfected with empty vector were used as negative control. The overexpression of *PADI2* was confirmed in the cultured cells using qRT-PCR. In the section above (3.3.2), the correlation analysis of co-expressed genes revealed that 15 genes have the highest correlating values. Ideally, all 15 genes can be further analysed to verify whether modulating *PADI2* expression may impact their mRNA abundance. However, based on the limitations of this study, two candidate genes, including *FZD5* and *ARHGEF10L,* were chosen for further expression analysis. These genes were chosen on the basis of their functional relevance in the EOC pathogenesis according to the literature. After cell transfection and PADI2 overexpression confirmation, qRT-PCR was used to determine which of the candidate genes from the correlation analysis are affected by modulating *PADI2* expression in OVCAR-4 cells. The qRT-PCR analysis of *FZD5* and *ARHGEF10L* mRNA expression showed consistent results with those observed in the correlation analysis. For example, *ARHGEF10L,* was positively correlated with *PADI2* expression in primary tumours and was also positively associated with *PADI2* mRNA in PADI2 overexpressing OVCAR-4 cells. (**Figure 3.2**).

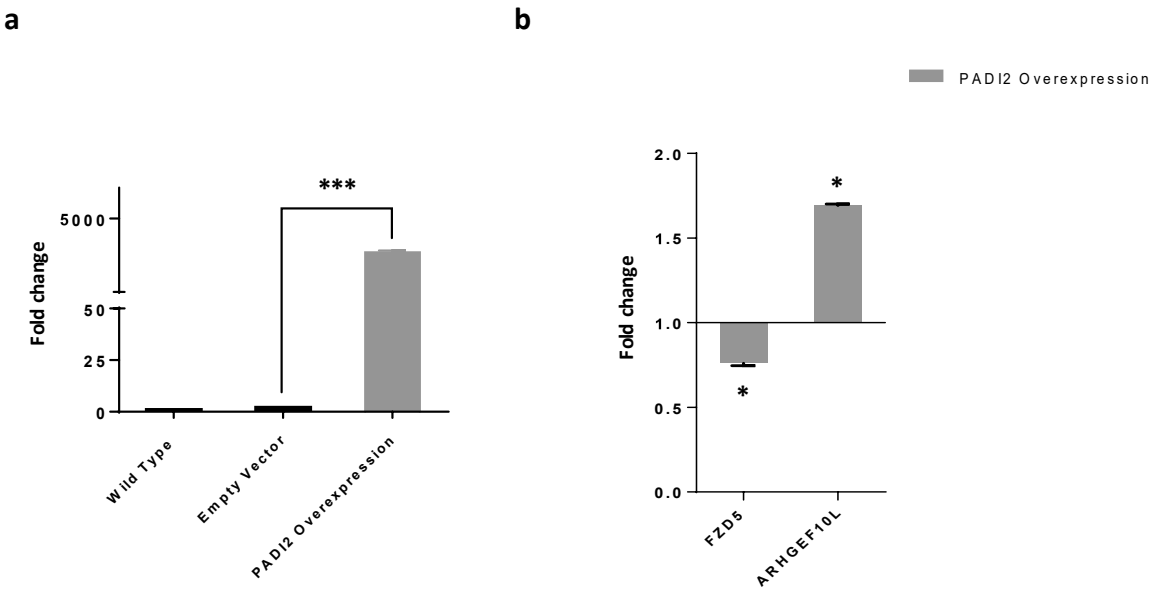

c **The comparison of the gene expression status between qRT-PCR (mRNA) and correlation analysis (Pearson's coefficient values)**

	FZD5	ARHGEF10L
Correlation analysis	⬇	⬆
qRT-PCR analysis	⬇	⬆

Figure 3.2. The determination of mRNA expression levels of *PADI2, FZD5,* and *ARHGEF10L* in PADI2 overexpressing OVCAR-4 cells using qRT-PCR. Cells were transiently transfected with a control empty vector and PADI2 overexpression vector. At 96 hours post-transfection and enrichment, expression levels were determined by qRT-PCR **(a)** *PADI2* expression in OVCAR-4 cells. Representative bar graphs of average PADI2 transcription levels normalised to 18S mRNA levels. **(b)** *FZD5* and *ARHGEF10L* in PADI2 overexpressing OVCAR-4 cells. The transcription levels of the target genes in the transfected cells were normalised with their mRNA levels to cells transfected with control empty vector. **(c)** The comparison of the gene expression status between qRT-PCR (mRNA) and correlation analysis (Pearson's coefficient values). Results are representative of the average fold change ± SD of triplicate independent experiments relative to the untreated controls. Bars are presented as mean ± SD (n = 3). *p≤0.05, ****p* 0.001.

3.4 DISCUSSION

3.4.1 The correlation between *PADI2* mRNA and OS of EOC patients

The effects of protein citrullination are widespread and vary according to the genomic context and interactions with PADIs (Ying *et al.*, 2009). While *PADI2* was initially characterised as an important epigenetic transcriptional regulator through H3 citrullination, recent studies suggest that *PADI2* promote the migration ability in breast cancer cells and participates in the apoptotic mechanisms of activated T lymphocytes (Hsu *et al.*, 2014; Wang *et al.*, 2016; Hosokawa *et al.*, 2018). Recently, McElwee reported that *PADI2* mRNA expression highly correlates with *HER2* in *HER2/ERBB2*-positive breast cancer subtype; one of the main breast cancer transcriptional subtypes (McElwee *et al.*, 2012c). Moreover, the up- or down-regulation of *PADI*2 expression was largely investigated in many types of cancer (Lin Wang *et al.*, 2017; Funayama *et al.*, 2017). However, the function of *PADI2* in EOC is not yet established. The aim of this chapter was to determine the novel role of *PADI2* mRNA expression in EOC by utilising both its correlation with the mRNA expression of co-expressed genes and its association with OS of EOC patients. This was achieved by employing *in silico* analysis of gene expression data from online cancer databases, including TCGA. Dr L. Machado initially explored the relationship between PADI2 expression and EOC by analysing primary tumour tissue microarrays arrays (TMA) collected from EOC patients with different disease subtypes (not only serous subtype). Given this unpublished data, *PADI2* expression was found to positively correlate with improved patient survival (**Appendix Figure S.3**). Based on the TMA data, the involvement of *PADI2* with EOC and extend that to patient prognosis was furthermore delineated. It is important to note that in contrast to the TMA EOC cohorts conducted on multiple EOC subtypes, the current study survival analysis of TCGA data was obtained from EOC patient cases with only serous EOC subtype. Thereafter, the analysis of the expression data collected from TCGA cBioPortal U133 and RNA-seq presented contrasting outcome to that observed in the TMA data; and that is PADI2 mRNA expression is associated with a lower survival rate of EOC patients. This is not surprising, given that the underlying assumption that *PADI2* expression patterns were measured in different patients' cohorts. The discrepancy of both outcomes resides not only in the fact that different data pools were used in each analysis, but in the inconsistency of the histological subtypes of EOC patient cases tested (Xue *et al.*, 2018). Thus, the current study outcome can represent the PADI2 association

with OC patient with serous disease subtype and not the other subtypes, such as endometrioid, mucinous and clear cell. In addition, several possible explanations might also be considered for the observed lack of consistency. For example, in mRNA expression analysis, the choice of fold change threshold for when genes are considered up- or downregulated may have a significant impact on the results. In addition, mRNA expression level is not always a good indicator for protein expression level, and this may alternately influence experimental outcomes. While this does not imply that mRNA detection cannot be utilised to produce meaningful results, but it does suggest that more sophisticated analysis may be required, such as multi-omics or include a wider/diverse data pool. Also, these gene expression detection and evaluation methods do not explain the effect of the tumour microenvironment on transcriptional regulation, gene expression and associated gene regulatory networks.

3.4.2 Determining the possible regulatory pathway of *PADI2* in EOC

Several studies have used different transcriptional profiling and protein-protein interaction (PPI) to potentially predict the function of genes and their downstream signalling pathways (Kabir *et al.*, 2018). The availability of extensive gene expression and PPI publicly-available data improved the detection of potential key regulators and molecular signatures in various diseases including cancer. However, these pathways are not universally defined, and different tools identify different signalling pathways for the same datasets. For example, in the current study, RNA-seq and U133 identified a number of highly regulated genes in EOC patients that are also co-expressed with *PADI2*; however, these genes were not previously known targets of *PADI2*. In a comprehensive and systematic genomics study by Wang *et al.*, (2016), using tumourigenesis-related PCR arrays and qRT-PCR, it was suggested that PADI2 contributes to breast cancer tumorigenesis by deregulating the expression of *ACSL4, BINC3* and *CA9* (Huifeng Wang *et al.*, 2016). Similar approaches were used in the current study. The second aim of this chapter was to determine the correlation and validate the association of the identified candidate genes with *PADI2* expression. This was achieved by analysing the correlation of co-expressed genes (obtained from TCGA), thereafter, the highest correlating genes were validated using qRT-PCR. The highest two correlating genes, including *FZD5* and *ARHGEF10L,* were also validated in PADI2 overexpressing OVCAR-4 cells. The qRT-PCR analysis identified that all the co-expressed genes analysed, including *FZD5* and *ARHGEF10L,* were also significantly deregulated in *PADI2* overexpressing OVCAR-4 cells. *ARHGEF10L* was found to be

positively correlated and associated with PADI2 expression, whereas, *FZD5* was inversely correlated/associated with PADI2. Collectively, these observations suggest that *FZD5* and *ARHGEF10L*, may be involved in the tumourigenic pathway of PADI2 in EOC.

Previous studies have shown that EOC progression and metastasis is a multistep process in which ECM and cancer cell cytoskeleton interactions play an important role (Smolle *et al.*, 2013; Gkretsi and Stylianopoulos, 2018). *FZD5* is known to increase the adhesion to ECM components, including collagen IV, fibronectin and vitronectin, its high expression also correlates with poor EOC patient prognosis. The upregulation of *FZD5* by the DNA-binding protein AT-Rich interactive Domain 3B (*ARID3B*), results in the activation of WNT5A/β-catenin signalling pathways, thereby, increasing tumour cell proliferation and development (Bobbs *et al.*, 2015). This finding agrees with other reports of EOC which indicated that *FZD5* expression correlates with advanced malignancy (Barbolina, Burkhalter and Stack, 2011; Bobbs *et al.*, 2015). Yoshioka *et al.*, (2012) also reached a similar conclusion. Several studies also suggested that *FZD5* can serve as both a biomarker and potential therapeutic target gene in cancer (Weeraratna *et al.*, 2002; Carmon and Loose, 2008). The present study showed that PADI2 overexpression in human EOC cell lines led to the downregulation of *FZD5*. Combined with the above findings, the present study also suggests that increased expression of *PADI2* may be involved in the biology of EOC by stimulating *FZD5* expression, subsequently hindering WNT5A/β-catenin signalling and leading to reduced proliferation. In addition, variants in genes encoding small GTPases, such as *ARHGEF10L*, which govern processes, including signal transduction, vesicle transport, cell proliferation and cell motility, are known to be associated with EOC (Earp *et al.*, 2018). While several Rho GTPases represent oncogenic activity by promoting cancer cell invasion, and progression in various cancers, other family members appear to act as tumour suppressors and are frequently mutated, deleted or downregulated in some cancers (Vega and Ridley, 2008). SNP rs2256787 is a common germline variation in *ARHGEF10L*, which encodes the Rho guanine nucleotide exchange factor 10-like protein, and is associated with 33% increased invasive endometrioid EOC risk (Earp *et al.*, 2018). PADI2 overexpression was shown to increase *ARHGEF10L* in EOC cells. Collectively, these findings and the current study supports the hypothesis that the PADI2-mediated downregulation of FZD5 and upregulation of *ARHGEF10L* expression may contribute to decreased adhesion and advanced tumour progression in EOC.

3.5 CONCLUSIONS

In summary, the results of TCGA data analysis in this chapter show that PADI2 expression is associated with lower OS and poor prognosis in EOC patients. This chapter also exploits a novel gene network interaction with *PADI2* using qRT-PCR. The data obtained from this analysis suggests that higher *PADI2* expression contributes to decreased EOC carcinogenesis by deregulating *FZD5* and *ARHGEF10L*. This chapter also outlines the basis of this thesis and the downstream studies observed in the coming chapters (4-6). In addition, this study potentially had basic methodology limitations. For example, some genes that may play vital roles in the biology of EOC were not included in the qRT-PCR analysis. Also, 0.7-fold change in gene mRNA expression was considered biologically significant, based on the instructions of the manufacturer. In addition, cultured cell lines were used to investigate the tumourigenic mechanisms. The observed mechanisms may not be entirely similar to the ones observed in tumour tissues or patient blood samples.

CHAPTER 4: The evolutionary history and structure and of PADI2

4.1 INTRODUCTION

Although *PADI2*-mediated citrullination is linked to the pathogenesis of many diseases including cancer, this PTM also contributes to protein moonlighting, an evolutionary acquired phenomenon that allows proteins to perform more than one biophysical or biochemical function within one polypeptide chain (Henderson and Martin, 2014). Studies based on experimental and computational analysis have indicated that the physiological and pathophysiological roles of PADI genes are conserved throughout evolution from bacteria to mammals (Vossenaar *et al.*, 2003). This conservation of PADI roles was linked to their highly conserved promoter regions that are associated with key regulatory elements and signalling pathways, such as transcription factors (e.g. SP1, SP3, NF-κB, etc., Adoue *et al.*, 2008). Interestingly, among the five PADI isoforms, *PADI2* is the most widely expressed member and phylogenetically most conserved isozyme suggesting it is the ancestral homologue of the PADI family of isozymes (Vossenaar *et al.*, 2003). A significant number of multigenic families' annotation studies have examined the phylogenetic relationship of PADI isozymes paralogues; however, the evolution of *PADI2* orthologues and its phylogenetic relationship across species was not fully explored.

Because important functions are conserved during evolution, the first step in analysis is to determine the homology of ortholog sequences. In contrast to the multigenic families' annotations of gene paralogs, gene orthologues annotation provide more accurate determination of evolutionary relationships and reveal significant functional similarities (Mirny and Gelfand, 2002). Various ortholog identification methods use sequence comparisons to test of homology and morphology, such as molecular phylogenies (Reaume and Sokolowski, 2011). Parsimony and maximum likelihood (ML) methods are the most established means of generating phylogenies (Ludwig et al., 2011). Given the large amount of genome sequencing data, the construction of ortholog groups using phylogenetic trees can identify functional divergence events of PADI2 across species (Weissenbach, 2016; Fang *et al.*, 2010).

4.2 AIMS AND OBJECTIVES

The aim of this chapter is to study the evolutionary history of *PADI2* based on the phylogenetic analysis of different orthologues sequences. This study will also focus on *PADI2* in its phylogenetic context to detect the evolutionarily conserved amino acid residues and predict functionally important catalytic residues.

1. Phylogenetic analysis of full length PADI2 orthologues (from NCBI database) to determine the orthology relationships and identify divergence events of *PADI2* across various species.

2. Reconstruction of PADI2 protein sequence and the assembly of 3D and 2D structures.

4.3 RESULTS

4.3.1 Phylogenetic analysis and evolutionary divergence of *PADI2* among 31 species

4.3.1.1 Phylogenetic analysis

The evolutionary analysis was performed on *PADI2* orthologues collected from 31 distinct species. The Mega7 codon-based alignment method and PhyML software were used to construct the PADI2 phylogenetic tree. *PADI2* orthologues were identified in mammals, including human primate (*Homo sapiens*), non-human primates (Rhesus monkey, Chimpanzee and Olive baboon), Rodents (Mouse, Rat, Alpine marmot and Molerat), chioptera bats (Rousette, flying fox and Opterus natalensis), Artiodactyla (Wild camel), ungulates (Horse and Ass), Carnivora (Dog and Giant panda), Aves class birds (Canary, Ruff, Eagle and Chicken) , fish (Bony tongue, Piranha, Catfish, Molly, Vulus, Rhinocerus, Barramundi perch and Poecilia mexicana) and Celastrales flowering plants (Japonicus) and amphibia (Frog). After sequence alignment, a total length of 1839bp nucleotide sequences was retrieved. The evolutionary relationship between *PADI2* orthologues was inferred using PhyML software ML phylogenetic tree. The reliability of the inferred phylogenetic tree was evaluated by bootstrap analysis (1000 replications), and bootstrap values were represented with branch support percentage (BSP) at each node. Bootstrap proportions of ≥70% that corresponds to a probability of ≥95% indicate the reliability of the population parameter in clades (Hillis and Bull, 1993). The bootstrap analysis of *PADI2* genes across 31 species corresponds to an overall reliable phylogenetic tree. However, low bootstrap values were detected in some tree branches; 41%, 69%, 43%, 36% and 32%. The ML phylogenetic tree showed the first major divergence event that separated the lineage into two clades; I and II with BSP of 100% and 99% respectively. The major separation logically appears between the two clades; clade-II which contains only teleost species and other invertebrate aquatic organisms and clade-I was formed from vertebrates' sequences, including mammals, aves and plants with the frog appearing basal to this clade. Clade-I gave rise to four sub-clades; Ia, Ib, Ic and Id. It is commonly known that sub-clades of a phylogenetic tree share more common ancestor than the one shared between clades, therefore, the tree subclades share a more common ancestor than that shared between clade-I and clade-II. it was also observed that each subclade is represented by a

different organism class. For example, subclade-Ia is represented by mammals, subclade-Ib is represented by plants, subclade-Ic is represented by aves or birds and subclade-Id is represented by amphibians. In clade-I, the separation of frog in subclade-Id from the other *PADI2* orthologues and its longest phylogenetic branch suggests that this lineage did undergo the least sequence variation. This may also indicate that this lineage occurred at an early stage and is likely to retain ancestral characteristics or may even be the ancestor of other organisms in the phylogeny (Crisp and Cook, 2005, **Figure 4.1**).

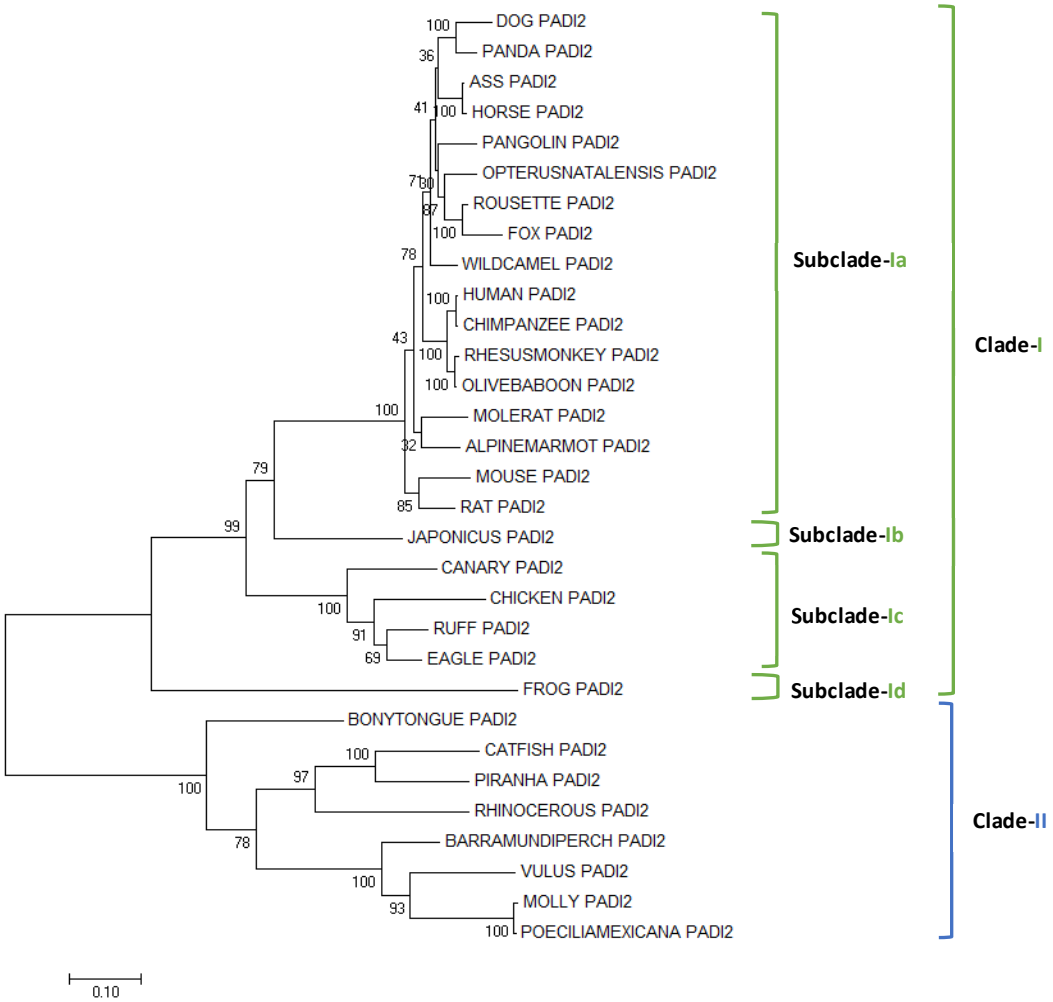

Figure 4.1. Phylogenetic analysis of *PADI2* orthologues obtained from 31 species. A bootstrapped unrooted phylogenetic tree was reconstructed using the maximum likelihood (PhyML) method using 31 aligned sequences of *PADI2* orthologues. Bootstrap values and numbers assigned to the branches are represented above and below the branches of each tree.

4.3.1.2 Phylogenetic analysis by maximum likelihood

PADI2 orthologues were further analysed to detect evidence of selection at codon sites using PAML software. The maximum likelihood method was used for detecting adaptive evolution in *PADI2*. The parameter (**ω**) ratios and the likelihood of sequence evolution was estimated by Empirical Bayes and represented in Models 0, 1a, 2, 3, 7 and 8. The likelihood results were then compared to detect variation in the **ω** ratio between sites and lineages. Therefore, the loglikelihood values from the null hypothesis models; M0, M1a and M7, were compared to the alternative analysis models; M3, M2 and M8 respectively. 2*(log likelihood M1a – log likelihood M2) $\chi 2$. The difference between the null and alternative hypothesis was measured by calculating the probability between the different models. In PAML, the comparison between site models detects positive selection only if the ω ratio averaged over all branches of the tree is (>1, Gharib and Robinson-Rechavi, 2013). The calculated *p*-values for likelihood ratio tests were not above 1 (≤1), therefore, were not significant between different models. This is indicative that there is no evidence of *PADI2* positive selection amongst all 31 species (**Table 4.1**).

Table 4.1. Log-likelihood values and parameter estimates for *PADI2* sequence in 31 vertebral species using PAML analysis

	Null Hypothesis				Alternative Hypothesis				
Test	**Model**	**Model description**	**Parameters**	**Log-likelihood**	**Model**	**Model description**	**Parameters**	**Log-likelihood**	**P-value**
Codon variation	0	One ratio	ω	23802.53	3	Discrete ratios	$\omega_0, \omega_1 \omega_2$	-23046.06	0
Natural selection	1a	Nearly neutral	$0 < \omega_0 < 1$ $\omega_1 = 1$	-23476.14	2a	Positive selection	$\omega_0 < 1$ $\omega_1 = 1$ $\omega_2 > 1$	-23476.14	1
Alternative selection (beta)	7	Beta	p, q	-23039.21	8	Beta & ω	$\omega_s > 1$	-23039.21	1

Positive selection sites are with P>95%

4.3.2 Overall amino acid sequence conservation in PADI2

Accurate sequence alignment of protein functions is the key to understanding their cellular physiology. The aligned nucleotide sequences of *PADI2* orthologues were used to predict the evolutionary status of the subsequent amino acid sequence. Full-length human PADI2 contains 664 amino acid residues, whereas sequence alignment analysis of *PADI2* orthologues resulted in a truncated protein sequence with a total length of 613 amino acids. The truncated PADI2 amino acid sequences were then colour coded by PyMOL to depict the evolutionary status of the corresponding amino acid (red: neutral, green: positive and yellow: conserved). The sequence alignment between more divergent species (e.g. between bonytongue and human) can result in minimal aligned sequence, subsequently leading to the identification of only highly conserved protein regions (McCauley *et al.*, 2007). The amino acid residues, which play an important role in protein function, are often conserved. These residues are usually clustered together in a functionally important locations, such as protein-ligand binding sites (Ahmad *et al.*, 2008). Therefore, an analysis of residue conservation is a reasonable approach to identify functionally important residue/sites in the PADI2 protein. Previously determined PADI2 domains (PAD, PAD_M and PAD_N), protein ligands (MPD, CA, ACT) (**supplementary material S3**) and Ca^{2+} ion binding sites by Slade *et al.*, (2015) were also mapped on the PADI2 amino acid sequence in the current study. Interestingly, PAD and PAD_M domains harbouring the active site and calcium binding sites (Ca3-5), have a higher proportion of conserved amino acid sequences (11%) and (16%), respectively, compared to PAD_N domain (37.5%). Also, highly conserved amino acid sequences were observed at Ca1, 2 and 6 binding sites (**Figure 4.2**).

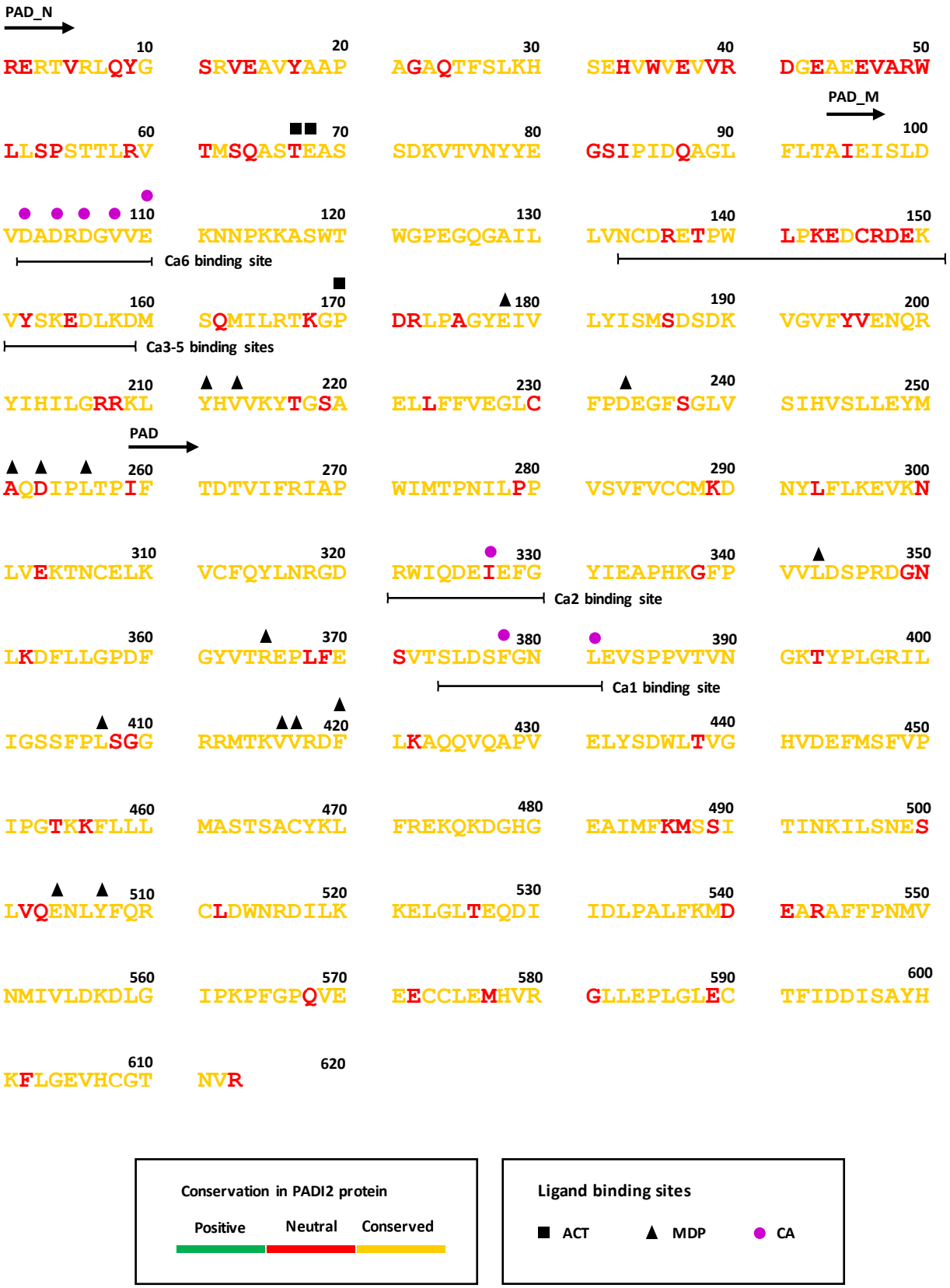
PAD_N
PAD_M
Ca6 binding site
Ca3-5 binding sites
PAD
Ca2 binding site
Ca1 binding site
Conservation in PADI2 protein
Positive
Neutral
Conserved
Ligand binding sites
ACT
MDP
CA

Figure 4.2. The retrieved amino acid sequence of human PADI2. The amino acids sequence alignment from phylogenetic analysis across 31 vertebral species as determined by Bayes Empirical Bayes output from PAML. The amino acid residues are represented by different colours, i.e. yellow; conserved, red; neutral selection and green; positive selection. The position of amino acid residues that correspond to the catalytic sites, including ligand binding sites and Ca^{2+} binding sites (Ca1-6), according to (Slade *et al.*, 2015) were mapped. The ligand binding sites of ACT, MDP and CA, are represented by different coloured shapes. ACT, acetate ion; MPD, (4S)-2-methyl-2,4-pentanediol; CA calcium ion.

4.3.3 Overall PADI2 3D/2D structures

Structural genomics efforts have enabled exponential growth in the determination of structure-based prediction of proteins' function. The aligned PADI2 codon selection data, were mapped to the published 3D/2D structures. The relationship between structure and conserved sequence features was examined by establishing the tertiary and secondary structure elements distribution. The PADI2 structure was shown in a similar orientation using the same colour scheme. The PADI2 sequence signatures (i.e. ligand binding sites) and protein domains were previously determined by Slade *et al.*, (2015). These signatures were re-mapped onto the truncated PADI2 3/2D structure. Online available tools, such as Pfam (HMMR), superfamily, Gene3D and EMBL-EBi were used to identify the position of the corresponding residues on the truncated PADI2 amino acid sequence. Collectively, these tools identified the different domains of PADI2 (i.e. N- and C- terminal domains) and recognised the positions of Ca^{2+} (Ca1-6) binding sites and ligand binding sites (MDP, CA and ACT). The C-terminal domain (residues 269–613), also known as PAD or α/β propeller domain, is a highly conserved domain that includes the proteins' active site and Ca1 and Ca6 binding sites (Linsky, 2012). The N-terminal domain is subdivided into two immunoglobulin-like subdomains: Immunoglobulin (Ig) subdomain or PAD_N (residues 3–94) and Immunoglobulin (Ig) subdomain II or PAD_M (residues 95–268). The majority of ligand binding sites are projected out of the binding pockets, which is formed by a relatively large external cavity that is highly accessible to solvents. These binding pockets mainly consist of conserved amino acid side chains, suggesting that these residues do not only play a role in ligand binding specificity, but also in interaction with partners, such as receptors (**Figure 4.3**).

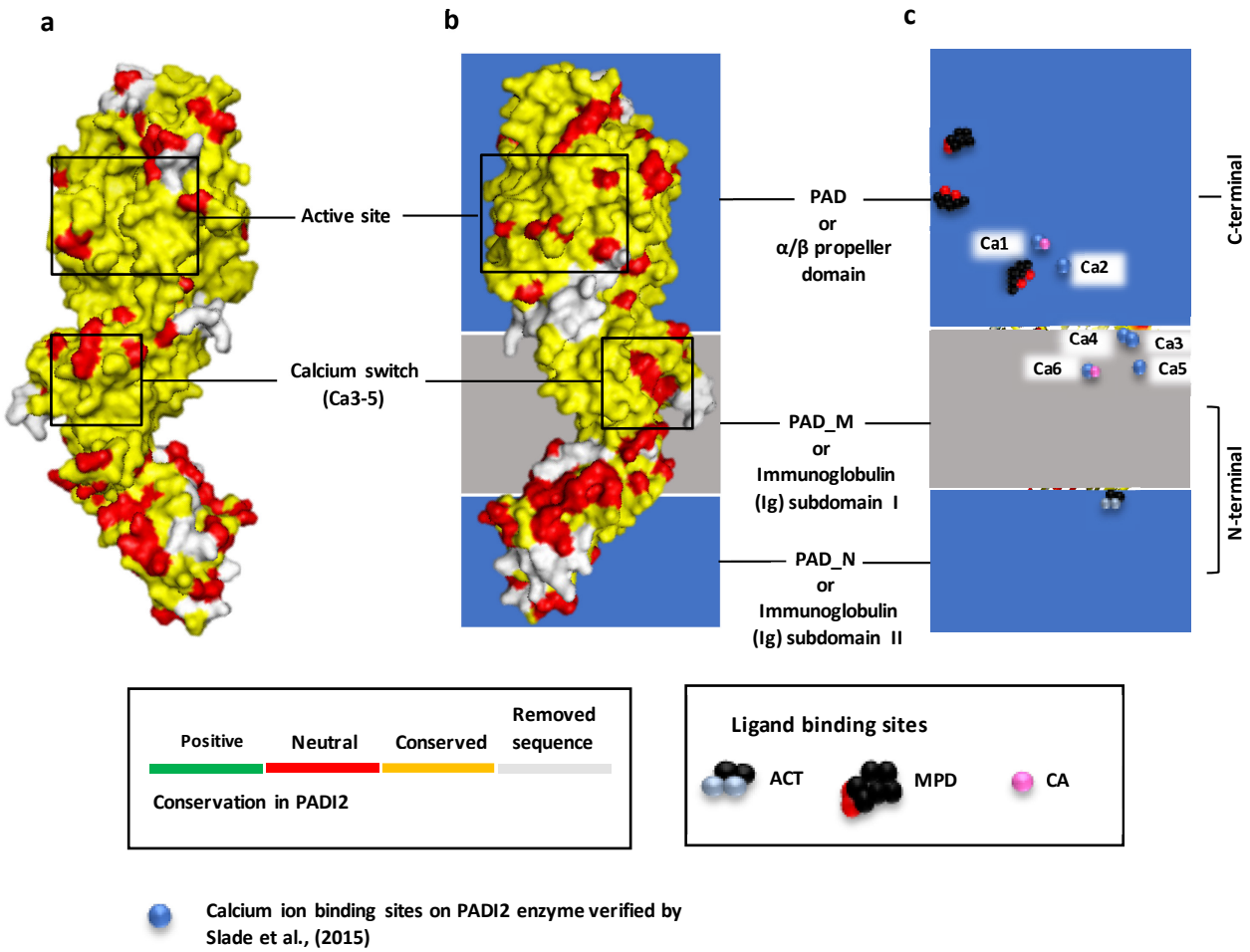

Figure 4.3 PADI2 3D and 2D structures. The amino acid residues are represented by different colours, i.e. yellow; conserved, red; neutral selection and green; positive selection. The position of amino acid residues that correspond to the catalytic sites, including ligand binding sites and Ca^{2+} binding sites (Ca1-6), according to (Slade *et al.*, 2015) were mapped. **(a)** PADI2 shows neutral and conserved selection. **(b)** An alternative view of PADI2 (rotated-180 degrees). **(c)** Ribbon presentation PADI2 tertiary structure including PADI2 domains. The ligand binding sites of ACT, MDP and CA, are represented by different coloured shapes. ACT, acetate ion; MPD, (4S)-2-methyl-2,4-pentanediol; CA calcium ion.

4.4 DISCUSSION

4.4.1 *In silico* identification and phylogenetic analysis of *PADI2* sequences across diverse species

PADI genes are expressed widely in various species and share significant identities at the level of their coding nucleotide sequences (Chavanas *et al.*, 2004). Although PADI isozyme sequences display high homology and their patterns of expression were suspected to concur this homology; however, each PADI gene has its specific pattern of expression depending on the tissue, cell type or cellular differentiation stage (Guerrin *et al.*, 2003). Previous work on PADI genes, along with the rapidly expanding availability of genomic sequence data, has enabled the examination and comparison of PADIs across diverse genomes. Several recent reports confirmed the expression of all five PADI isotypes in mammals, such as human (*Homo sapiens*), rat (*Rattus norvegicus*) and mouse (Mus musculus), (Ying *et al.*, 2009). The five mammalian PADI isozymes are highly conserved with 70-90% amino acid sequence homology between human paralogs (Méchin *et al.*, 2007). Furthermore, PADI genes are clustered on a single chromosomal locus (chromosome 1p36.1) and display high nucleotide sequence homology in exons with the same exon/intron structure (Ying *et al.*, 2012).

It has been proposed that genes with highly conserved sequences is suggestive of functional significance and therefore are likely to be under selective constraint (Bergmiller et al., 2012; Davies et al., 2015). Mammalian *PADI2* is the most phylogenetically conserved PADI isozyme, and it contains amino acid residues corresponding to two highly conserved domains involved in the enzymes' catalytic activity and Ca^{2+} binding sites (Rebl *et al.*, 2010). The importance of *PADI2* enzyme and hypercitrullination have been established in many neurodegenerative human disorders and cancers (Chirivi *et al.*, 2013). However, the mechanisms regulating PADI2 activation and its physiological roles in a non-pathologic setting remain poorly understood (Chirivi *et al.*, 2013). While the origin and evolution of the PADI isotypes have been previously studied, the evolutionary history of *PADI2* in various organisms is not yet elucidated. The aim of this chapter was to determine the protein structure and evolutionary relationships of *PADI2* orthologues across various species. This was achieved by employing various tools to establish the phylogenetic relationship of full length *PADI2* orthologues and the reconstruction of PADI2 3D and 2D structures. The phylogenetic analysis of gene expression in diverse species can serve as the foundation for "evolutionary synthetic biology," to provide better understanding

of cellular pathway evolution, macromolecular machines and other emergent properties of early life (Losos *et al.*, 2013; Yuan *et al.*, 2014). While this approach was devised for P*ADI2* individually in this thesis, this gene has been previously explored in a multigene family phylogenetic analysis that includes all PADI isoforms and other comparative methods for the analysis of gene evolution (Magnadóttir *et al.*, 2018; Wang and Wang, 2013; Witalison *et al.*, 2015). However, a limited number of studies have investigated *PADI2* phylogenetic evolution, among a small range of different species, including rhesus monkey, chimpanzee, mouse, dog, chicken, rat, frog and zebrafish (Hosokawa *et al.*, 2018). These studies showed that human *PADI2* orthologues were found to be conserved amongst all five organisms. Likewise, the current study included a larger number and more diverse species (i.e. 31 organisms), including fish, aves, mammals and amphibians, in addition to newly available sequences from species, such as Miniopterus Natalensis bat (Stoffberg *et al.,* 2004). While the oldest marsupial and placental mammals divergence were estimated between 125 and 175 million years ago, various estimates place the teleost-bony fish divergence at almost 400 million years ago (Grimholt *et al.*, 2015). The identification of *PADI2* in teleost fish (bony fish species, e.g. Catfish, Piranha, Molly, Bonytongue and Vulus) is exciting, as it indicates that PADI2 is of a very ancient origin and will likely be found in most, if not all, cartilaginous and teleost fish species. The bony tongue fish (Osteoglossomorpha), belong to the most ancient living teleost groups, this fish represent a phylogenetic link between the old world fish and the modern teleost (O'Neill *et al.*, 1998). However, the much more diverse and familiar species of teleost arose at about the same time as modern birds and placental mammals including humans (*Homo sapiens*), Olive baboon, about 120 to 60 million years ago (Near *et al.*, 2012). PADI2 also occurred in more recently evolved species such as horse (55 million years), Donkey (*Ass*, 5000 years) and variety of bat species (35 million years). This study provides evidence for conservation and concerted evolution of *PADI2* sequence in some of the oldest and newly diverged species.

The most important finding presented in this study is that *PADI2* is highly conserved throughout evolution. The use of 31 different species, with diverse annotation levels and evolutionary distances, contributed to the robustness of the results obtained from both phylogenetic and structural analysis of PADI2 in the current study. The PADI2 sequence conservation resulted in a reliable phylogenetic relationship that may correlate with the structural and physiological traits of the organisms associated. It may also contribute to further the understanding of the conserved roles of *PADI2* throughout phylogeny. Indeed, the

depth and breadth of conservation of PADI2 sequence is indicative of possible vital regulatory and/or developmental roles (Carroll, 2008; Rokas, 2008; Ingham *et al.*, 2011).

4.4.2 Functional analysis of PADI2 domains

While sequence and phylogenetic analysis provide a relatively simple way of viewing protein sequence divergence, the comparison of protein tertiary structure 3D models can provide more insight into a protein's evolution. Previously, researchers have examined the detection of functional 3D patterns associated with atom interactions or/and active sites (Nebel *et al.*, 2007). Slade et al., (2015) previously determined the PADI2 3D structure using its full-length amino acids component (human PADI2 comprises of 668 amino acids) to build the crystal structure. They also showed the organisation of PADI2 domains and identified functionally significant residues that are associated with the active site and other functionally important sites, such as Ca^{2+} binding sites (Slade et al., 2015). Herein, the aligned PADI2 codon selection data obtained from the sequence alignment of 31 species, were mapped to the published 3D/2D structures. The previously identified PADI2 domains and key residues were also re-mapped on the truncated PADI2 3D structure in this study. The findings in this study illustrate the important utility of 3D protein structure in the interpretation of important information about the function of the PADI2 protein (Medvedeva *et al.*, 2015). The most important functional residues reside in relatively more conserved domains of PADI2 protein. For example, among the identified PADI2 domains, the PAD domain which includes the active site and PAD_M domain that contains the calcium switch, show the highest amino acid sequence conservation; 89% and 84% (conserved amino acid sequence), respectively. Whereas, PAD_N domain shows the least amino acid sequence conservation (62.5%). This is not surprising, since it was previously hypothesised that the calcium-switch (Ca3–5) is a key regulator of PADI2 function and may be evolutionarily maintained to sustain its function. By convention, domains are defined as conserved, functionally independent protein sequences, which use a core structural motif to bind or process ligands (Castagnoli *et al.*, 2004; Kuriyan and Cowburn, 1997; Doolittle, 1995). The folding of a domain is mainly based on a complex network of sequential inter-molecular interactions in time. These interactions have significant implications for domain integrity, particularly if the core of a protein domain is largely structurally conserved (Slade *et al.*, 2015).

Moreover, del Sol *et al.*, (2006) showed that residues mediating the enzyme's function, such as catalytic residues, those forming the ligand-binding pocket, or residues involved in protein-protein interactions, have high centrality values (residues located in a central position of protein crystal structure). A more detailed study by Sol et al., (2015) on 46 different protein families, revealed that a total of 80% of these proteins central domains/positions corresponded to active site residues or residues in direct contact with catalytically important sites. Furthermore, the geometrical analysis of the functional sites of these enzymes also revealed that centrally conserved amino acids can be predictors for the catalytic site residues and are clustered with functionally important active site residues situated in protein surface clefts or cavities. These studies show that residue centrality, as an inherent fold characteristic, maybe evolutionarily maintained to sustain a proteins' function (del Sol *et al.*, 2006b). While, mammalian PADI2 shares 70–95% amino acid sequence homology with other PADI family members, the residues corresponding to the calcium-binding sites (Ca3– 5) that reside in the centrally located PAD_M domain are highly conserved throughout evolution (Raijmakers *et al.*, 2007). Given that the centrally located calcium switch (Ca3–5) are highly conserved among PADI2 orthologues and all the PADI paralogs, this may furthermore indicate its importance as a key regulator of PADI2 activity/function. It may also suggest that it is likely a universal feature of the PADIs. In contrast to Ca3-6, the Ca1 and Ca2 sites are located in the PAD domain containing the active site. Ca1 and Ca2 bind calcium ions independently of the other calcium binding sites. The active site of PADI2 was found to be highly conserved, even where sequence identity was very low. Collectively, residues that correspond to both active site and Ca^{2+} binding sites are highly conserved as a results of evolutionary constraints placed upon the residues corresponding to these sites, which need to be in an optimal position to be most effective during catalysis (Jack *et al.*, 2016).

4.5 CONCLUSIONS

In summary, the *PADI2* gene was found in diverse vertebrate and invertebrate organisms with conserved gene and protein characteristics. The important characteristics of the PADI2 protein structure were identified/re-mapped and found to be conserved among various species. These characteristics include important amino acid residues that correspond to functionally important catalytic sites, such as Ca^{2+} binding sites and ligand binding sites. These findings are particularly important as they imply that *PADI2* is evolutionarily maintained to

sustain its important function and is also suggestive of a role for PADI2 in regulation and/or development (Carroll, 2008; Rokas, 2008; Ingham *et al.*, 2011).

CHAPTER 5: Potential role of PADI2-mediated citrullination in EOC pathogenesis

5.1 INTRODUCTION

The identification of new biomarkers specific to cancer subtypes and individual patients is crucial for developing personalised treatment, in terms of evaluating both disease risk and therapy response (Hayes *et al.*, 2014). Thus, cancer biomarkers can also serve in diagnosis and contribute to improving the outcome of cancer chemotherapy (Kamel and Al-Amodi, 2017). The PADI2 enzyme and citrullinated proteins are associated with various human diseases including cancer. In addition, increasing clinical evidence suggests that PADI2 has important roles in tumour progression. PADI2 was previously identified as an oncogene, potential biomarker and important therapeutic target in breast cancer (McElwee *et al.*, 2012; Wang *et al.*, 2016). The dysregulation of PADI2 expression was shown to affect cellular activity in various cancers, such as breast, prostate and colorectal; however, the role of PADI in EOC is yet to be investigated. This study aims to elucidate the role of PADI2 in EOC. Given the emerging links between *PADI2* and tumorigenesis, a better understanding of the upstream mechanisms that induce *PADI2* expression, and the downstream mechanisms by which PADI2 regulate cell activity will contribute to better understanding of the EOC biology. Furthermore, the overexpression of PADI2 enzyme and its activity at critical points of tumour progression raises the possibility that this enzyme, and the resulting post-translational modifications, may have utility as a novel EOC biomarker and therapeutic target. There have been conflicting studies on the role of PADI2 in cancer. On the one hand, numerous reports have revealed that *PADI2* expression contributes to the tumorigenesis of some cancers and is associated with poor patient prognosis (McElwee *et al.*, 2012; Wang *et al.*, 2016; Horibata *et al.*, 2017). Conversely, other studies indicated that PADI2 expression reduced tumour growth and its downregulation is an early event of carcinogenesis (Cantarino *et al.*, 2016; Funayama *et al.*, 2017). Collectively, these inconsistent observations suggest that PADI2 can act as either a tumour promoter or a suppressor in a context. These observations also suggest that PADI2 may have different roles in different cancers or cancer subtypes. For this purpose, investigating PADI2's role in different molecular EOC subtypes may provide more insight into the mechanisms regulating PADI2-subtype specific function and downstream effect on cellular activity, including proliferation, apoptosis, autophagy, necrosis and aggregation.

It was previously determined that PADIs are Ca^{2+}-dependent enzymes that require Ca^{2+} concentrations ranging from 40µM to 3.3mM to efficiently citrullinate protein substrates (Damgaard *et al.*, 2014). Furthermore, according to a crystallographic study by Slade *et al.*, (2015), they confirmed that Ca^{2+} is a key regulator and a critical prerequisite for PADI2 enzyme-substrate binding. However, the conditions required for this reaction to take place in *in vitro* cultures are unknown. The current novel work aims to elucidate whether high Ca^{2+} concentrations are required to induce PADI2 function in *in vitro*.

5.2 AIMS AND OBJECTIVES

The aim of this chapter is to elucidate the role of PADI2 overexpression and explore its Ca^{2+}-dependent regulation *in vitro.* The effect of PADI2 overexpression on downstream effect on cellular activity, including proliferation, apoptosis, autophagy, necrosis and cellular aggregation was evaluated in human OVCAR-4 and mouse ID8-Luc2 cells. In addition, this work determines whether PADI2 expression contributes to tumorigenesis by increasing resistance to cisplatin chemotherapy in EOC cells. The objectives were to:

1. Determine the endogenous expression levels of PADI2 in a panel of nine EOC cell lines.

2. Transfect a human PADI2 overexpression construct into the mouse ID8-Luc2 and human OVCAR-4 cell lines to determine the effect upon citrullination within these cells.

3. Measure the functional effect of overexpressing PADI2 in EOC cell lines on cell proliferation apoptosis, autophagy, necrosis and cellular aggregation.

5.3 RESULTS

5.3.1 Detection of PADI2 endogenous expression in EOC cell lines

The deregulation of PADI2 expression was previously linked to human cancer development and progression (Liu *et al.*, 2014). To study the function of PADI2 in EOC and assess whether it affects cellular chemoresistance to cisplatin, PADI2 expression was initially evaluated in a panel of nine EOC cell lines.

5.3.1.1 Optimisation of PADI2 and PADI4 monoclonal antibodies for Western blotting

It is possible for an antibody to be sensitive for a protein of interest but still cross-react with other closely related proteins and therefore lack specificity. To optimise the specificity of PADI2 monoclonal antibody, PADI4 recombinant protein was also used as an experimental validation control to determine if there was a cross-reactivity with Western blotting experiments. A PADI4 monoclonal antibody was also used to detect the optimum amount of PADI4 recombinant protein required to be detected by Western blotting.

Both anti-PADI2 (Santa Cruz, USA) and anti-PADI4 (Abcam, UK) antibodies' sensitivity were initially optimised using serial dilutions of recombinant proteins and thereafter analysed using SDS-page and Western blotting. 1µg was determined as the optimal recombinant protein concentration required as loading positive control for both PADI2 and PADI4 recombinant proteins (**Figure 5.1**).

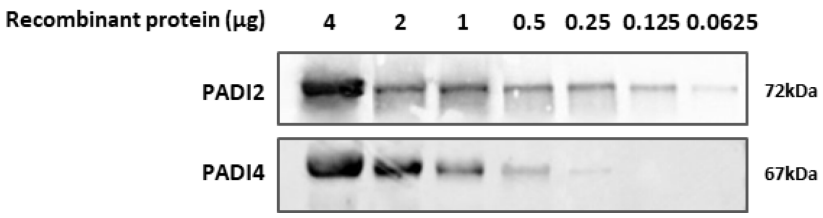

Figure 5.1. Western blotting and SDS-page analysis of the recombinant PADI2 and PADI4 proteins different concentrations. Both anti-PADI2 and anti-PADI4 antibodies' sensitivity were initially optimised using serial dilutions of recombinant proteins and thereafter analysed using SDS-page and Western blotting**.** Results are representative of three independent experiments.

5.3.1.2 Expression of endogenous PADI2 in EOC cell lines

To determine whether endogenous PADI2 is expressed in EOC cell lines, qRT-PCR and Western blot analysis was performed on a panel of nine EOC cell lines, including SKOV-3, ID8-Luc2, OVCAR-3, OVCAR-4, OVCAR-5, OVCAR-8, OVCA-433, OAW42 and TOV-112D (**Figure 5.2a and 5.2b**). Although, PADI2 mRNA expression levels were significantly higher in TOV-112D, OVCAR-8, and OVCAR-3 compared with the remaining cell lines. However, the subsequent analysis by Western blotting showed that PADI2 protein was not expressed in any of the cell lines tested. In parallel, recombinant PADI2 protein and C2C12, murine muscle cell line, were used as positive controls to confirm PADI2 antibody's sensitivity.

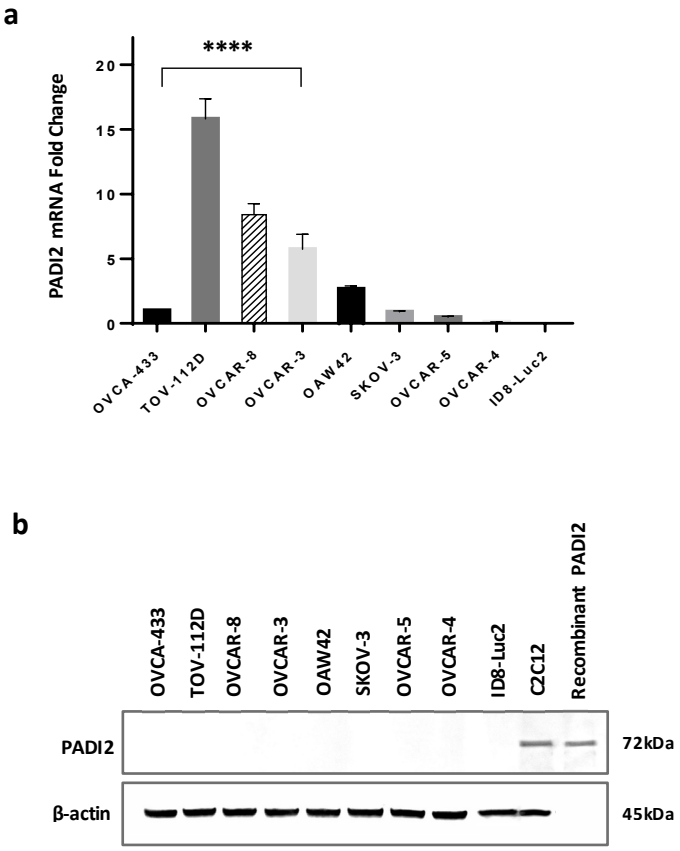

Figure 5.2. The expression of endogenous PADI2 in EOC cell lines. (a) Transcript levels of PADI2 were determined by qRT-PCR. Representative bar graphs of average PADI2 transcription levels normalised to 18S mRNA levels. Results are representative of the average fold change ± SD of triplicate independent experiments relative to the untreated controls. Bars are presented as mean ± SD (n = 3). ****$p \leq 0.0001$. (**b)** Cell lysates were analysed by SDS-PAGE and Western blotting using antibodies specific to PADI2. Recombinant PADI2 and C2C12; murine muscle cell line, were used as positive controls. Results are representative of independent experiments.

5.3.2 PADI2 overexpression analysis in EOC cell lines

5.3.2.1 Determination of pcDNA3.1+-DYK PADI2 and empty vector plasmids transfection efficiency in EOC cell lines by flow cytometry

PADI2 overexpression vector (pcDNA3.1+-DYK) and empty vector (pcDNA3.1+-DYK) were co-transfected with a fluorescent GFP containing plasmid (pCMV-GFP) into SKOV-3 and ID8-Luc2 cell lines. Transfection efficiency was then assessed using flow cytometry. Plasmid DNA (pcDNA3.1+-DYK and GFP plasmids) was transfected into cells at different ratios (1:1 and 3:2, to give a total amount of 5µg). At 48 hours post-transfection, cells were trypsinised and re-suspended in PBS/10% FCS. Transfection efficiency was then assessed by measuring the intracellular GFP expression using flow cytometry. To determine the transfection efficiency of the co-expressed plasmid in cells, the collected flow cytometry data was then analysed using Flowing software. In the analysis, cellular debris were excluded by gating cells on the forward and side scatter (FSC linear and SSC log) parameters and the background fluorescence intensity of mock-transfected (treated with Lipofectamine 3000) cells were subtracted to eliminate background fluorescence (**Figure 5.3a**). The histograms produced by the Flowing software, represented the transfection efficiency (x-axis) percentages of control empty vector and PADI2 overexpression vector in SKOV-3 and ID8-Luc2 cells. The transfection efficiency at 2.5µg DNA of co-transfected control empty vector and PADI2 overexpression vector in SKOV-3 cells were 50.8% and 51.9%, and in ID8-Luc2; 51.1% and 30.3%, respectively. Whereas the transfection efficiency at 3µg DNA in SKOV-3 cells were 42.4% and 38.6%, respectively (**Figure 5.3b**).

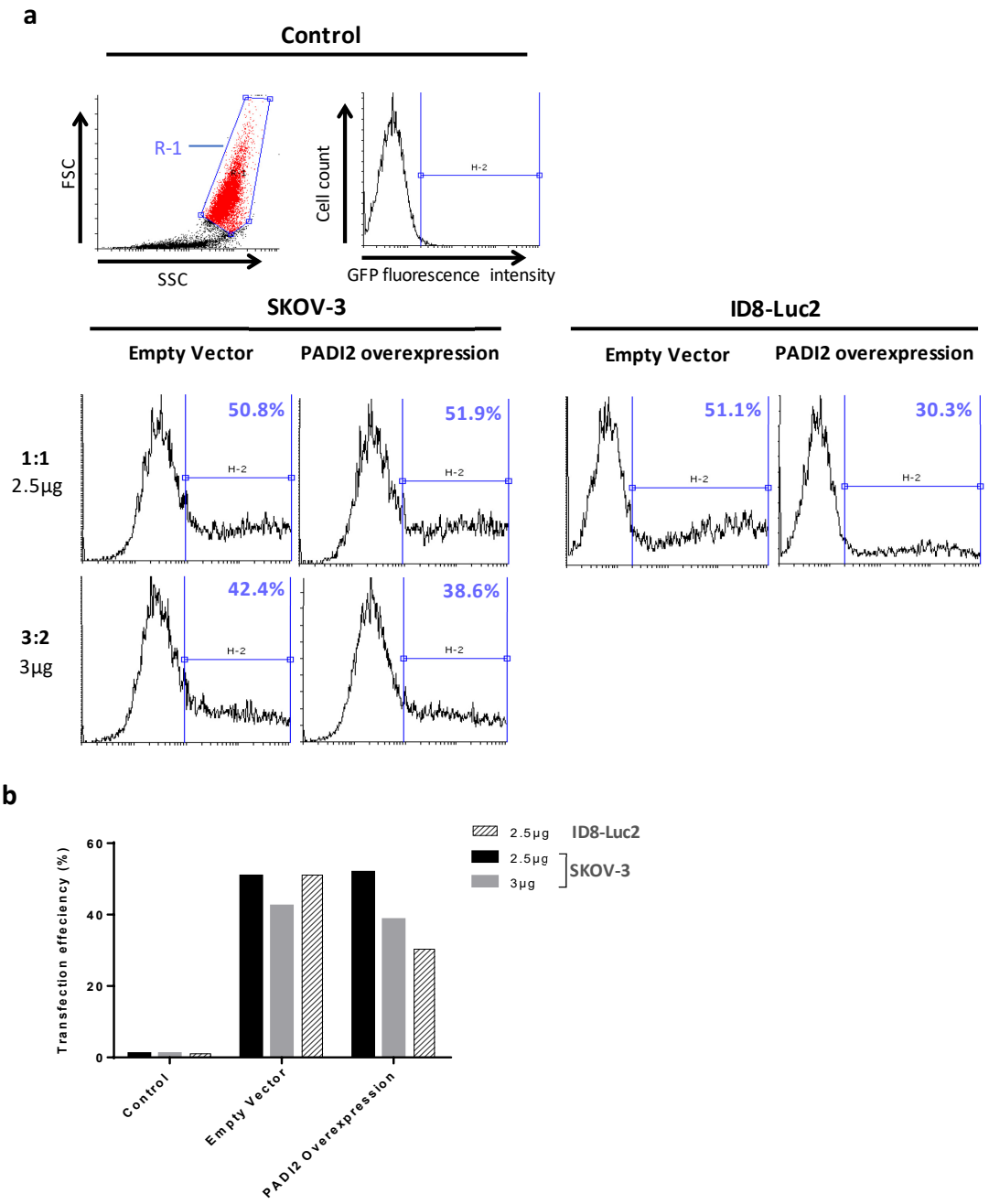

Figure 5.3. Flow cytometry analysis of PADI2 expression vector and empty vector transfection efficiency in SKOV-3 and ID8-Luc2 cell lines. Cells were transiently co-transfected with 2.5 µg GFP (pCMV) at different concentrations (2.5-3µg) of the PADI2 overexpression vector or control empty vector using Lipofectamine 3000. The concentration of the co-transfected GFP vector with each of the expression vectors are also indicated with ratio values (for clarification). At 48 hours post-transfection, cells were resuspended in PBS/10% FBS and then analysed by flow cytometry. **(a)** Representative dot plot of side scatter and forward scatter displaying the gated events of viable cells (R-1). The flow cytometric histograms were analysed to determine the transfection efficiency percentages by measuring the average fluorescence intensity relative to the control (Lipofectamine 3000). The marker H-2 that encompasses the GFP fluorescent peak in histograms was used to evaluate transfection efficiency percentages. **(b)** Bar graph representation of plasmids transfection efficiency percentages in EOC cell lines.

5.3.2.2 Enrichment of SKOV-3 and ID8-Luc2 cells transfected with PADI2 gene

To allow more accurate interpretation of the effects of PADI2 overexpression in EOC cell lines, optimal concentrations of the mammalian antibiotic, geneticin (G418), enrichment was determined. This was achieved by applying different antibiotic concentrations to non-transfected cells for seven days. The cell viability was then determined using trypan blue method (**Figure 5.4a**). On day two of enrichment, IC50 values were then determined by plotting the cell viability percentages on a semi-log-dose-response graph. 50% of the cell population died in SKOV-3 and ID8-Luc2 lines at G418 concentrations; 988.6µg/ml and 729.7µg/ml in SKOV-3 and ID8-Luc2, respectively (**Figure 5.4b**).

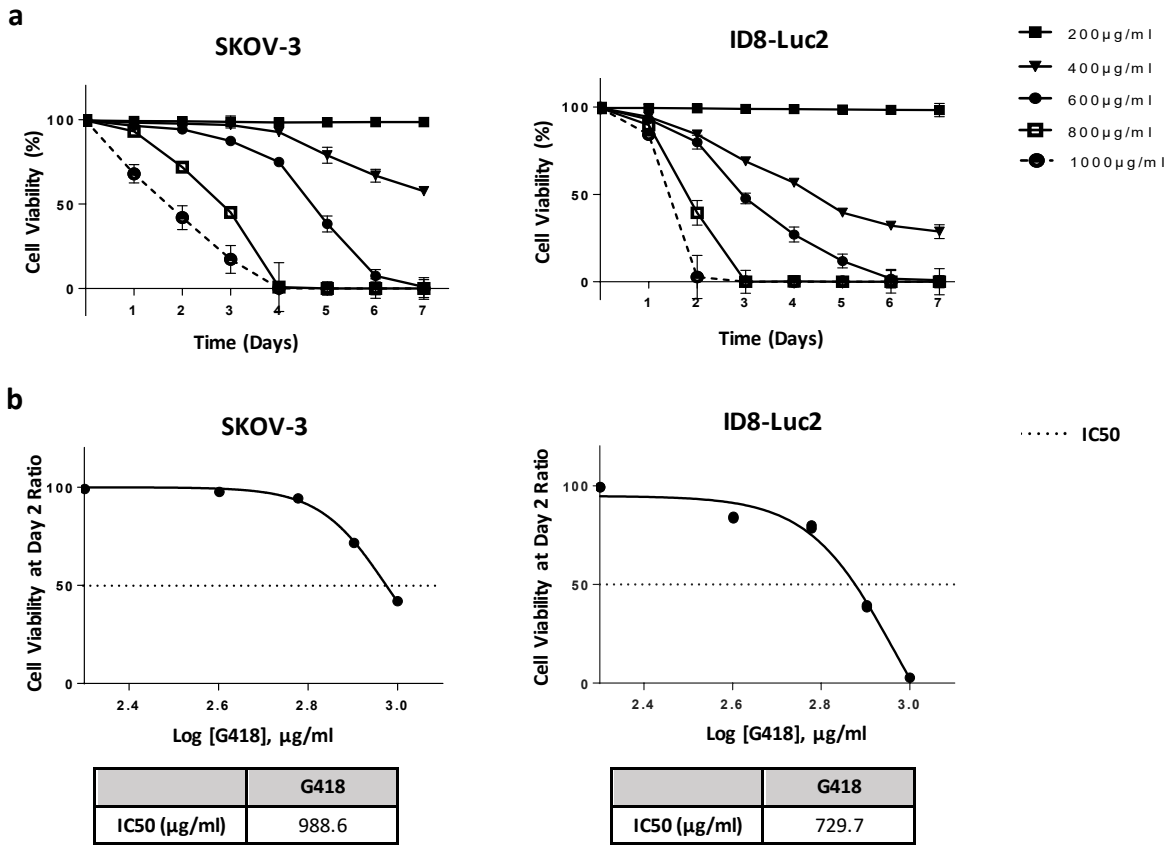

	G418
IC50 (µg/ml)	988.6

	G418
IC50 (µg/ml)	729.7

Figure 5.4. The percentage of cell viability in SKOV-3 and ID8-Luc2 cells after treatment with G418 (200-1000µg/ml). (a) Cells were incubated for total of seven days and cell viability was measured every 24 hours using 1% trypan blue. Percentage viability values were represented in time-kill curves. **(b)** G418 Log-dose response curves were used to determine the IC50 values at day two; 988.6µg/ml and 729.7µg/ml in SKOV-3 and ID8-Luc2, respectively. Results are representative of the average percentages of ± SD of duplicate independent experiments relative to the untreated controls. Bars are presented as mean ± SD (n = 3).

5.3.2.3 PADI2 overexpression was absent in the human cell line SKOV-3 and did not affect protein citrullination in the murine cell line ID8-Luc2

To determine whether PADI2 expression levels affect the total citrullination in SKOV-3 and ID8-Luc2 cell lines, first, cell lines were transfected with 2.5µg PADI2 overexpression vector or control empty vector for a duration of 48 hours. The transfected cells were then subjected to G418-enrichment for additional 48 hours. The surviving cells were resistant to G418, indicating successful delivery of plasmids into cells. At 96 hours post transfection and enrichment, the mRNA and protein expressions levels of PADI2 were detected in each cell line using qRT-PCR and Western blotting, respectively. The two detection methods produced inconsistent results in SKOV-3 cell lines (**Figure 5.5a and 5.5b)**. *PADI2* mRNA expression was detected in PADI2 overexpressing SKOV-3 cells; however, subsequent analysis of the transfected cells by Western blotting did not detect protein expression. Conversely, both the *PADI2* mRNA and protein expression was detected in PADI2 overexpressing ID8-Luc2 cells (**Figure 5.5c and 5.5d**). PADI gene family members share similar sequences and functional domains, therefore PADI4 recombinant was used to confirm the specificity of the PADI2 antibody. Since it was previously established that Ca^{2+} induces the activation of PADI isozymes and subsequently catalyse PADI2-citrullination reaction. Therefore, it is important to assess this *in vitro*, and determine whether increasing e[Ca^{2+}] could affect the total PADI2-induced citrullination in PADI2 overexpressing cells. At 96 hours post transfection, PADI2 overexpressing ID8-Luc2 cells were incubated in 1mM $CaCl_2$ (e[Ca^{2+}]) for a duration of 72 hours. However, citrullination was not detected irrespective of Ca^{2+} treatment (**Figure 5.5d**).

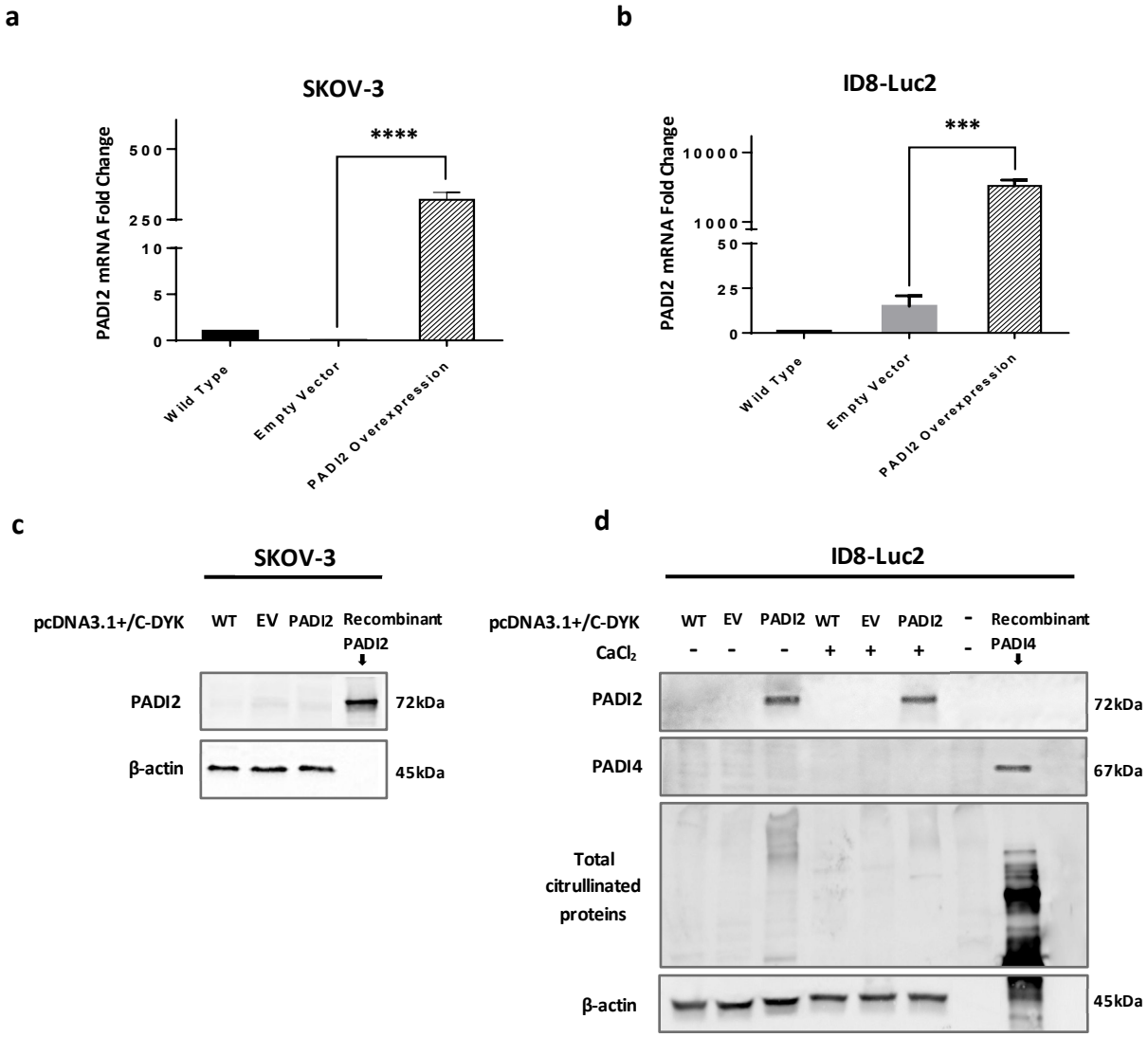

Figure 5.5. The effect of overexpressing PADI2 on total protein citrullination in SKOV-3 and ID8-Luc2 cell lines treated with $CaCl_2$. Cells were transiently transfected with PADI2 overexpression vector (PADI2) and control empty vector (EV). **(a)** and **(b)** At 96 hours post-transfection and enrichment, *PADI2* mRNA expression levels were determined by qRT-PCR. Representative bar graphs of average PADI2 transcription levels normalised to 18S mRNA levels. Results are representative of the average fold change ± SD of triplicate independent experiments relative to the untreated controls. Bars are presented as mean ± SD (n = 3). ***$p \leq 0.001$; and ****$p \leq 0.0001$. **(c)** and **(d)** At 96 hours post-transfection and enrichment, cells were incubated in the presence and absence of 1mM $CaCl_2$ for 72 hours. Cell lysates were assessed for PADI2 protein and total citrullination by Western blot using antibodies specific to PADI2 and citrulline. Recombinant PADI2 and C2C12, murine muscle cell line, were used as positive controls. Representative blots for quantification of PAD2 were normalized to β-actin in the lower panel.

To better examine the effect of PADI2 overexpression in EOC, it was helpful to use more than one EOC cell line. Furthermore, using different cancer cell lines will help better explore the possible functions of PADI2 in EOC tumorigenesis. Since PADI2 protein was not detected in PADI2 overexpressing SKOV-3 cells (**Figure 5.5b**), as a result, this cell line was not used as *in vitro* model to examine PADI2 function in EOC. Therefore, the OVCAR-4 cell line was selected as an alternative EOC cell line model. Similarly, G418 IC50 values were initially determined for OVCAR-4 cell line, followed by transfection experiments, qPCR and Western blotting analysis of OVCAR-4 control empty vector and PADI2 overexpression transfected cells.

5.3.2.4 Enrichment of OVCAR-4 cells transfected with PADI2 gene

Cell viability was determined using trypan blue method. On day two of enrichment, IC50 values were then determined by plotting the cell viability percentages on a semi-log-dose-response graph (**Figure 5.6a**). 50% of the cell population died in OVCAR-4 cell line at G418 concentration estimated to 943.6µg/ml (**Figure 5.6b**).

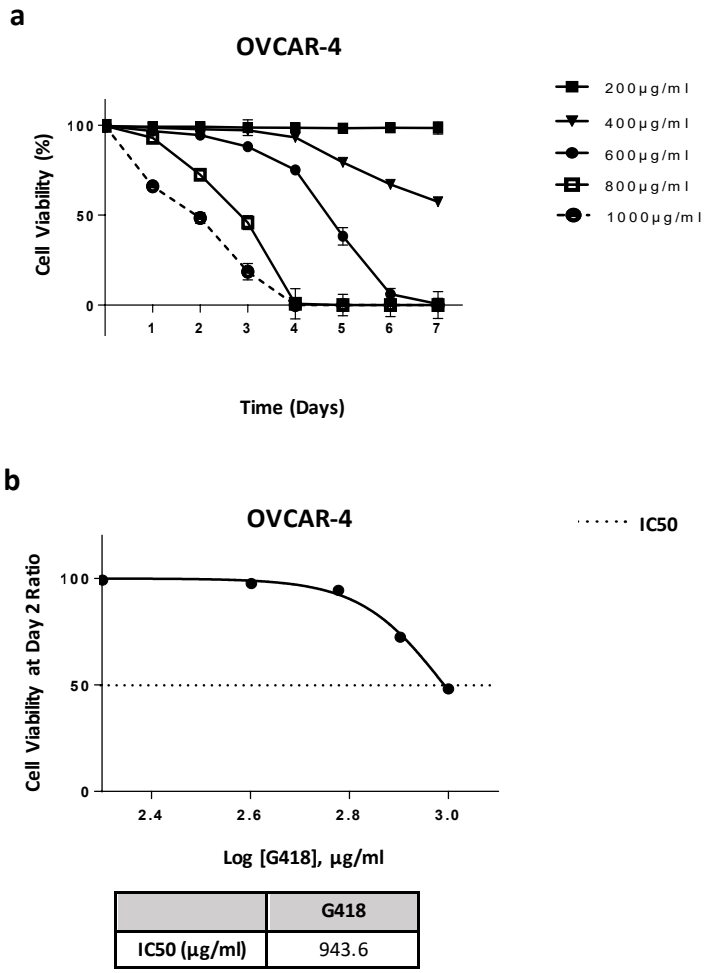

	G418
IC50 (µg/ml)	943.6

Figure 5.6. The percentage cell viability of OVCAR-4 cells in the presence of G418 (200-1000µg/ml). (a) Cells were incubated for total of seven days and cell viability was measured every 24 hours using 1% trypan blue. Percentage viability values were represented in time-kill curves. **(b)** G418 Log-dose response curves were used to determine the IC50 value at day two; 943.6µg/ml. Results are representative of the average percentages of ± SD of duplicate independent experiments relative to the untreated controls. Bars are presented as mean ± SD (n = 3).

5.3.2.5 PADI2 overexpression induced protein citrullination in OVCAR-4

To determine whether the PADI2 expression levels affect the total citrullination in OVCAR-4, cells were transfected with PADI2 overexpression vector and control empty vector for 48 hours. The transfected cells were enriched by G418 for additional 48 hours. After the confirmation of successful PADI2 mRNA and protein overexpression, at 96 hours post-transfection and enrichment, PADI2 overexpressing OVCAR-4 cells were incubated in 1mM $CaCl_2$ (e[Ca^{2+}]) for 72 hours consecutive. Total citrullination was then detected in cells treated with 1mM $CaCl_2$ (**Figure 5.7**).

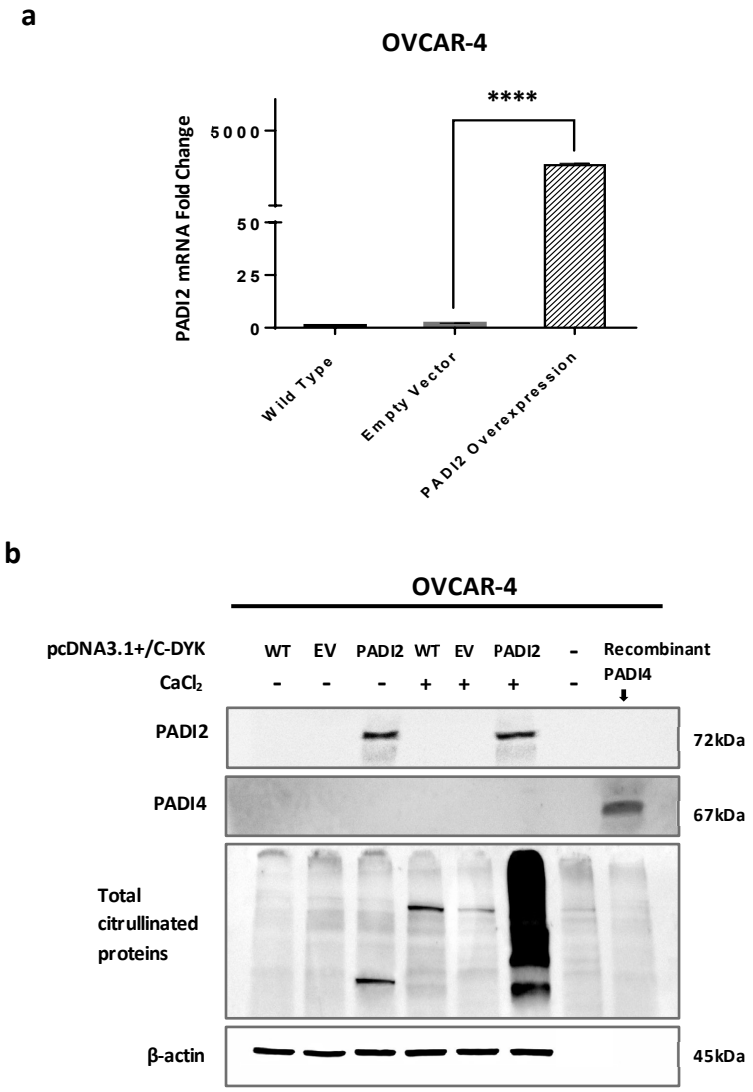

Figure 5.7. PADI2 overexpression induced total protein citrullination in OVCAR-4 cell line treated with $CaCl_2$. Cells were transiently transfected with PADI2 overexpression vector (PADI2) and control empty vector (EV). **(a)** At 96 hours post-transfection and enrichment, *PADI2* mRNA expression levels were determined by qRT-PCR. Representative bar graphs of average PADI2 transcription levels normalised to 18S mRNA levels. Results are representative of the average fold change ± SD of triplicate independent experiments relative to the untreated controls. Bars are presented as mean ± SD (n = 3). ****$p \leq 0.0001$. **(b)** At 96 hours post-transfection and mammalian selection, cells were incubated in the presence and absence of 1mM $CaCl_2$ for 72 hours. Cell lysates were assessed for PADI2 protein and total citrulline protein by Western blot using antibodies specific to PADI2 and citrulline. Recombinant PADI2 and C2C12; murine muscle cell line, were used as positive controls.

5.3.3 PADI2 overexpression can alter EOC cell activity *in vitro*

The aim of the present study was to assess the role of PADI2 in EOC cells, to determine whether increasing PADI2 expression affected EOC cellular activity. Therefore, PADI2 overexpression was assessed in EOC cell proliferation, apoptosis, autophagy, necrosis and cellular aggregation.

5.3.3.1 The effect of PADI2 overexpression on the proliferation of EOC cells

5.3.3.1.1 PADI2 overexpression did not affect the proliferation of OVCAR-4 or ID8-Luc2 cells

To investigate the role of PADI2 in EOC proliferation, OVCAR-4 and ID8-Luc2 wild type were transiently transfected with PADI2 overexpression and vector control empty vector. At 96 hours post-transfection, cells were seeded into 96-well plates at cell density of $1x10^4$. Cell proliferation was then determined using WST-1 assay. There was no statistically significant difference between wild type, control empty vector and PADI2 overexpression vector transfected cell lines (**Figure 5.8**).

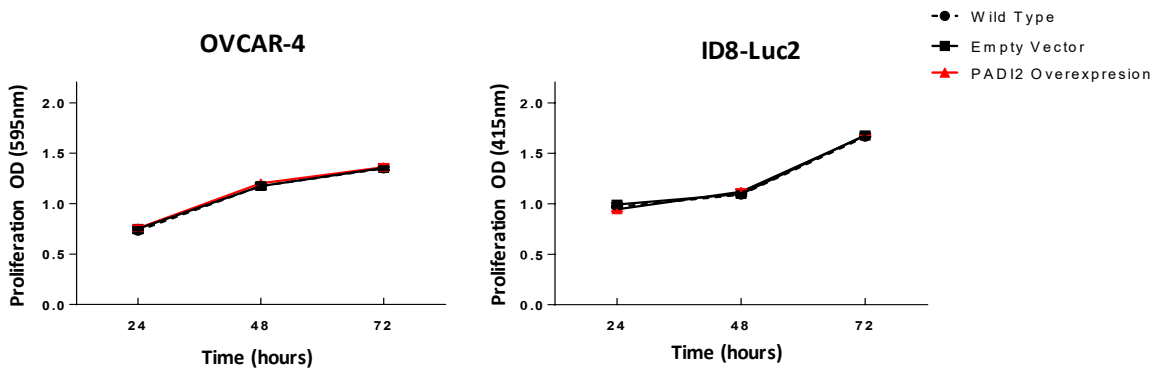

Figure 5.8. PADI2 overexpression did not affect cell proliferation in OVCAR-4 and ID8-Luc2 cells. Cells were transiently transfected with PADI2 expression vector and control empty vector. At 96 hours post-transfection and enrichment, cell proliferation was measured using WST-1 assay for duration of 72 hours. Results are representative of the average percentages of ± SD of triplicate independent experiments relative to the untreated controls. Bars are presented as mean ± SD (n = 3).

5.3.3.1.2 The effect of PADI2 overexpression and increased e[Ca^{2+}] on OVCAR-4 and ID8-Luc2 cell proliferation

Since Ca^{2+} is a known to activate PADI2 and may induce PADI2-mediated citrullination as observed in OVCAR-4 (section above **5.3.3.5)**, therefore, $CaCl_2$ was added to the cell culture media of both OVCAR-4 and ID8-Luc2 cell lines. The growth medium used for cell culture contained pre-existing concentrations of Ca^{2+}, which were previously indicated by the manufacturing company (RPMI: 1.05mM and DMEM: 0.43mM). Ca^{2+}, as a major intracellular second messenger, regulates multiple physiological functions in cells, including cell survival and cell death. Therefore, it is important to evaluate the Ca^{2+} concentrations required for PADI2 activity while maintaining viable cells. To examine the effect of increasing e[Ca^{2+}] on PADI2 activity in EOC, the effect of the addition of $CaCl_2$ was assessed in PADI2 overexpressing OVCAR-4 and ID8-Luc2 cells. At 96 hours post-transfection and enrichment, cells were incubated in media containing increasing concentrations of 0.05-2.5mM CaCl2 for 24, 48 and 72 hours. Cell proliferation was then determined using WST-1 assay. Overall, PADI2 overexpression significantly decreased cell proliferation in OVCAR-4 cells treated with $CaCl_2$ at all concentrations. The lowest cell proliferation percentages were observed when PADI2 overexpressing OVCAR-4 cells were treated with 1mM $CaCl_2$. Conversely, the incubation of PADI2 overexpressing ID8-Luc2 cells in increasing $CaCl_2$ concentrations, resulted in an inconsistent pattern of cell proliferation at all incubation times (**Figure 5.9a**). A microscopic view of OVCAR-4 cell proliferation at 72 hours post-treatment with increasing concentrations of 0.05-2.5 $CaCl_2$mM (**Figure 5.9b**).

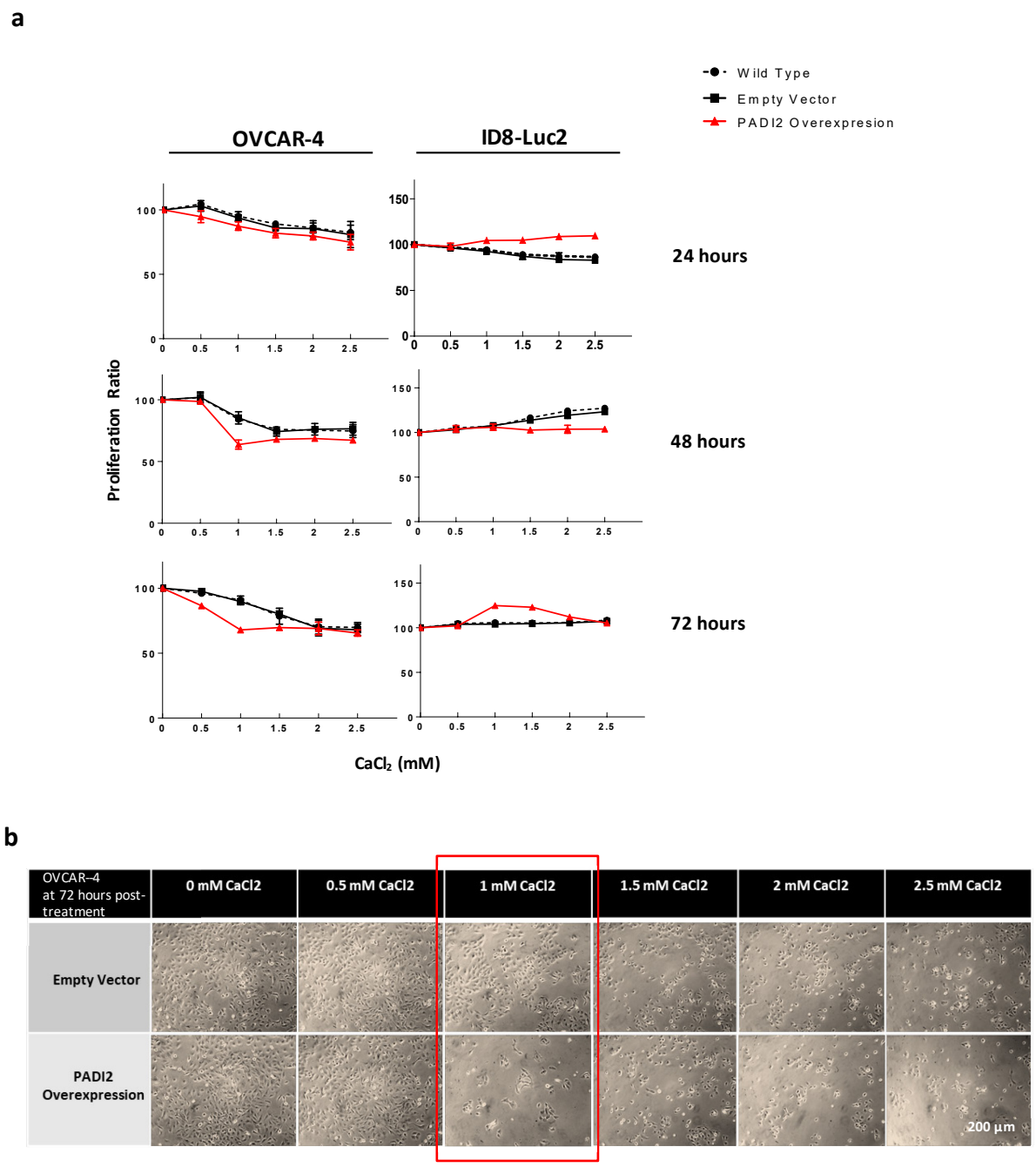

Figure 5.9. The effect of PADI2 overexpression on cell proliferation in OVCAR-4 and ID8-Luc2 cells incubated with increasing concentrations of $CaCl_2$. Cell proliferation was analysed by WST-1 assay. **(a)** OVCAR-4 and ID8-Luc2 cells were transiently transfected with PADI2 overexpression vector and control empty vector. At 96 hours post transfection and enrichment, cells were incubated in increasing concentrations of 0.5-2.5mM $CaCl_2$ for a duration of 72 hours. **(b)** Representative senescence-associated with exposing PADI2 overexpressing OVCAR-4 cells to increasing concentration of 0.5-2m.5mM $CaCl_2$ for 72 hours. Results are representative of the average percentages of ± SD of triplicate independent experiments relative to the untreated controls. Bars are presented as mean ± SD (n = 3). ****$p \leq 0.0001$.

5.3.3.1.3 OVCAR-4 cells are more susceptible to cisplatin drug treatment than ID8-Luc2 cells

The vast majority of previous and current studies frequently evaluate the cytotoxicity and inhibitory effect of a potential biomarker or oncogene with commonly used chemotherapeutic drugs. Evaluating the utility of a novel biomarker will help identify reliable biomarkers that can be used in a clinical context. As previously mentioned, (introduction chapter 1.6), cisplatin is the most commonly used chemotherapeutic treatment for EOC patients, therefore, it was used as a positive control in this study to assess the utility of PADI2 as a potential biomarker and therapeutic target for EOC. To enable better assessment of PADI2, it was important to first evaluate OVCAR-4 and ID8-Luc2 sensitivity to cisplatin treatment. Therefore, cisplatin drug efficacy was initially determined in wild type (non-transfected) OVCAR-4 and ID8-Luc2 cells.

In the current study, e[Ca^{2+}] was shown to promote PADI2 activity in EOC cells and therefore downstream experiments on PADI2 activity will involve the addition of e[Ca^{2+}] (**Figure 5.9**). Since Ca^{2+} is also a key regulator of cisplatin-induced ROS, and was previously shown to alleviate oxidative stress, subsequently increasing cisplatin sensitivity in human EOC cells (Ma *et al.*, 2016). Thus, it was crucial to evaluate cisplatin drug efficacy with or without the addition of $CaCl_2$ treatment. This was achieved by incubating cells with increasing cisplatin concentrations of 1-100µg/ml in the presence of 1mM $CaCl_2$ for a duration of 72 hours. All cell proliferation percentages were then plotted on a semi-log-dose-response graph to report drug exposure time and evaluate IC50 values. The inhibitory rate was determined by WST-1 assay. IC50 values were significantly decreased in OVCAR-4 and ID8-Luc2 cells treated with Cisplatin in the presence and absence of $CaCl_2$, at all incubation periods (**Figure 5.10**).

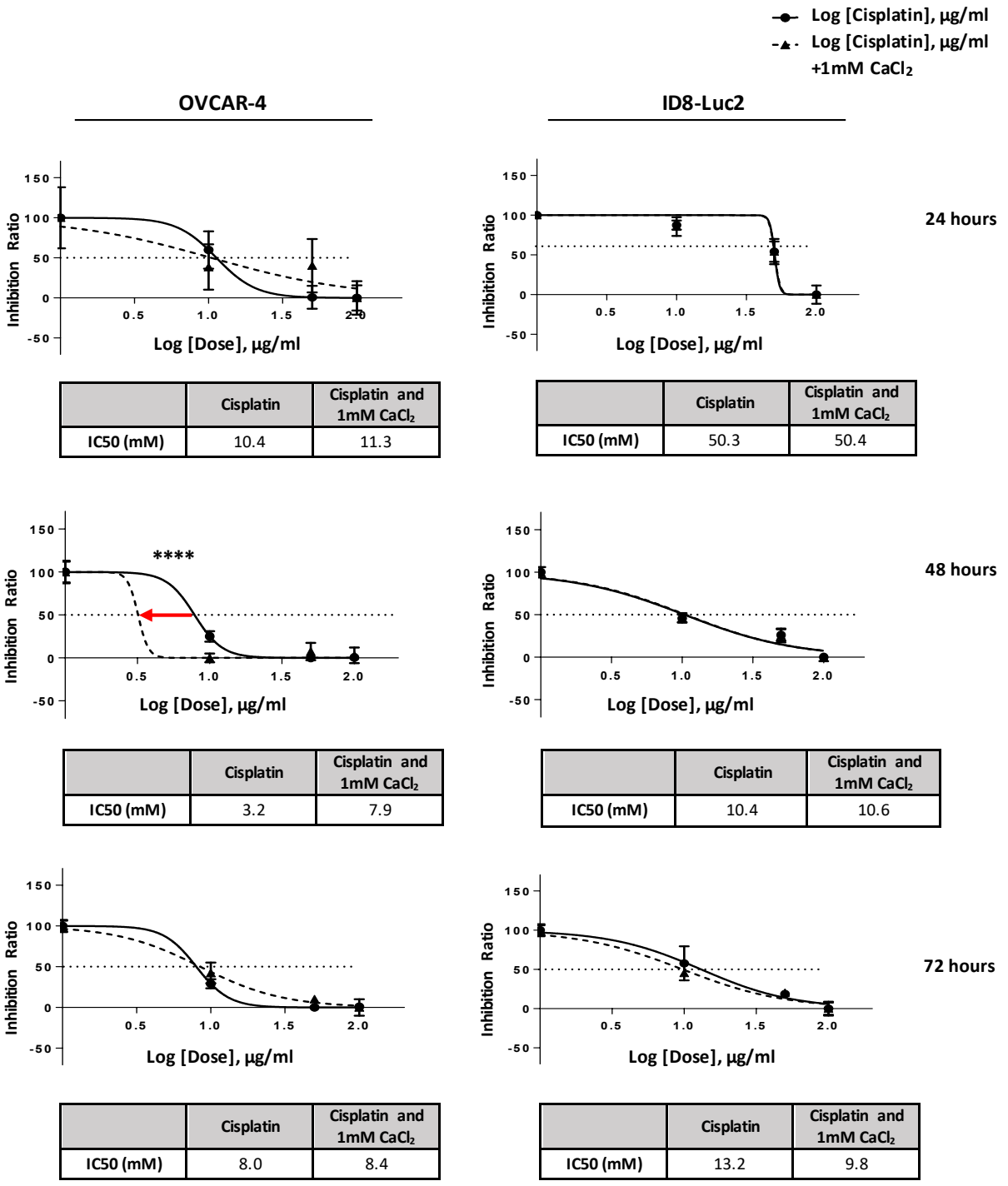

	Cisplatin	Cisplatin and 1mM $CaCl_2$
IC50 (mM)	10.4	11.3

	Cisplatin	Cisplatin and 1mM $CaCl_2$
IC50 (mM)	50.3	50.4

	Cisplatin	Cisplatin and 1mM $CaCl_2$
IC50 (mM)	3.2	7.9

	Cisplatin	Cisplatin and 1mM $CaCl_2$
IC50 (mM)	10.4	10.6

	Cisplatin	Cisplatin and 1mM $CaCl_2$
IC50 (mM)	8.0	8.4

	Cisplatin	Cisplatin and 1mM $CaCl_2$
IC50 (mM)	13.2	9.8

Figure 5.10. The evaluation of cisplatin drug efficacy in EOC cells treated with 1mM $CaCl_2$. Wild type non-transfected cells were incubated in increasing concentrations of 1-100µg/ml cisplatin in the presence and absence of 1mM $CaCl_2$ for a duration of 72 hours. Cell proliferation was analysed by WST-1 assay. IC50 values were then determined by plotting the cell inhibition rate with the corresponding drug concentration on a dose-response curve. OVCAR-4 cells were more susceptible to cisplatin than ID8-luc2 cells. Results are representative of the average percentages of ± SD of triplicate independent cell proliferation experiments relative to cells incubated in the absence of cisplatin. Results are representative of the average percentages of ± SD of triplicate independent experiments relative to untreated and 0.05% DMSO treated controls. Bars are presented as mean ± SD (n = 3). **** $p \leq 0.0001$.

5.3.3.1.4 Exploring the utility of PADI2 as a potential biomarker in EOC

After assessing cisplatin drug efficacy in wild type OVCAR-4 and ID8-Luc2 cells, as explained in the results section above (**5.3.3.1.3**), cisplatin was then used as a positive control to assess the utility of PADI2 as a potential biomarker and therapeutic target in EOC. To do so, wild type OVCAR-4 and ID8-Luc2 cells were transiently transfected with PADI2 overexpression vector and control empty vector. At 96 hours post-transfection and enrichment, PADI2 overexpressing OVCAR-4 and ID8-Luc2 cells were incubated in 1mM $CaCl_2$ and increasing cisplatin concentrations of 1-100µg/ml for the duration of 72 hours. Cell proliferation was then determined using a WST-1 assay. Cisplatin treatment significantly reduced cell proliferation in PADI2-overexpressing OVCAR-4 and ID8-Luc2 cells (**Figure 5.11 and Figure 5.12**).

However, the addition of 1mM $CaCl_2$, significantly reduced the cisplatin drug efficacy in OVCAR-4 cells, only for the first 48 hours of incubation. This $CaCl_2$-induced reduction in cisplatin cytotoxicity subsequently increased cell proliferation significantly in both control and PADI2 overexpressing cells at 24 and 48 hours. Cisplatin cytotoxicity was recovered at 72 hours in PADI2 overexpressing cells, and proliferation percentages were consistent with those treated with cisplatin without 1mM $CaCl_2$. Thus, PADI2 overexpression significantly increased cisplatin cytotoxicity in a Ca^{2+}-dependent manner in OVCAR-4 cells (incubated with 1mM $CaCl_2$, **Figure 5.11**). Conversely, in ID8-Luc2 cells, PADI2 overexpression significantly reduced cisplatin cytotoxicity, independently of e[Ca^{2+}] treatment. The addition of 1mM $CaCl_2$ did not have any effect on ID8-Luc2-cisplatin sensitivity. Thus, PADI2 overexpression significantly reduced cisplatin cytotoxicity in ID8-Luc2 cells, independently of e[Ca^{2+}] treatment, at all incubation times (**Figure 5.11**).

To better illustrate the effect of PADI2 on cisplatin cytotoxicity in OVCAR-4 and ID8-Luc2 cells, the proliferation data obtained by measuring the impact of PADI2 overexpression on optimal IC50 values of cisplatin (50µg/ml) and $CaCl_2$ (1mM) were demonstrated in a bar graph (**Figure 5.12**). In OVCAR-4, PADI2 overexpression relatively decreased cell proliferation by 21% and 22% in a Ca^{2+}-dependent manner at 48 and 72 hours, respectively. Also, cisplatin cytotoxicity was significantly increased by 10% in PADI2 overexpressing OVCAR-4 cells (relative to control) in a Ca^{2+}-dependent manner at 72 hours (**Figure 5.12**). Conversely, in ID8-Luc2, PADI2 overexpression relatively increased cell proliferation by 20%, independently of e[Ca^{2+}] treatment, at 72 hours. Also, cisplatin cytotoxicity was significantly reduced by 21% and 24%

in PADI2 overexpressing OVCAR-4 cells (relative to control) in a Ca^{2+}-dependent manner at 48 and 72 hours, respectively (**Figure 5.12**).

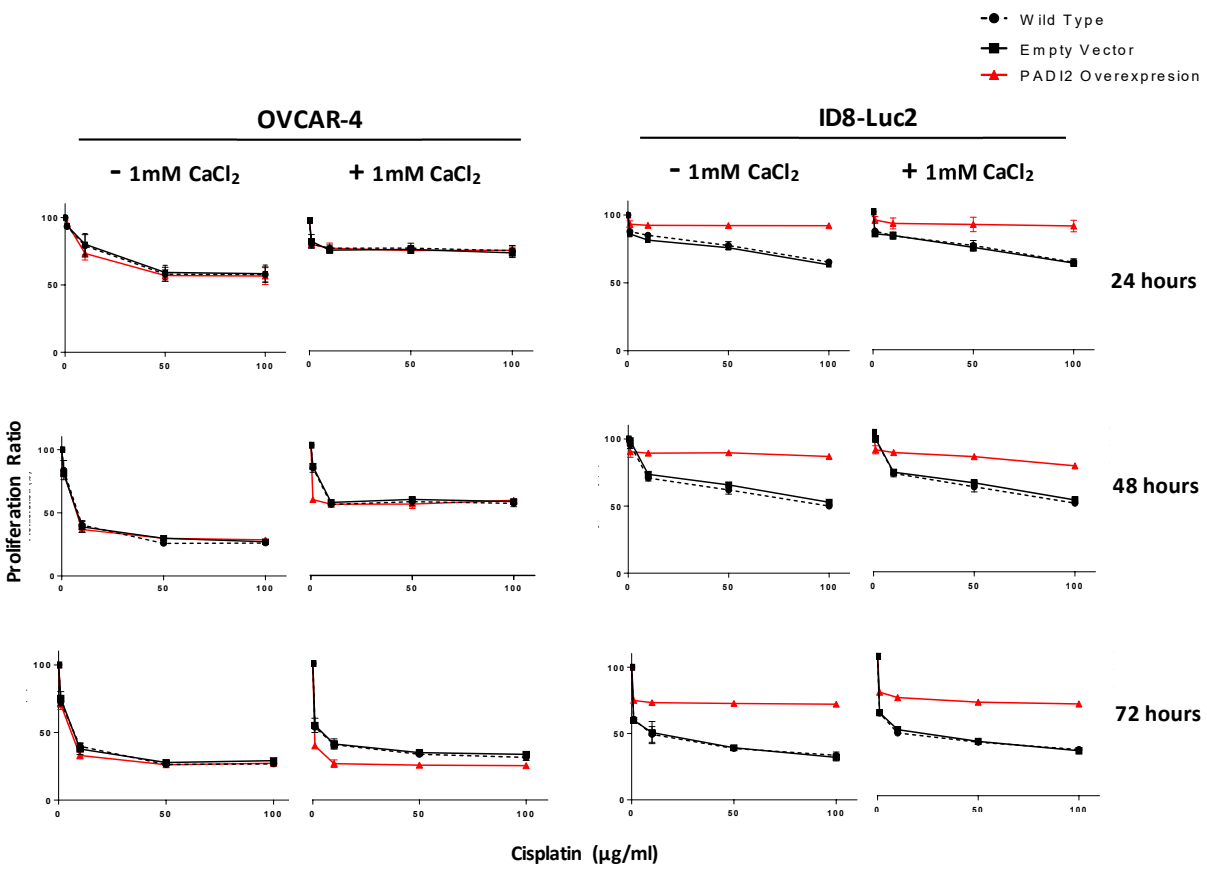

Figure 5.11. The effect of PADI2 overexpression on cisplatin cytotoxicity in EOC cells incubated with 1mM $CaCl_2$. Cell proliferation was analysed by WST-1 assay. OVCAR-4 and ID8-Luc2 cells were transiently transfected with a control empty vector and PADI2 overexpression vector. At 96 hours post transfection and enrichment, cells were treated with various concentrations of 1-100µg/ml cisplatin in the presence or absence of 1mM $CaCl_2$ for total of 72 hours. The addition of 1mM $CaCl_2$ subsequently reduced cisplatin cytotoxicity in wild type, control empty vector and PADI2 overexpressing OVCAR-4 cells. Cisplatin cytotoxicity was not affected by the addition of 1mM $CaCl_2$ in wild type, control empty vector and PADI2 overexpressing ID8-Luc2 cells. Results are representative of the average percentages of ± SD of triplicate independent experiments relative to the untreated and 0.05% DMSO treated controls. Bars are presented as mean ± SD (n = 3).

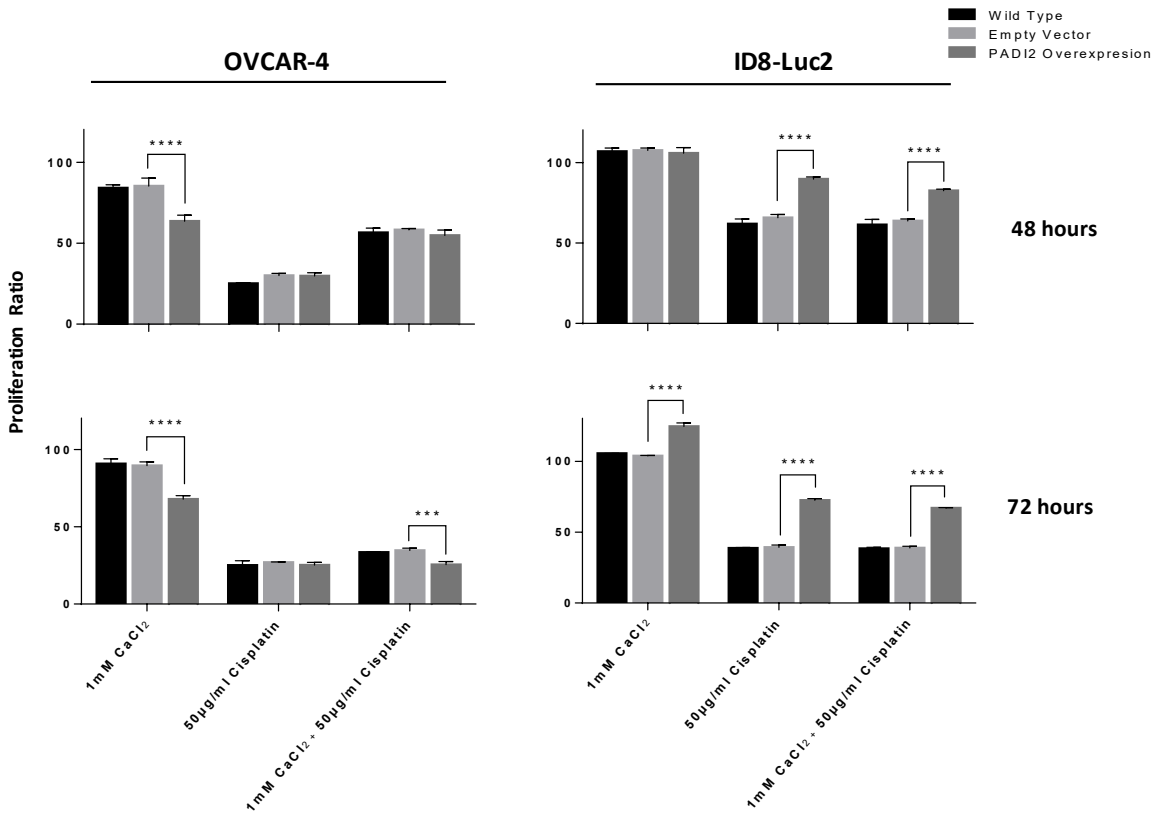

Figure 5.12. The effect of PADI2 overexpression on the cytotoxicity of 50µg/ml cisplatin in EOC cells incubated with 1mM $CaCl_2$. Cell proliferation was analysed by WST-1 assay. OVCAR-4 and ID8-Luc2 cells were transiently transfected with control empty vector and PADI2 overexpression vector. At 96 hours post transfection and enrichment, cells were treated with 50µg/ml cisplatin in the presence and absence of 1mM $CaCl_2$ for total of 72 hours**.** Results are representative of the average percentages of ± SD of triplicate independent experiments relative to the untreated and 0.05% DMSO treated controls. Bars are presented as mean ± SD (n = 3). ***$p \leq 0.001$; ****$p \leq 0.0001$.

5.3.4 The effect of PADI2 overexpression on OVCAR-4 cell apoptosis

Since the proliferation data showed that PADI2 overexpression reduced cell proliferation and increased cisplatin cytotoxicity in OVCAR-4 cells in a Ca^{2+}-dependent manner. Thereafter, the effect of PADI2 overexpression was furthermore explored in other cellular activities, including cell apoptosis. This was achieved by incubating PADI2 overexpressing OVCAR-4 cells (after 96 hours post-transfection and enrichment) with 1mM $CaCl_2$, 50µg/ml cisplatin, 50µg/ml cisplatin with 1mM $CaCl_2$, 50µg/ml cisplatin with 2mM $CaCl_2$ for 48 and 72 hours. Interestingly, it was shown that PADI2 overexpression significantly induced cell apoptosis by 20% and 34% (relative to control), in a Ca^{2+}-dependent manner, at 48 and 72 hours, respectively. These results further validated the ones obtained from proliferation data. However, unlike the previous observation in proliferation data, there was no significant increase in cisplatin-induced apoptosis in PADI2-overexpressing cells irrespective of 1mM $CaCl_2$ treatment, there was no difference relative to control (**Figure 5.13**).

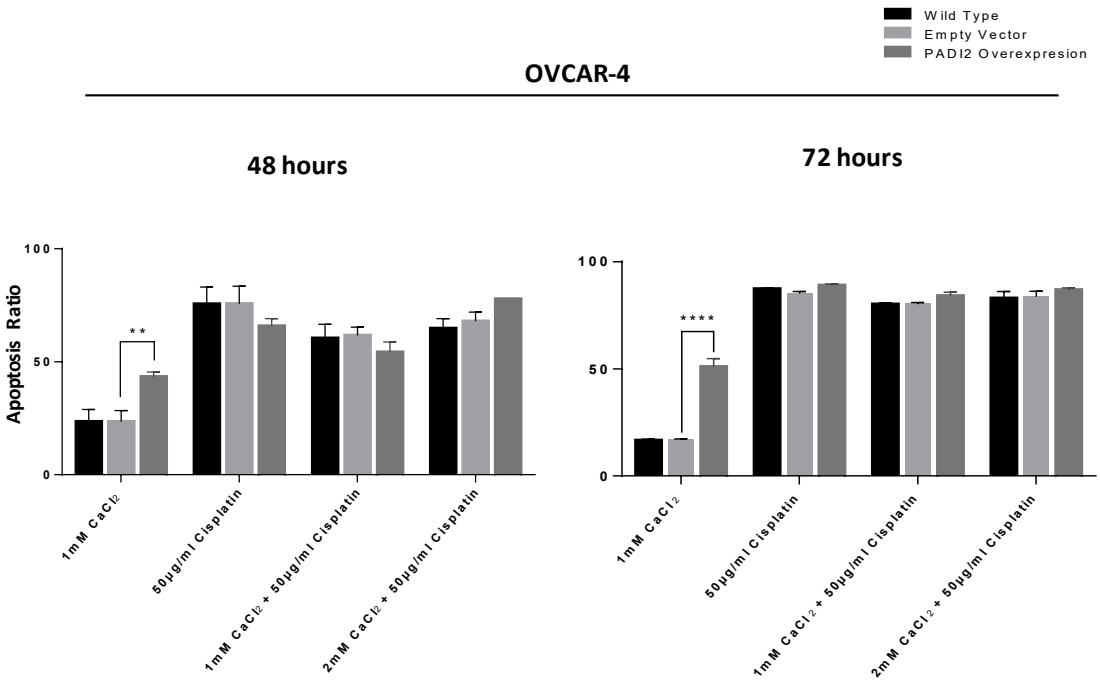

Figure 5.13. The effect of PADI2 overexpression on cisplatin-induced apoptosis in OVCAR-4 incubated with 1mM $CaCl_2$. Cell apoptosis was measured by apoptosis detection kit. OVCAR-4 cells were transiently transfected with a control empty vector and PADI2 overexpression vector. At 96 hours post transfection and enrichment, cells were incubated with 1mM $CaCl_2$ and cisplatin 50µg/ml in the presence and absence of $CaCl_2$ 1mM or 2mM for total of 72 hours. Results are representative of the average percentages of ± SD of triplicate independent cell proliferation experiments relative to the untreated and 0.05% DMSO treated controls. Bars are presented as mean ± SD (n = 3), $^{**}p \leq 0.01$; $^{****}p \leq 0.0001$.

5.3.5 The effect of PADI2 overexpression on autophagy and necrosis in OVCAR-4 cells

To further confirm previous observations from proliferation and apoptosis data, cell autophagy and necrosis were also investigated in OVCAR-4. OVCAR-4 wild type cells were transiently transfected with PADI2 overexpression vector and control empty vector. At 96 hours post-transfection and enrichment, cells were then incubated with increasing concentrations of $CaCl_2$ (1-3mM) for 48 and 72 hours. Chloroquine and Earle's balanced salt solution (EBSS) were used as positive control treatments in this experiment. EBSS is an autophagy inducer, and chloroquine is a autophagy inhibitor. Consistent with the cell proliferation and apoptosis data, PADI2 overexpression significantly increased cell autophagy by 26%, 34%, 33% (relative to control), in OVCAR-4 cells treated with 1mM, 2mM and 3mM $CaCl_2$, respectively, at 48 hours. Likewise, at 72 hours, PADI2 overexpression significantly increased cell autophagy by 38%, 24%, 18% (relative to control), in OVCAR-4 cells treated with 1mM, 2mM and 3mM $CaCl_2$, respectively (**Figure 5.14a**). Whereas, in cell necrosis analysis, PADI2 overexpressing cells showed a marked increase in necrotic death upon 3mM $CaCl_2$ treatment relative to control (**Figure 5.14b**).

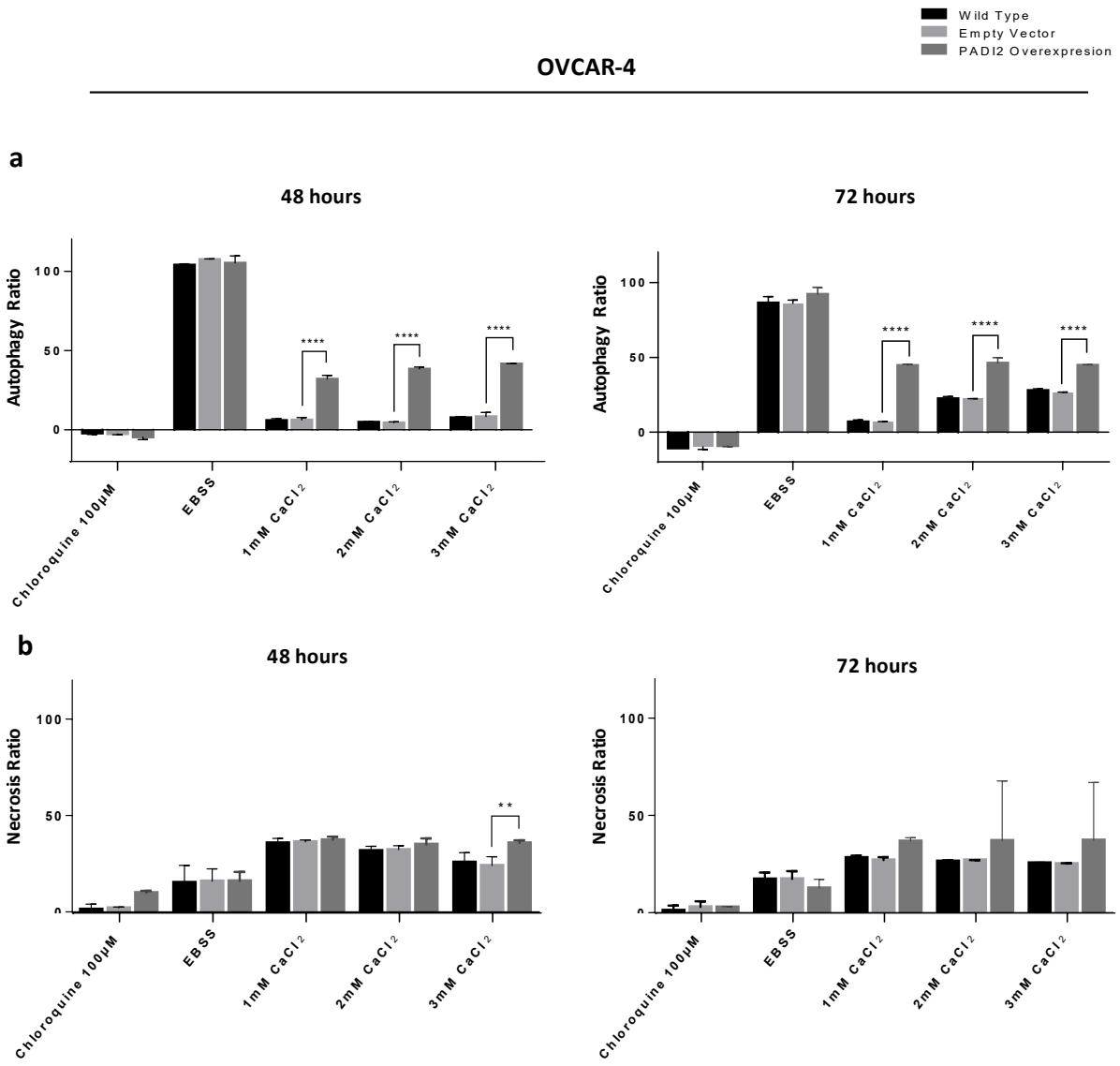

Figure 5.14. The effect of PADI2 overexpression on autophagy and necrosis in OVCAR-4 cells incubated with increasing concentrations of $CaCl_2$. OVCAR-4 cells were transiently transfected with PADI2 overexpression vector and control empty vector. At 96 hours post-transfection and enrichment, cells were incubated in increasing concentration of 1-3mM $CaCl_2$ for total a duration of 72 hours. Cells were also treated with autophagy positive controls; 100µM chloroquine autophagy inhibitor and EBSS autophagy inducer positive control. **(a)** Represent autophagy results and **(b)** represent necrosis results. Results are representative of the average percentages of ± SD of triplicate independent cell proliferation experiments relative to the untreated and 0.05% DMSO treated controls. Bars are presented as mean ± SD (n = 3). * $p \leq 0.05$, p ≤ 0.01, **** $p \leq 0.0001$. EBSS, serum starved cell media.

5.3.6 The effect of PADI2 overexpression on OVCAR-4 cell aggregation

It was previously shown that PADI2 modulates epithelial-mesenchymal plasticity in cancer by modulating intracellular interactions (Horibata *et al.*, 2017). Since 3D cell cultures also exhibit intracellular junctions that are similar to the *in vivo* states compared to classic monolayer cultures. Therefore, 3D cultures did provide suitable system to explore whether PADI2 overexpression may affect cell adhesion in EOC. Following transfection and enrichment, the hanging drop protocol was used to aggregate OVCAR-4 cells. Once assembled, cell aggregates were incubated for further 72 hours with or without 1mM $CaCl_2$. Spheroid morphological differences were also observed using inverted microscope. The spheroids in wild type and control cells did not increase in size but progressively compacted (as observed with inverted microscope) in the presence 1mM $CaCl_2$. When compared to control cells, the diameter area of PADI2 overexpressing OVCAR-4 spheroids significantly decreased by 94% in the presence of 1mM $CaCl_2$ (**Figure 5.16a**). More interestingly, even when OVCAR-4 cells were not incubated in 1mM $CaCl_2$, PADI2 overexpressing cells demonstrated less organised and more dispersed aggregate structures (**Figure 5.16b**).

a

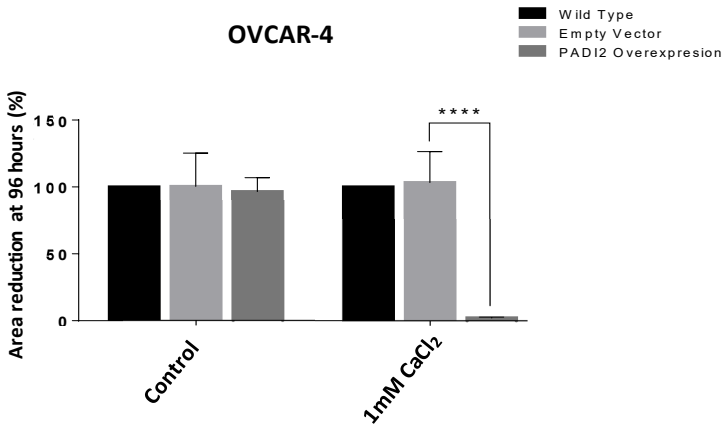

b

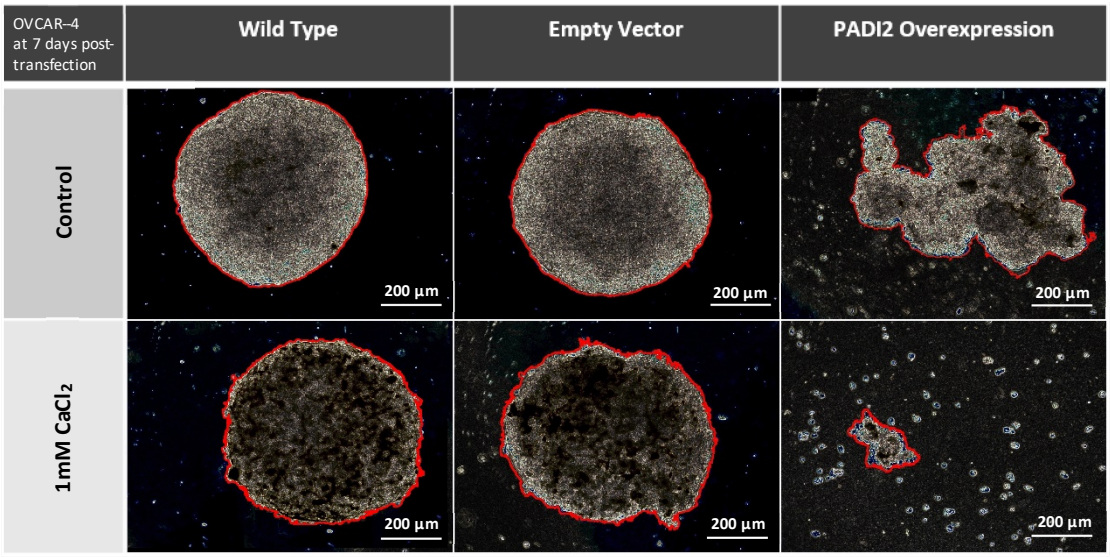

Figure 5.16. PADI2 disrupts aggregate formation in OVCAR-4 treated with 1mM $CaCl_2$. OVCAR-4 cells were transiently transfected with PADI2 overexpression vector and control empty vector. At 96 hours post-transfection and enrichment, cellular aggregates were initially cultured using hanging drop protocol. Once assembled, cell aggregates were further incubated in the presence and absence of 1mM $CaCl_2$. **(a)** Spheroid structures diameter and density were analysed using ImageJ. **(b)** Spheroid morphological differences observed using inverted microscope. Results are representative of the average percentages of ± SD of triplicate independent cell proliferation experiments relative to the untreated and 0.05% DMSO treated controls. Bars are presented as mean ± SD (n = 3). $****p \leq 0.0001$.

5.4 DISCUSSION

5.4.1 Endogenous PADI2 expression in EOC cell lines

PADI2 deregulation was shown to be an early event in the development of cancer (Cantarino *et al.*, 2016). Previous findings suggest that PADI2 can serve as a biomarker or independent predictor of breast cancer (Wang *et al.*, 2016; McElwee *et al.*, 2012). Although PADI2 was deregulated in many cancers, the role of PADI2 in the pathogenesis of EOC was not explored previously (McElwee *et al.*, 2014; McElwee *et al.*, 2012; Wang *et al.*, 2017; Funayama *et al.*, 2017). Hence, the aim of this research was to examine whether PADI2 plays a role in EOC tumorigenesis. Initially, endogenous PADI2 was assessed to establish the protein expression levels, thereafter, the downstream investigations were planned accordingly. All the EOC cell lines examined in the current study showed minimal to no PADI2 mRNA expression and its protein was not detected in any cell line. The reason for this observation is unclear; however, it is important to report that most of the cell lines used in this study were pre-defined as HGS (except for TOV-112D and ID8-Luc2 cell lines). Well-defined EOC histological and molecular subtypes are characterised by a consistent pattern of expression of specific genes, such as biomarkers and oncogenes, that commonly correlate with subtype differentiation (Köbel *et al.*, 2008). Notably, while some gene expression/mutation strongly correlate with one subtype, but their prevalence may not be detected in other disease subtypes. For example, the aberrant p53 expression induced by a *TP53* mutation is one of the most frequent genetic alternations characterising around 90% of HGS (Na *et al.*, 2017). This p53 aberrant expression was rarely detected in other EOC subtypes (Kurman and Shih, 2016). PADI2 expression may be detected in specific cell subtypes of EOC, such as clear cell, mucinous, LGS, and undifferentiated. A future validation of this work would include EOC cell lines representing different disease subtypes and determine whether PADI2 expression is detected in other subtypes. Since high PADI2 expression was shown to associate with decreased proliferation and increased apoptosis of EOC human OVCAR-4 cells. This finding combined with the fact that endogenous PADI2 was not detected in any of the EOC cell lines tested in this study, suggests the absence of PADI2 expression in these cell lines, could be one of the underlying causes of cancer development.

5.4.2 The effect of e[Ca^{2+}] treatment on PADI2-mediated citrullination in EOC cells

5.4.2.1 e[Ca^{2+}] treatment induced PADI2-mediated citrullination in OVCAR-4 cells

Previous studies reported that *PADI2* expression levels correlates with citrullination events in cancer cells, indicating a possible role of PADI2-meidated citrullination in cancer (Cantarino *et al.*, 2016). PADI2 is thought to exist in an "inactive" form under insufficient i[Ca^{2+}] levels. Recently, Slade *et al.,* (2015) used x-ray crystallography diffraction method and determined that PADI2 enzyme is activated by relatively high Ca^{2+} concentrations between 1-10mM. This regulatory method is yet to be confirmed *in vitro* studies. One of the aims of this chapter was to examine the implications of increasing e[Ca^{2+}] on PADI2 activity and furthermore explore whether Ca^{2+}-PADI2 activation affects the overall citrullination and downstream cellular activity in EOC cell lines. After overexpressing PADI2 in EOC cells, citrullinated proteins were only detected in OVCAR-4 cells cultured with 1mM $CaCl_2$. These observations confirm previous findings by Slade *et al.*, (2015); that high Ca^{2+} concentration (≥1mM) may be required for activating PADI2-mediated citrullination. In line with these findings, Vossenaar, (2004) found that vimentin, a known PADI2 target in RA, is specifically citrullinated after Ca^{2+}-influx in macrophages, which are abundant in the inflamed RA synovium (Lewallen *et al.*, 2014). Others also reported that all PADI isozymes generally require Ca^{2+} concentrations around 0.2-0.5mM for half-maximal activity and 2-2.5mM for full enzymatic activity (Kearney *et al.*, 2005; Arita *et al.*, 2004; Damgaard *et al.*, 2014). However, the cytosolic and nucleoplasmic Ca^{2+} concentrations existing under normal physiological conditions are lower than the concentrations required for PADI activity. The highest noted e[Ca^{2+}] concentration in plasma was estimated to be 1.1-1.3mM (Darrah *et al.*, 2013). Moreover, the highest i[Ca^{2+}] concentration achieved by primary human cells does not exceed 100µM and higher i[Ca^{2+}] concentrations are observed in cells undergoing apoptosis (Vossenaar, 2004; Darrah *et al.*, 2013). PADI2-meditaed citrullination possibly requires a high concentration of both, i[Ca^{2+}] and e[Ca^{2+}]. However, the i[Ca^{2+}] levels were not measured in this study. Therefore, additional future work might be required to determine whether the addition of e[Ca^{2+}] and possibly subsequent increase in i[Ca^{2+}] concentrations, is responsible for PADI2 activation and subsequent citrullination. This can be achieved by using the Ca^{2+} indicator dye Fura-2 AM, a poly-amino carboxylic acid that binds to free i[Ca^{2+}] and is excited at 340 nm and 380 nm (Gahete *et al.*, 2012).

5.4.2.2 Citrullination was not detected in ID8-Luc2 cells

In contrast to OVCAR-4, Ca^{2+} treatment did not induce citrullination in PADI2 overexpressing ID8-Luc2 cells. Indeed, PADI2 overexpression was confirmed in ID8-Luc2; however, citrullination was not detected. The inconsistency of outcomes between both PADI2 overexpressing OVCAR-4 and ID8-Luc2 cell lines may be as a result of several contributing factors. It may be indicative of subsequent outcome of cell heterogeneity. Each of the cell lines; OVCAR-4 and ID8-Luc2, represent different EOC disease subtype; serous EOC and undefined subtype, respectively. This heterogeneity complicates the understanding of the underlying PADI2-regulating mechanisms, but provides the ability to capture EOC heterogeneity based on the activity of PADI2 and its associated regulatory pathways (Huang *et al.*, 2003).

While the basics of cell culture experiments share certain similarities, cell culture conditions vary widely for each cell type (Yao and Asayama, 2017). Different culture conditions, including growth medium, FBS% and other cell growth requirement, are often cell type-specific and can contribute to different phenotypes being expressed (Neumann *et al.*, 2010). For example, the cell lines used in this study were cultured in different growth medium; OVCAR-4 cells were cultured in RPMI, whereas, ID8-Luc2 cells were cultured in DMEM growth media containing insulin. It was previously shown that insulin protects pancreatic acinar cells from stress-induced cytosolic Ca^{2+}-influx or overload, thereby, avoiding mitochondrial dysfunction and apoptosis (Lanner *et al.*, 2006). Similarly, the insulin present in DMEM growth media may inhibit or delay Ca^{2+} influx by hindering the function of calcium chelators, thereby, reducing Ca^{2+} entry into ID8-Luc2 cells. Due to the low i[Ca^{2+}] levels in ID8-Luc2, PADI2 enzyme remain inactive and therefore no citrullination was detected.

Other environmental factors, such as cell culture passaging, can alter the gene expression pattern and proliferation rate of cell lines (Neumann *et al.*, 2010). For example, in contrast to rapidly proliferating ID8-Luc2 cells, OVCAR-4 are slow to moderately proliferating cell populations, which show a constant pheno- and/or genotype for prolonged cultivation periods. Extended cultivation of OVCAR-4 cells, may alter their *in vivo* phenotype. Therefore, only limited amounts of OVCAR-4 cells were collected, and low quantities of mRNA were obtained for molecular analysis. As a result, OVCAR-4 cells were regularly grown over several passages to obtain sufficient cellular material to carry out the required experiments (Neumann *et al.*, 2010). In this situation, it is increasingly difficult to determine whether the

cell population after a prolonged cultivation period still harbours the identical gene profile detected in HGS EOC population shortly after isolation from the tissue (Neumann *et al.*, 2010; Marques *et al.*, 2017). Furthermore, passaging may result in a selection pressure for parts of the cell population in cell lines. For example, ID8-Luc2 are less adherent, therefore, a part of the cell population was removed from the culture flask during passaging steps prior to collection and that may alter the overall gene expression profile in higher passages compared to earlier passages.

5.4.3 The effect of PADI2 overexpression and increasing e[Ca^{2+}] on EOC cellular activity

Previous studies on PADI2 mainly focused on its role in disease by evaluating the subsequent effects of increasing or decreasing its expression. These studies led to the identification of possible targets for PADI2, including apoptotic or cell migration-related and chromatin associated proteins (Sharma *et al.*, 2019; Horibata *et al.*, 2017; Falcão *et al.*, 2018). However, the precise mechanisms regulating PADI2 activation and underlying interactions in cancer remain unclear. It was previously established that PADI isozyme require high Ca^{2+} levels to retain proper enzymatic activity (Zhou *et al.*, 2018). However, this Ca^{2+}-dependent activation of PADI2 was not previously explored *in vitro* or in EOC. Since Ca^{2+} is also a key regulator of several cellular processes, and the disruption of i[Ca^{2+}] homeostasis is involved in cancer (Giorgi *et al.*, 2012; Sun *et al.*, 2016). Therefore, the effect of increasing Ca^{2+} was initially evaluated and IC50 values were determined. Followed by the assessment of the subsequent effect of increasing Ca^{2+} concentration on PADI2 activity and the downstream cellular activity in EOC cell lines. One of the aims of this chapter was to investigate whether the increase of PADI2 activity possibly by Ca^{2+}, may affect cell proliferation, aggregation, apoptosis, autophagy, necrosis and aggregation.

5.4.3.1 The effect of PADI2 overexpression on cisplatin-induced cytotoxicity and EOC cell proliferation

The vast majority of previous and current studies frequently evaluated the cytotoxicity and inhibitory effect of potential biomarkers or oncogenes with commonly used chemotherapeutic drugs (e.g. cisplatin). Evaluating the utility of a novel biomarker will help identify reliable biomarkers that can be used in a clinical context. As previously mentioned,

(introduction chapter 1.6), cisplatin is the most commonly used chemotherapeutic treatment for EOC patients, therefore, it was used as a positive control in this study, to assess the utility of PADI2 as a potential biomarker in EOC.

5.4.3.1.1 PADI2 reduced proliferation and increased cisplatin cytotoxicity in OVCAR-4 cells

The present study demonstrated that PADI2 overexpression significantly decreased OVCAR-4 cell proliferation only when treated with ≥1mM Ca^{2+}. The gradual decrease in cell proliferation was observed in a time- and dose-dependent manner. In addition, Ca^{2+}-induced PADI2 activity significantly enhanced OVCAR-4-cisplatin cytotoxicity at 72 hours. Given that the proliferation experiments were carried out over a total incubation period of 72 hours, longer incubation times might be required to definitively confirm whether PADI2 activity is associated with increased cisplatin cytotoxicity in EOC cells. Collectively, these results suggest that PADI2 overexpression in OVCAR-4 may reduce the proliferative activity of EOC cells only when accompanied with high Ca^{2+} levels. Interestingly, other studies reached similar conclusions; however, they examined the role of PADI2 in cancer without including exogenous Ca^{2+} treatment (Cantarino *et al.*, 2016; Funayama *et al.*, 2017).

5.4.3.1.2 PADI2 decreased cisplatin cytotoxicity in ID8-Luc2 cells

The overexpression of PADI2 in ID8-Luc2 cells incubated with increasing concentrations of e[Ca^{2+}], generated discrepant conclusions. There was a general inconsistency of cellular behaviour in response to increasing e[Ca^{2+}] in PADI2 expressing ID8-Luc2 cells. For example, the cell proliferation measured in PADI2 overexpressing ID8-Luc2 increased for the first 24 hours of incubation, while at 72 hours, opposite results existed. This Ca^{2+}- and PADI2 overexpression-induced discrepancy in ID8-Luc2 cell proliferation patterns resulted in inconclusive results. In addition, PADI2 overexpression significantly reduced cisplatin cytotoxicity in ID8-Luc2 cells, independently of exogenous Ca^{2+} treatment or induced citrullination. Collectively, these results suggest that PADI2 activity may be regulated by other mechanisms in ID8-Luc2 cells, that do not include Ca^{2+} or citrullination.

When comparing both cell lines, in OVCAR-4, increasing e[Ca^{2+}] and possibly activating PADI2 in a Ca^{2+}-dependent manner, subsequently decreased the cell proliferation, possibly through

citrullination. However, the effect of PADI2 overexpression and activity on ID8-Luc2 is controversial and remains undetermined. The discrepancy between both cell lines in response to PADI2 overexpression suggests that there may be undiscovered factors that can modulate PADI2 activity in EOC. In addition, PADI2 may exert its different roles through epigenetic mechanisms or may be responsible for regulating other PTMs-associated downstream pathways in EOC. These results also show that PADI2 behaves differently in different cancer subtypes, suggesting a subtype-specific role. Since the human-derived OVCAR-4 and mouse-derived ID8-Luc2 cell lines used in this study represent different histological and molecular EOC subtypes as well as different organisms, therefore, each cell line may exhibit different molecular as well as clinical parameters (Hernandez *et al.*, 2016; Rojas *et al.*, 2016; Lengyel *et al.*, 2014; Mitra *et al.*, 2015). OVCAR-4 represents HGS EOC and these cells were retrieved from platinum-refractory patients (Lengyel *et al.*, 2014; Hernandez *et al.*, 2016). Whereas, ID8-Luc2 is presented in most research as EOC subtype (no specific subtypes, Mitra *et al.*, 2015). Each subtype is represented by a distinct genomic, transcriptomic changes and signalling pathways, that reflect on the intratumor heterogeneity (Rojas *et al.*, 2016). This heterogeneity may define the unique cellular environment specific for a particular cancer type, in which PADI2 exerts its cell-specific role in cellular activity (Wang *et al.*, 2017). Therefore, the mechanisms regulating PADI2 expression and activation possibly through increasing e[Ca^{2+}]/i[Ca^{2+}], require a thorough investigation. The distinction of cell line models may also allow the assessment of therapeutic efficacy in a context that would include intratumor heterogeneity.

Differences in tumour biology between mouse and human cancers are also evident with regard to the tumour type spectrums within the same cancer gene-orthologues mutations (Zhang *et al.*, 2013) . Around 99% of mouse genes have a homolog in the human genome, and for 80% of these genes, this homology is mostly found in the conserved syntenic interval of the mouse gene orthologues (Guénet, 2005). For instance, human *p53* mutations result predominantly in some sarcomas and carcinomas, whereas mutations in mouse *p53* result in multiple lymphomas and sarcomas (Jacks *et al.*, 1994; Zhang *et al.*, 2013). It is commonly found that the mouse genome harbours genes that are orthologues to human genes but variable in terms of copy number (Guénet, 2005). Therefore, a genetically engineered cancer mouse model may recapitulate many, but not all, aspects of human cancers. Since the mouse is a different organism, PADI2 activation in mouse-derived cell lines may be regulated by other mechanisms distinct from the ones present in human cell lines.

5.4.3.3 PADI2 induced autophagy and apoptosis in OVCAR-4 cells in a Ca^{2+}- and citrullination-dependent manner

It was suggested earlier in this research that PADI2 overexpression in OVCAR-4 resulted in the reduction of cell proliferation in a Ca^{2+}- and citrullination-dependent manner. Similar to the proliferation data, the overexpression of PADI2 in OVCAR-4 cell, increased autophagy and apoptosis in a Ca^{2+}-dependent manner. The factors modulating PADI2-induced autophagy and apoptosis are possibly initiated by similar mechanism as described before for proliferation and could be linked to increased i[Ca^{2+}] influx/overload thereby, inducing PADI2-mediated increase in OVCAR-4 cells autophagy and apoptosis. It was previously established that targeting autophagic pathways inhibits the growth of HGS EOC cells and holds promise as a potential and novel therapeutic target (Zhan *et al.*, 2016). The haploinsufficiency analysis HGS EOCs network implicates autophagy as a major disrupted pathway as a result of coincident gene deletions (Delaney *et al.*, 2017). The activation of autophagy was also previously linked to PADIs co-activation during apoptosis-induced oxidative stress in gastrointestinal caners (Song and Yu, 2019). A more direct link between autophagy and PADI2 activity was provided by Liu and Lin, (2017), found that PADI2 triggers ER stress and induce autophagy in Jurkat T cells by downregulating the transcription of p62 and inducing the accumulation of autophagic-related proteins, including LC3-II (microtubule-associated proteins 1A/1B light chain 3B), autophagy related 5 (ATG5) and autophagy related 12 (ATG12). Cell autophagy is also known to induce PADI2-mediated protein citrullination (e.g. vimentin) onto MHC-II cross-molecules and subsequent activation of $CD4^+$ T-helper cells (Crotzer and Blum, 2009; Brentville *et al.*, 2016). Citrullinated proteins can drive apoptosis, promote autophagic processing, therefore, resulting in antigenic presentation by antigen presenting cells, subsequently inducing tumour inflammation. PADI-induced tumour inflammation and the subsequent antigenic presentation was shown to induce CD4+/CD8+-mediated tumour clearance in melanoma and lung cancer models (Moaaz and Lotfy, 2017; Valesini *et al.*, 2015). Collectively, these findings suggest that modulating cell apoptosis and autophagy could be another way by which PADI2 regulates controlled and Ca^{2+}-dependent cell death in OVCAR-4 cells. These findings also clearly represent a variety of potential pathways by which PADI2 regulates its downstream effect on cellular activity; however, the underlying mechanisms remain elusive and may involve citrullination-dependent pathways.

5.4.3.4 PADI2 did not induce necrosis in OVCAR-4 cells

In contrast to the proliferation, autophagy and apoptosis, PADI2 overexpression in OVCAR-4 did induce cell necrosis only in response to e[Ca^{2+}] concentrations higher than ≥3mM. Exposing cells to higher e[Ca^{2+}] concentrations than the those observed under physiological conditions, led to a relatively significant increase in cell necrosis only at 48 hours.

5.4.3.5 PADI2 role in cell adhesion and aggregation

The interaction of cell-cell and cell-ECM adhesion play a significant role in cancer cell adhesion, aggregation and migration (Arcangeli *et al.*, 2014; Turel and Rao, 1998; Zhong and Rescorla, 2012). Alterations in cell-cell adhesion receptors, such as cadherins, integrins and cell surface proteoglycans, contribute to cancer progression and metastasis (Rosso *et al.*, 2017). In EOC, the deregulation of cell adhesion molecules, including cadherin switching during EMT, loss or induction of adhesion molecules, mesenchymal markers (e.g. E-cadherin), ß1 integrins and proteoglycans (e.g. Collagen II) were found to induce aggregation of EOC cells (Liao *et al.*, 2014; Powan *et al.*, 2017; Fernández, 2011; Casey *et al.*, 2001). The current study shows that overexpressing PADI2 in OVCAR-4 cells impaired the formation of EOC aggregates independently of e[Ca^{2+}] supplementation and resulted in more dispersed aggregated cell colonies. Interestingly, exposing PADI2 overexpressing OVCAR-4 cells to high e[Ca^{2+}] (1mM $CaCl_2$), disrupted the aggregate establishment entirely. Similar results were reported by Yuzhalin *et al.*, (2018) and Song and Yu, (2019), who found that increased PADIs-mediated citrullination resulted in the downregulation of E-cadherin and concurrently disrupted cell aggregation and impaired metastatic growth in gastrointestinal cancers. Collectively, these findings provide evidence that PADI2 disrupts the formation of cancer cell aggregates, by modulating the expression of key cell-adhesion molecules involved in this process, possibly through citrullinating adhesion molecules, such as E-cadherin.

The dissociation of cell aggregates *in vivo,* increases cancer cell susceptibility to cancer therapeutic treatments, including chemotherapy and radiotherapy (Weiswald *et al.*, 2015). The PADI2-mediated dissociation of EOC aggregates *in vivo* can lead to successful efforts of sensitising EOC cells to chemotherapeutic treatment, thereby, inducing cancer cell apoptosis. Thus, the detection of PADI2 expression patterns can be used as a prognostic indicator or predictor of chemotherapeutic outcome in EOC patients. For example, the detection of high

PADI2 expression in an EOC patient sample, may indicate successful chemotherapeutic outcome. In addition, future advancement, such as gene therapy, can be utilised to produce patient tailored therapy, by inducing PADI2 expression in EOC patients as a priming step to disrupt cell aggregates, subsequently sensitising drug-resistant EOC subtypes to chemotherapeutic treatment.

5.5 CONCLUSIONS

In conclusion, the present study presents evidence, using the human-derived OVCAR-4 EOC cell line, that PADI2 is a crucial physiological Ca^{2+}-dependent modulator in human EOC, and its overexpression contributes to lower cell proliferation and aggregation and increased autophagy and apoptosis, through protein citrullination. The overexpression of PADI2 expression also increases cisplatin cytotoxicity in OVCAR-4 cells. Conversely, the PADI2 overexpression of decreased cisplatin cytotoxicity in the mouse-derived ID8-Luc2 cells. Overall, the results presented in this chapter can serve as a guide to select appropriate cell lines representing different histological and molecular subtype of EOC for future *in vitro* patient tailored therapeutic studies in EOC. This study potentially had intrinsic methodology limitations. PADI2 overexpression and downstream functional studies were carried in out two cell line models, each representing a different organism (human and mouse). The molecular mechanisms regulating PADI2 and its subsequent mediated functional activity in one cell line may not be completely similar to the mechanisms observed in another cell line.

CHAPTER 6: Targeted mutagenesis of the *PADI2* locus using CRISPR/Cas9 genome editing

6.1 INTRODUCTION

Genome-editing technology is widely used for DNA engineering to inactivate or modify specific genes in functional studies and therapeutic intervention techniques (Sánchez-Rivera and Jacks, 2015). The application of such tools has a significant impact on the understanding of the genetic basis behind various cancers (Kannan and Ventura, 2015). Cancer development is a multistep process triggered by germline and somatic mutations (Hanahan and Weinberg, 2000). The recently developed clustered regularly interspaced short palindromic repeats (CRISPR)-associated proteins (CRISPR/Cas9) system provides a robust and multiplexable genome editing tool, that enables more precise genomic editing and facilitates the elucidation of target gene function in cancer biology (Chen *et al.*, 2016). The CRISPR/Cas system is endogenously found in a variety of bacterial species with acquired adaptive immune systems and serve as a defence mechanism against invading viruses (Rath *et al.*, 2015; Chylinski *et al.*, 2014). This defence mechanism relies on RNA-guided recognition and cleavage of invasive viral and plasmid DNA (Rath *et al.*, 2015). The CRISPR part of the system functions as an "immune memory" which stores the unique viral DNA sequence in-between sections of regularly interspaced palindromic repeated segments. The CRISPR-associated proteins (Cas) part of the system catalyses site-specific cleavage of the targeted DNA sequences of invading viruses. Single guide RNA (sgRNA) in the CRISPR/Cas9 system, is used to guide the Cas9 nuclease to the target genomic site containing the protospacer adjacent motif (PAM) sequence, NGG, located at the 5'- end of the target sequence (Dabrowska *et al.*, 2018). Modified variants of this system have been used for genome editing applications in various organisms. Cas9-induced double-strand breaks (DSBs) at ~3bp upstream from PAM are mainly repaired by error-prone non-homologous end joining (NHEJ), resulting in random indel mutations (e.g. insertion/deletion) and consequent premature translation termination and transcript degradation (Jiang and Doudna, 2017). Alternatively, the homology-directed repair (HDR) mechanism can repair the DSB precisely using a homologous repair template (Jiang and Doudna, 2017; Wang *et al.*, 2016). Mutations generated by the CRISPR/Cas9 system can be characterised by sequencing amplicons comprising the complete target site. Next generation sequencing (NGS) and Sanger sequencing are commonly used approaches to analyse bulk

amplicon mixture or individual cloned fragments (Zischewski *et al.*, 2017). Recently, CRISPR/Cas9 system has been modified into diverse innovative tools for targeting a large-scale cancer driver genes and oncogenes (Xiao *et al.*, 2018). More recently, the CRISPR/Cas9 system has been utilised to engineer immune cells for cancer immunotherapy, such as chimeric antigen receptor T (CART) cells (Wu and Cao, 2019; Fan *et al.*, 2018).

In this study, the CRISPR/Cas9 tool was used to disrupt the *PADI2* locus in SKOV-3 and ID8-Luc2 cell lines. The Cas9 endonuclease was targeted to exons 1 and 7 using sgRNA sequences specific to the *PADI2* locus. Thereafter, DNA was specifically cleaved at ~3-bp upstream of PAM to induce DSBs that will be potentially repaired by NHEJ, subsequently resulting in indels. The genomic cleavage assay and Sanger sequencing approaches were then utilised to determine whether CRISPR/Cas9 targeted mutagenesis of the *PADI2* locus was successful.

6.2 AIMS AND OBJECTIVES

The aim of this chapter was to knockout PADI2 in human SKOV-3 and mouse ID8-Luc2 EOC cell lines, using CRISPR/Cas9 system.

1. Design sgRNAs that target PADI2 locus in both human and mouse genomes.

2. Transfect CRISPR/Cas9-sgRNA complex constructs into the mouse ID8-Luc2 and human SKOV-3 cell lines to genetically delete PADI2 locus.

3. Characterise the efficiency and specificity of CRISPR/Cas9-PADI2 knockout in EOC cells using cleavage assay and Sanger sequencing.

6.3 RESULTS

6.3.1 Restriction digest analysis of CRISPR/Cas9 plasmids

E. coli DH5-α cells were transformed with CRISPR/Cas9 sgRNA1 or CRISPR/Cas9 sgRNA 2 and spread onto LB ampicillin plates for selection of the transformed colonies. The growth of bacterial colonies was indicative of cells harbouring the plasmids. Plasmid DNA was then extracted and analysed using restriction enzyme digestion by *SacI* enzyme and resolved on 1% TAE Agarose (**Figure 6.1**).

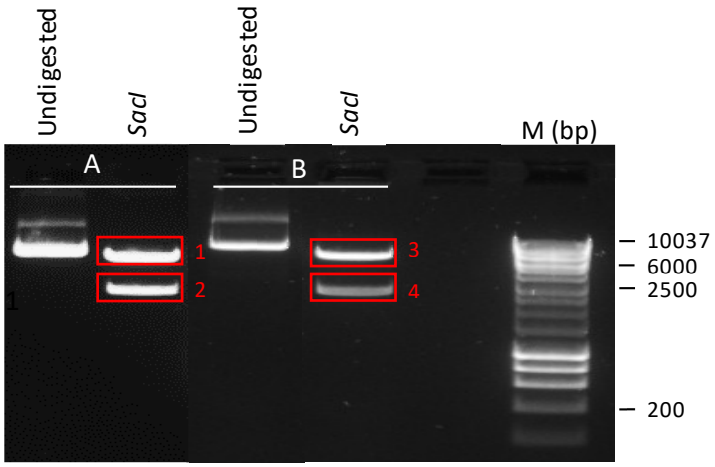

Figure 6.1. Agarose gel electrophoresis analysis of the restriction enzyme digests fragments using *SacI* (a) CRISPR/Cas9 sgRNA1 and (b) CRISPR/Cas9 sgRNA2. Restriction digest product was resolved on 1% Agarose gel electrophoresis TAE. Bands 1 and 3 are visible at 6579bp and bands 2 and 4 are visible at 2598bp. Results are representative of three independent experiments. Lane M: DNA Hyperladder (1kb).

6.3.2 Flow cytometric analysis of CRISPR/Cas9 plasmids transfection efficiency in EOC cell lines

CRISPR/Cas9 (pX459) sgRNA1 or sgRNA2 plasmids were co-transfected with a fluorescent GFP-containing plasmid (pCMV-GFP) into SKOV-3 and ID8-Luc2 cell lines. To thoroughly investigate the efficiency of CRISPR/Cas9 plasmid transfection and systematically optimise experimental parameters, plasmid DNA (sgRNA plasmid and GFP plasmid) was transfected at different ratios (1:1, 4:1 and 3:2,) to give a total of 5µg of plasmid DNA. After incubation for 48 hours, cells were then trypsinised and re-suspended in PBS/10% FCS. Transfection efficiency was then assessed by measuring the intracellular GFP expression using flow cytometry. The flow cytometric data collected was analysed using Flowing software to determine the transfection efficiency of plasmids in cells. In the analysis, cellular debris were excluded by gating cells on the forward and side scatter (FSC linear and SSC log) parameters. When analysing co-transfected cells, the background fluorescence intensity of mock-transfected (treated with Lipofectamine 3000) cells were subtracted to eliminate background fluorescence (**Figure 6.2a**). The histograms produced by the Flowing software indicated the transfection efficiency (x-axis) percentages of control empty vector and PADI2 overexpression vector in SKOV-3 and ID8-Luc2 cell lines. The transfection efficiency of the both sgRNA1 and sgRNA2 plasmids co-transfected ID8-Luc2 cells at 1:1 ratio, exhibited transfection efficiencies of 39.81% and 48.07%, respectively. While, the transfection efficiencies of sgRNA1 detected in SKOV-3 were 41.1%, 55.1% and 48.6%, at 1:1, 3:1 and 4:1 ratios, respectively. The transfection efficiencies of sgRNA2 detected in SKOV-3 were; 40.7%, 57.7% and 54.9%, at 1:1, 3:1 and 4:1 ratios, respectively (**Figure 6.2a and 6.2b**).

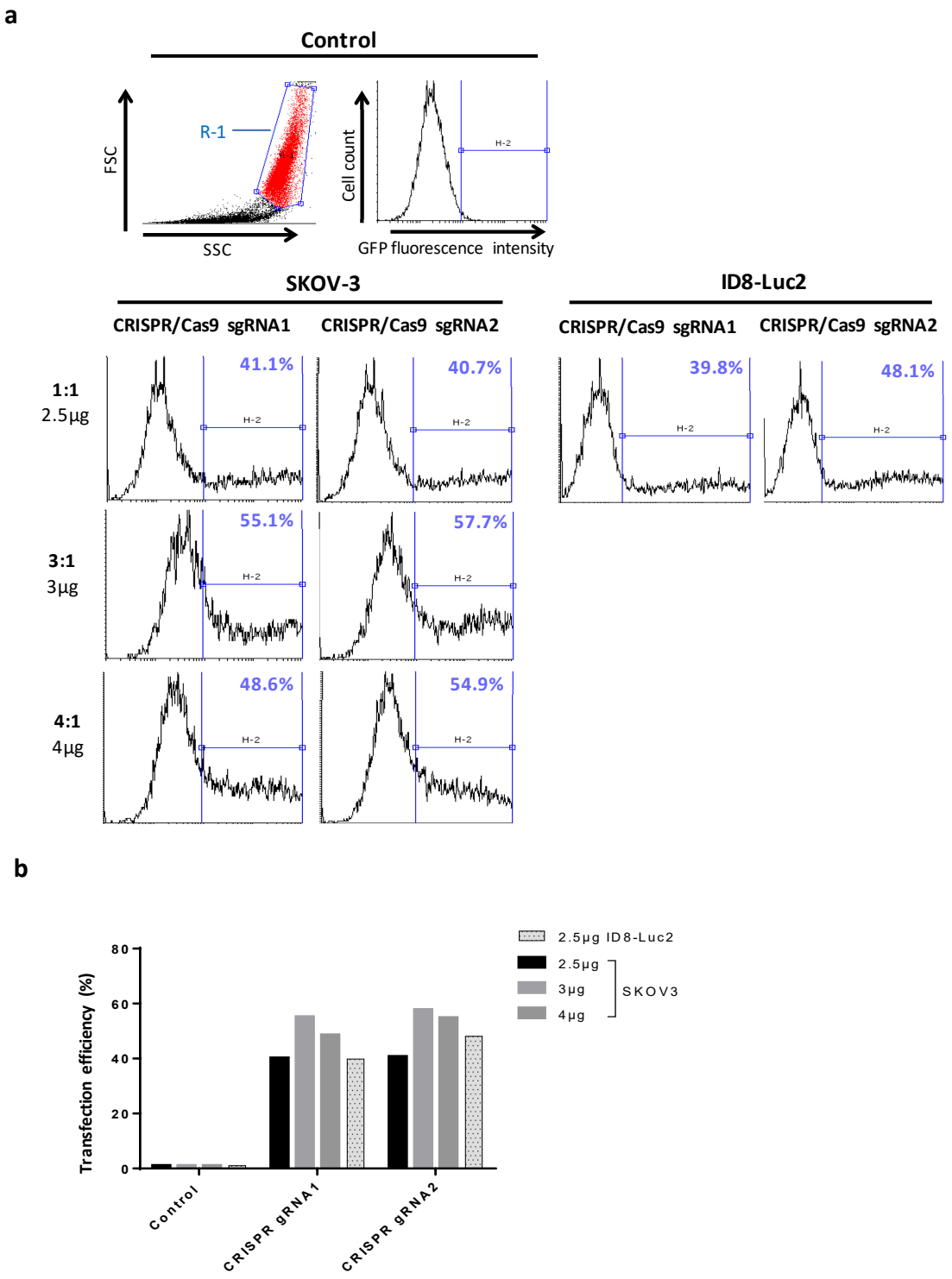

Figure 6.2. Flow cytometry analysis of CRISPR/Cas9 transfection efficiency in SKOV3 and ID8-Luc2 cell lines. A total amount of 5µg of plasmid DNA was co-transfected into cells at different ratios; 1:1, 4:1 and 3:2 in SKOV-3 and 1:1 in ID8-Luc2 of GFP (pCMV): CRISPR/Cas9 sgRNA1 or CRISPR/Cas9 sgRNA2 vectors, using Lipofectamine 3000. At 48 hours post-transfection, cells were re-suspended in PBS+10% FBS and analysed using flow cytometry. **(a)** Representative dot plots of side scatter and forward scatter displaying the gated events of viable cells (R-1) and non-viable cells (black). The flow cytometric histograms representing GFP fluorescent peak (H-2 marker) were used evaluate transfection efficiency percentages of Cas9 transfected cells relative to the control untreated cells (Lipofectamine 3000 treated). **(b)** Bar graph representation of plasmids transfection efficiency percentages in cell lines.

6.3.3 Enrichment of CRISPR/Cas9 transfected cell population using the mammalian selection antibiotic: puromycin

To allow more accurate interpretation of the effects of CRISPR/Cas9-induced mutagenesis in PADI2 locus, optimal concentrations of the mammalian antibiotics, puromycin, for enrichment were determined. This was achieved by applying different antibiotic concentrations to non-transfected cells for seven days. The cell viability percentage was then determined using trypan blue method (**Figure 6.3a**). On day two of enrichment, IC50 values were then determined by plotting the cell viability percentages on a semi-log-dose-response graph. 50% of the cell population died in SKOV-3 and ID8-Luc2 lines at Puromycin concentrations 2.63µg/ml and 2.96µg/ml of in SKOV-3 and ID8-Luc2, respectively (**Figure 6.3b**).

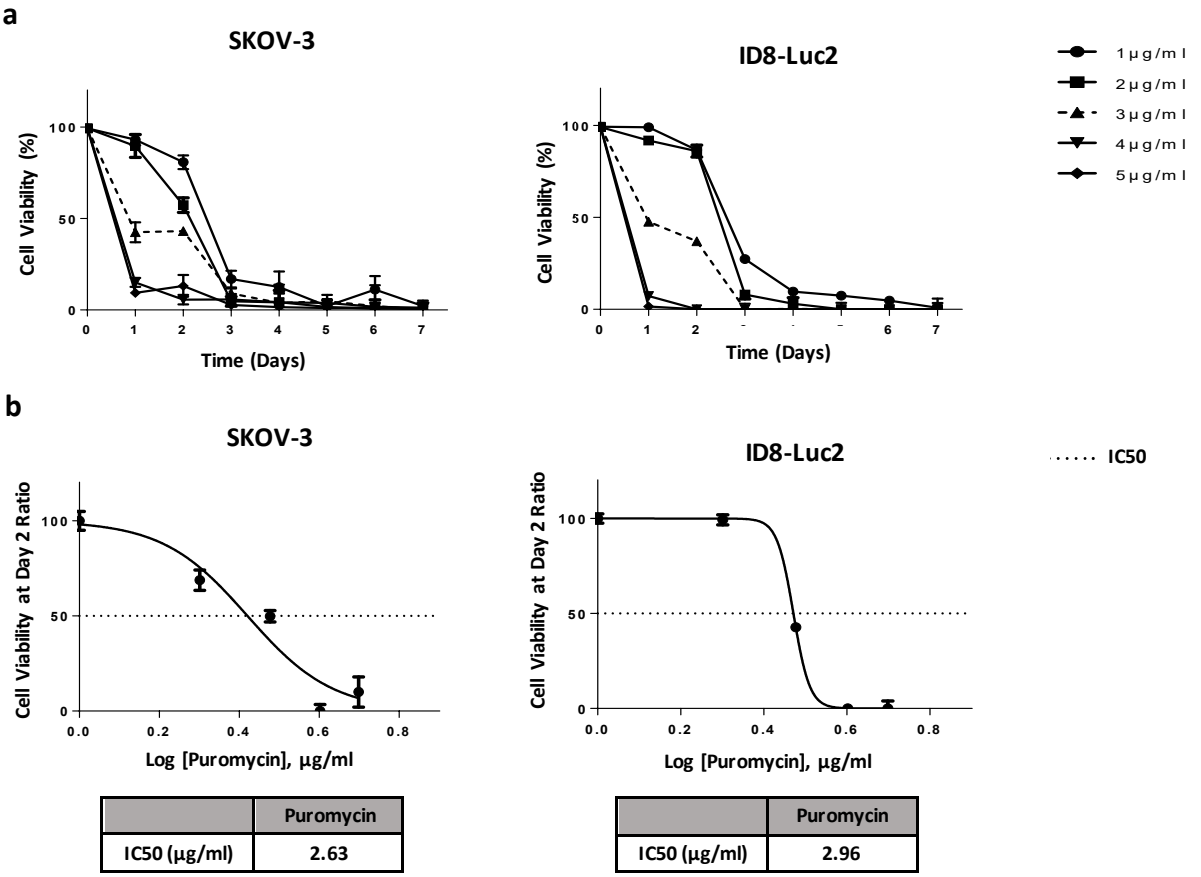

	Puromycin
IC50 (µg/ml)	2.63

	Puromycin
IC50 (µg/ml)	2.96

Figure 6.3. The percentage of cell viability in SKOV3 and ID8-Luc2 cells after treatment with puromycin (1-5µg/ml). (a) Cells were incubated for total of seven days and cell viability was measured every 24 hours using 1% Trypan blue. Percentage viability values were represented in time-kill curves. **(b)** Puromycin Log-dose response curves were used to determine the IC50 value at day two; 2.63µg/ml and 2.96µg/ml in SKOV-3 and ID8-Luc2, respectively. Results are representative of the average percentages of ± SD of duplicate independent experiments relative to the untreated controls. Bars are presented as mean ± SD (n = 3).

6.3.4 Gradient optimisation of sgRNA1 and sgRNA primers for PCR amplification

CRISPR/Cas9 was used to induce mutations in exon 1 and 7 in the *PADI2* locus of SKOV-3 and ID8-Luc2. The designed chimeric sgRNA sequences (20bp excluding PAM) containing a complementarity region to the *PADI2* locus on the human and mouse genome were used to delete a segment of the genomic DNA (>100bp) up- stream of the targeted sequence. The targeted deletions guided by sgRNA and subsequent repair and generation of indels were then confirmed by PCR analysis using primers flanking the targeted regions. The sgRNA1 and sgRNA2 forward and reverse primer sets; A, B, C and D, were designed to generate a 400-450bp DNA template including the sgRNA-guided deletion junction by PCR amplification (**Figure 6.4**). The designed primers optimal annealing temperatures (Ta) were determined using the gradient PCR program. The PCR products were then resolved by agarose gel electrophoresis (2%) which allowed the visualisation of specific amplicons corresponding to the expected band size (400-500bp). Based on these experiments, the optimal Ta selected for primers A, C and D was 63.8°C, and primer B Ta was selected at 55.8°C (**Figure 6.5**).

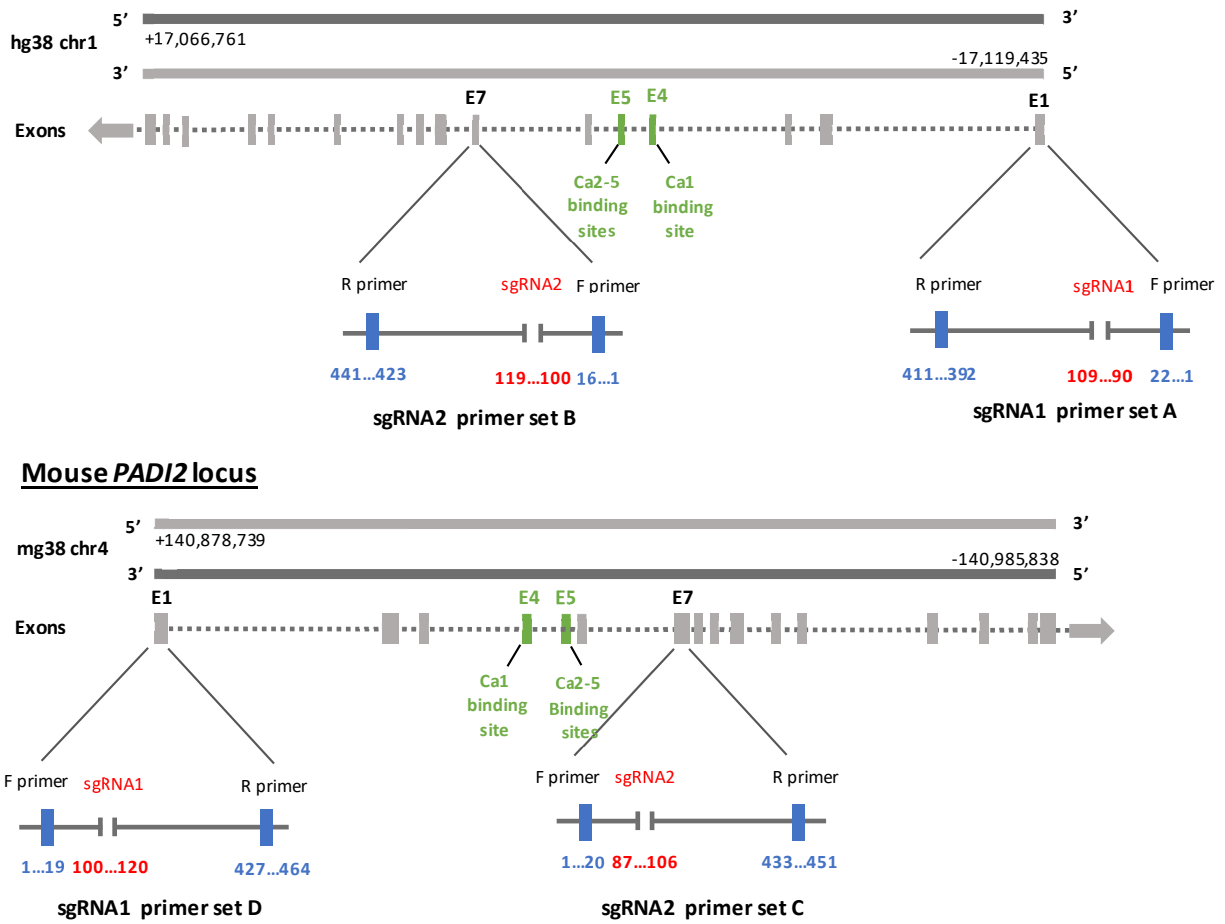

Figure 6.4 Schematic representation of sgRNA1 and sgRNA2 target sites and their corresponding designed primers in *PADI2* locus DNA sequence including Ca^{2+} binding sites.

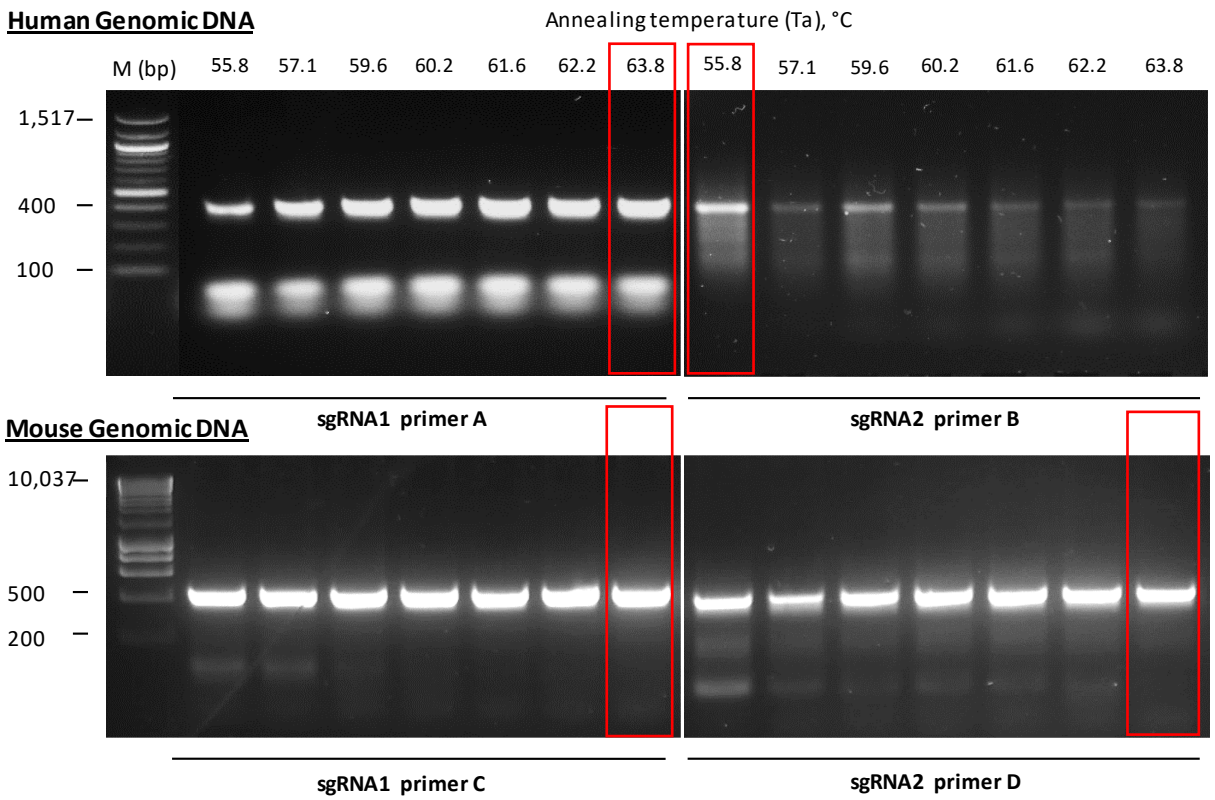

Figure 6.5. Agarose gel electrophoresis analysis of purified human and mouse genomic DNA amplified by PCR to determine the optimal annealing temperature of CRISPR/Cas9 sgRNA1 and CRISPR/Cas9 sgRNA2 primers. This was achieved by setting gradient annealing temperatures between 55.8-63.8°C. Red boxes indicates the optimal annealing temperatures selected for further downstream analyses. The following cycling conditions were used: activation 95°C, 10 minutes, denaturation 95°C, 30 seconds, annealing 55.8°C -63.3°C, 30 seconds, elongation 72°C, 30 seconds. PCR products were then resolved on 2% Agarose gel and the length of the expected band size was 400bp. M, Molecular weight marker (bp).

6.3.5 Detection of the sgRNA: CRISPR/Cas9- mediated cleavage of *PADI2* locus by genomic cleavage assay

After optimising PCR amplification conditions for the targeted region, sgRNA primers were then employed in the PCR-based GeneArt genomic cleavage detection assay to detect CRISPR/Cas9-mediated gene editing. At 96 hours post-transfection and enrichment, DNA corresponding to the edited region was amplified using previously optimised annealing conditions for sgRNA primer sets: A, B, C and D, along with the manufacturer's pre-determined Ta for kit/control primers. This PCR amplicon was then denatured and re-annealed by heating and slow cooling steps. After CRISPR/Cas9 cleavage, if an aberrant NHEJ event has occurred, a heteroduplex will form between amplicons of different lengths (e.g., mutant and wild type amplicons), leading to a DNA distortion that is then recognised and cleaved by T7 endonuclease 1 (T7E1); is a structure-selective enzyme that detects structural deformities (e.g. mismatched and ssDNA) in heteroduplexed DNA (Mashal *et al.*, 1995, Figure **6.6a**). The band patterns of the cleaved products are compared between non-transfected and CRISPR/Cas9 edited samples to determine the frequency of mutations. The cleaved products were then analysed by gel electrophoresis, the bands of full length and cleaved PCR products were visualized and used to evaluate editing efficiency and indel frequency (Sentmanat *et al.*, 2018; Wu *et al.*, 2014). Based on the gel electrophoresis analysis, the detection enzyme mediated-cleavage of PCR product in CRISPR/Cas9-sgRNA1 transfected SKOV-3 cells displayed multiple cleaved PCR amplicons bands (each band represent an indel) indicating successful editing of PADI2 locus. The intensity of each band was then calculated (using Image J software and normalized to the non-transfected cells level) to determine the mutation or indel frequency in the edited population. The mutation frequency of each indel band; a, b and c, was measured to be 32.1%, 34.6% and 8.3%, respectively. Conversely, no indels were detected in SKOV-3 cells transfected with CRISPR/Cas9-sgRNA2. Cleaved PCR amplicons were not detected in ID8-Luc2 cells transfected with CRISPR/Cas9 sgRNA1 or CRISPR/Cas9 sgRNA2 (**Figure 6.6b**). CRISPR/Cas9 sgRNA1-mediated mutagenesis in SKOV-3 *PADI2* locus was further analysed by Sanger sequencing to confirm and quantify indel formation.

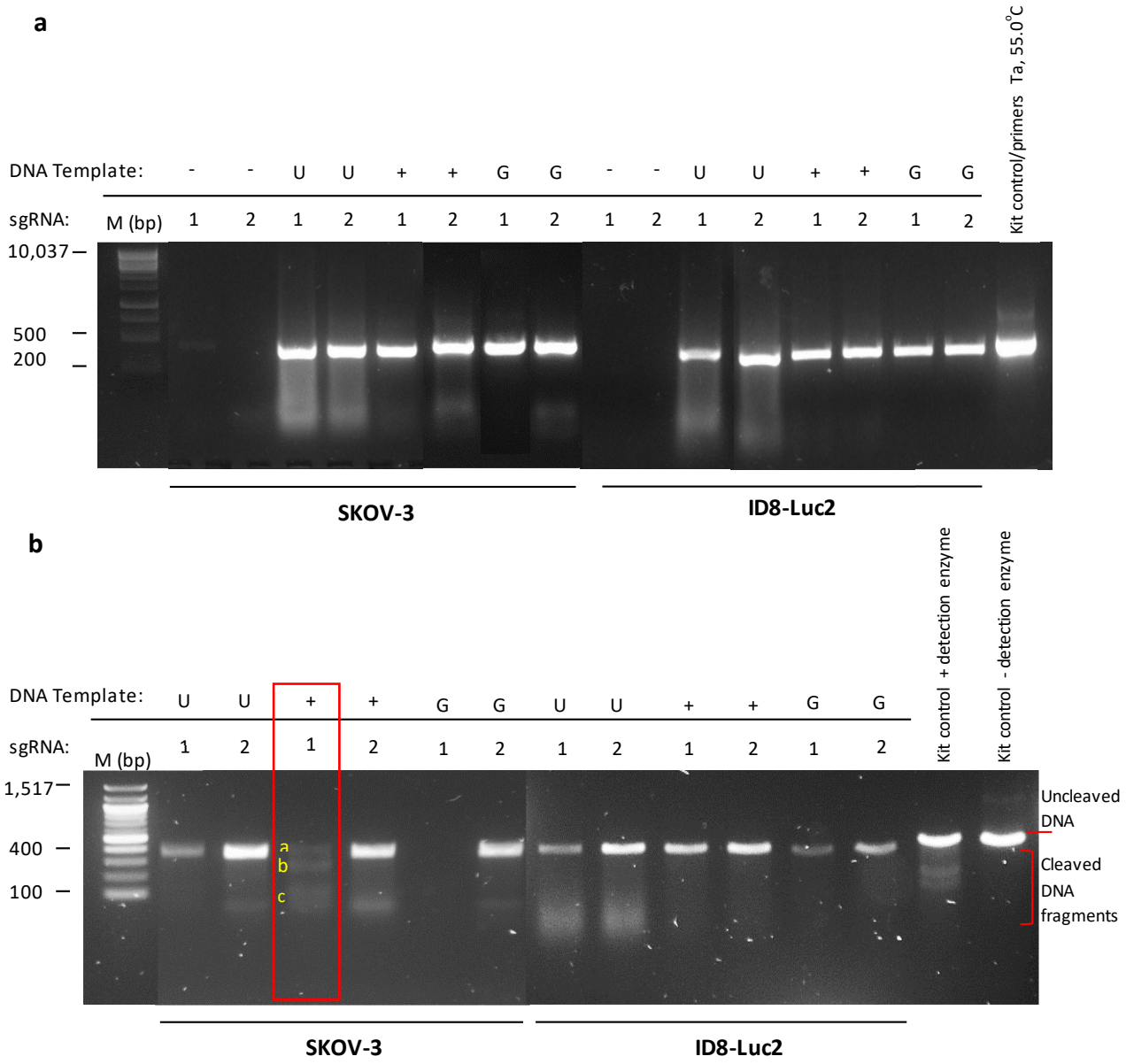

Figure 6.6. Agarose gel electrophoresis analysis of the extracted Genomic DNA from CRISPR/Cas9 sgRNA1 or sgRNA2 transfected SKOV-3 and ID8-Luc2. At 96 hours post-transfection and enrichment, Genomic DNA was extracted from; CRISPR/Cas9 transfected polyclonal populations (+) and non-transfected cells (U). **(a)** The extracted DNA was then amplified by PCR using the optimised sgRNA1 and sgRNA2 primers**.** The PCR amplification conditions for kit/control primers were pre-determined by the manufacturer's protocol (Ta: 55oC). The previously optimised CRISPR-Cas sgRNA primer sets: A, B, C and D, were amplified using the optimal Ta selected. The following cycling conditions were used: activation 95°C, 10 minutes, denaturation 95°C, 30 seconds, annealing 55.8°C or 63.3°C, 30 seconds, elongation 72°C, 30 seconds. PCR products were then resolved on 2% Agarose gel and the expected band size was 400bp. **(b)** After re-annealing, samples were treated with and without the detection enzyme. Treated samples were then resolved on a 2% Agarose gel. CRISPR/Cas9 treated cell lines showing bands after digestion (indicated with red box) were selected and used for further experiments. The intensity of each band was then calculated using Image J to determine the indel frequency in the edited population; bands a, b and c represent a mutation frequency of 32.1%, 34.6% and 8.3%, respectively.; Kit control/Primers, Human and mouse purified genomic DNA (G), were used as control. M, Molecular weight marker (100bp or 1kb).

6.3.6 Sanger sequencing analysis of CRISPR/Cas9 sgRNA1-mediated mutagenesis in SKOV-3 *PADI2* locus

Sanger sequencing was used to confirm the CRISPR/Cas9-sgRNA1-induced mutagenesis of the *PADI2* locus and identify the indels generated by NHEJ cell repair system in polyclonal SKOV-3 cell population. Sanger sequencing is a targeted sequencing technique that uses oligonucleotide primers to seek out specific DNA regions (Robin *et al.*, 2018). Sanger sequencing was performed using the CRISPR/Cas9-sgRNA1 edited SKOV-3 PCR product generated in a similar manner as previously explained in section **6.3.4 and 6.3.5**. Sanger sequencing products of the whole edited SKOV-3 cell population (containing non-homozygous edited events) were analysed using Synthego software-tracking of indels by decomposition (TIDE) to generate DNA trace chromatograms. TIDE decodes the mixed chromatogram signals from the edited polyclonal cell population to accurately determine the mutation frequency of each deletion and insertion size by comparing and decomposing Sanger traces (Brinkman *et al.*, 2014). Sequence indels were detected by comparing the chromatogram peak heights between the DNA trace files of non-transfected SKOV-3 and CRISPR/Cas9-sgRNA transfected SKOV-3. However, the absolute peak heights in a chromatogram is dependent on the amount of template DNA in the sequencing reaction, therefore, relative (rather than absolute) peak heights were initially determined for each trace. This normalization is performed by comparing the CRISPR/Cas9 edited nucleotide's peak height to that of the non-transfected cells. After sequence alignment, a range of deletions and insertions (represented after DNA DSBs) were detected in exon 1. The TIDE-coupled Sanger sequencing confirmed previous observations from cleavage detection assay; CRISPR/Cas9 sgRNA1 induced mutagenesis resulted in indel formation at DSBs site in SKOV-3 *PADI2* locus. The TIDE analysis of Sanger sequencing-DNA chromatograms identified 29 indel events with overall few insertion events than deletion events within the edited *PADI2* locus of which the majority was deletions (56.5%) with fewer insertion events (17.8%) and a ratio of 3.8 : 1; deletions to insertions, based on two independent experiments. The highest mutational activity for CRISPR/Cas9 sgRNA1 was detected at -1 deletions and +1 insertion sites, each represented with the highest targeted indel frequency percentage of 13.3% an 10.8%, respectively (**Figure 6.7b** and **6.7c**).

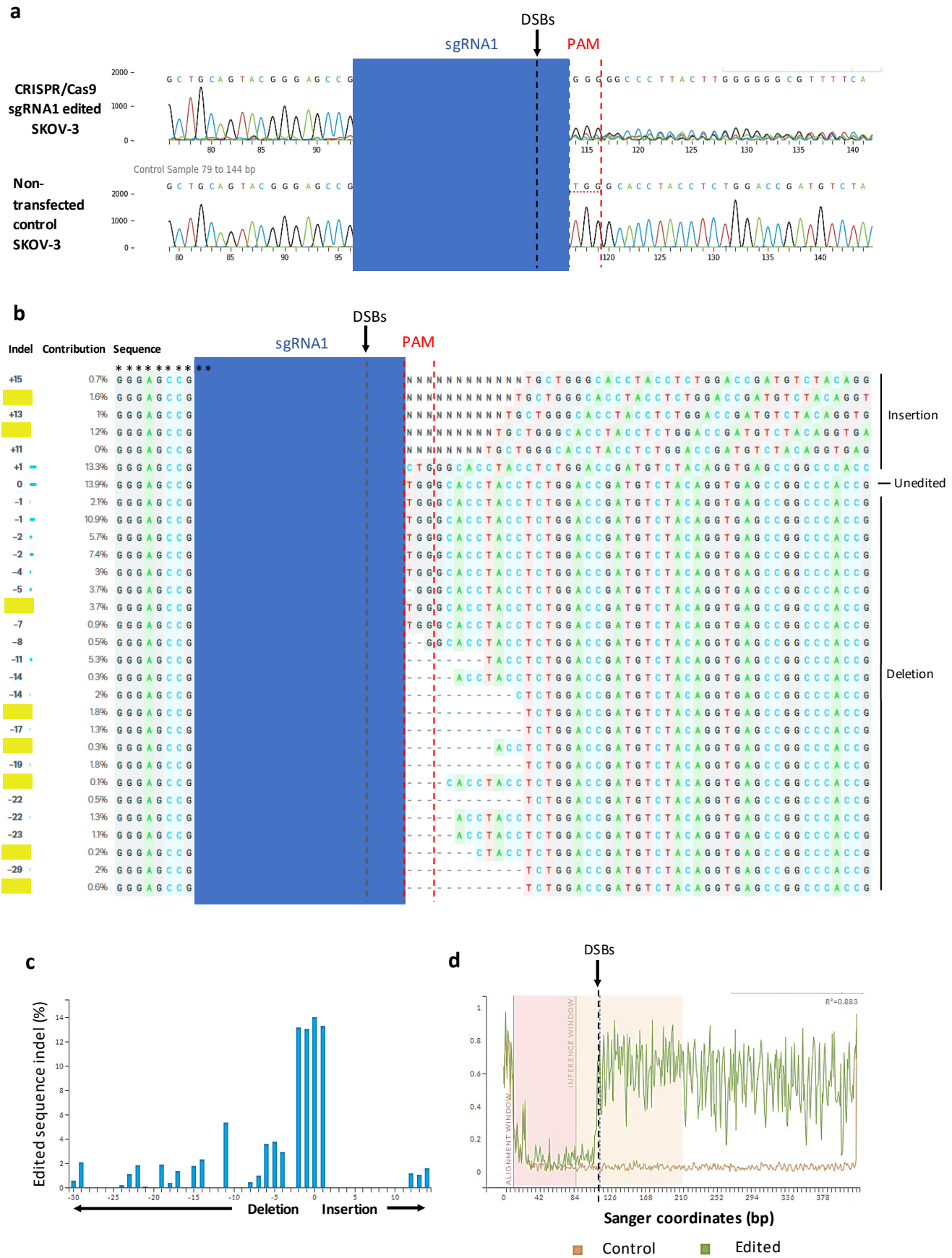
a
DSBs
sgRNA1
PAM
CRISPR/Cas9 sgRNA1 edited SKOV-3
Non-transfected control SKOV-3
Control Sample 79 to 144 bp
b
Indel
Contribution
Sequence
DSBs
sgRNA1
PAM
Insertion
Unedited
Deletion
c
Edited sequence indel (%)
Deletion
Insertion
d
DSBs
INFERENCE WINDOW
ALIGNMENT WINDOW
Sanger coordinates (bp)
Control
Edited

Figure 6.7. Sanger sequencing analysis of CRISPR/Cas9 sgRNA1-mediated mutagenesis of *PADI2* locus in SKOV-3. A PCR product encoding the region of interest was amplified from the genomic DNA of whole cell population using primers flanking the targeted site, which was then analysed by Sanger sequencing. **(a)** The DNA chromatograms of TIDE (tracking of indels by decomposition) algorithms compared the CRISPR/Cas9 edited and non-transfected sequence alignments. The black arrow indicates the expected site of cleavage. **(b)** Normalised contributions showing the inferred sequences present in the edited population and their relative proportions. Cut sites are represented by black vertical dotted lines. **(c)** Indel plot displays the inferred distribution of indels in the entire edited population of genomes. **(d)** The discordance plot details the level of alignment per base between the non-transfected and CRISPR/Cas9 edited sample in the inference window (the region around the cute site). On the plot, the green line and orange line should be close together before the cut site, with a typical CRISPR/Cas9 edit resulting in a jump in the discordance near the cut site and continuing to remain far apart after the cut site (representing an elevated level of sequence discordance). The blue box region represents the guide sequence. The vertical red doted, and black doted lines represent the PAM site and cleavage site of Cas9 (DSBs, double strand breaks), respectively. (-) Deletions or (+) insertions were found near the PAM sequence, *; consensus sequence and yellow boxes represent non-frameshift indels. Results are representative of two independent experiments.

6.4 DISCUSSION

6.4.1 CRISPR-mediated *PADI2* knock out in EOC cell lines

Among its many applications, CRISPR/Cas9 has shown a promising potential in clinical applications and has prompted the emergence of novel molecular targets for cancer therapy (Zhan *et al.*, 2019; Martinez-Lage *et al.*, 2018). CRISPR-Cas9-mediated gene therapy can be exploited for precise genome editing therapeutics and future preclinical target validation (Martinez-Lage *et al.*, 2018). The availability of various virtual or computational CRISPR/Cas9 libraries and databases facilitate high-throughput screening to identify gene signatures involved in carcinogenesis, progression, metastasis and tolerance (Ma *et al.*, 2017; Fan *et al.*, 2018). These signatures can therefore be explored in downstream analysis *in vitro*, and *in vivo* animal models to reveal novel functions and their consequent effect on the biology of cancer (Fan *et al.*, 2018). This knowledge enabled the evaluation of small molecules drugs and antibodies targeting oncogenic signalling pathways for cancer therapy. Recently, CRISPR/Cas9 system was used in preclinical and clinical cancer studies to validate potential therapeutic targets and associated druggable target proteins to better guide future drug discovery efforts (Fan *et al.*, 2018). Huang *et al.*, (2017) used CRISPR/Cas9-mediated knockout of maternal embryonic leucine zipper kinase (*MELK*), an established oncogene in basal breast cancer, to validate whether MELK is necessary for the survival of basal breast cancer. Other studies used CRISPR/Cas9-mediated *p53, BRCA1, PTEN and* nuclear factor *1 (NF1)* and *BRCA2* knockout to investigate the biology of HGS EOC (Walton *et al.*, 2017; Walton *et al.*, 2016). Collectively, these findings provide a general framework and represent promising potential of CRISPR/Cas9 technology to accelerate the discovery of novel molecular targets and gene signatures (Nault, 2017). Previous studies provided genetic evidence that *PADI2* may function as an oncogene by mediating the tumourigenic processes and inducing inflammation within the tumour microenvironment (Wang *et al.*, 2016). Although PADI2 expression has been linked to some female reproductive organ cancers, the role of *PADI2* in EOC oncogenesis is poorly understood. Herein, the main aim of this chapter was to generate genetically modified PADI2-knockout EOC cells, that can be utilised in future studies to enhance the understanding of PADI2 function in EOC. After transfection studies, the efficiency CRISPR/Cas9 system was validated by analysing the edited region by multiple methods.

6.4.2 Detection of the sgRNA: CRISPR/Cas9- mediated gene editing of the *PADI2* locus in EOC cell lines

Herein, the results obtained by cleavage detection assay provided the foundation for interpreting the diverse outcomes from CRISPR/Cas9-sgRNA complex-mediated PADI2 knockout. Surprisingly, successful editing of PADI2 locus was only confirmed in the human-derived SKOV-3 cell line transfected with CRISPR/Cas9 guided with sgRNA1. This result suggests that the selected sgRNA1 was specific to the targeted sequence in the human genome and not in the mouse genome. In addition, CRISPR/Cas9 guided with sgRNA2, did not knockout PADI2 in both human and mouse cell lines. This result shows that the CRISPR/Cas9-sgRNA2 complex have low specificity or low Cas9 binding affinity to the targeted sequence in both human and mouse genomes. However, troubleshooting methods will be required to determine the factors that may have contributed to this unsuccessful CRISPR/Cas9-targeted *PADI2* manipulation in ID8-Luc2 cells.

Current studies aiming to improve target specificity determined that a CRISPR/Cas9 or CRISPR/Cas9-sgRNA complex efficiency is dependent on the number of alleles for each gene that may vary depending on the specific cell line used or organism. In line with these findings, a number of studies also evaluated the efficiency of one CRISPR/Cas9 complex across different target sites and determined that specific target sites are inherently more effective (Wang *et al.*, 2014; Chari *et al.*, 2015; Moreno-Mateos *et al.*, 2015; Wilson *et al.*, 2018). These findings led to a series of large-scale screens of CRISPR/Cas9-sgRNA complex activity across various target sites and organisms/cell types, aimed to identify the specific features contributing to on-target efficiency (Horlbeck *et al.*, 2016; Moreno-Mateos *et al.*, 2015; Chari *et al.*, 2015; Wilson *et al.*, 2018). One study aimed to increase the on-target efficiency by modifying the sgRNA structures. This was achieved by limiting the GC content, avoiding poly-T sequences and including a 'G' directly up-stream of the PAM sequence (i.e. an **G**NGG motif). Building on this research, CRISPR-associated computational tools are regularly optimised to minimise potential guide specificity (off-target effects) while also maximise guide efficiency (on-target activity) by analysing the features of the target sites (Wilson *et al.*, 2018). Another successful approach was discussed by Zheng *et al.*, (2014), also aimed to improve CRISPR/Cas9-sgNRA complex by combining two sgRNA cassettes (separated by tRNA pattern) targeting the same gene in one single delivery system. This multiple sgRNA-mediated editing process resulted in a large fragment deletion of the targeted gene and subsequent high and effective genome-wide mutation frequency. This method strictly depends on two sgRNAs binding to the DNA

with a defined orientation and spacing, significantly reducing the probability that a suitable target site will occur more than once in a genome and therefore enhancing the specificity (Tsai *et al.*, 2014). However, having multiple sgRNA expression cassettes on the same construct limits the cloning capacity and increases off-target mutations (Chira *et al.*, 2017; Chen *et al.*, 2015). Therefore, testing individual sgRNA systems is required as a primary step to characterise sgRNA-specific-induced gene mutation and potential off-target deletions.

Recently, various methods have been developed to improve *Cas9*-sgRNA complex specificity by utilising natural or engineered *Cas9* orthologues, engineering the *Cas9* protein/sgRNA, or modulating the kinetics and regulation of the CRISPR components in the cell (Tycko *et al.*, 2016). Hence, *Cas9* activity is not only determined by the specific target site, but also by the mode of *Cas9*/sgRNA delivery, gene of interest and cell type (Tycko *et al.*, 2016). For example, He *et al.*, (2018) showed that CRISPR/Cas9-targeted manipulation of the OC–related DNA methyltransferase 1 (*DNMT1*) gene was only successful when combined with lipid-mediated delivery system (i.e. folate receptor-targeted liposome (F-LP)) for precise genome editing. These methods can be used in the future to develop more efficient CRISPR/Cas9-sgRNA delivery system that will successfully target *PADI2* in ID8-Luc2 cells. Despite the fact that CRISPR/Cas9 gene editing was not successful in ID8-Luc2 in this study; Walton *et al.*, (2017) reported generating ID8 cells with deletions in number of tumour suppressor genes using the CRISPR/Cas9.

6.4.3 Targeted Sanger sequencing detection of CRISPR/Cas9-sgRNA1 mediated mutagenesis of PADI2 locus in SKOV-3 cells

TIDE-coupled Sanger sequencing analysis confirmed successful mutation of the PADI2 locus in the CRISPR/Cas9-sgRNA1 edited SKOV-3 cell population. This observation was determined by comparing the sequence identity of SKOV-3 edited cell pool with the wild type cells. The DNA trace chromatograms produced by TIDE analysis, displayed the precise site confirming that Cas9-induced DSBs has occurred exactly 3bp upstream of the PAM sequence. It was also detected by the TIDE analysis that around 14% of the CRISPR/Cas9 edited SKOV-3 population remain unedited. The reasons that account for the ability of these cells to escape chromosomal CRISPR targeting are not entirely understood. It is possible that the trans-acting factors, such as anti-CRISPR proteins (i.e. AcrIIC4 and AcrIIC5) may inhibit the expression or activity of Cas9 in specific cancer cell phenotypes, leading to higher tolerance of CRISPR within the transfected population (Lee *et al.*, 2018). It is known that the mutational outcomes are

not random and are dependent on the DNA sequence at the targeted site (Allen *et al.*, 2018). Therefore, the characterisation of these outcome can predict repair profiles reproducibility, Cas9-gRNA efficacy and reveal the biological impact on the targeted sequence (Allen *et al.*, 2018). Thereafter, the detailed analysis of DNA trace sequence by TIDE also provided invaluable information of the edited sequences. The TIDE-generated indel frequencies, were used to characterise the mutation/genetic outcome of CRISPR/Cas9-sgRNA1 edited SKOV-3 population. The detected frequency of insertion events (17.8%) were less than the deletion events (56.5%). The high deletion frequency reflects on the spontaneous joining between the distant ends of two DSBs and repaired by NHEJ (Taylor *et al.,* 2004).

Deletions and insertions of one to three nucleotides represent around 70% of all unique coding indels (Lin *et al.*, 2017; Allen *et al.*, 2018). Indels have the propensity to generate highly mutagenic peptides via creation of a shifted novel open reading frame (Turajlic *et al.*, 2017). CRISPR/Cas9-induced indel mutations that cause a FS (FS indels) create a novel open reading frame that commonly result in complete gene dysfunction by producing truncated polypeptides and/or nonsense-mediated mRNA decay, thereby, knocking out target gene (Turajlic *et al.*, 2017). In the current study, the indel mutations that causes FS are substantially high (21 FS indels) representing 62% of the indels and the remaining are non-frame shift (NFS) indels (8 FS indels) 38%. For example, NFS coding indels included more rare variants, such as -21 (0.1%), whereas, FS indels, included more frequent indels, such as +1 indels found in 13.3% of the polyclonal edited population. Collectively, the number of FS indels was greater than expected, which is not surprising since FS are thought to be more deleterious, and mutants with FS are more likely to increase DNA damage and result in premature termination of translation (Taylor, Ponting and Copley, 2004).

6.5 CONCLUSIONS

In summary, this work provides a novel platform, using CRISPR/Cas9 technology for successful PADI2 knockout. The designed sgRNA1 successfully guided the Cas9 nuclease to the target genomic site on PADI2 locus (exon 1), thereby generating the knockout cell line. This CRISPR/Cas9-sgRNA1 complex can therefore be used in future studies to elucidate the role of PADI2 in EOC. Despite the understanding gained from analysing CRISPR/Cas9 mediated mutagenesis in SKOV-3 using cleavage assay and Sanger sequencing, more extensive analysis

may be required to further investigate sgRNA1 comprehensive specificity. The off-target effect of engineered nucleases is a main concern, particularly in therapeutic applications in a clinical context. The off-target mutations can be found at very low frequencies and below the detection limit of the cleavage assay or Sanger sequencing but can be revealed by NGS. Great advances have been made in recent years in developing methods for identifying off-target sites to determine the safe application of CRISPR/Cas system in a clinical context.

CHAPTER 7: Discussion

The discovery of new EOC biomarkers contributes to improved diagnosis, prognosis, therapeutic response and monitoring of cancer patients (Toss and Cristofanilli, 2015; Yurkovetsky *et al.*, 2010; Sidhu and Capalash, 2017). At present, there is a need for highly reliable and predictive prognostic biomarkers for EOC to enable the stratification of patient risk, facilitate treatment choice and improve patient counselling. Like many tumour markers, PADI2 expression was found to be frequently dysregulated in malignant tumours (Copeland *et al.*, 2009; Bannister and Kouzarides, 2011). This aberrant expression, or dysregulation of PADI2 deregulates the expression of other proteins, including transcription factors (e.g. p53 and p21), key signalling molecules (e.g. RhoA, Rac1 and Cdc42) and is involved in the dysregulation of cell cycle related genes (e.g. *CXCR2*, Patch *et al.*, 2015; Guo *et al.*, 2017; Horibata *et al.*, 2017; Song and Yu, 2019). Therefore, PADI2-induced dysregulations contribute to its potent role in the progression of some cancers or suppression of others (Wang *et al.*, 2016; McElwee *et al.*, 2012). Previous studies also provided genetic evidence that PADI2 may function as mediator of tumorigenesis (Wang, *et al.*, 2016). PADI2 mRNA expression was also found to correlate with *HER2/ERBB2* expression in HER2/ERBB2+ breast cancers and gastrointestinal cancers (McElwee *et al.*, 2012; Bertucci *et al.*, 2004; Guo and Fast, 2011; Guo *et al.*, 2017; Funayama *et al.*, 2017). Although PADI2 expression has been previously linked to female reproductive organ cancers, the role of PADI2 in EOC is unexplored. The detailed role of Ca^{2+} in PADI2 enzyme activation, and subsequent citrullination in cancer remains largely unknown. (Guo *et al.*, 2017). One of the main aims of this study was to assess whether high PADI2 expression conferred a survival advantage in EOC patients by examining TCGA primary tumour data. The role of PADI2 as a modulator of pathogenesis and therapeutic target was investigated *in vitro* EOC cell lines by assessing the effect of its overexpression on proliferation, apoptosis, cellular aggregation, autophagy and necrosis. In the context of combined therapy, PADI2 expression was assessed to determine its impact on cisplatin drug efficacy in EOC cells. In addition, PADI2 correlation and putative interactions with other genes was explored to provide a new understanding of PADI2 regulatory pathways and novel gene targets by which it carries out its role in EOC. Another aim of this research was to develop a CRISPR/Cas9-sgRNA tool to genetically edit/disrupt the PADI2 locus by inducing NHEJ-based mutations that result in non-templated insertions and deletions. Finally, one of the main aims of this thesis was to examine the PADI2 evolutionary history and identify PADI2-functionally important residuesby

assessing the evidence for natural selection amongst 31 orthologues sequences. All these aims were achieved in this thesis work.

7.1 PADI2 deregulates the expression of various genes involved in EOC tumorigenesis

Uncontrolled cellular proliferation, cell death and increased invasion and metastasis are known hallmarks of cancer. Underlying these hallmarks are genome instability, which generates the genetic diversity in cancer cells required as a substrate to accelerate the acquisition of replicative immortality, and inflammation (Hanahan and Weinberg, 2000; Hanahan and Weinberg, 2011). While previous studies have shown that PADI2 is involved in proliferation, invasion and inflammation of cancer cells, the mechanisms by which PADI2 expression and consequent citrullination may regulate these processes remain largely unknown. Herein, the pathway by which *PADI2* is involved in cancer was explored by evaluating the impact of PADI2 overexpression and the consequent alteration of the expression of some genes involved in tumour progression and signal transduction. The correlating genes identified from analysing the TCGA co-expression data were validated in PADI2 overexpressing OVCAR-4 cells using qRT-PCR. Thus, the mRNA expression analysis verified decreased and increased expression of *FZD5* and *ARHGEF10,* respectively. The increased expression of *FZD5,* was previously shown to be associated with poor patient outcome in EOC malignancy (Barbolina *et al.*, 2011; Bobbs *et al.*, 2015; Verardo *et al.*, 2014; Torchiaro *et al.*, 2016). Therefore, PADI2-mediated decrease in FZD5 expression may contribute improved survival outcome in EOC patient. Whereas, Rho-GTPase activating proteins, such as *ARHGEF10L,* are positively associated with good prognosis (Aleskandarany *et al.*, 2019; Zhao *et al.*, 2014). PADI2 may render the progression of EOC by upregulating the expression of *ARHGEF10L* and downregulating *FZD5*, subsequently reducing *FZD5*-mediated ECM adhesion in EOC (Bobbs *et al.*, 2015), although further functional studies are required. The observed PADI2-mediated deregulation of these genes could be a direct or indirect consequence of the irreversible nature of citrullination and subsequent differential expression (Darrah and Andrade, 2018).

7.2 PADI2 expression associated with different survival outcomes in EOC patients

In this study, the role of PADI2 in EOC was evaluated in the human-derived OVCAR-4 and mouse-derived ID8-Luc2 cell lines. The role of PADI2 was assessed by exploring the impact of its overexpression on downstream cellular activity, including cell proliferation, apoptosis, autophagy, necrosis and aggregation. The relationship between *PADI2* expression and OS of EOC patients was initially established by Dr L. Machado (unpublished data), by analysing primary tumour TMAs collected from EOC patients, where higher PADI2 expression was found to positively correlate with improved patient survival (**Appendix Figure S.3**). Thus, the TMA data indicates that PADI2 mRNA expression is significantly associated with improved patient prognosis and higher OS with an increase in mean survival of 22 months. To confirm the TMA findings, the current study explored *PADI2* mRNA expression association with OS of EOC patients by analysing primary tumour clinical data obtained from TCGA cbioPortal. Well characterised bioinformatics and statistical approaches were then employed to investigate the survival rate of EOC patients from U133 and RNA-seq cohorts in correspondence to *PADI2* mRNA expression levels. In contrast to the TMA data, the survival analysis of *PADI2* mRNA expression data indicated that high levels of *PADI2* mRNA was associated with decreased (rather than increased) OS in EOC patients by 11 months. It is important to note that this inconsistency between both the TMA and TCGA studies which led to inconclusive conclusions was a result of each study analysis was conducted using different patient cohorts with different OC subtypes. For example, the current study survival analysis of TCGA data was obtained from EOC patient cases with only serous subtype, whereas the TMA cohort contained OC patients with various OC subtypes. Thereafter, the analysis of the expression data collected from TCGA cBioPortal U133 and RNA-seq presented contrasting outcome to that observed in the TMA data; and that is PADI2 mRNA expression is associated with a lower survival rate of EOC patients. This is not surprising, given that the underlying assumption that PADI2 expression patterns were measured in different patients' cohorts. The discrepancy of both outcomes resides not only in the fact that different data pools were used in each analysis, but in the inconsistency of the histological subtypes of EOC patient cases tested (Xue et al., 2018). Guo *et al.*, (2017) previously used immunohistochemistry to assess whether PADI2 was expressed in ovarian cancer TMAs in comparison to normal TMAs. The Guo group found that significant PADI2 expression was detected in 34.1% of cervical squamous cell carcinomas, 95% of breast-invasive ductal carcinomas, 88% of oesophageal cancers, 97.5% of colon adenocarcinomas, 62.8% of gastric adenocarcinomas, 55.2% of liver hepatocellular

carcinomas, 30% of ovarian serous papillary adenocarcinomas, 92.5% of lung cancers, 90% of papillary thyroid carcinoma samples and 58.5% of rectal adenocarcinomas and (Guo *et al.*, 2017).

7.3 Endogenous PADI2 expression was not detected in any of the EOC cell lines tested

As mentioned above (in section 7.2), Guo *et al.*, (2017) reported that PADI2 expression was significantly increased in only 30% of ovarian serous adenocarcinomas tissues in comparison to 95% of breast cancer and 97.5% of colon cancer. Correspondingly, Protein Atlas analysis of EOC TMAs indicated that only 10% of EOC tissue had high endogenous PADI2 expression; however, the TMA cohort only included few EOC cases (28 cases). In line with Guo's group and Protein Atlas' findings, the current study shows that EOC cell lines displayed weak endogenous PADI2 mRNA expression and its protein was not detected. Collectively, these findings suggest that low endogenous PADI2 expression may contribute to lower risk of EOC, therefore, PADI2 expression is suppressed in EOC cancer cells. However, the unpublished TMA data disagrees with the above findings.

7.4 The overexpression of PADI2 altered EOC cellular function *in vitro*

Discordant results were also observed between the two cell lines examined in the study. For example, PADI2 overexpression significantly reduced cisplatin cytotoxicity in ID8-luc2 cells, resulting in a significant increase of cell proliferation and induced cell-cisplatin resistance. This PADI2-mediated cisplatin resistance in ID8-Luc2 was observed in a Ca^{2+}- and citrullination-independent manner. The reasons for this result are currently unclear but may indicate that PADI2 contributes to EOC tumorigenesis (in some context) and its overexpression leads to increased ID8-Luc2 cell resistance to cisplatin in the absence of citrullination, and irrespective of the Ca^{2+} concentrations in the extracellular medium. Multiple studies correspondingly reported that PADI2 overexpression promotes cell proliferation in tumours, such as breast and prostate cancers (Cherrington *et al.*, 2012; McElwee, Mohanan *et al.*, 2012; Wang *et al.*, 2017). However, this cell line model may not recapitulate what occurs in primary tumours given this human protein was expressed in a mouse cell line and was defective in mediating citrullination. Collectively, these observations agree with the data obtained from cBioPortal demonstrating PADI2 expression association with poor EOC patient prognosis but disagrees

with prior TMA data. It is important to state that the TMA data was collected from EOC patients with various disease subtypes, whereas the RNA-seq and U133 data were collected from patient with serous disease subtype only.

In contrast to ID8-Luc2 cells, PADI2 overexpression in the human-derived OVCAR-4 was shown to increase citrullination in a Ca^{2+} -dependent and citrullination-dependent manner. In addition, PADI2 overexpression significantly increased apoptosis and autophagy, decreased proliferation and cellular aggregation in response to high Ca^{2+} levels (≥1mM Ca^{2+}). Notably, PADI2 overexpression also resulted in increased total protein citrullination in PADI2 overexpressing cells incubated in 1mM Ca^{2+}. These findings indicate that PADI2 may mediate OVCAR-4 cellular activity in a Ca^{2+}- and citrullination- dependent manner. Thus, these results suggest that the overexpression of PADI2 suppresses cell proliferation and induces apoptosis and autophagy of OVCAR-4 cells through catalysis of protein citrullination, and that the downregulation of PADI2 expression might therefore contribute to ovarian carcinogenesis. These cell functional studies support the TMA unpublished data (**Appendix Figure S.3**) and disagrees with TCGA cBioPortal data (**Figure 3.1**). Funayama *et al.*, (2017) correspondingly reported that PADI2 suppresses the proliferation in colonic epithelial cells by catalysing protein citrullination, but in this study the effect of Ca^{2+} on PADI2 was not investigated. Combined with the previous findings from the co-expression analysis, PADI2 may suppress proliferation and aggregation OVCAR4 cells via *FZD5* and *ARHGEF10L* signalling pathways.

Whatever the reasons for this discrepancy in PADI2 function in the different cell lines used in this study, a probable speculation is the epigenetic or/and genetic intratumor heterogeneity (Schwarz *et al.*, 2014; Burrell *et al.*, 2013; Assenov *et al.*, 2018). This heterogeneity complicates the understanding of the underlying PADI2-regulating mechanisms, but provides the ability to capture EOC heterogeneity based on the activity of PADI2 and its associated regulatory pathways (Huang *et al.*, 2003). Therefore, multiple signalling pathways may be involved in the regulation of PADI2 and these pathways may differ depending on the molecular context that infers the heterogeneity. This discrepant pattern was also observed amongst different studies, all investigating the role of PADI2 in breast cancer tumorigenesis. For example, one study found that PADI2 overexpression promoted the proliferation of MCF-7 cells (Cherrington *et al.*, 2012). Conversely, in another study by Wang *et al.*, (2016), PADI2 overexpression was found to contribute to breast cancer tumorigenesis not by inducing proliferation or apoptosis, but by promoting cancer cell migration and invasion. Collectively, all these reports combined with the findings from this study, demonstrate that PADI2 may have different functions in

different cells lines (and primary tumours), possibly depending on the genomic content of each cell lines. Interestingly, all the above studies by Wang, McElwee and Cherrington groups, commenced detecting PADI2 function after overexpression or inhibition studies in the absence of exogenous Ca^{2+} treatment.

It is also important to point out, that ID8-Luc2 is a mouse-derived EOC cell line model. The mouse cell lines are the most widely used model in cancer research due to their ability to preserve temporal disease development, including stromal compartments and coevolution of cancer (Zhang *et al.*, 2013; Walrath *et al.*, 2010). Even though animal models are likely to reflect similar regulatory molecular mechanisms observed in human disease, they are probably subject to the different evolutionary pressures as conventional cancer cell lines during propagation (Perlman, 2016). To understand the different outcomes observed in human-derived OVCAR-4 and mouse-derived ID8-Luc2 cell lines, the human and mouse *PADI2* aligned sequences were compared using an EMBL-Pairwise sequence alignment tool. The comparison of both orthologues demonstrated that mouse *PADI2* has a 11.7% difference in nucleotide sequence and a 2.9% amino acid difference between mouse and human PADI2 (**Appendix Figure S.1** and **Figure S.2**). Supporting the observations from EMBL-Pairwise sequence alignment, Bayesian phylogenetic analysis using DNA sequences, further supported good homology between human and mouse *PADI2* orthologues. However, on the phylogenetic tree, the homologous human and mouse *PADI2* were located on divergent taxa within subclade (Ia), indicating genomic biodiversity. This differentiation in phylogenetic taxa can demonstrate a different protein function/responsiveness to certain regulators: these theories have been previously discussed by Chu *et al.*, (2018). Collectively, these findings can also provide further clarification and possible reasons for the discrepant effects of PADI2 overexpression between OVCAR-4 and ID8-Luc2 cells.

7.5 The evolutionary history of PADI2 and how is it related to structure and function?

Phylogenetic analysis and codon-based selection tests were used to reconstruct the evolutionary history and ancestral reconstruction of *PADI2* orthologues. This technique attempts to computationally dissect and study the evidence for natural selection by assessing the divergence points occurring amongst *PADI2* orthologues sequences retrieved from 31 organisms. Following the phylogenetic analysis, PADI2 3D/2D structures were mapped to the published structures of the aligned PADI2 codon selection data, thereby, allowing the

identification of the conserved amino acid residues that correspond to important sites on PADI2, such as active binding site and Ca^{2+} binding sites.

7.5.1 PADI2 is a phylogenetically conserved gene

The highly conserved protein sequences are thought to maintain an important function (Robson *et al.*, 2002; Sadeque *et al.*, 2010). The phylogenetic approach was previously employed for P*ADI2* by Hosakawa group, who examined a small range of different species, including rhesus monkey, chimpanzee, mouse, dog, chicken, rat, frog, and zebrafish (Hosokawa *et al.*, 2018). That study showed that *PADI2* orthologues were conserved amongst all tested species. Likewise, this thesis also assessed P*ADI2* phylogenetic history but in larger number (i.e. 31 species) and more diverse species, including fish, aves, mammals and amphibians, in addition to newly available sequences from species, such as Miniopterus Natalensis bat (Stoffberg et al., 2004). In the Bayesian phylogenetic analysis using *PADI2* ortholog DNA sequences, the calculated *p*-values for likelihood ratio tests were not significant between all 31 organisms; thus, indicating no evidence of *PADI2* positive selection amongst distinct species, and suggesting that *PADI2* is highly conserved throughout evolution. In line with these findings, Vossenaar *et al.*, (2003) also showed that the physiological and pathophysiological roles of PADI isozymes are conserved throughout evolution from bacteria to mammals. Moreover, Hosokawa *et al.*, (2018) phylogenetic analysis of all PADI isozymes also show *PADI2* is the most phylogenetically conserved PADI isozyme and is predicted to be the ancestral homologue of the other PADI isozymes. One of the most exciting findings in this thesis, was the identification of conserved *PADI2* sequences even in teleost fish, such as Catfish, Piranha, Molly, Bonytongue and Vulus, that diverged almost 400 million years ago. This indicates that *PADI2* is of a very ancient origin and may likely be found in most, if not all, cartilaginous and teleost fish species.

Moreover, in prior phylogenetic studies, evolutionarily conserved genes, such as *PADI2,* are a consequence of extensive purifying selection that eliminates deleterious mutations (Pollock, 2002). Thus, reducing the level of a genes' diversity within species, as well as a decreasing its rate of evolutionary change between species (Nei, 2007). Protein folds that tolerate mutations better are more likely to evolve functional innovations (Abrusán and Marsh, 2016), therefore, *PADI2* functional importance may reside in its sequence conservation. Further analysis using a Genic Intolerance tool of *PADI2* residual variation Intolerance indicate that *PADI2* has fewer

common functional mutations than expected. The residual variation intolerance score showed that for PADI2, 80.22% of the mutations that may occur in the sequence are intolerant and are likely to be disease-causing. In addition, the cBioPortal genetic alteration analysis detected that PADI2 was altered in only 6% of EOC primary tumours. Collectively, these findings indicate that PADI2 is highly conserved and possibly has low mutational robustness, i.e. the ability to accept mutations without change. Therefore, PADI2 is robust against accepting destabilising mutations and the presence of mutations in the PADI2 genome (e.g. missense) are more likely to cause protein dysfunction (Abrusán and Marsh, 2016).

7.5.2 Conserved Ca^{2+} binding sites on PADI2 enzyme indicate its subsequent activation in a Ca^{2+}-dependent manner

Ca^{2+} binding sites (Ca1-6) are located in PAD and PAD_M domains containing the highest proportion of conserved amino acid residues (89%) and (84%), respectively. The amino acid residues corresponding to Ca1, 2 and 6 binding sites were more conserved than those observed for Ca3-5, which is indicative of regulatory importance of PADI2 enzyme activation. In accordance with this observation, Slade *et al.*, (2015) showed that Ca1 and Ca6 do play a critical role in the activation of PADI2 enzymes by promoting the relief of active-site shielding. Followed by Ca3-5-induced conformational changes, thereby, promoting Ca2 binding and subsequently generating a catalytically competent enzyme by rearranging residues (i.e. arginine347) within the active site (Slade *et al.*, 2015). The protein conformational changes are essential for the function or catalysis carried out by the protein, such examples can be observed within the PADI family: binding of Ca^{2+} to acidic concave surfaces of PADI4 was shown to stabilise the unstable domains and therefore organise the active site of the protein (Arita *et al.*, 2004; Liu *et al.*, 2017). Collectively, the 3D/2D structure and evolutionary study provided insights into the biochemical and molecular dependency of PADI2 activation on Ca^{2+} and catalysing Ca^{2+}-dependent citrullination in cancer cell lines. The functional data obtained in this study provide evidence conferring the crucial interplay between Ca^{2+} and PADI2 in cellular activity, where PADI2 overexpression and high Ca^{2+} concentrations conferred survival disadvantage in human OVCAR-4 cells.

7.6 Successful CRISPR/Cas9-mediated knockout of *PADI2* in EOC cell lines

The work in this thesis provides a novel platform using CRISPR/Cas9 gene editing for successful PADI2 knockout. The designed sgRNA1 successfully guided the Cas9 nuclease to the target genomic site on PADI2 locus (exon 1), thereby generating the knockout cell line. This developed CRISPR/Cas9-sgRNA1 tool can therefore be used in future studies to elucidate the role of PADI2 in EOC. This CRISPR/Cas9-sgRNA complex can be therefore utilised to monitor the effect of multiple pharmacological and chemical intervention in PADI2-knockout cells. The application of such tools has a significant impact on understanding the genetic basis behind various types of cancers in association with PADI2. However, this tool was not used in the current study due to the lack of PADI2 expression in cell lines. The reason for this lack of PADI2 expression in all cell lines examined compared with primary tumour tissue is currently unclear by may represent the inability to propagate and culture established PADI2 cell lines from primary clinical material.

7.7 Limitations and future work

The research detailed in this thesis has advanced the understanding of the role of PADI2 in EOC, whilst also revealing several possible avenues for future research. A role for PADI2 has been previously well established in neurodegenerative disease and its mediation of citrullination has been linked to various cancers. The role of PADI2 in EOC was not explored previously, therefore, this thesis work is novel and provides the fundamental principles of PADI2 activity and its potential role in EOC.

As described in chapter 3, the TCGA cBioPortal data was obtained from primary tumour EOC patients with serous disease subtype. However, including different disease subtype or analysing other cohorts that include only non-serous subtypes, would provide a more comprehensive assessment of PADI2 and whether its expression and association with serous EOC patients is subtype-specific. In addition, some of the identified novel co-expressed genes that may play important roles in PADI2-mediated pathways in EOC, were not included in the qRT-PCR analysis and require further examination. In addition, in chapter 5, PADI2 overexpression studies *in vitro,* included empty vector and wild type (non-transfected) EOC cells as negative controls. However, plasmids harbouring a kinase deficient PADI2 may be required for further elucidation of cell function and to confirm the findings obtained from

overexpression studies. PADI2 mediates protein citrullination in OVCAR4 cells, thus decreasing cell proliferation and aggregation and increasing apoptosis and autophagy.

This work was the first to address the role of PADI2 in EOC, therefore, this thesis contains optimisation steps that formed a starting point of this novel work and enabled enhanced characterisation of the downstream effects of PADI2 overexpression *in vitro* EOC cellular activity. This study also evaluated the efficacy of cisplatin drug in OVCAR-4 and ID8-Luc2 EOC cell lines. In addition, cultured cell lines were used to investigate the tumourigenic mechanisms. The observed mechanisms may not be entirely similar to the mechanisms in primary tumour tissues or patient blood samples. Typical cell culture medium is replete with metabolites and growth factors, among others, for which cells normally must compete *in vivo* (Hecht *et al.*, 2016). Whether cell lines can mimic tumour cell gene expression patterns and cellular activity by altering the culture medium conditions is a question yet to be fully explored.

In a clinical context, PADI2 expression can be initially assessed in EOC patients. Next, EOC patients will be given a dedicated course of cisplatin (e.g. 3-6 cycles) and followed by post-treatment assessment of patients' response to the chemotherapy treatment. If resistant to cisplatin and PADI2 is high in their tumour, a combination therapy including cisplatin and Cl-amidine, a known PADI inhibitor, might be used to improve chemotherapeutic response by hindering PADI2-mediated EOC cells resistance to cisplatin treatment. This can be assessed initially using *in vivo* mouse models. In contrast, if sensitive and PADI2 expression was high, patients can be provided with Ca^{2+} supplementation as part of combination therapy to activate PADI2-increased cisplatin efficacy and perhaps decrease the chemotherapy treatment time. Future studies can include investigating the role of PADI2 in cancer inflammation and whether it could be used as part of an immunotherapy approach using $CD4^{+}$ T cells targeting citrullinated epitopes (i.e. targets of PADI2 in EOC).

Additionally, this work has developed CRISPR/Cas9-sgRNA complex for editing the PADI2 locus in human cell lines as described in chapter 6. Whilst the CRISPR/Cas9 editing system is a highly specific novel approach for genome editing, the potential for off-target effects remain to be fully characterised. Genome-wide off-target effects were not determined in this study. By sequencing the whole genome by NGS, it is possible to identify not only off-target effects but also structural variants, such as rearrangements, inversions, major deletions and duplications (Zischewski *et al.*, 2017). New research by Kocak *et al.*, (2019), suggested using engineered

hairpin secondary RNA secondary structures combined with different variants of Cas9 or Cas12a, to increase CRISPR systems specificity.

7.8 Concluding remarks

This thesis provides evidence that PADI2 expression is associated with EOC patient survival time and as a functionally conserved protein is also involved *in vitro* in EOC cellular activity. PADI2 acts as a novel mediator in EOC cells in a cell line-specific manner, and its overexpression induces differential effects on cellular activity, reflecting the complexity of PADI2 biological regulation. On the one hand, PADI2 significantly reduced cisplatin efficacy/cytotoxicity independently of exogenous Ca2+ supplementation or induced citrullination in the mouse-derived EOC cell line. However, the mechanisms by which PADI2 reduces cisplatin cytotoxicity or whether a cofactor is required for its interaction in ID8-Luc2 cells, remains unknown. Conversely, PADI2 overexpression contributes to decreased proliferation/aggregation and increased apoptosis/autophagy in human-derived serous EOC cells in a Ca^{2+}- and citrullination-dependent manner. PADI2 affects EOC tumorigenesis in human-derived cells by regulating the expression of *ARHGEF10L* and *FZD5*, which were previously shown to be involved in EOC. It is envisioned that the continued research and identification of other potential regulatory mechanisms by which PADI2 reduces aggregation of EOC cells will help to predict chemotherapy treatment outcome in clinical EOC patients. It can also be used as part of tailored patient treatment by identifying PADI2 as a potential biomarker in EOC, and its high expression can be accompanied with oral Ca^{2+} supplements, to increase cisplatin efficacy in EOC patients.

a

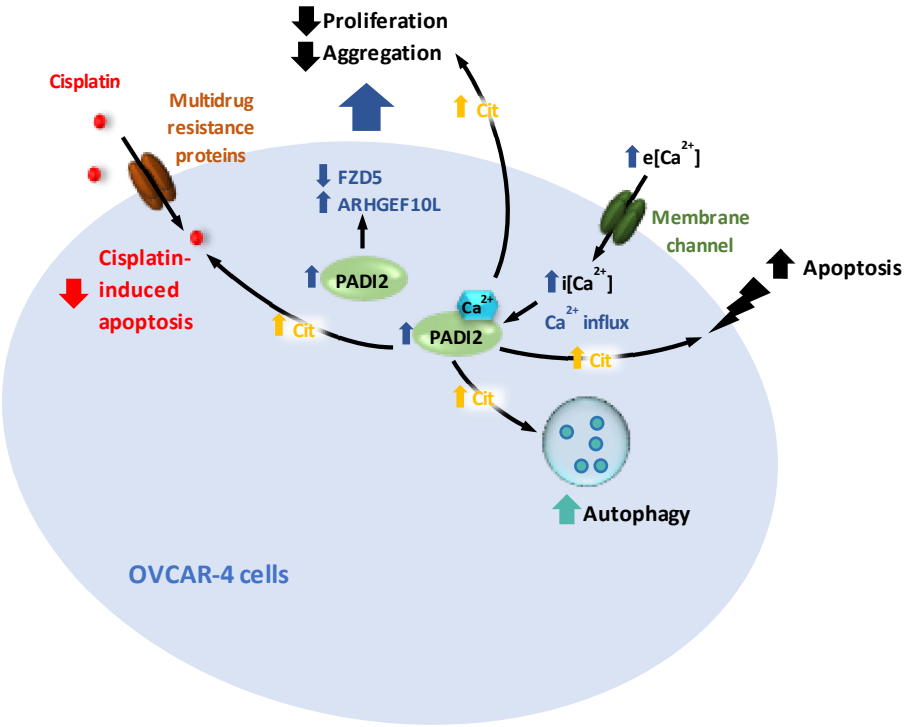
Proliferation
Aggregation
Cisplatin
Multidrug resistance proteins
Cit
e[Ca2+]
FZD5
ARHGEF10L
Membrane channel
Cisplatin-induced apoptosis
PADI2
i[Ca2+]
Apoptosis
Ca2+
Ca2+ influx
Cit
PADI2
Cit
Cit
Autophagy
OVCAR-4 cells

b

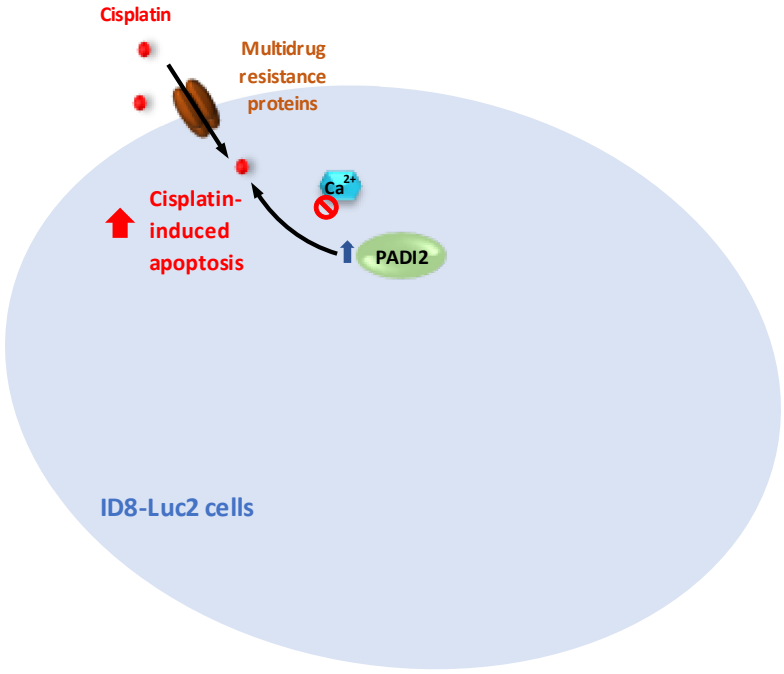
Cisplatin
Multidrug resistance proteins
Ca2+
Cisplatin-induced apoptosis
PADI2
ID8-Luc2 cells

7.1 Schematic representation of the combined findings from this thesis work. The proposed mechanism of PADI2 function in EOC. PADI2 activation and downstream regulatory pathways were assessed in human-derived OVCAR-4 cells and mouse-derived ID8-Luc2 cells. **(a)** In OVCAR-4 cells, PADI2 overexpression led to a significant reduction in the proliferation and cellular aggregation, and increased apoptosis and autophagy in a Ca^{2+}- and citrullination-dependent manner. Higher *PADI2* expression was also associated with the deregulation of *FZD5* and *ARHGEF10L* independently of Ca^{2+} treatment. By reducing the expression of *FZD5,* known to increase the adhesion to ECM, and increasing GTPases *ARHGEF10L* expression, PADI2 contributes to reduced aggregation and proliferation. PADI2 overexpression also induced cisplatin cytotoxicity, by sensitising cells to treatment and leading to higher drug efficacy. **(b)** In ID8-Luc2 cells, PADI2 overexpression significantly decreased cisplatin cytotoxicity independently of e[Ca^{2+}] or induced citrullination, leading to reduced drug efficacy and increased cell survival and resistance. Abbreviations: *FZD,* frizzled class receptor 5; *ARHGEF10L;* Rho guanine nucleotide exchange factor (GEF) 10-like, Ca^{2+}, calcium; ECM, extracellular matrix.

REFERENCES

Abrusán, G., Marsh, J.A. (2016) Alpha helices are more robust to mutations than beta strands. *PLOS computational biology*. **12**(12), e1005242.

Adoue, V., Chavanas, S., Coudane, F., Méchin, M.-C., Caubet, C., Ying, S., Dong, S., Duplan, H., Charveron, M., Takahara, H., Serre, G., Simon, M. (2008) Long-range enhancer differentially regulated by c-Jun and JunD controls peptidylarginine deiminase-3 gene in keratinocytes. *Journal of molecular biology*. **384**(5), 1048–1057.

Aggarwal, S.K. (1998) Calcium modulation of toxicities due to Cisplatin. *Metal-based drugs*. **5**(2), 77–81.

Ahmad, S., Keskin, O., Sarai, A., Nussinov, R. (2008) Protein–DNA interactions: structural, thermodynamic and clustering patterns of conserved residues in DNA-binding proteins. *Nucleic acids research*. **36**(18), 5922–5932.

Al-Bahlani, S., Fraser, M., Wong, A.Y.C., Sayan, B.S., Bergeron, R., Melino, G., Tsang, B.K. (2011) P73 regulates cisplatin-induced apoptosis in ovarian cancer cells via a calcium/calpain-dependent mechanism. *Oncogene*. **30**(41), 4219–4230.

Al-Ibraheemi, A., Wahed, A. (2013) Pitfalls in Tumor Markers Testing. *Accurate Results in the Clinical Laboratory*. 177–193.

Aldape, K., Zadeh, G., Mansouri, S., Reifenberger, G., von Deimling, A. (2015) Glioblastoma: pathology, molecular mechanisms and markers. *Acta neuropathologica*. **129**(6), 829–848.

Aleskandarany, M.A., Surridge, R., Mukherjee, A., Caldas, C., Diez-Rodriguez, M., Ashankyty, I., Albrahim, K.I., Elmouna, A.M., Aneja, R., Martin, S.G., Ellis, I.O., Green, A.R., Rakha, E.A. (2019) Rho-GTPase activating-protein 18: a biomarker associated with good prognosis in invasive breast cancer. *British journal of cancer*. **117**(8), 1176-1184.

Allen, F., Crepaldi, L., Alsinet, C., Strong, Alexander J., Kleshchevnikov, V., De Angeli, P., Páleníková, P., Khodak, A., Kiselev, V., Kosicki, M., Bassett, A.R., Harding, H., Galanty, Y., Muñoz-Martínez, F., Metzakopian, E., Jackson, S.P., Parts, L. (2018) Predicting the mutations generated by repair of Cas9-induced double-strand breaks. *Nature biotechnology*. **37**(1), 64–72.

Allen, F., Crepaldi, L., Alsinet, C., Strong, Alexander J, Kleshchevnikov, V., De Angeli, P., Palenikova, P., Kosicki, M., Bassett, A.R., Harding, H., Galanty, Y., Muñoz-Martínez, F., Metzakopian, E., Jackson, S.P., Parts, L. (2018) Mutations generated by repair of Cas9-induced double strand breaks are predictable from surrounding sequence. *Nature Biotechnology*. **37**(1), 64-72.

Alvero, A.B., Chen, R., Fu, H.-H., Montagna, M., Schwartz, P.E., Rutherford, T., Silasi, D.-A., Steffensen, K.D., Waldstrom, M., Visintin, I., Mor, G. (2009) Molecular phenotyping of human ovarian cancer stem cells unravels the mechanisms for repair and chemoresistance. *Cell cycle*. **8**(1), 158–166.

Aman, A., Piotrowski, T. (2010) Cell migration during morphogenesis. *Developmental biology*. **341**(1), 20–33.

Amler, L.C. (2010) HER3 mRNA as a predictive biomarker in anticancer therapy. *Expert opinion on biological therapy*. **10**(9), 1343–1355.

Anglesio, M.S., Kommoss, S., Tolcher, M.C., Clarke, B., Galletta, L., Porter, H., Damaraju, S., Fereday, S., Winterhoff, B.J., Kalloger, S.E., Senz, J., Yang, W., Steed, H., Allo, G., Ferguson, S., Shaw, P., Teoman, A., Garcia, J.J., Schoolmeester, J.K., Bakkum-Gamez, J., Tinker, A. V, Bowtell, D.D., Huntsman, D.G., Gilks, C.B., McAlpine, J.N. (2013) Molecular characterization of mucinous ovarian tumours supports a stratified treatment approach with HER2 targeting in 19% of carcinomas. *The journal of pathology*. **229**(1), 111–120.

Antalis, T.M., Hodge, K.M. (2013) Testisin. *Handbook of proteolytic enzymes*, 3000–3003.

Anzilotti, C., Pratesi, F., Tommasi, C., Migliorini, P. (2010) Peptidylarginine deiminase 4 and citrullination in health and disease. *Autoimmunity reviews*. **9**(3), 158–160.

Arcangeli, A., Crociani, O., Bencini, L. (2014) Interaction of tumour cells with their microenvironment: ion channels and cell adhesion molecules. A focus on pancreatic cancer. *The royal society of biological sciences*. **369**(1638).

Arita, K., Hashimoto, H., Shimizu, T., Nakashima, K., Yamada, M., Sato, M. (2004) Structural basis for Ca2+-induced activation of human PAD4. *Nature structural & molecular biology*. **11**(8), 777–783.

Assenov, Y., Brocks, D., Gerhäuser, C. (2018) Intratumor heterogeneity in epigenetic patterns. *Seminars in cancer biology*. **51**, 12–21.

Audagnotto, M., Dal Peraro, M. (2017) Protein post-translational modifications: In silico prediction tools and molecular modeling. *Computational and structural biotechnology journal*. **15**, 307–319.

Aysal, A., Karnezis, A., Medhi, I., Grenert, J.P., Zaloudek, C.J., Rabban, J.T. (2012) Ovarian endometrioid adenocarcinoma. *The american journal of surgical pathology*. **36**(2), 163–172.

Baba, T., Convery, P.A., Matsumura, N., Whitaker, R.S., Kondoh, E., Perry, T., Huang, Z., Bentley, R.C., Mori, S., Fujii, S., Marks, J.R., Berchuck, A., Murphy, S.K. (2009) Epigenetic regulation of CD133 and tumorigenicity of CD133+ ovarian cancer cells. *Oncogene*. **28**(2), 209–218.

Bannister, A.J., Kouzarides, T. (2011) Regulation of chromatin by histone modifications. *Cell research*. **21**(3), 381–395.

Barbolina, M.V., Burkhalter, R.J., Stack, M.S. (2011) Diverse mechanisms for activation of Wnt signalling in the ovarian tumour microenvironment. *Biochemical journal*. **437**(1), 1–12.

Baron, A.T., Wilken, J.A., Haggstrom, D.E., Goodrich, S.T., Maihle, N.J. (2009) Clinical implementation of soluble EGFR (sEGFR) as a theragnostic serum biomarker of breast, lung and ovarian cancer. *IDrugs : the investigational drugs journal*. **12**(5), 302–8.

Bast, R.C., Hennessy, B., Mills, G.B., Mills, G.B. (2009) The biology of ovarian cancer: new opportunities for translation. *Nature reviews. Cancer*. **9**(6), 415–28.

Beaufort, C.M., Helmijr, J.C.A., Piskorz, A.M., Hoogstraat, M., Ruigrok-Ritstier, K., Besselink, N.,

Murtaza, M., van IJcken, W.F.J., Heine, A.A.J., Smid, M., Koudijs, M.J., Brenton, J.D., Berns, E.M.J.J., Helleman, J. (2014) Ovarian Cancer Cell Line Panel (OCCP): Clinical importance of in vitro morphological subtypes. *PLoS one*. **9**(9), e103988.

Bélanger, A.-S., Tojcic, J., Harvey, M., Guillemette, C. (2010) Regulation of UGT1A1 and HNF1 transcription factor gene expression by DNA methylation in colon cancer cells. *BMC molecular biology*. **11**, 9.

Bell, D., Berchuck, A., Birrer, M., Chien, J., Cramer, D.W., Dao, F., Dhir, R., DiSaia, P., Gabra, H., Glenn, P., Godwin, A.K., Gross, J., Hartmann, L., Huang, M., Huntsman, D.G., Iacocca, M., Imielinski, M., Kalloger, S., Karlan, B.Y., Levine, D.A., Mills, G.B., Morrison, C., Mutch, D., Olvera, N., Orsulic, S., Park, K., Petrelli, N., Rabeno, B., Rader, J.S., Sikic, B.I., Smith-McCune, K., Sood, A.K., Bowtell, D., Penny, R., Testa, J.R., Chang, K., Dinh, H.H., Drummond, J.A., Fowler, G., Gunaratne, P., Hawes, A.C., Kovar, C.L., Lewis, L.R., Morgan, M.B., Newsham, I.F., Santibanez, J., Reid, J.G., Trevino, L.R., Wu, Y.-Q., Wang, M., Muzny, D.M., Wheeler, D.A., Gibbs, R.A., Getz, G., Lawrence, M.S., Cibulskis, K., Sivachenko, A.Y., Sougnez, C., Voet, D., Wilkinson, J., Bloom, T., Ardlie, K., Fennell, T., Baldwin, J., Gabriel, S., Lander, E.S., Ding, L., Fulton, R.S., Koboldt, D.C., McLellan, M.D., Wylie, T., Walker, J., O'Laughlin, M., Dooling, D.J., Fulton, L., Abbott, R., Dees, N.D., Zhang, Q., Kandoth, C., Wendl, M., Schierding, W., Shen, D., Harris, C.C., Schmidt, H., Kalicki, J., Delehaunty, K.D., Fronick, C.C., Demeter, R., Cook, L., Wallis, J.W., Lin, L., Magrini, V.J., Hodges, J.S., Eldred, J.M., Smith, S.M., Pohl, C.S., Vandin, F., Raphael, B.J., Weinstock, G.M., Mardis, E.R., Wilson, R.K., Meyerson, M., Winckler, W., Getz, G., Verhaak, R.G.W., Carter, S.L., Mermel, C.H., Saksena, G., Nguyen, H., Onofrio, R.C., Lawrence, M.S., Hubbard, D., Gupta, S., Crenshaw, A., Ramos, A.H., Ardlie, K., Chin, L., Protopopov, A., Zhang, Juinhua, Kim, T.M., Perna, I., Xiao, Y., Zhang, H., Ren, G., Sathiamoorthy, N., Park, R.W., Lee, E., Park, P.J., Kucherlapati, R., Absher, D.M., Waite, L., Sherlock, G., Brooks, J.D., Li, J.Z., Xu, J., Myers, R.M., Laird, P.W., Cope, L., Herman, J.G., Shen, H., Weisenberger, D.J., Noushmehr, H., Pan, F., Triche Jr, T., Berman, B.P., Van Den Berg, D.J., Buckley, J., Baylin, S.B., Spellman, P.T., Purdom, E., Neuvial, P., Bengtsson, H., Jakkula, L.R., Durinck, S., Han, J., Dorton, S., Marr, H., Choi, Y.G., Wang, V., Wang, N.J., Ngai, J., Conboy, J.G., Parvin, B., Feiler, H.S., Speed, T.P., Gray, J.W., Levine, D.A., Socci, N.D., Liang, Y., Taylor, B.S., Schultz, N., Borsu, L., Lash, A.E., Brennan, C., Viale, A., Sander, C., Ladanyi, M., Hoadley, K.A., Meng, S., Du, Y., Shi, Y., Li, L., Turman, Y.J., Zang, D., Helms, E.B., Balu, S., Zhou, X., Wu, J., Topal, M.D., Hayes, D.N., Perou, C.M., Getz, G., Voet, D., Saksena, G., Zhang, Junihua, Zhang, H., Wu, C.J., Shukla, S., Cibulskis, K., Lawrence, M.S., Sivachenko, A., Jing, R., Park, R.W., Liu, Y., Park, P.J., Noble, M., Chin, L., Carter, H., Kim, D., Karchin, R., Spellman, P.T., Purdom, E., Neuvial, P., Bengtsson, H., Durinck, S., Han, J., Korkola, J.E., Heiser, L.M., Cho, R.J., Hu, Z., Parvin, B., Speed, T.P., Gray, J.W., Schultz, N., Cerami, E., Taylor, B.S., Olshen, A., Reva, B., Antipin, Y., Shen, R., Mankoo, P., Sheridan, R., Ciriello, G., Chang, W.K., Bernanke, J.A., Borsu, L., Levine, D.A., Ladanyi, M., Sander, C., Haussler, D., Benz, C.C., Stuart, J.M., Benz, S.C., Sanborn, J.Z., Vaske, C.J., Zhu, J., Szeto, C., Scott, G.K., Yau, C., Hoadley, K.A., Du, Y., Balu, S., Hayes, D.N., Perou, C.M., Wilkerson, M.D., Zhang, N., Akbani, R., Baggerly, K.A., Yung, W.K., Mills, G.B., Weinstein, J.N., Penny, R., Shelton, T., Grimm, D., Hatfield, M., Morris, S., Yena, P., Rhodes, P., Sherman, M., Paulauskis, J., Millis, S., Kahn, A., Greene, J.M., Sfeir, R., Jensen, M.A., Chen, J., Whitmore, J., Alonso, S., Jordan, J., Chu, A., Zhang, Jinghui, Barker, A., Compton, C., Eley, G., Ferguson, M., Fielding, P., Gerhard, D.S., Myles, R., Schaefer, C., Mills Shaw, K.R.,

Vaught, J., Vockley, J.B., Good, P.J., Guyer, M.S., Ozenberger, B., Peterson, J., Thomson, E. (2011) Integrated genomic analyses of ovarian carcinoma. *Nature*. **474**(7353), 609–615.

Berek, J.S., Crum, C., Friedlander, M. (2015) Cancer of the ovary, fallopian tube, and peritoneum. *International journal of gynecology & obstetrics*. **143**, 59-78.

Bermudez, Y., Yang, H., Saunders, B.O., Cheng, J.Q., Nicosia, S. V., Kruk, P.A. (2007) VEGF- and LPA-induced telomerase in human ovarian cancer cells is Sp1-dependent. *Gynecologic oncology*. **106**(3), 526–537.

Berry, D.C., Croniger, C.M., Ghyselinck, N.B., Noy, N. (2012) Transthyretin blocks retinol uptake and cell signaling by the holo-retinol-binding protein receptor STRA6. *Molecular and cellular biology*. **32**(19), 3851–3859.

Bertucci, F., Borie, N., Ginestier, C., Groulet, A., Charafe-Jauffret, E., Adélaïde, J., Geneix, J., Bachelart, L., Finetti, P., Koki, A., Hermitte, F., Hassoun, J., Debono, S., Viens, P., Fert, V., Jacquemier, J., Birnbaum, D. (2004) Identification and validation of an ERBB2 gene expression signature in breast cancers. *Oncogene*. **23**(14), 2564–2575.

Bettermann, K., Benesch, M., Weis, S., Haybaeck, J. (2012) SUMOylation in carcinogenesis. *Cancer letters*. **316**(2), 113–125.

Bhattacharya, R., Nicoloso, M., Arvizo, R., Wang, E., Cortez, A., Rossi, S., Calin, G.A., Mukherjee, P. (2009) MiR-15a and MiR-16 control Bmi-1 expression in ovarian cancer. *Cancer research*. **69**(23), 9090–9095.

Bhattacharya, S.K., Crabb, J.S., Bonilha, V.L., Gu, X., Takahara, H., Crabb, J.W. (2006) Proteomics Implicates peptidyl arginine deiminase 2 and optic nerve citrullination in glaucoma pathogenesis. *Investigative Opthalmology & Visual Science*. **47**(6), 2508.

Bicker, K.L., Thompson, P.R. (2013) The protein arginine deiminases: Structure, function, inhibition, and disease. *Biopolymers*. **99**(2), 155–163.

Birrer, M.J., Konstantinopoulos, P., Penson, R.T., Roche, M., Ambrosio, A., Stallings, T.E., Matulonis, U., Bradley, C.R. (2011) A phase II trial of iniparib (BSI-201) in combination with gemcitabine/carboplatin (GC) in patients with platinum-resistant recurrent ovarian cancer. *Journal of clinical oncology*. **29**(15), 5005–5005.

Bobbs, A., Gellerman, K., Hallas, W.M., Joseph, S., Yang, C., Kurkewich, J., Cowden Dahl, K.D. (2015a) ARID3B directly regulates ovarian cancer promoting genes. *PLOS one*. **10**(6), e0131961.

Bolton, K.L., Chenevix-Trench, G., Goh, C., Sadetzki, S., Ramus, S.J., Karlan, B.Y., Lambrechts, D., Despierre, E., Barrowdale, D., McGuffog, L., Healey, S., Easton, D.F., Sinilnikova, O., Benítez, J., García, M.J., Neuhausen, S., Gail, M.H., Hartge, P., Peock, S., Frost, D., Evans, D.G., Eeles, R., Godwin, A.K., Daly, M.B., Kwong, A., Ma, E.S.K., Lázaro, C., Blanco, I., Montagna, M., D'Andrea, E., Nicoletto, M.O., Johnatty, S.E., Kjær, S.K., Jensen, A., Høgdall, E., Goode, E.L., Fridley, B.L., Loud, J.T., Greene, M.H., Mai, P.L., Chetrit, A., Lubin, F., Hirsh-Yechezkel, G., Glendon, G., Andrulis, I.L., Toland, A.E., Senter, L., Gore, M.E., Gourley, C., Michie, C.O., Song, H., Tyrer, J., Whittemore, A.S., McGuire, V., Sieh, W., Kristoffersson, U., Olsson, H., Borg, Å., Levine, D.A., Steele, L., Beattie, M.S., Chan, S., Nussbaum, R.L., Moysich, K.B., Gross, J., Cass, I., Walsh, C., Li, A.J., Leuchter, R., Gordon, O., Garcia-Closas, M.,

Gayther, S.A., Chanock, S.J., Antoniou, A.C., Pharoah, P.D.P., EMBRACE, kConFab Investigators, Cancer Genome Atlas Research Network (2012) Mutations and Survival in Women With Invasive Epithelial Ovarian Cancer. *JAMA*. **307**(4), 382.

Bose, T., Cieślar-Pobuda, A., Wiechec, E. (2015) Role of ion channels in regulating Ca^{2+} homeostasis during the interplay between immune and cancer cells. *Cell death & disease*. **6**(2), e1648.

Brentville, V.A., Metheringham, R.L., Gunn, B., Symonds, P., Daniels, I., Gijon, M., Cook, K., Xue, W., Durrant, L.G. (2016) Citrullinated vimentin presented on MHC-II in tumor cells is a target for CD4+ T-cell-mediated antitumor immunity. *Cancer research*. **76**(3), 548–560.

Brinkman, E.K., Chen, T., Amendola, M., van Steensel, B. (2014) Easy quantitative assessment of genome editing by sequence trace decomposition. *Nucleic acids research*. **42**(22), 168–168.

Bristow, R.E., Chang, J., Ziogas, A., Campos, B., Chavez, L.R., Anton-Culver, H. (2015) Impact of national cancer institute comprehensive cancer centers on ovarian cancer treatment and survival. *Journal of the american college of surgeons*. **220**(5), 940–950.

Bristow, R.E., Chi, D.S. (2006) Platinum-based neoadjuvant chemotherapy and interval surgical cytoreduction for advanced ovarian cancer: A meta-analysis. *Gynecologic oncology*. **103**(3), 1070–1076.

Brown, J., Frumovitz, M. (2014) Mucinous tumors of the ovary: current thoughts on diagnosis and management. *Current oncology reports*. **16**(6), 389.

Burke, W.M., Jin, X., Lin, H.J., Huang, M., Liu, R., Reynolds, R.K., Lin, J. (2001) Inhibition of constitutively active STAT3 Suppresses growth of human ovarian and breast cancer cells. *Oncogene*. **20**(55), 7925–7934.

Bürkle, A. (2001) Posttranslational modification predator ± prey and parasite ± host interactions. *Encyclopedia of genetics elsevier Inc.* **4**(12), 1533.

Burrell, R.A., McGranahan, N., Bartek, J., Swanton, C. (2013) The causes and consequences of genetic heterogeneity in cancer evolution. *Nature*. **501**(7467), 338–345.

Camp, R.L., Dolled-Filhart, M., Rimm, D.L. (2004) X-Tile: A New Bio-Informatics Tool for Biomarker Assessment and Outcome-Based Cut-Point Optimization. *Clinical cancer research*. **10**(21), 7252–7259.

Campbell, I.G., Russell, S.E., Choong, D.Y.H., Montgomery, K.G., Ciavarella, M.L., Hooi, C.S.F., Cristiano, B.E., Pearson, R.B., Phillips, W.A. (2004) Mutation of the ***PIK3CA*** gene in ovarian and breast cancer. *Cancer research*. **64**(21), 7678–7681.

Cannistra, S.A. (2004) Cancer of the ovary. *New england journal of medicine*. **351**(24), 2519–2529.

Canonici, A., Ivers, L., Conlon, N.T., Pedersen, K., Gaynor, N., Browne, B.C., O'Brien, N.A., Gullo, G., Collins, D.M., O'Donovan, N., Crown, J. (2018) HER-targeted tyrosine kinase inhibitors enhance response to trastuzumab and pertuzumab in HER2-positive breast cancer. *Investigational new drugs*. **37**(3), 441-451.

Cantarino, N., Musulen, E., Valero, V., Peinado, M.A., Perucho, M., Moreno, V., Forcales, S.-V.,

Douet, J., Buschbeck, M. (2016) Downregulation of the deiminase PADI2 is an early event in colorectal carcinogenesis and indicates poor prognosis. *Molecular cancer research*. **14**(9), 841–848.

Carmon, K. S., Loose, D.S. (2008) Secreted frizzled-related protein 4 regulates two Wnt7a signaling pathways and inhibits proliferation in endometrial cancer cells. *Molecular cancer research*. **6**(6), 1017–1028.

Carmon, Kendra S., Loose, D.S. (2008) Wnt7a interaction with FZD5 and detection of signaling activation using a split eGFP. *Biochemical and biophysical research communications*. **368**(2), 285–291.

Carracedo, A., Pandolfi, P.P. (2008) The PTEN-PI3K pathway: of feedbacks and cross-talks. *Oncogene*. **27**(41), 5527–41.

Carroll, S.B. (2008) Evo-Devo and an expanding evolutionary synthesis: a genetic theory of morphological evolution. *Cell*. **134**(1), 25–36.

Casey, R.C., Burleson, K.M., Skubitz, K.M., Pambuccian, S.E., Oegema, T.R., Ruff, L.E., Skubitz, A.P.N. (2001) β1-Integrins regulate the formation and adhesion of ovarian carcinoma multicellular spheroids. The american journal of pathology. **159**(3), 2071-2080.

Castagnoli, L., Costantini, A., Dall'Armi, C., Gonfloni, S., Montecchi-Palazzi, L., Panni, S., Paoluzi, S., Santonico, E., Cesareni, G. (2004) Selectivity and promiscuity in the interaction network mediated by protein recognition modules. *FEBS Letters*. **567**(1), 74–79.

Cau, L., Pendaries, V., Lhuillier, E., Thompson, P.R., Serre, G., Takahara, H., Méchin, M.-C., Simon, M. (2017) Lowering relative humidity level increases epidermal protein deimination and drives human filaggrin breakdown. *Journal of dermatological science*. **86**(2), 106–113.

Causey, C.P., Jones, J.E., Slack, J.L., Kamei, D., Jones, L.E., Subramanian, V., Knuckley, B., Ebrahimi, P., Chumanevich, A.A., Luo, Y., Hashimoto, H., Sato, M., Hofseth, L.J., Thompson, P.R., Thompson, P.R. (2011) The development of N-α-(2-carboxyl)benzoyl-N(5)-(2-fluoro-1-iminoethyl)-l-ornithine amide (o-F-amidine) and N-α-(2-carboxyl)benzoyl-N(5)-(2-chloro-1-iminoethyl)-l-ornithine amide (o-Cl-amidine) as second generation protein arginine deiminase (PAD) inhibitors. *Journal of medicinal chemistry*. **54**(19), 6919–35.

Cerami, E., Gao, J., Dogrusoz, U., Gross, B.E., Sumer, S.O., Aksoy, B.A., Jacobsen, A., Byrne, C.J., Heuer, M.L., Larsson, E., Antipin, Y., Reva, B., Goldberg, A.P., Sander, C., Schultz, N. (2012) The cBio cancer genomics portal: an open platform for exploring multidimensional cancer genomics data: Figure 1. *Cancer discovery*. **2**(5), 401–404.

De Ceuleneer, M., Van Steendam, K., Dhaenens, M., Deforce, D. (2012) In vivo relevance of citrullinated proteins and the challenges in their detection. *Proteomics*. **12**(6), 752–760.

Chan, J.K., Tian, C., Monk, B.J., Herzog, T., Kapp, D.S., Bell, J., Young, R.C., Gynecologic Oncology Group (2008) Prognostic factors for high-risk early-stage epithelial ovarian cancer. *Cancer*. **112**(10), 2202–2210.

Chang, L.C., Huang, C.F., Lai, M.-S., Shen, L.J., Wu, F.L.L., Cheng, W.F. (2018) Prognostic factors in epithelial ovarian cancer: A population-based study. *PLOS one*. **13**(3), 0194993.

Chang, M.C., Chen, C.A., Chen, P.J., Chiang, Y.C., Chen, Y.L., Mao, T.L., Lin, H.W., Lin Chiang, W.H., Cheng, W.F. (2012) Mesothelin enhances invasion of ovarian cancer by inducing MMP-7 through MAPK/ERK and JNK pathways. *Biochemical journal*. **442**(2), 293–302.

Chang, M.C., Chen, C.A., Hsieh, C.Y., Lee, C.N., Su, Y.N., Hu, Y.H., Cheng, W.F. (2009) Mesothelin inhibits paclitaxel-induced apoptosis through the PI3K pathway. *Biochemical journal*. **424**(3), 449–458.

Chang, X. (2005) Localization of peptidylarginine deiminase 4 (PADI4) and citrullinated protein in synovial tissue of rheumatoid arthritis. *Rheumatology*. **44**(1), 40–50.

Chang, X., Fang, K. (2010) PADI4 and tumourigenesis. *Cancer cell international*. **10**(1), 7.

Chang, X., Han, J. (2006) Expression of peptidylarginine deiminase type 4 (PAD4) in various tumors. *Molecular carcinogenesis*. **45**(3), 183–196.

Chari, R., Mali, P., Moosburner, M., Church, G.M. (2015) Unraveling CRISPR-Cas9 genome engineering parameters via a library-on-library approach. *Nature methods*. **12**(9), 823–826.

Chavanas, S., Méchin, M.C., Nachat, R., Adoue, V., Coudane, F., Serre, G., Simon, M. (2006b) Peptidylarginine deiminases and deimination in biology and pathology: Relevance to skin homeostasis. *Journal of dermatological science*. **44**(2), 63–72.

Chavanas, S., Méchin, M.C., Takahara, H., Kawada, A., Nachat, R., Serre, G., Simon, M. (2004) Comparative analysis of the mouse and human peptidylarginine deiminase gene clusters reveals highly conserved non-coding segments and a new human gene, PADI6. *Gene*. **330**, 19–27.

Chen, H., Ye, D., Xie, X., Chen, B., Lu, W. (2004) VEGF, VEGFRs expressions and activated STATs in ovarian epithelial carcinoma. *Gynecologic oncology*. **94**(3), 630–635.

Chen, S., Sun, H., Miao, K., Deng, C.X. (2016) CRISPR-Cas9: from genome editing to cancer research. *International journal of biological sciences*. **12**(12), 1427–1436.

Chen, X., Xu, F., Zhu, C., Ji, J., Zhou, X., Feng, X., Guang, S. (2015) Dual sgRNA-directed gene knockout using CRISPR/Cas9 technology in Caenorhabditis elegans. *Scientific reports*. **4**(1), 7581.

Cherrington, Brian D, Morency, E., Struble, A.M., Coonrod, S.A., Wakshlag, J.J. (2010) Potential role for peptidylarginine deiminase 2 (PAD2) in citrullination of canine mammary epithelial cell histones. *PloS one*. **5**(7), 11768.

Cherrington, B.D., Zhang, X., McElwee, J.L., Morency, E., Anguish, L.J., Coonrod, S.A. (2012) Potential role for PAD2 in gene regulation in breast cancer cells. *PLoS one*. **7**(7), 41242.

Chetrit, A., Hirsh-Yechezkel, G., Ben-David, Y., Lubin, F., Friedman, E., Sadetzki, S. (2008) Effect of *BRCA1/2* mutations on long-term survival of patients with invasive ovarian cancer: the national israeli study of ovarian cancer. *Journal of clinical oncology*. **26**(1), 20–25.

Chin, L., Meyerson, M. (2008) Comprehensive genomic characterization defines human glioblastoma genes and core pathways. *Nature*. **455**(7216), 1061–8.

Chira, S., Gulei, D., Hajitou, A., Zimta, A.A., Cordelier, P., Berindan-Neagoe, I. (2017)

CRISPR/Cas9: transcending the reality of genome editing. *Molecular therapy - nucleic acids*. **7**, 211–222.

Chorawala, M.R., Oza, P.M., Shah, G.B. (2012) Mechanisms of anticancer drugs resistance: an overview. *International journal of pharmaceutical sciences and drug research*. **4**(1), 1-09.

Chrun, E.S., Modolo, F., Daniel, F.I. (2017) Histone modifications: A review about the presence of this epigenetic phenomenon in carcinogenesis. *Pathology - Research and Practice*. **213**(11), 1329–1339.

Chu, H.D., Nguyen, K.H., Watanabe, Y., Le, D.T., Pham, T.L.T., Mochida, K., Tran, L.P. (2018) Identification, structural characterization and gene expression analysis of members of the nuclear factor-y family in chickpea (cicer arietinum l.) under dehydration and abscisic acid treatments. *International journal of molecular sciences*. **19**(11).

Chui, M.H., Ryan, P., Radigan, J., Ferguson, S.E., Pollett, A., Aronson, M., Semotiuk, K., Holter, S., Sy, K., Kwon, J.S., Soma, A., Singh, N., Gallinger, S., Shaw, P., Arseneau, J., Foulkes, W.D., Gilks, C.B., Clarke, B.A. (2014) The histomorphology of lynch syndrome–associated ovarian carcinomas. *The American journal of surgical pathology*. **38**(9), 1173–1181.

Chylinski, K., Makarova, K.S., Charpentier, E., Koonin, E. V (2014) Classification and evolution of type II CRISPR-Cas systems. *Nucleic acids research*. **42**(10), 6091–105.

Colomer, A.T., Jiménez, A.M., Bover Barceló, M.I. (2008) Laparoscopic treatment and staging of early ovarian cancer. *Journal of minimally invasive gynecology*. **15**(4), 414–419.

Colón, M., Pleil, J.D., Hartlage, T.A., Lucia Guardani, M., Helena Martins, M. (2001) Survey of volatile organic compounds associated with automotive emissions in the urban airshed of São Paulo, Brazil. *Atmospheric environment*. **35**(23), 4017–4031.

Comamala, M., Pinard, M., Thériault, C., Matte, I., Albert, A., Boivin, M., Beaudin, J., Piché, A., Rancourt, C. (2011) Downregulation of cell surface CA125/MUC16 induces epithelial-to-mesenchymal transition and restores EGFR signalling in NIH:OVCAR3 ovarian carcinoma cells. *British journal of cancer*. **104**(6), 989–999.

Cook, K., Daniels, I., Symonds, P., Pitt, T., Gijon, M., Xue, W., Metheringham, R., Durrant, L., Brentville, V. (2018) Citrullinated α-enolase is an effective target for anti-cancer immunity. *Oncoimmunology*. **7**(2), 1390642.

Copeland, R.A., Solomon, M.E., Richon, V.M. (2009) Protein methyltransferases as a target class for drug discovery. *Nature reviews drug discovery*. **8**(9), 724–732.

Crisp, M., Cook, L. (2005) Do early branching lineages signify ancestral traits? *Trends in Ecology & Evolution*. **20**(3), 122–128.

Di Cristofano, A., Pesce, B., Cordon-Cardo, C., Pandolfi, P.P. (1998) Pten is essential for embryonic development and tumour suppression. *Nature genetics*. **19**(4), 348–55.

Crotzer, V.L., Blum, J.S. (2009) Autophagy and its role in MHC-mediated antigen presentation. *Journal of immunology*. **182**(6), 3335.

Cyster, J.G. (2005) Chemokines, sphingosine-1-phosphate, and cell migration in secondary lymphoid organs. *Annual review of immunology*. **23**(1), 127–159.

D'Andrilli, G., Giordano, A., Bovicelli, A. (2008) Epithelial ovarian cancer: the role of cell cycle genes in the different histotypes. *The open clinical cancer journal*. **2**(1), 7–12.

Dabrowska, M., Czubak, K., Juzwa, W., Krzyzosiak, W.J., Olejniczak, M., Kozlowski, P. (2018) qEva-CRISPR: a method for quantitative evaluation of CRISPR/Cas-mediated genome editing in target and off-target sites. *Nucleic acids research*. **46**(17), 101.

Dahiya, N., Becker, K.G., Wood, W.H., Zhang, Y., Morin, P.J. (2011) Claudin-7 is frequently overexpressed in ovarian cancer and promotes invasion. *PLoS one*. **6**(7), 22119.

Damgaard, D., Senolt, L., Nielsen, M.F., Pruijn, G.J., Nielsen, C.H. (2014) Demonstration of extracellular peptidylarginine deiminase (PAD) activity in synovial fluid of patients with rheumatoid arthritis using a novel assay for citrullination of fibrinogen. *Arthritis research & therapy*. **16**(6).

Darling, A.L., Uversky, V.N. (2018) Intrinsic disorder and posttranslational modifications: the darker side of the biological dark matter. *Frontiers in genetics*. **9**, 158.

Darrah, E., Andrade, F. (2018) Rheumatoid arthritis and citrullination. *Current opinion in rheumatology*. **30**(1), 72–78.

Darrah, E., Giles, J.T., Ols, M.L., Bull, H.G., Andrade, F., Rosen, A. (2013) Erosive rheumatoid arthritis is associated with antibodies that activate PAD4 by increasing calcium sensitivity. *Science translational medicine*. **5**(186), 186.

Darrah, E., Rosen, A., Giles, J.T., Andrade, F. (2012) Peptidylarginine deiminase 2, 3 and 4 have distinct specificities against cellular substrates: novel insights into autoantigen selection in rheumatoid arthritis. *Annals of the rheumatic diseases*. **71**(1), 92–98.

Ben David, Y., Chetrit, A., Hirsh-Yechezkel, G., Friedman, E., Beck, B.D., Beller, U., Ben-Baruch, G., Fishman, A., Levavi, H., Lubin, F., Menczer, J., Piura, B., Struewing, J.P., Modan, B., National Israeli Study of Ovarian Cancer (2002) Effect of *BRCA* mutations on the length of survival in epithelial ovarian tumors. *Journal of clinical oncology*. **20**(2), 463–466.

Dekou, V., Whincup, P., Papacosta, O., Ebrahim, S., Lennon, L., Ueland, P.M., Refsum, H., Humphries, S.E., Gudnason, V. (2001) The effect of the C677T and A1298C polymorphisms in the methylenetetrahydrofolate reductase gene on homocysteine levels in elderly men and women from the British regional heart study. *Atherosclerosis*. **154**(3), 659–66.

Delaney, J.R., Patel, C.B., Willis, K.M., Haghighiabyaneh, M., Axelrod, J., Tancioni, I., Lu, D., Bapat, J., Young, S., Cadassou, O., Bartakova, A., Sheth, P., Haft, C., Hui, S., Saenz, C., Schlaepfer, D.D., Harismendy, O., Stupack, D.G. (2017) Haploinsufficiency networks identify targetable patterns of allelic deficiency in low mutation ovarian cancer. *Nature communications*. **8**, 14423.

Denman, R.B. (2005) PAD: the smoking gun behind arginine methylation signaling? *BioEssays*. **27**(3), 242–246.

Dhar, S.K., St. Clair, D.K. (2009) Nucleophosmin blocks mitochondrial localization of p53 and apoptosis. *Journal of biological chemistry*. **284**(24), 16409–16418.

Doolittle, R.F. (1995) The Multiplicity of domains in proteins. *Annual review of biochemistry*. **64**(1), 287–314.

Dressman, H.K., Berchuck, A., Chan, G., Zhai, J., Bild, A., Sayer, R., Cragun, J., Clarke, J., Whitaker, R.S., Li, L., Gray, J., Marks, J., Ginsburg, G.S., Potti, A., West, M., Nevins, J.R., Lancaster, J.M. (2007) An integrated genomic-based approach to individualized treatment of patients with advanced-stage ovarian cancer. *Journal of clinical oncology*. **25**(5), 517–525.

Duan, Z., Bradner, J., Greenberg, E., Mazitschek, R., Foster, R., Mahoney, J., Seiden, M. V. (2007) 8-Benzyl-4-oxo-8-azabicyclo[3.2.1]oct-2-ene-6,7-dicarboxylic acid (SD-1008), a novel janus kinase 2 inhibitor, increases chemotherapy sensitivity in human ovarian cancer cells. *Molecular pharmacology*. **72**(5), 1137–1145.

Durante, P., Raleigh, X., Gómez, M.E., Campos, G., Ryder, E. (1996) Isozyme analysis of human polymorphonuclear leukocyte phosphofructokinase from insulin resistant individuals. *Biochemical and biophysical research communications*. **225**(3), 975–82.

Durbin, R.M., Altshuler, D.L., Durbin, R.M., Abecasis, G.R., Bentley, D.R., Chakravarti, A., Clark, A.G., Collins, F.S., De La Vega, F.M., Donnelly, P., Egholm, M., Flicek, P., Gabriel, S.B., Gibbs, R.A., Knoppers, B.M., Lander, E.S., Lehrach, H., Mardis, E.R., McVean, G.A., Nickerson, D.A., Peltonen, L., Schafer, A.J., Sherry, S.T., Wang, Jun, Wilson, R.K., Gibbs, R.A., Deiros, D., Metzker, M., Muzny, D., Reid, J., Wheeler, D., Wang, Jun, Li, J., Jian, M., Li, G., Li, R., Liang, H., Tian, G., Wang, B., Wang, Jian, Wang, W., Yang, H., Zhang, X., Zheng, Huisong, Lander, E.S., Altshuler, D.L., Ambrogio, L., Bloom, T., Cibulskis, K., Fennell, T.J., Gabriel, S.B., Jaffe, D.B., Shefler, E., Sougnez, C.L., Bentley, D.R., Gormley, N., Humphray, S., Kingsbury, Z., Koko-Gonzales, P., Stone, J., McKernan, K.J., Costa, G.L., Ichikawa, J.K., Lee, C.C., Sudbrak, R., Lehrach, H., Borodina, T.A., Dahl, A., Davydov, A.N., Marquardt, P., Mertes, F., Nietfeld, W., Rosenstiel, P., Schreiber, S., Soldatov, A. V., Timmermann, B., Tolzmann, M., Egholm, M., Affourtit, J., Ashworth, D., Attiya, S., Bachorski, M., Buglione, E., Burke, A., Caprio, A., Celone, C., Clark, S., Conners, D., Desany, B., Gu, L., Guccione, L., Kao, K., Kebbel, A., Knowlton, J., Labrecque, M., McDade, L., Mealmaker, C., Minderman, M., Nawrocki, A., Niazi, F., Pareja, K., Ramenani, R., Riches, D., Song, W., Turcotte, C., Wang, S., Mardis, E.R., Wilson, R.K., Dooling, D., Fulton, L., Fulton, R., Weinstock, G., Durbin, R.M., Burton, J., Carter, D.M., Churcher, C., Coffey, Alison, Cox, A., Palotie, A., Quail, M., Skelly, T., Stalker, J., Swerdlow, H.P., Turner, D., De Witte, A., Giles, S., Gibbs, R.A., Wheeler, D., Bainbridge, M., Challis, D., Sabo, A., Yu, F., Yu, J., Wang, Jun, Fang, X., Guo, X., Li, R., Li, Yingrui, Luo, R., Tai, S., Wu, H., Zheng, Hancheng, Zheng, X., Zhou, Y., Li, G., Wang, Jian, Yang, H., Marth, G.T., Garrison, E.P., Huang, W., Indap, A., Kural, D., Lee, W.-P., Fung Leong, W., Quinlan, A.R., Stewart, C., Stromberg, M.P., Ward, A.N., Wu, J., Lee, C., Mills, R.E., Shi, X., Daly, M.J., DePristo, M.A., Altshuler, D.L., Ball, A.D., Banks, E., Bloom, T., Browning, B.L., Cibulskis, K., Fennell, T.J., Garimella, K. V., Grossman, S.R., Handsaker, R.E., Hanna, M., Hartl, C., Jaffe, D.B., Kernytsky, A.M., Korn, J.M., Li, H., Maguire, J.R., McCarroll, S.A., McKenna, A., Nemesh, J.C., Philippakis, A.A., Poplin, R.E., Price, A., Rivas, M.A., Sabeti, P.C., Schaffner, S.F., Shefler, E., Shlyakhter, I.A., Cooper, D.N., Ball, E. V., Mort, M., Phillips, A.D., Stenson, P.D., Sebat, J., Makarov, V., Ye, Kenny, Yoon, S.C., Bustamante, C.D., Clark, A.G., Boyko, A., Degenhardt, J., Gravel, S., Gutenkunst, R.N., Kaganovich, M., Keinan, A., Lacroute, P., Ma, X., Reynolds, A., Clarke, L., Flicek, P., Cunningham, F., Herrero, J., Keenen, S., Kulesha, E., Leinonen, R., McLaren, W.M., Radhakrishnan, R., Smith, R.E., Zalunin, V., Zheng-Bradley, X., Korbel, J.O., Stütz, A.M., Humphray, S., Bauer, M., Keira Cheetham, R., Cox, T.,

Eberle, M., James, T., Kahn, S., Murray, L., Chakravarti, A., Ye, Kai, De La Vega, F.M., Fu, Y., Hyland, F.C.L., Manning, J.M., McLaughlin, S.F., Peckham, H.E., Sakarya, O., Sun, Y.A., Tsung, E.F., Batzer, M.A., Konkel, M.K., Walker, J.A., Sudbrak, R., Albrecht, M.W., Amstislavskiy, V.S., Herwig, R., Parkhomchuk, D. V., Sherry, S.T., Agarwala, R., Khouri, H.M., Morgulis, A.O., Paschall, J.E., Phan, L.D., Rotmistrovsky, K.E., Sanders, R.D., Shumway, M.F., Xiao, C., McVean, G.A., Auton, A., Iqbal, Z., Lunter, G., Marchini, J.L., Moutsianas, L., Myers, S., Tumian, A., Desany, B., Knight, J., Winer, R., Craig, D.W., Beckstrom-Sternberg, S.M., Christoforides, A., Kurdoglu, A.A., Pearson, J. V., Sinari, S.A., Tembe, W.D., Haussler, D., Hinrichs, A.S., Katzman, S.J., Kern, A., Kuhn, R.M., Przeworski, M., Hernandez, R.D., Howie, B., Kelley, J.L, Cord Melton, S., Abecasis, G.R., Li, Yun, Anderson, P., Blackwell, T., Chen, W., Cookson, W.O., Ding, J., Min Kang, H., Lathrop, M., Liang, L., Moffatt, M.F., Scheet, P., Sidore, C., Snyder, Matthew, Zhan, X., Zöllner, S., Awadalla, P., Casals, F., Idaghdour, Y., Keebler, J., Stone, E.A., Zilversmit, M., Jorde, L., Xing, J., Eichler, E.E., Aksay, G., Alkan, C., Hajirasouliha, I., Hormozdiari, F., Kidd, J.M., Cenk Sahinalp, S., Sudmant, P.H., Mardis, E.R., Chen, K., Chinwalla, A., Ding, L., Koboldt, D.C., McLellan, M.D., Dooling, D., Weinstock, G., Wallis, J.W., Wendl, M.C., Zhang, Q., Durbin, R.M., Albers, C.A., Ayub, Q., Balasubramaniam, S., Barrett, J.C., Carter, D.M., Chen, Y., Conrad, D.F., Danecek, P., Dermitzakis, E.T., Hu, M., Huang, N., Hurles, M.E., Jin, H., Jostins, L., Keane, T.M., Quang Le, S., Lindsay, S., Long, Q., MacArthur, D.G., Montgomery, S.B., Parts, L., Stalker, J., Tyler-Smith, C., Walter, K., Zhang, Y., Gerstein, M.B., Snyder, Michael, Abyzov, A., Balasubramanian, S., Bjornson, R., Du, J., Grubert, F., Habegger, L., Haraksingh, R., Jee, J., Khurana, E., Lam, H.Y.K., Leng, J., Jasmine Mu, X., Urban, A.E., Zhang, Z., Li, Yingrui, Luo, R., Marth, G.T., Garrison, E.P., Kural, D., Quinlan, A.R., Stewart, C., Stromberg, M.P., Ward, A.N., Wu, J., Lee, C., Mills, R.E., Shi, X., McCarroll, S.A., Banks, E., DePristo, M.A., Handsaker, R.E., Hartl, C., Korn, J.M., Li, H., Nemesh, J.C., Sebat, J., Makarov, V., Ye, Kenny, Yoon, S.C., Degenhardt, J., Kaganovich, M., Clarke, L., Smith, R.E., Zheng-Bradley, X., Korbel, J.O., Humphray, S., Keira Cheetham, R., Eberle, M., Kahn, S., Murray, L., Ye, Kai, De La Vega, F.M., Fu, Y., Peckham, H.E., Sun, Y.A., Batzer, M.A., Konkel, M.K., Walker, J.A., Xiao, C., Iqbal, Z., Desany, B., Blackwell, T., Snyder, Matthew, Xing, J., Eichler, E.E., Aksay, G., Alkan, C., Hajirasouliha, I., Hormozdiari, F., Kidd, J.M., Chen, K., Chinwalla, A., Ding, L., McLellan, M.D., Wallis, J.W., Hurles, M.E., Conrad, D.F., Walter, K., Zhang, Y., Gerstein, M.B., Snyder, Michael, Abyzov, A., Du, J., Grubert, F., Haraksingh, R., Jee, J., Khurana, E., Lam, H.Y.K., Leng, J., Jasmine Mu, X., Urban, A.E., Zhang, Z., Gibbs, R.A., Bainbridge, M., Challis, D., Coafra, C., Dinh, H., Kovar, C., Lee, S., Muzny, D., Nazareth, L., Reid, J., Sabo, A., Yu, F., Yu, J., Marth, G.T., Garrison, E.P., Indap, A., Fung Leong, W., Quinlan, A.R., Stewart, C., Ward, A.N., Wu, J., Cibulskis, K., Fennell, T.J., Gabriel, S.B., Garimella, K. V., Hartl, C., Shefler, E., Sougnez, C.L., Wilkinson, J., Clark, A.G., Gravel, S., Grubert, F., Clarke, L., Flicek, P., Smith, R.E., Zheng-Bradley, X., Sherry, S.T., Khouri, H.M., Paschall, J.E., Shumway, M.F., Xiao, C., McVean, G.A., Katzman, S.J., Abecasis, G.R., Blackwell, T., Mardis, E.R., Dooling, D., Fulton, L., Fulton, R., Koboldt, D.C., Durbin, R.M., Balasubramaniam, S., Coffey, Allison, Keane, T.M., MacArthur, D.G., Palotie, A., Scott, C., Stalker, J., Tyler-Smith, C., Gerstein, M.B., Balasubramanian, S., Chakravarti, A., Knoppers, B.M., Abecasis, G.R., Bustamante, C.D., Gharani, N., Gibbs, R.A., Jorde, L., Kaye, J.S., Kent, A., Li, T., McGuire, A.L., McVean, G.A., Ossorio, P.N., Rotimi, C.N., Su, Y., Toji, L.H., Tyler-Smith, C., Brooks, L.D., Felsenfeld, A.L., McEwen, J.E., Abdallah, A., Juenger, C.R., Clemm, N.C., Collins, F.S., Duncanson, A., Green, E.D., Guyer, M.S., Peterson, J.L., Schafer, A.J.,

Abecasis, G.R., Altshuler, D.L., Auton, A., Brooks, L.D., Durbin, R.M., Gibbs, R.A., Hurles, M.E., McVean, G.A. (2010) A map of human genome variation from population-scale sequencing. *Nature*. **467**(7319), 1061–1073.

Durrant, L.G., Metheringham, R.L., Brentville, V.A. (2016) Autophagy, citrullination and cancer. *Biochemistry research international.* **12**(6), 1055–1056.

Earp, M., Tyrer, J.P., Winham, S.J., Lin, H.-Y., Chornokur, G., Dennis, J., Aben, K.K.H., Anton-Culver, H., Antonenkova, N., Bandera, E. V., Bean, Y.T., Beckmann, M.W., Bjorge, L., Bogdanova, N., Brinton, L.A., Brooks-Wilson, A., Bruinsma, F., Bunker, C.H., Butzow, R., Campbell, I.G., Carty, K., Chang-Claude, J., Cook, L.S., Cramer, D.W., Cunningham, J.M., Cybulski, C., Dansonka-Mieszkowska, A., Despierre, E., Doherty, J.A., Dörk, T., du Bois, A., Dürst, M., Easton, D.F., Eccles, D.M., Edwards, R.P., Ekici, A.B., Fasching, P.A., Fridley, B.L., Gentry-Maharaj, A., Giles, G.G., Glasspool, R., Goodman, M.T., Gronwald, J., Harter, P., Hein, A., Heitz, F., Hildebrandt, M.A.T., Hillemanns, P., Hogdall, C.K., Høgdall, E., Hosono, S., Iversen, E.S., Jakubowska, A., Jensen, A., Ji, B.-T., Jung, A.Y., Karlan, B.Y., Kellar, M., Kiemeney, L.A., Kiong Lim, B., Kjaer, S.K., Krakstad, C., Kupryjanczyk, J., Lambrechts, D., Lambrechts, S., Le, N.D., Lele, S., Lester, J., Levine, D.A., Li, Z., Liang, D., Lissowska, J., Lu, K., Lubinski, J., Lundvall, L., Massuger, L.F.A.G., Matsuo, K., McGuire, V., McLaughlin, J.R., McNeish, I., Menon, U., Milne, R.L., Modugno, F., Moysich, K.B., Ness, R.B., Nevanlinna, H., Odunsi, K., Olson, S.H., Orlow, I., Orsulic, S., Paul, J., Pejovic, T., Pelttari, L.M., Permuth, J.B., Pike, M.C., Poole, E.M., Rosen, B., Rossing, M.A., Rothstein, J.H., Runnebaum, I.B., Rzepecka, I.K., Schernhammer, E., Schwaab, I., Shu, X.-O., Shvetsov, Y.B., Siddiqui, N., Sieh, W., Song, H., Southey, M.C., Spiewankiewicz, B., Sucheston-Campbell, L., Tangen, I.L., Teo, S.-H., Terry, K.L., Thompson, P.J., Thomsen, L., Tworoger, S.S., van Altena, A.M., Vergote, I., Vestrheim Thomsen, L.C., Vierkant, R.A., Walsh, C.S., Wang-Gohrke, S., Wentzensen, N., Whittemore, A.S., Wicklund, K.G., Wilkens, L.R., Woo, Y.-L., Wu, A.H., Wu, X., Xiang, Y.-B., Yang, H., Zheng, W., Ziogas, A., Lee, A.W., Pearce, C.L., Berchuck, A., Schildkraut, J.M., Ramus, S.J., Monteiro, A.N.A., Narod, S.A., Sellers, T.A., Gayther, S.A., Kelemen, L.E., Chenevix-Trench, G., Risch, H.A., Pharoah, P.D.P., Goode, E.L., Phelan, C.M. (2018) Variants in genes encoding small GTPases and association with epithelial ovarian cancer susceptibility. *PLOS ONE*. **13**(7), e0197561.

English, D.P., Santin, A.D. (2013) Claudins overexpression in ovarian cancer: potential targets for Clostridium Perfringens Enterotoxin (CPE) based diagnosis and therapy. *International journal of molecular sciences*. **14**(5), 10412–37.

Falcão, A.M., Meijer, M., Scaglione, A., Rinwa, P., Agirre, E., Liang, J., Larsen, S.C., Heskol, A., Frawley, R., Klingener, M., Varas-Godoy, M., Raposo, A.A.S.F., Ernfors, P., Castro, D.S., Nielsen, M.L., Casaccia, P., Castelo-Branco, G. (2018) PADI2-mediated citrullination is required for efficient oligodendrocyte differentiation and myelination. *Cell reports.* **9**(1), 425348.

Fan, M., Zhuang, Q., Chen, Y., Ding, T., Yao, H., Chen, L., He, X., Xu, X. (2014) B7-H4 expression is correlated with tumor progression and clinical outcome in urothelial cell carcinoma. *International journal of clinical and experimental pathology*. **7**(10), 6768–75.

Fan, P., He, Z.Y., Xu, T., Phan, K., Chen, G.G., Wei, Y.Q. (2018) Exposing cancer with CRISPR-Cas9: from genetic identification to clinical therapy. *Translational Cancer*

Research. **7**(3), 817–827.

Fang, G., Bhardwaj, N., Robilotto, R., Gerstein, M.B. (2010) Getting started in gene orthology and functional analysis. *PLoS computational biology*. **6**(3), 1000703.

Fernández, M.L. (2011) Identification of new molecules and biomarkers involved in the initiation and progression of ovarian cancer. *Universitat Autònoma de Barcelona*.

Fischerova, D., Zikan, M., Semeradova, I., Slama, J., Kocian, R., Dundr, P., Nemejcova, K., Burgetova, A., Dusek, L., Cibula, D. (2017) Ultrasound in preoperative assessment of pelvic and abdominal spread in patients with ovarian cancer: a prospective study. *Ultrasound in obstetrics & gynecology*. **49**(2), 263–274.

Florea, A.M., Büsselberg, D. (2006) Occurrence, use and potential toxic effects of metals and metal compounds. *BioMetals*. **19**(4), 419–427.

Folkman, J. (1990) Endothelial cells and angiogenic growth factors in cancer growth and metastasis. Introduction. *Cancer metastasis reviews*. **9**(3), 171–4.

Foster, I. (2008) Cancer: A cell cycle defect. *Radiography*. **14**(2), 144–149.

Fotopoulou, C., Richter, R., Braicu, E.I., Schmidt, S.C., Lichtenegger, W., Sehouli, J. (2010) Can complete tumor resection be predicted in advanced primary epithelial ovarian cancer? A systematic evaluation of 360 consecutive patients. *European journal of surgical oncology*. **36**(12), 1202–1210.

Friedl, P., Wolf, K. (2003) Tumour-cell invasion and migration: diversity and escape mechanisms. *Nature reviews cancer*. **3**(5), 362–374.

Fuhrmann, J., Clancy, K.W., Thompson, P.R. (2015) Chemical biology of protein arginine modifications in epigenetic regulation. *Chemical Reviews*. **115**(11), 5413–5461.

Funayama, R., Taniguchi, H., Mizuma, M., Fujishima, F., Kobayashi, M., Ohnuma, S., Unno, M., Nakayama, K. (2017) Protein-arginine deiminase 2 suppresses proliferation of colon cancer cells through protein citrullination. *Cancer Science*. **108**(4), 713–718.

Fury, M.G., Zhang, W., Christodoulopoulos, I., Zieve, G.W. (1997) Multiple protein: protein interactions between the snRNP common core proteins. *Experimental cell research*. **237**(1), 63–9.

Gahete, M., Luque, R., Castaño, J. (2012) Measurement of Free Cytosolic Calcium Concentration ([Ca2+]i) in Single CHO-K1 Cells. *Bio-protocol*. **2**(22).

Gao, J., Aksoy, B.A., Dogrusoz, U., Dresdner, G., Gross, B., Sumer, S.O., Sun, Y., Jacobsen, A., Sinha, R., Larsson, E., Cerami, E., Sander, C., Schultz, N. (2013) Integrative analysis of complex cancer genomics and clinical profiles using the cBioPortal. *Science signaling*. **6**(269), pl1.

Gao, Z., Xu, X., McClane, B., Zeng, Q., Litkouhi, B., Welch, W.R., Berkowitz, R.S., Mok, S.C., Garner, E.I.O. (2011) C terminus of clostridium perfringens enterotoxin downregulates cldn4 and sensitizes ovarian cancer cells to taxol and carboplatin. *Clinical cancer research*. **17**(5), 1065–1074.

Garziera, M., Cecchin, E., Canzonieri, V., Sorio, R., Giorda, G., Scalone, S., De Mattia, E., Roncato, R., Gagno, S., Poletto, E., Romanato, L., Sartor, F., Polesel, J., Toffoli, G. (2018) Identification of novel somatic TP53 Mutations in patients with high-grade serous ovarian cancer (HGSOC) using next-generation sequencing (NGS).

International journal of molecular sciences. **19**(5).

Gatza, M.L., Silva, G.O., Parker, J.S., Fan, C., Perou, C.M. (2014) An integrated genomics approach identifies drivers of proliferation in luminal-subtype human breast cancer. *Nature genetics*. **46**(10), 1051–1059.

George, J., Alsop, K., Etemadmoghadam, D., Hondow, H., Mikeska, T., Dobrovic, A., deFazio, A., Smyth, G.K., Levine, D.A., Mitchell, G., Bowtell, D. D., Bowtell, David D (2013) Nonequivalent gene expression and copy number alterations in high-grade serous ovarian cancers with brca1 and brca2 mutations. *Clinical cancer research*. **19**(13), 3474–3484.

Gershenson, D.M., Sun, C.C., Lu, K.H., Coleman, R.L., Sood, A.K., Malpica, A., Deavers, M.T., Silva, E.G., Bodurka, D.C. (2006) Clinical behavior of stage II-IV low-grade serous carcinoma of the ovary. *Obstetrics & gynecology*. **108**(2), 361–368.

Gharib, W.H., Robinson-Rechavi, M. (2013) The branch-site test of positive selection is surprisingly robust but lacks power under synonymous substitution saturation and variation in GC. *Molecular biology and evolution*. **30**(7), 1675–86.

Gilks, C.B., Ionescu, D.N., Kalloger, S.E., Köbel, M., Irving, J., Clarke, B., Santos, J., Le, N., Moravan, V., Swenerton, K., Cheryl (2008) Tumor cell type can be reproducibly diagnosed and is of independent prognostic significance in patients with maximally debulked ovarian carcinoma. *Human pathology*. **39**(8), 1239–1251.

Giorgi, C., Baldassari, F., Bononi, A., Bonora, M., De Marchi, E., Marchi, S., Missiroli, S., Patergnani, S., Rimessi, A., Suski, J.M., Wieckowski, M.R., Pinton, P. (2012) Mitochondrial Ca(2+) and apoptosis. *Cell calcium*. **52**(1), 36–43.

Gkouskou, K.K., Ioannou, M., Pavlopoulos, G.A., Georgila, K., Siganou, A., Nikolaidis, G., Kanellis, D.C., Moore, S., Papadakis, K.A., Kardassis, D., Iliopoulos, I., McDyer, F.A., Drakos, E., Eliopoulos, A.G. (2016) Apolipoprotein A-I inhibits experimental colitis and colitis-propelled carcinogenesis. *Oncogene*. **35**(19), 2496–2505.

Gkretsi, V., Stylianopoulos, T. (2018) Cell Adhesion and Matrix Stiffness: Coordinating cancer cell invasion and metastasis. *Frontiers in oncology*. **8**, 145.

Glick, D., Barth, S., Macleod, K.F. (2010) Autophagy: cellular and molecular mechanisms. *The journal of pathology*. **221**(1), 3–12.

González-Martín, A., Sánchez-Lorenzo, L., Bratos, R., Márquez, R., Chiva, L. (2014) First-line and maintenance therapy for ovarian cancer: current status and future directions. *Drugs*. **74**(8), 879–889.

Gopinathan, G., Milagre, C., Pearce, O.M.T., Reynolds, L.E., Hodivala-Dilke, K., Leinster, D.A., Zhong, H., Hollingsworth, R.E., Thompson, R., Whiteford, J.R., Balkwill, F. (2015) Interleukin-6 stimulates defective angiogenesis. *Cancer research*. **75**(15), 3098–107.

Gray, H.J., Bell-McGuinn, K., Fleming, G.F., Cristea, M., Xiong, H., Sullivan, D., Luo, Y., McKee, M.D., Munasinghe, W., Martin, L.P. (2018) Phase I combination study of the PARP inhibitor veliparib plus carboplatin and gemcitabine in patients with advanced ovarian cancer and other solid malignancies. *Gynecologic oncology*. **148**(3), 507–514.

Grimholt, U., Tsukamoto, K., Azuma, T., Leong, J., Koop, B.F., Dijkstra, J.M. (2015) A

comprehensive analysis of teleost MHC class I sequences. *BMC evolutionary biology*. **15**(1), 32.

Chirivi, R., Rosmalen, J.W. van, Jenniskens, G.J., Pruijn, G.J., Raats, J.M. (2013) Citrullination: a target for disease intervention in multiple sclerosis and other inflammatory diseases? *Journal of clinical & cellular immunology*. **4**(03), 1–8.

Guan, B., Wang, T.L., Shih, I.M. (2011) ARID1A, a factor that promotes formation of swi/snf-mediated chromatin remodeling, is a tumor suppressor in gynecologic cancers. *Cancer research*. **71**(21), 6718–6727.

Guénet, J.L. (2005) The mouse genome. *Genome research*. **15**(12), 1729–40.

Guerrin, M., Ishigami, A., Méchin, M.C., Nachat, R., Valmary, S., Sebbag, M., Simon, M., Senshu, T., Serre, G. (2003) cDNA cloning, gene organization and expression analysis of human peptidylarginine deiminase type I. *The biochemical journal*. **370**(1), 167–74.

Guertin, M.J., Zhang, X., Anguish, L., Kim, S., Varticovski, L., Lis, J.T., Hager, G.L., Coonrod, S.A. (2014) Targeted H3R26 deimination specifically facilitates estrogen receptor binding by modifying nucleosome structure. *PLoS genetics*. **10**(9), 1004613.

Guo, Q., Fast, W. (2011) Citrullination of Inhibitor of growth 4 (ing4) by peptidylarginine deminase 4 (PAD4) disrupts the interaction between ING4 and p53. *Journal of biological chemistry*. **286**(19), 17069–17078.

Guo, W., Zheng, Y., Xu, B., Ma, F., Li, C., Zhang, X., Wang, Y., Chang, X. (2017) Investigating the expression, effect and tumorigenic pathway of PADI2 in tumors. *OncoTargets and therapy*. **10**, 1475–1485.

Guo, Y., Sheng, Q., Li, J., Ye, F., Samuels, D.C., Shyr, Y. (2013) Large Scale Comparison of Gene Expression Levels by Microarrays and RNAseq Using TCGA Data. *PLoS ONE*. **8**(8), 71462.

György, B., Tóth, E., Tarcsa, E., Falus, A., Buzás, E.I. (2006a) Citrullination: A posttranslational modification in health and disease. *The international journal of biochemistry & Cell Biology*. **38**(10), 1662–1677.

György, B., Tóth, E., Tarcsa, E., Falus, A., Buzás, E.I. (2006b) Citrullination: A posttranslational modification in health and disease. *The international journal of biochemistry & cell biology*. **38**(10), 1662–1677.

Haile, S., Lal, A., Myung, J.K., Sadar, M.D. (2011) FUS/TLS is a co-activator of androgen receptor in prostate cancer cells. *PloS one*. **6**(9), 24197.

Hanahan, D., Weinberg, R.A. (2011) Hallmarks of Cancer: The Next Generation. *Cell*. **144**(5), 646–674.

Hanahan, D., Weinberg, R.A. (2000) The hallmarks of cancer. *Cell*. **100**(1), 57–70.

Hayes, D.F., Markus, H.S., Leslie, R.D., Topol, E.J. (2014) Personalized medicine: risk prediction, targeted therapies and mobile health technology. *BMC Medicine*. **12**(1), 37.

He, Z.Y., Zhang, Y.G., Yang, Y.H., Ma, C.C., Wang, P., Du, W., Li, L., Xiang, R., Song, X.R., Zhao, X., Yao, S.H., Wei, Y.Q. (2018) *In vivo* ovarian cancer gene therapy using CRISPR-Cas9. *Human gene therapy*. **29**(2), 223–233.

Hecht, V.C., Sullivan, L.B., Kimmerling, R.J., Kim, D.H., Hosios, A.M., Stockslager, M.A., Stevens, M.M., Kang, J.H., Wirtz, D., Vander Heiden, M.G., Manalis, S.R. (2016) Biophysical changes reduce energetic demand in growth factor-deprived lymphocytes. *The Journal of cell biology*. **212**(4), 439–47.

Hedgepeth, S.C., Garcia, M.I., Wagner, L.E., Rodriguez, A.M., Chintapalli, S. V, Snyder, R.R., Hankins, G.D. V, Henderson, B.R., Brodie, K.M., Yule, D.I., van Rossum, D.B., Boehning, D., Boehning, D. (2015) The BRCA1 tumor suppressor binds to inositol 1,4,5-trisphosphate receptors to stimulate apoptotic calcium release. *The Journal of biological chemistry*. **290**(11), 7304–13.

Helland, Å., Anglesio, M.S., George, J., Cowin, P.A., Johnstone, C.N., House, C.M., Sheppard, K.E., Etemadmoghadam, D., Melnyk, N., Rustgi, A.K., Phillips, W.A., Johnsen, H., Holm, R., Kristensen, G.B., Birrer, M.J., Pearson, R.B., Børresen-Dale, A.-L., Huntsman, D.G., deFazio, A., Creighton, C.J., Smyth, G.K., Bowtell, D.D.L., Bowtell, D.D.L. (2011) Deregulation of MYCN, LIN28B and LET7 in a molecular subtype of aggressive high-grade serous ovarian cancers. *PLoS ONE*. **6**(4), 18064.

Henderson, B., Martin, A.C.R. (2014) Protein moonlighting: a new factor in biology and medicine. *Biochemical society transactions*. **42**(6), 1671–8.

Hernandez, L., Kim, M.K., Lyle, L.T., Bunch, K.P., House, C.D., Ning, F., Noonan, A.M., Annunziata, C.M. (2016) Characterization of ovarian cancer cell lines as in vivo models for preclinical studies. *Gynecologic oncology*. **142**(2), 332–40.

Hernández, R., Lino-Silva, L.S., Cantú de León, D., Pérez-Montiel, M.D., Luna-Ortiz, K. (2012) Ovarian undifferentiated carcinoma with voluminous mesenteric presentation. *International journal of surgery case reports*. **3**(11), 551–554.

Hillis, D.M., Bull, J.J. (1993) An empirical test of bootstrapping as a method for assessing confidence in phylogenetic analysis. *Systematic biology*. **42**(2), 182–192.

Horibata, S., Rogers, K.E., Sadegh, D., Anguish, L.J., McElwee, J.L., Shah, P., Thompson, P.R., Coonrod, S.A. (2017a) Role of peptidylarginine deiminase 2 (PAD2) in mammary carcinoma cell migration. *BMC Cancer*. **17**(1), 378.

Horlbeck, M.A., Witkowsky, L.B., Guglielmi, B., Replogle, J.M., Gilbert, L.A., Villalta, J.E., Torigoe, S.E., Tjian, R., Weissman, J.S. (2016) Nucleosomes impede Cas9 access to DNA in vivo and in vitro. *eLife*. **5**, 12677**.**

Hsu, P.C., Liao, Y.F., Lin, C.L., Lin, W.H., Liu, G.Y., Hung, H.C. (2014) Vimentin is involved in peptidylarginine deiminase 2-induced apoptosis of activated jurkat cells. *Molecules and cells*. **37**(5), 426–434.

Huang, E., Ishida, S., Pittman, J., Dressman, H., Bild, A., Kloos, M., D'Amico, M., Pestell, R.G., West, M., Nevins, J.R. (2003) Gene expression phenotypic models that predict the activity of oncogenic pathways. *Nature Genetics*. **34**(2), 226–230.

Huang, H.-T., Seo, H.-S., Zhang, T., Wang, Y., Jiang, B., Li, Q., Buckley, D.L., Nabet, B., Roberts, J.M., Paulk, J., Dastjerdi, S., Winter, G.E., McLauchlan, H., Moran, J., Bradner, J.E., Eck, M.J., Dhe-Paganon, S., Zhao, J.J., Gray, N.S. (2017) MELK is not necessary for the proliferation of basal-like breast cancer cells. *eLife*. **6,** 26693**.**

Huang, J., Zhang, L., Greshock, J., Colligon, T.A., Wang, Y., Ward, R., Katsaros, D., Lassus, H., Butzow, R., Godwin, A.K., Testa, J.R., Nathanson, K.L., Gimotty, P.A., Coukos, G.,

Weber, B.L., Degenhardt, Y. (2011) Frequent genetic abnormalities of the PI3K/AKT pathway in primary ovarian cancer predict patient outcome. *Genes, Chromosomes and cancer*. **50**(8), 606–618.

Huizing, M.T., Misser, V.H., Pieters, R.C., ten Bokkel Huinink, W.W., Veenhof, C.H., Vermorken, J.B., Pinedo, H.M., Beijnen, J.H. (1995) Taxanes: a new class of antitumor agents. *Cancer investigation*. **13**(4), 381–404.

Hunter, S.M., Anglesio, M.S., Ryland, G.L., Sharma, R., Chiew, Y.-E., Rowley, S.M., Doyle, M.A., Li, J., Gilks, C.B., Moss, P., Allan, P.E., Stephens, A.N., Huntsman, D.G., deFazio, A., Bowtell, D.D., Group, A.O.C.S., Gorringe, K.L., Campbell, I.G. (2015) Molecular profiling of low grade serous ovarian tumours identifies novel candidate driver genes. *Oncotarget*. **6**(35), 37663–77.

Hunter, S.M., Gorringe, K.L., Christie, M., Rowley, S.M., Bowtell, D.D., Campbell, I. G., Campbell, Ian G (2012) Pre-Invasive Ovarian mucinous tumors are characterized by CDKN2A and RAS pathway aberrations. *Clinical cancer research*. **18**(19), 5267–5277.

Hurwitz, H., Fehrenbacher, L., Novotny, W., Cartwright, T., Hainsworth, J., Heim, W., Berlin, J., Baron, A., Griffing, S., Holmgren, E., Ferrara, N., Fyfe, G., Rogers, B., Ross, R., Kabbinavar, F. (2004) Bevacizumab plus irinotecan, fluorouracil, and leucovorin for metastatic colorectal Cancer. *New england journal of medicine*. **350**(23), 2335–2342.

Inagaki, M., Takahara, H., Nishi, Y., Sugawara, K., Sato, C. (1989) Ca2+-dependent deimination-induced disassembly of intermediate filaments involves specific modification of the amino-terminal head domain. *The Journal of biological chemistry*. **264**(30), 18119–27.

Ingham, P.W., Nakano, Y., Seger, C. (2011) Mechanisms and functions of Hedgehog signalling across the metazoa. *Nature reviews genetics*. **12**(6), 393–406.

Innamaa, A., Jackson, L., Asher, V., Van Shalkwyk, G., Warren, A., Hay, D., Bali, A., Sowter, H., Khan, R. (2013) Expression and prognostic significance of the oncogenic K2P potassium channel KCNK9 (TASK-3) in ovarian carcinoma. *Anticancer research*. **33**(4), 1401–8.

Iorio, M. V., Visone, R., Di Leva, G., Donati, V., Petrocca, F., Casalini, P., Taccioli, C., Volinia, S., Liu, C.G., Alder, H., Calin, G.A., Menard, S., Croce, C.M. (2007) MicroRNA signatures in human ovarian cancer. *Cancer research*. **67**(18), 8699–8707.

Ireland, J.M., Unanue, E.R. (2012) Processing of proteins in autophagy vesicles of antigen-presenting cells generates citrullinated peptides recognized by the immune system. *Scientific Reports.* **8**(3), 429–430.

Ishida-Yamamoto, A., Senshu, T., Eady, R.A.J., Takahashi, H., Shimizu, H., Akiyama, M., Iizuka, H. (2002) Sequential reorganization of cornified cell keratin filaments involving filaggrin-mediated compaction and keratin 1 deimination. *Journal of investigative dermatology*. **118**(2), 282–287.

Jack, B.R., Meyer, A.G., Echave, J., Wilke, C.O. (2016) Functional sites induce long-range evolutionary constraints in enzymes G. A. Petsko, ed. *PLOS biology*. **14**(5), 1002452.

Jacks, T., Remington, L., Williams, B.O., Schmitt, E.M., Halachmi, S., Bronson, R.T., Weinberg, R.A. (1994) Tumor spectrum analysis in p53-mutant mice. *Current Biology*. **4**(1), 1–7.

Jain, R.K., Duda, D.G., Clark, J.W., Loeffler, J.S. (2006) Lessons from phase III clinical trials on anti-VEGF therapy for cancer. *Nature Clinical Practice Oncology*. **3**(1), 24–40.

Jazaeri, A.A., Awtrey, C.S., Chandramouli, G.V.R., Chuang, Y.E., Khan, J., Sotiriou, C., Aprelikova, O., Yee, C.J., Zorn, K.K., Birrer, M.J., Barrett, J.C., Boyd, J. (2005) Gene expression profiles associated with response to chemotherapy in epithelial ovarian cancers. *Clinical cancer research*. **11**(17), 6300–6310.

Jia, Z.H., Jia, Y., Guo, F.J., Chen, J., Zhang, X.W., Cui, M.H. (2017) Phosphorylation of STAT3 at Tyr705 regulates MMP-9 production in epithelial ovarian cancer. *PLOS ONE*. **12**(8), e0183622.

Jiang, F., Doudna, J.A. (2017) CRISPR–Cas9 structures and mechanisms. *Annual review of biophysics*. **46**(1), 505–529.

Jiang, L., Hickman, J.H., Wang, S.-J., Gu, W. (2015) Dynamic roles of p53-mediated metabolic activities in ROS-induced stress responses. *Cell cycle*. **14**(18), 2881–2885.

Jiang, Z., Cui, Y., Wang, L., Zhao, Y., Yan, S., Chang, X. (2013) Investigating citrullinated proteins in tumour cell lines. *World journal of surgical oncology*. **11**(1), 260.

Jin, Z., Ogata, S., Tamura, G., Katayama, Y., Fukase, M., Yajima, M., Motoyama, T. (2003) Carcinosarcomas (malignant mullerian mixed tumors) of the uterus and ovary: a genetic study with special reference to histogenesis. *International journal of gynecological pathology*. **22**(4), 368–373.

Johnson, S.K., Ramani, V.C., Hennings, L., Haun, R.S. (2007) Kallikrein 7 enhances pancreatic cancer cell invasion by shedding E-cadherin. *Cancer*. **109**(9), 1811–1820.

Jones, J.E., Causey, C.P., Knuckley, B., Slack-Noyes, J.L., Thompson, P.R. (2009) Protein arginine deiminase 4 (PAD4): Current understanding and future therapeutic potential. *Current opinion in drug discovery & development*. **12**(5), 616–27.

Jones, J.E., Slack, J.L., Fang, P., Zhang, X., Subramanian, V., Causey, C.P., Coonrod, S.A., Guo, M., Thompson, P.R. (2012) Synthesis and screening of a haloacetamidine containing library to identify PAD4 selective inhibitors. *ACS chemical biology*. **7**(1), 160–5.

Jordan, M.A., Wilson, L. (2004) Microtubules as a target for anticancer drugs. *Nature reviews cancer*. **4**(4), 253–265.

Jordan, S., Steer, C., DeFazio, A., Quinn, M., Obermair, A., Friedlander, M., Francis, J., O'Brien, S., Goss, G., Wyld, D., Webb, P., Webb, P. (2013) Patterns of chemotherapy treatment for women with invasive epithelial ovarian cancer – A population-based study. *Gynecologic Oncology*. **129**(2), 310–317.

Kabir, M.H., Patrick, R., Ho, J.W.K., O'Connor, M.D. (2018) Identification of active signaling pathways by integrating gene expression and protein interaction data. *BMC systems biology*. **12**(S9), 120.

Kamel, H.F.M., Al-Amodi, H.S.A.B. (2017) Exploitation of gene expression and cancer biomarkers in paving the path to era of personalized medicine. *Genomics,*

proteomics & bioinformatics. **15**(4), 220–235.

Kan, R., Jin, M., Subramanian, V., Causey, C.P., Thompson, P.R., Coonrod, S.A. (2012) Potential role for PADI-mediated histone citrullination in preimplantation development. *BMC developmental biology*. **12**(1), 19.

Kan, R., Yurttas, P., Kim, B., Jin, M., Wo, L., Lee, B., Gosden, R., Coonrod, S.A. (2011) Regulation of mouse oocyte microtubule and organelle dynamics by PADI6 and the cytoplasmic lattices. *Developmental biology*. **350**(2), 311–322.

Kannan, R., Ventura, A. (2015) The CRISPR revolution and its impact on cancer research. *Swiss medical weekly*. **145**, 14230.

Katsumoto, T., Mitsushima, A., Kurimura, T. (1990) The role of the vimentin intermediate filaments in rat 3Y1 cells elucidated by immunoelectron microscopy and computer-graphic reconstruction. *Biology of the cell*. **68**(2), 139–46.

Kaye, S.B., Lubinski, J., Matulonis, U., Ang, J.E., Gourley, C., Karlan, B.Y., Amnon, A., Bell-McGuinn, K.M., Chen, L.M., Friedlander, M., Safra, T., Vergote, I., Wickens, M., Lowe, E.S., Carmichael, J., Bella, K. (2011) Phase II, open-label, randomized, multicenter study comparing the efficacy and safety of olaparib, a poly (ADP-Ribose) polymerase inhibitor, and pegylated liposomal doxorubicin in. *Article in journal of clinical oncology*. **30**(4), 372-379.

Kearney, P.L., Bhatia, M., Jones, N.G., Yuan, L., Glascock, M.C., Catchings, K.L., Yamada, M., Thompson, P.R. (2005) Kinetic Characterization of protein arginine deiminase 4: a transcriptional corepressor implicated in the onset and progression of rheumatoid arthritis †. *Biochemistry*. **44**(31), 10570–10582.

Keniry, M., Parsons, R. (2008) The role of PTEN signaling perturbations in cancer and in targeted therapy. *Oncogene*. **27**(41), 5477–85.

Kim, S., Han, Y., Kim, S.I., Kim, H.S., Kim, S.J., Song, Y.S. (2018) Tumor evolution and chemoresistance in ovarian cancer. *npj Precision Oncology*. **2**(1), 20.

King, M.C., Marks, J.H., Mandell, J.B. (2003) Breast and ovarian cancer risks due to inherited mutations in BRCA1 and BRCA2. *Science*. **302**(5645), 643–646.

Kinose, Y., Sawada, K., Nakamura, K., Kimura, T. (2014) The role of micrornas in ovarian cancer. *BioMed research international*. **2014**, 1–11.

Klareskog, L., Amara, K., Malmström, V. (2014) Adaptive immunity in rheumatoid arthritis. *Current opinion in rheumatology*. **26**(1), 72–79.

Klucky, B., Mueller, R., Vogt, I., Teurich, S., Hartenstein, B., Breuhahn, K., Flechtenmacher, C., Angel, P., Hess, J. (2007) Kallikrein 6iInduces E-Cadherin shedding and promotes cell proliferation, migration, and invasion. *Cancer research*. **67**(17), 8198–8206.

Knuckley, B., Causey, C.P., Jones, J.E., Bhatia, M., Dreyton, C.J., Osborne, T.C., Takahara, H., Thompson, P.R. (2010) Substrate specificity and kinetic studies of pads 1, 3, and 4 identify potent and selective inhibitors of protein arginine deiminase 3. *Biochemistry*. **49**(23), 4852–4863.

Kobayashi, E., Ueda, Y., Matsuzaki, S., Yokoyama, T., Kimura, T., Yoshino, K., Fujita, M., Kimura, T., Enomoto, T. (2012) Biomarkers for screening, diagnosis, and monitoring of ovarian cancer. *Cancer epidemiology biomarkers & prevention*. **21**(11), 1902–

1912.

Köbel, M., Kalloger, S.E., Boyd, N., McKinney, S., Mehl, E., Palmer, C., Leung, S., Bowen, N.J., Ionescu, D.N., Rajput, A., Prentice, L.M., Miller, D., Santos, J., Swenerton, K., Gilks, C.B., Huntsman, D. (2008) Ovarian carcinoma subtypes are different diseases: implications for biomarker studies. *PLoS medicine*. **5**(12), e232.

Köbel, M., Kalloger, S.E., Santos, J.L., Huntsman, D.G., Gilks, C.B., Swenerton, K.D. (2010) Tumor type and substage predict survival in stage I and II ovarian carcinoma: Insights and implications. *Gynecologic oncology*. **116**(1), 50–56.

Kocak, D.D., Josephs, E.A., Bhandarkar, V., Adkar, S.S., Kwon, J.B., Gersbach, C.A. (2019) Increasing the specificity of CRISPR systems with engineered RNA secondary structures. *Nature biotechnology*. **37**(1), 657–666.

Konecny, G.E., Wang, C., Hamidi, H., Winterhoff, B., Kalli, K.R., Dering, J., Ginther, C., Chen, H.-W., Dowdy, S., Cliby, W., Gostout, B., Podratz, K.C., Keeney, G., Wang, H.-J., Hartmann, L.C., Slamon, D.J., Goode, E.L. (2014) Prognostic and therapeutic relevance of molecular subtypes in high-grade serous ovarian Cancer. *JNCI: Journal of the national cancer institute*. **106**(10).

Kovala, A.T., Harvey, K.A., Mcglynn, P., Boguslawski, G., Garcia, J.G.N., English, D. (2000) High-efficiency transient transfection of endothelial cells for functional analysis. *FASEB J*. **14**, 2486–2494.

Kubo, F., Takeichi, M., Nakagawa, S. (2003) Wnt2b controls retinal cell differentiation at the ciliary marginal zone. *Development*. **130**(3), 587–98.

Kumar, S., Stecher, G., Tamura, K. (2016) MEGA7: molecular evolutionary genetics analysis version 7.0 for bigger datasets. *Molecular biology and evolution*. **33**(7), 1870–1874.

Kuo, K.T., Mao, T.L., Chen, X., Feng, Y., Nakayama, K., Wang, Y., Glas, R., Ma, M.J., Kurman, R.J., Shih, I.M., Wang, T.L. (2010) DNA copy numbers profiles in affinity-purified ovarian clear cell carcinoma. *Clinical cancer research*. **16**(7), 1997–2008.

Kuriyan, J., Cowburn, D. (1997) Modular peptide recognition domains in eukaryotic signaling. *Annual review of biophysics and biomolecular structure*. **26**(1), 259–288.

Kurman, R.J., Shih, I.M. (2011) Molecular pathogenesis and extraovarian origin of epithelial ovarian cancer—Shifting the paradigm. *Human pathology*. **42**(7), 918–931.

Kurman, R.J., Shih, I.M. (2016) The dualistic model of ovarian carcinogenesis revisited, revised, and expanded. *The american journal of pathology*. **186**(4).

Kurman, R.J., Shih, I.M. (2010) The origin and pathogenesis of epithelial ovarian cancer: a proposed unifying theory. *The american journal of surgical pathology*. **34**(3), 433–443.

Kuroda, T., Hirohashi, Y., Torigoe, T., Yasuda, K., Takahashi, A., Asanuma, H., Morita, R., Mariya, T., Asano, T., Mizuuchi, M., Saito, T., Sato, N. (2013) ALDH1-high ovarian cancer stem-like cells can be isolated from serous and clear cell adenocarcinoma cells, and ALDH1 high expression is associated with poor prognosis. *PLoS one*. **8**(6), e65158.

Kursunluoglu, G., Taskiran, D., Ayar Kayali, H. (2018) The Investigation of the antitumor agent

toxicity and capsaicin effect on the electron transport chain enzymes, catalase activities and lipid peroxidation levels in lung, heart and brain tissues of rats. *Molecules*. **23**(12), 3267.

L Hollis, R., Gourley, C., L Hollis, R., Gourley, C. (2016) Genetic and molecular changes in ovarian cancer. *Cancer biology & medicine*. **13**(2), 236–247.

Lamensa, J.W., Moscarello, M.A. (1993) Deimination of human myelin basic protein by a peptidylarginine deiminase from bovine brain. *Journal of neurochemistry*. **61**(3), 987–96.

Landen, C.N., Goodman, B., Katre, A.A., Steg, A.D., Nick, A.M., Stone, R.L., Miller, L.D., Mejia, P. V., Jennings, N.B., Gershenson, D.M., Bast, R.C., Coleman, R.L., Lopez-Berestein, G., Sood, A.K. (2010) Targeting aldehyde dehydrogenase cancer stem cells in ovarian cancer. *Molecular cancer therapeutics*. **9**(12), 3186–3199.

Langie, S.A.S., Koppen, G., Desaulniers, D., Al-Mulla, F., Al-Temaimi, R., Amedei, A., Azqueta, A., Bisson, W.H., Brown, D., Brunborg, G., Charles, A.K., Chen, T., Colacci, A., Darroudi, F., Forte, S., Gonzalez, L., Hamid, R.A., Knudsen, L.E., Leyns, L., Lopez de Cerain Salsamendi, A., Memeo, L., Mondello, C., Mothersill, C., Olsen, A.-K., Pavanello, S., Raju, J., Rojas, E., Roy, R., Ryan, E., Wegman, P., Salem, H.K., Scovassi, A.I., Singh, N., Vaccari, M., Van Schooten, F.J., Valverde, M., Woodrick, J., Zhang, L., van Larebeke, N., Kirsch-Volders, M., Collins, A.R. (2015) Causes of genome instability: the effect of low dose chemical exposures in modern society. *Carcinogenesis*. **36**(1), S61–S88.

Lanner, J.T., Katz, A., Tavi, P., Sandstrom, M.E., Zhang, S.J., Wretman, C., James, S., Fauconnier, J., Lannergren, J., Bruton, J.D., Westerblad, H. (2006) The role of Ca2+ influx for insulin-mediated glucose uptake in skeletal muscle. *Diabetes*. **55**(7), 2077–2083.

Leamon, C.P., Lovejoy, C.D., Nguyen, B. (2013) Patient selection and targeted treatment in the management of platinum-resistant ovarian cancer. *Pharmacogenomics and personalized medicine*. **6**, 113–25.

Lee, J., Mir, A., Edraki, A., Garcia, B., Amrani, N., Lou, H.E., Gainetdinov, I., Pawluk, A., Ibraheim, R., Gao, X.D., Liu, P., Davidson, A.R., Maxwell, K.L., Sontheimer, E.J. (2018) Potent Cas9 inhibition in bacterial and human cells by acriic4 and acriic5 anti-CRISPR proteins. *mBio*. **9**(6), e02321.

Lee, Y.-H., Coonrod, S.A., Kraus, W.L., Jelinek, M.A., Stallcup, M.R. (2005) Regulation of coactivator complex assembly and function by protein arginine methylation and demethylimination. *Proceedings of the national academy of sciences*. **102**(10), 3611–3616.

Lehmann, S., Bykov, V.J.N., Ali, D., Andrén, O., Cherif, H., Tidefelt, U., Uggla, B., Yachnin, J., Juliusson, G., Moshfegh, A., Paul, C., Wiman, K.G., Andersson, P.O. (2012) Targeting p53 in vivo: a first-in-human study with p53-targeting compound apr-246 in refractory hematologic malignancies and prostate cancer. *Journal of clinical oncology*. **30**(29), 3633–3639.

Lengyel, E., Burdette, J.E., Kenny, H.A., Matei, D., Pilrose, J., Haluska, P., Nephew, K.P., Hales, D.B., Stack, M.S. (2014) Epithelial ovarian cancer experimental models. *Oncogene*. **33**(28), 3619–33.

Lewallen, D.M., Bicker, K.L., Madoux, F., Chase, P., Anguish, L., Coonrod, S., Hodder, P.,

Thompson, P.R. (2014) A FluoPol-ABPP PAD2 high-throughput screen identifies the first calcium site inhibitor targeting the PADs. *ACS Chemical biology*. **9**(4), 913–921.

Li, Pingxin, Li, M., Lindberg, M.R., Kennett, M.J., Xiong, N., Wang, Y. (2010) PAD4 is essential for antibacterial innate immunity mediated by neutrophil extracellular traps. *The journal of experimental medicine*. **207**(9), 1853–1862.

Li, P, Wang, D., Yao, H., Doret, P., Hao, G., Shen, Q., Qiu, H., Zhang, X., Wang, Y., Chen, G., Wang, Y. (2010) Coordination of PAD4 and HDAC2 in the regulation of p53-target gene expression. *Oncogene*. **29**(21), 3153–3162.

Li, P., Yao, H., Zhang, Z., Li, M., Luo, Y., Thompson, P.R., Gilmour, D.S., Wang, Y. (2008) Regulation of p53 target gene expression by peptidylarginine deiminase 4. *Molecular and cellular biology*. **28**(15), 4745–4758.

Liang, Z.D., Long, Y., Tsai, W.B., Fu, S., Kurzrock, R., Gagea-Iurascu, M., Zhang, F., Chen, H.H.W., Hennessy, B.T., Mills, G.B., Savaraj, N., Kuo, M.T. (2012) Preclinical development mechanistic basis for overcoming platinum resistance using copper chelating agents. *Molecular cancer therapeutics*. **11**(11), 2483-2494

Liao, J., Qian, F., Tchabo, N., Mhawech-Fauceglia, P., Beck, A., Qian, Z., Wang, X., Huss, W.J., Lele, S.B., Morrison, C.D., Odunsi, K. (2014) Ovarian cancer spheroid cells with stem cell-like properties contribute to tumor generation, metastasis and chemotherapy resistance through hypoxia-resistant metabolism. *PLoS one*. **9**(1), e84941.

Lin, M., Whitmire, S., Chen, J., Farrel, A., Shi, X., Guo, J. (2017) Effects of short indels on protein structure and function in human genomes. *Scientific reports*. **7**(1), 9313.

Linsky, T.W. (2012) Studies on the mechanism and inhibition of enzymes in the pentein superfamily. *University of texas libraries.* **7**(2), 18515.

Liu, G.-Y., Liao, Y.F., Chang, W.H., Liu, C.C., Hsieh, M.C., Hsu, P.C., Tsay, G.J., Hung, H.C. (2006) Overexpression of peptidylarginine deiminase IV features in apoptosis of haematopoietic cells. *Apoptosis*. **11**(2), 183–196.

Liu, G.Y., Lin, Y.H. (2017) T Helper subset cell activation and activated t cell autonomous death (ACAD) dedicated by peptidylarginine deiminase 2 through an ER stress and autophagy mechanism. *Immunotherapy*. **3**(2), 1325.

Liu, M.X., Siu, M.K., Liu, S.S., Yam, J.W., Ngan, H.Y., Chan, D.W., Liu, M.X., Siu, M.K., Liu, S.S., Yam, J.W., Ngan, H.Y., Chan, D.W. (2014) Epigenetic silencing of microRNA-199b-5p is associated with acquired chemoresistance via activation of JAG1-Notch1 signaling in ovarian cancer. *Oncotarget*. **5**(4), 944–958.

Liu, Y.L., Lee, C.Y., Huang, Y.N., Chen, H.Y., Liu, G.Y., Hung, H.C. (2017) Probing the roles of calcium-binding sites during the folding of human peptidylarginine deiminase 4. *Scientific reports*. **7**(1), 2429.

Liu, Y.L., Tsai, I.C., Chang, C.W., Liao, Y.F., Liu, G.Y., Hung, H.C. (2013) Functional roles of the non-catalytic calcium-binding sites in the n-terminal domain of human peptidylarginine deiminase 4. *PLoS one*. **8**(1), e51660.

López-Cortés, A., Paz-y-Miño, C., Cabrera-Andrade, A., Barigye, S.J., Munteanu, C.R., González-Díaz, H., Pazos, A., Pérez-Castillo, Y., Tejera, E. (2018) Gene prioritization,

communality analysis, networking and metabolic integrated pathway to better understand breast cancer pathogenesis. *Scientific reports*. **8**(1), 16679.

Losos, J.B., Arnold, S.J., Bejerano, G., Brodie, E.D., Hibbett, D., Hoekstra, H.E., Mindell, D.P., Monteiro, A., Moritz, C., Orr, H.A., Petrov, D.A., Renner, S.S., Ricklefs, R.E., Soltis, P.S., Turner, T.L., Turner, T.L. (2013) Evolutionary biology for the 21st century. *PLoS biology*. **11**(1), e1001466.

Loveday, C., Turnbull, C., Ramsay, E., Hughes, D., Ruark, E., Frankum, J.R., Bowden, G., Kalmyrzaev, B., Warren-Perry, M., Snape, K., Adlard, J.W., Barwell, J., Berg, J., Brady, A.F., Brewer, C., Brice, G., Chapman, C., Cook, J., Davidson, R., Donaldson, A., Douglas, F., Greenhalgh, L., Henderson, A., Izatt, L., Kumar, A., Lalloo, F., Miedzybrodzka, Z., Morrison, P.J., Paterson, J., Porteous, M., Rogers, M.T., Shanley, S., Walker, L., Breast Cancer Susceptibility Collaboration (UK), B.C.S.C., Eccles, D., Evans, D.G., Renwick, A., Seal, S., Lord, C.J., Ashworth, A., Reis-Filho, J.S., Antoniou, A.C., Rahman, N. (2011) Germline mutations in RAD51D confer susceptibility to ovarian cancer. *Nature genetics*. **43**(9), 879–882.

Ludwig, W., Oliver Glöckner, F., Yilmaz, P. (2011) The Use of rRNA gene sequence data in the classification and identification of prokaryotes. *Methods in microbiology*. **38**, 349–384.

Luo, Y., Arita, K., Bhatia, M., Knuckley, B., Lee, Y.H., Stallcup, M.R., Sato, M., Thompson, P.R. (2006) Inhibitors and inactivators of protein arginine deiminase 4: functional and structural characterization. *Biochemistry*. **45**(39), 11727–36.

Luster, A.D., Alon, R., von Andrian, U.H. (2005) Immune cell migration in inflammation: present and future therapeutic targets. *Nature immunology*. **6**(12), 1182–1190.

Lynch, H.T., Casey, M.J., Snyder, C.L., Bewtra, C., Lynch, J.F., Butts, M., Godwin, A.K. (2009) Hereditary ovarian carcinoma: heterogeneity, molecular genetics, pathology, and management. *Molecular oncology*. **3**(2), 97–137.

Ma, L., Boucher, J.I., Paulsen, J., Matuszewski, S., Eide, C.A., Ou, J., Eickelberg, G., Press, R.D., Zhu, L.J., Druker, B.J., Branford, S., Wolfe, S.A., Jensen, J.D., Schiffer, C.A., Green, M.R., Bolon, D.N. (2017) CRISPR-Cas9–mediated saturated mutagenesis screen predicts clinical drug resistance with improved accuracy. *Proceedings of the national academy of sciences*. **114**(44), 11751–11756.

Ma, L., Wang, H., Wang, C., Su, J., Xie, Q., Xu, L., Yu, Y., Liu, S., Li, S., Xu, Y., Li, Z. (2016) Failure of elevating calcium induces oxidative stress tolerance and imparts cisplatin resistance in ovarian cancer cells. *Aging and disease*. **7**(3), 254–66.

Macgregor, P.F., Squire, J.A. (2002) Application of Microarrays to the analysis of gene expression in cancer. *Clinical chemistry*. **48**(8).

Maddirevula, S., Coskun, S., Awartani, K., Alsaif, H., Abdulwahab, F.M., Alkuraya, F.S. (2017) The human knockout phenotype of *PADI6* is female sterility caused by cleavage failure of their fertilized eggs. *Clinical genetics*. **91**(2), 344–345.

Maehama, T., Dixon, J.E. (1998) The tumor suppressor, PTEN/MMAC1, dephosphorylates the lipid second messenger, phosphatidylinositol 3,4,5-trisphosphate. *The Journal of biological chemistry*. **273**(22), 13375–8.

Magnadóttir, B., Hayes, P., Hristova, M., Bragason, B.T., Nicholas, A.P., Dodds, A.W.,

Guðmundsdóttir, S., Lange, S. (2018) Post-translational protein deimination in cod (Gadus morhua L.) ontogeny novel roles in tissue remodelling and mucosal immune defences? *Developmental & comparative immunology*. **87**, 157–170.

Marinho, A.T., Lu, H., Pereira, S.A., Monteiro, E., Gabra, H., Recchi, C. (2019) Anti-tumorigenic and platinum-sensitizing effects of apolipoprotein a1 and apolipoprotein A1 mimetic peptides in ovarian cancer. *Frontiers in pharmacology*. **9,** 1524.

Martín-Cameán, M., Delgado-Sánchez, E., Piñera, A., Diestro, M.D., De Santiago, J., Zapardiel, I. (2016) The role of surgery in advanced epithelial ovarian cancer. *Ecancermedicalscience*. **10**, 666.

Martinez-Lage, M., Puig-Serra, P., Menendez, P., Torres-Ruiz, R., Rodriguez-Perales, S. (2018) CRISPR/Cas9 for cancer therapy: hopes and challenges. *Biomedicines*. **6**(4), 105.

Mashal, R.D., Koontz, J., Sklar, J. (1995) Detection of mutations by cleavage of DNA heteroduplexes with bacteriophage resolvases. *Nature genetics*. **9**(2), 177–183.

Matsuda, K., Yoshida, K., Taya, Y., Nakamura, K., Nakamura, Y., Arakawa, H. (2002) p53AIP1 regulates the mitochondrial apoptotic pathway. *Cancer research*. **62**(10), 2883–9.

Matsumoto, T., Yamazaki, M., Takahashi, H., Kajita, S., Suzuki, E., Tsuruta, T., Saegusa, M. (2015) Distinct β-Catenin and PIK3CA mutation profiles in endometriosis-associated ovarian endometrioid and clear cell carcinomas. *American journal of clinical pathology*. **144**(3), 452–463.

Mattson, M.P., Chan, S.L. (2003) Calcium orchestrates apoptosis. *Nature cell biology*. **5**(12), 1041–1043.

McCauley, J.L., Kenealy, S.J., Margulies, E.H., Schnetz-Boutaud, N., Gregory, S.G., Hauser, S.L., Oksenberg, J.R., Pericak-Vance, M.A., Haines, J.L., Mortlock, D.P. (2007) SNPs in multi-species conserved sequences (mcs) as useful markers in association studies: a practical approach. *BMC genomics*. **8**(1), 266.

McConechy, M.K., Ding, J., Senz, J., Yang, W., Melnyk, N., Tone, A.A., Prentice, L.M., Wiegand, K.C., McAlpine, J.N., Shah, S.P., Lee, C.-H., Goodfellow, P.J., Gilks, C.B., Huntsman, D.G. (2014) Ovarian and endometrial endometrioid carcinomas have distinct CTNNB1 and PTEN mutation profiles. *Modern pathology*. **27**(1), 128–134.

McElwee, J.L., Mohanan, S., Griffith, O.L., Breuer, H.C., Anguish, L.J., Cherrington, B.D., Palmer, A.M., Howe, L.R., Subramanian, V., Causey, C.P., Thompson, P.R., Gray, J.W., Coonrod, S.A. (2012) Identification of PADI2 as a potential breast cancer biomarker and therapeutic target. *BMC cancer*. **12**, 500.

McElwee, J.L., Mohanan, S., Horibata, S., Sams, K.L., Anguish, L.J., McLean, D., Cvita, I., Wakshlag, J.J., Coonrod, S.A. (2014) PAD2 Overexpression in Transgenic Mice Promotes Spontaneous Skin Neoplasia. *Cancer Research*. **74**(21), 6306–6317.

McLean, G.W., Carragher, N.O., Avizienyte, E., Evans, J., Brunton, V.G., Frame, M.C. (2005) The role of focal-adhesion kinase in cancer — a new therapeutic opportunity. *Nature reviews cancer*. **5**(7), 505–515.

Méchin, M.C., Sebbag, M., Arnaud, J., Nachat, R., Foulquier, C., Adoue, V., Coudane, F., Duplan, H., Schmitt, A.M., Chavanas, S., Guerrin, M., Serre, G., Simon, M. (2007) Update on peptidylarginine deiminases and deimination in skin physiology and severe human diseases. *International journal of cosmetic science*. **29**(3), 147–168.

Medeiros Tavares Marques, J.C., Cornélio, D.A., Nogueira Silbiger, V., Ducati Luchessi, A., de Souza, S., Batistuzzo de Medeiros, S.R. (2017) Identification of new genes associated to senescent and tumorigenic phenotypes in mesenchymal stem cells. *Scientific reports*. **7**(1), 17837.

Medvedeva, I.V., Demenkov, P.S., Ivanisenko, V.A. (2015) Computer analysis of protein functional sites projection on exon structure of genes in Metazoa. *BMC genomics*. **16**(13), S2.

Michaely, P., Li, W.P., Anderson, R.G.W., Cohen, J.C., Hobbs, H.H. (2004) The modular adaptor protein ARH is required for low density lipoprotein (LDL) binding and internalization but not for LDL receptor clustering in coated pits. *The Journal of biological chemistry*. **279**(32), 34023–31.

Michl, P., Barth, C., Buchholz, M., Lerch, M.M., Rolke, M., Holzmann, K.H., Menke, A., Fensterer, H., Giehl, K., Löhr, M., Leder, G., Iwamura, T., Adler, G., Gress, T.M. (2003) Claudin-4 expression decreases invasiveness and metastatic potential of pancreatic cancer. *Cancer research*. **63**(19), 6265–71.

Ming, M., He, Y.Y. (2012) PTEN in DNA damage repair. *Cancer letters*. **319**(2), 125–129.

Mirny, L.A., Gelfand, M.S. (2002) Using orthologous and paralogous proteins to identify specificity determining residues. *Genome biology*. **3**(3).

Mishra, S.K., Watkins, S.C., Traub, L.M. (2002) The autosomal recessive hypercholesterolemia (ARH) protein interfaces directly with the clathrin-coat machinery. *Proceedings of the national academy of sciences of the united states of america*. **99**(25), 16099–104.

Mitra, A.K., Davis, D.A., Tomar, S., Roy, L., Gurler, H., Xie, J., Lantvit, D.D., Cardenas, H., Fang, F., Liu, Y., Loughran, E., Yang, J., Sharon Stack, M., Emerson, R.E., Cowden Dahl, K.D., V Barbolina, M., Nephew, K.P., Matei, D., Burdette, J.E. (2015) In vivo tumor growth of high-grade serous ovarian cancer cell lines. *Gynecologic oncology*. **138**(2), 372-377.

Miyamoto, M., Takano, M., Goto, T., Kato, M., Sasaki, N., Tsuda, H., Furuya, K. (2013) Clear cell histology as a poor prognostic factor for advanced epithelial ovarian cancer: a single institutional case series through central pathologic review. *Journal of gynecologic oncology*. **24**(1), 37–43.

Moaaz, M., Lotfy, H. (2017) The interplay of interleukin-17A (IL-17A) and breast cancer tumor microenvironment as a novel approach to increase tumor immunogenicity. *Immunotherapy*. **3**(2).

Mohamed, B.M., Boyle, N.T., Schinwald, A., Murer, B., Ward, R., Mahfoud, O.K., Rakovich, T., Crosbie-Staunton, K., Gray, S.G., Donaldson, K., Volkov, Y., Prina-Mello, A. (2018) Induction of protein citrullination and auto-antibodies production in murine exposed to nickel nanomaterials. *Scientific reports*. **8**(1), 679.

Mohanan, S., Cherrington, Brian D, Horibata, S., McElwee, J.L., Thompson, P.R., Coonrod, S.A. (2012) Potential role of peptidylarginine deiminase enzymes and protein citrullination in cancer pathogenesis. *Biochemistry research international*. **2012**, 895343.

Montagnana, M., Danese, E., Giudici, S., Franchi, M., Guidi, G.C., Plebani, M., Lippi, G. (2011)

HE4 in ovarian cancer: from Discovery to clinical application. *Advances in clinical chemistry*. **55**, 1–20.

Moreno-Mateos, M.A., Vejnar, C.E., Beaudoin, J.D., Fernandez, J.P., Mis, E.K., Khokha, M.K., Giraldez, A.J. (2015) CRISPRscan: designing highly efficient sgRNAs for CRISPR-Cas9 targeting in vivo. *Nature methods*. **12**(10), 982–8.

Mortier, A., Gouwy, M., Van Damme, J., Proost, P. (2011) Effect of posttranslational processing on the in vitro and in vivo activity of chemokines. *Experimental cell research*. **317**(5), 642–654.

Moynahan, M.E., Pierce, A.J., Jasin, M. (2001) BRCA2 is required for homology-directed repair of chromosomal breaks. *Molecular cell*. **7**(2), 263–72.

Murugaesu, N., Chew, S.K., Swanton, C. (2013) Adapting clinical paradigms to the challenges of cancer clonal evolution. *The american journal of pathology*. **182**(6), 1962–1971.

Mutch, D.G., Prat, J. (2014) 2014 FIGO staging for ovarian, fallopian tube and peritoneal cancer. *Gynecologic oncology*. **133**(3), 401–404.

Na, K., Sung, J.Y., Kim, H.S. (2017) TP53 mutation status of tubo-ovarian and peritoneal high-grade serous carcinoma with a wild-type p53 immunostaining pattern. *Anticancer research*. **37**(12), 6697–6703.

Nachat, R., Méchin, M.C., Takahara, H., Chavanas, S., Charveron, M., Serre, G., Simon, M. (2005) Peptidylarginine deiminase isoforms 1–3 are expressed in the epidermis and involved in the deimination of K1 and filaggrin. *Journal of investigative dermatology*. **124**(2), 384–393.

Nam, E.J., Kim, Y.T. (2008) Alteration of cell-cycle regulation in epithelial ovarian cancer. *International journal of gynecological cancer*. **18**(6), 1169–1182.

Nault, J.C. (2017) Cancer gene discovery in hepatocellular carcinoma: The CRISPR/CAS9 accelerator. *Gastroenterology*. **152**(5), 941–943.

Naumann, R.W., Coleman, R.L., Burger, R.A., Sausville, E.A., Kutarska, E., Ghamande, S.A., Gabrail, N.Y., DePasquale, S.E., Nowara, E., Gilbert, L., Gersh, R.H., Teneriello, M.G., Harb, W.A., Konstantinopoulos, P.A., Penson, R.T., Symanowski, J.T., Lovejoy, C.D., Leamon, C.P., Morgenstern, D.E., Messmann, R.A. (2013) A randomized phase ii trial comparing vintafolide (ec145) and pegylated liposomal doxorubicin (PLD) in Combination versus PLD alone in patients with platinum-resistant ovarian cancer. *Journal of clinical oncology*. **31**(35), 4400–4406.

Near, T.J., Eytan, R.I., Dornburg, A., Kuhn, K.L., Moore, J.A., Davis, M.P., Wainwright, P.C., Friedman, M., Smith, W.L. (2012) Resolution of ray-finned fish phylogeny and timing of diversification. *Proceedings of the national academy of sciences of the united states of america*. **109**(34), 13698–703.

Nebel, J.C., Herzyk, P., Gilbert, D.R. (2007) Automatic generation of 3D motifs for classification of protein binding sites. *BMC bioinformatics*. **8**, 321.

Nei, M. (2007) The new mutation theory of phenotypic evolution. *Proceedings of the national academy of sciences of the united states of america*. **104**(30), 12235–42.

Neumann, E., Riepl, B., Knedla, A., Lefèvre, S., Tarner, I.H., Grifka, J., Steinmeyer, J., Schölmerich, J., Gay, S., Müller-Ladner, U. (2010) Cell culture and passaging alters

gene expression pattern and proliferation rate in rheumatoid arthritis synovial fibroblasts. *Arthritis research & therapy*. **12**(3), R83.

Nicholas, A.P., Bhattacharya, S.K. (2014) Protein Deimination in Human Health and Disease. Springer international. **6**, 1-474

Nick, A.M., Coleman, R.L., Ramirez, P.T., Sood, A.K. (2015) A framework for a personalized surgical approach to ovarian cancer. *Nature reviews clinical oncology*. **12**(4), 239–245.

Di Nicolantonio, F., Mercer, S.J., Knight, L.A., Gabriel, F.G., Whitehouse, P.A., Sharma, S., Fernando, A., Glaysher, S., Di Palma, S., Johnson, P., Somers, S.S., Toh, S., Higgins, B., Lamont, A., Gulliford, T., Hurren, J., Yiangou, C., Cree, I.A. (2005) Cancer cell adaptation to chemotherapy. *BMC cancer*. **5**, 78.

Nolen, B.M., Lokshin, A.E. (2014) Pancreatic and ovarian cancer biomarkers. *Biomarkers in toxicology*, 759–770.

Novetsky, A.P., Thompson, D.M., Zighelboim, I., Thaker, P.H., Powell, M.A., Mutch, D.G., Goodfellow, P.J. (2013) Lithium chloride and inhibition of glycogen synthase kinase 3β as a potential therapy for serous ovarian cancer. *International journal of gynecological cancer*. **23**(2), 361–366.

O'Malley, C.D., Shema, S.J., Cress, R.D., Bauer, K., Kahn, A.R., Schymura, M.J., Wike, J.M., Stewart, S.L. (2012) The implications of age and comorbidity on survival following epithelial ovarian cancer: summary and results from a centers for disease control and prevention study. *Journal of women's health*. **21**(9), 887–894.

O'Neill, D.F., Powell, J.F.F., Standen, E.M., Youson, J.H., Warby, C.M., Sherwood, N.M. (1998) Gonadotropin-releasing hormone (GnRH) in ancient teleosts, the bonytongue fishes: putative origin of salmon GnRH. *General and comparative endocrinology*. **112**(3), 415–425.

Obata, K., Morland, S.J., Watson, R.H., Hitchcock, A., Chenevix-Trench, G., Thomas, E.J., Campbell, I.G. (1998) Frequent PTEN/MMAC mutations in endometrioid but not serous or mucinous epithelial ovarian tumors. *Cancer research*. **58**(10), 2095–7.

Okudela, K., Mitsui, H., Suzuki, T., Woo, T., Tateishi, Y., Umeda, S., Saito, Y., Tajiri, M., Masuda, M., Ohashi, K. (2014) Expression of HDAC9 in lung cancer--potential role in lung carcinogenesis. *International journal of clinical and experimental pathology*. **7**(1), 213–20.

Olsen, I., Singhrao, S.K., Potempa, J. (2018) Citrullination as a plausible link to periodontitis, rheumatoid arthritis, atherosclerosis and Alzheimer's disease. *Journal of oral microbiology*. **10**(1), 1487742.

Patch, A.M., Christie, E.L., Etemadmoghadam, D., Garsed, D.W., George, Joshy, Fereday, S., Nones, K., Cowin, P., Alsop, K., Bailey, P.J., Kassahn, K.S., Newell, F., Quinn, M.C.J., Kazakoff, S., Quek, K., Wilhelm-Benartzi, C., Curry, E., Leong, H.S., Hamilton, A., Mileshkin, L., Au-Yeung, G., Kennedy, C., Hung, J., Chiew, Y.-E., Harnett, P., Friedlander, M., Quinn, M., Pyman, J., Cordner, S., O'Brien, P., Leditschke, J., Young, G., Strachan, K., Waring, P., Azar, W., Mitchell, C., Traficante, N., Hendley, J., Thorne, H., Shackleton, M., Miller, D.K., Arnau, G.M., Tothill, R.W., Holloway, T.P., Semple, T., Harliwong, I., Nourse, C., Nourbakhsh, E., Manning, S., Idrisoglu, S., Bruxner, T.J.C., Christ, A.N., Poudel, B., Holmes, O., Anderson, M., Leonard, C.,

Lonie, A., Hall, N., Wood, S., Taylor, D.F., Xu, Q., Fink, J.L., Waddell, Nick, Drapkin, R., Stronach, E., Gabra, H., Brown, R., Jewell, A., Nagaraj, S.H., Markham, E., Wilson, P.J., Ellul, J., McNally, O., Doyle, M.A., Vedururu, R., Stewart, C., Lengyel, E., Pearson, J. V., Waddell, Nicola, deFazio, A., Grimmond, S.M., Bowtell, D.D.L., Bowtell, D.D.L. (2015) Whole–genome characterization of chemoresistant ovarian cancer. *Nature*. **521**(7553), 489–494.

Pearton, D.J., Dale, B.A., Presland, R.B. (2002) Functional analysis of the profilaggrin N-terminal peptide: identification of domains that regulate nuclear and cytoplasmic distribution. *Journal of investigative dermatology*. **119**(3), 661–669.

Peiretti, M., Bristow, R.E., Zapardiel, I., Gerardi, M., Zanagnolo, V., Biffi, R., Landoni, F., Bocciolone, L., Aletti, G.D., Maggioni, A. (2012) Rectosigmoid resection at the time of primary cytoreduction for advanced ovarian cancer. A multi-center analysis of surgical and oncological outcomes. *Gynecologic oncology*. **126**(2), 220–223.

Perlman, R.L. (2016) Mouse models of human disease: An evolutionary perspective. *Evolution, medicine, and public health*. **2016**(1), 170–6.

Piura, B., Rabinovich, A., Yanai-Inbar, I. (2001) Three primary malignancies related to BRCA mutation successively occurring in a BRCA1 185delAG mutation carrier. *European journal of obstetrics, gynecology, and reproductive biology*. **97**(2), 241–4.

Poliaková, M., Aebersold, D.M., Zimmer, Y., Medová, M. (2018) The relevance of tyrosine kinase inhibitors for global metabolic pathways in cancer. *Molecular cancer*. **17**(1), 27.

Pollock, D.D. (2002) Genomic biodiversity, phylogenetics and coevolution in proteins. *Applied bioinformatics*. **1**(2), 81–92.

Powan, P., Luanpitpong, S., He, X., Rojanasakul, Y., Chanvorachote, P. (2017) Molecular Pathways in Cell Signaling: Detachment-induced E-cadherin expression promotes 3D tumor spheroid formation but inhibits tumor formation and metastasis of lung cancer cells. *American journal of physiology - cell physiology*. **313**(5), C556.

Prat, J. (2012) New insights into ovarian cancer pathology. *Annals of oncology*. **23**(10), 111–117.

Prat J (2012) Ovarian carcinomas: five distinct diseases with different origins, genetic alterations, and clinicopathological features. *Virchows archiv*. **460**(3), 237–249.

Prieske, K., Prieske, S., Joosse, S.A., Trillsch, F., Grimm, D., Burandt, E., Mahner, S., Schmalfeldt, B., Milde-Langosch, K., Oliveira-Ferrer, L., Woelber, L. (2017) Loss of BRCA1 promotor hypermethylation in recurrent high-grade ovarian cancer. *Oncotarget*. **8**(47), 83063–83074.

Pruitt, K.D., Brown, G.R., Hiatt, S.M., Thibaud-Nissen, F., Astashyn, A., Ermolaeva, O., Farrell, C.M., Hart, J., Landrum, M.J., McGarvey, K.M., Murphy, M.R., O'Leary, N.A., Pujar, S., Rajput, B., Rangwala, S.H., Riddick, L.D., Shkeda, A., Sun, H., Tamez, P., Tully, R.E., Wallin, C., Webb, D., Weber, J., Wu, W., DiCuccio, M., Kitts, P., Maglott, D.R., Murphy, T.D., Ostell, J.M. (2014) RefSeq: an update on mammalian reference sequences. *Nucleic acids research*. **42**(1), 756–763.

Pujade-Lauraine, E., Hilpert, F., Weber, B., Reuss, A., Poveda, A., Kristensen, G., Sorio, R., Vergote, I., Witteveen, P., Bamias, A., Pereira, D., Wimberger, P., Oaknin, A., Mirza,

M.R., Follana, P., Bollag, D., Ray-Coquard, I. (2014) Bevacizumab Combined With Chemotherapy for Platinum-Resistant Recurrent Ovarian Cancer: The AURELIA Open-Label Randomized Phase III Trial. *Journal of clinical oncology*. **32**(13), 1302–1308.

Raijmakers, R., Zendman, A.J.W., Egberts, W.V., Vossenaar, E.R., Raats, J., Soede-Huijbregts, C., Rutjes, F.P.J.T., van Veelen, P.A., Drijfhout, J.W., Pruijn, G.J.M. (2007) Methylation of arginine residues interferes with citrullination by peptidylarginine deiminases in vitro. *Journal of molecular biology*. **367**(4), 1118–1129.

Rais, J., Jafri, A., Siddiqui, S., Tripathi, M., Arshad, M. (2017) Phytochemicals in the treatment of ovarian cancer. *Frontiers in bioscience*. **9**, 67–75.

Rajabi, M., Mousa, S.A. (2017) The role of angiogenesis in cancer treatment. *Biomedicines*. **5**(2).

Rastogi, M., Gupta, S., Sachan, M., Rastogi, M., Gupta, S., Sachan, M. (2016) Biomarkers towards ovarian cancer diagnostics: present and future prospects. *Brazilian archives of biology and technology*. **59**(1), 16160070.

Rath, D., Amlinger, L., Rath, A., Lundgren, M. (2015) The CRISPR-Cas immune system: Biology, mechanisms and applications. *Biochimie*. **117**, 119–128.

Rauh-Hain, J.A., Krivak, T.C., Del Carmen, M.G., Olawaiye, A.B. (2011) Ovarian cancer screening and early detection in the general population. *Reviews in obstetrics & gynecology*. **4**(1), 15–21.

Reaume, C., Sokolowski, M. (2011) Conservation of gene function in behaviour. *Philosophical transactions of the Royal Society of London. Series B, Biological sciences*. **366**(1574), 2100–10.

Rebl, A., Köllner, B., Anders, E., Wimmers, K., Goldammer, T. (2010a) Peptidylarginine deiminase gene is differentially expressed in freshwater and brackish water rainbow trout. *Molecular biology reports*. **37**(5), 2333–2339.

Robin, N.H., Farmer, M.B., Gomes, A., Korf, B. (2018) Genetic testing techniques. *Pediatric cancer genetics.* **5**, 47–64.

Robson, F., Costa, M.M.R., Hepworth, S.R., Vizir, I., Pin˜eiro, M., Reeves, P.H., Putterill, J., Coupland, G. (2002) Functional importance of conserved domains in the flowering-time gene CONSTANS demonstrated by analysis of mutant alleles and transgenic plants. *The plant journal*. **28**(6), 619–631.

Rojas, V., Hirshfield, K.M., Ganesan, S., Rodriguez-Rodriguez, L. (2016) Molecular characterization of epithelial ovarian cancer: implications for diagnosis and treatment. *International journal of molecular sciences*. **17**(12).

Rokas, A. (2008) The origins of multicellularity and the early history of the genetic toolkit for animal development. *Annual review of genetics*. **42**(1), 235–251.

Romanidis, K., Nagorni, E.A., Halkia, E., Pitiakoudis, M. (2014) The role of cytoreductive surgery in advanced ovarian cancer: the general surgeon's perspective. *Journal of balkan union of oncology*. **19**(3), 598–604.

Rooth, C. (2013) Ovarian cancer: risk factors, treatment and management. *British journal of nursing*. **22**(Sup17), S23–S30.

Rosen, D.G., Mercado-Uribe, I., Yang, G., Bast, R.C., Amin, H.M., Lai, R., Liu, J. (2006) The role of constitutively active signal transducer and activator of transcription 3 in ovarian tumorigenesis and prognosis. *Cancer*. **107**(11), 2730–2740.

Rosen, E.M. (2013) BRCA1 in the DNA damage response and at telomeres. *Frontiers in genetics*. **4**, 85.

Rosso, M., Majem, B., Devis, L., Lapyckyj, L., Besso, M.J., Llauradó, M., Abascal, M.F., Matos, M.L., Lanau, L., Castellví, J., Sánchez, J.L., Pérez Benavente, A., Gil-Moreno, A., Reventós, J., Santamaria Margalef, A., Rigau, M., Vazquez-Levin, M.H. (2017) E-cadherin: A determinant molecule associated with ovarian cancer progression, dissemination and aggressiveness. *PloS one*. **12**(9), e0184439.

Roy, R., Chun, J., Powell, S.N. (2012) BRCA1 and BRCA2: different roles in a common pathway of genome protection. *Nature reviews cancer*. **12**(1), 68–78.

Rutten, M.J., van de Vrie, R., Bruining, A., Spijkerboer, A.M., Mol, B.W., Kenter, G.G., Buist, M.R. (2015) Predicting surgical outcome in patients with international federation of gynecology and obstetrics stage III or IV ovarian cancer using computed tomography. *International journal of gynecological cancer*. **25**(3), 407–415.

Ryland, G.L., Hunter, S.M., Doyle, M.A., Rowley, S.M., Christie, M., Allan, P.E., Bowtell, D.D., Gorringe, K.L., Campbell, I.G., Campbell, I.G. (2013) *RNF43* is a tumour suppressor gene mutated in mucinous tumours of the ovary. *The journal of pathology*. **229**(3), 469–476.

Sadeque, A., Barsky, M., Marass, F., Kruczkiewicz, P., Upton, C. (2010) JaPaFi: A novel program for the identification of highly conserved dna sequences. *Viruses*. **2**(9), 1867–85.

Salani, R., Kurman, R.J., Giuntoli, R., Gardner, G., Bristow, R., Wang, T.L., shih, I.M. (2008) Alteration of cell-cycle regulation in epithelial ovarian cancer. *International Journal of Gynecological Cancer*. **18**(3), 487–491.

Salani, R., Santillan, A., Zahurak, M.L., Giuntoli, R.L., Gardner, G.J., Armstrong, D.K., Bristow, R.E. (2007) Secondary cytoreductive surgery for localized, recurrent epithelial ovarian cancer. *Cancer*. **109**(4), 685–691.

Sánchez-Rivera, F.J., Jacks, T. (2015) Applications of the CRISPR-Cas9 system in cancer biology. *Nature reviews. Cancer*. **15**(7), 387–95.

Sato, E., Olson, S.H., Ahn, J., Bundy, B., Nishikawa, H., Qian, F., Jungbluth, A.A., Frosina, D., Gnjatic, S., Ambrosone, C., Kepner, J., Odunsi, T., Ritter, G., Lele, S., Chen, Y.T., Ohtani, H., Old, L.J., Odunsi, K. (2005) Intraepithelial CD8+ tumor-infiltrating lymphocytes and a high CD8+/regulatory T cell ratio are associated with favorable prognosis in ovarian cancer. *Proceedings of the national academy of sciences*. **102**(51), 18538–18543.

Sato, N., Tsunoda, H., Nishida, M., Morishita, Y., Takimoto, Y., Kubo, T., Noguchi, M. (2000) Loss of heterozygosity on 10q23.3 and mutation of the tumor suppressor gene PTEN in benign endometrial cyst of the ovary: possible sequence progression from benign endometrial cyst to endometrioid carcinoma and clear cell carcinoma of the ovary. *Cancer research*. **60**(24), 7052.

Schmeler, K.M., Sun, C.C., Bodurka, D.C., T. Deavers, M., Malpica, A., Coleman, R.L., Ramirez, P.T., Gershenson, D.M. (2008) Neoadjuvant chemotherapy for low-grade serous

carcinoma of the ovary or peritoneum. *Gynecologic oncology*. **108**(3), 510–514.

Schorge, J.O., McCann, C., Del Carmen, M.G. (2010) Surgical debulking of ovarian cancer: what difference does it make? *Reviews in obstetrics & gynecology*. **3**(3), 111–117.

Schwartz, D.R., Kardia, S.L.R., Shedden, K.A., Kuick, R., Michailidis, G., Taylor, J.M.G., Misek, D.E., Wu, R., Zhai, Y., Darrah, D.M., Reed, H., Ellenson, L.H., Giordano, T.J., Fearon, E.R., Hanash, S.M., Cho, K.R. (2002) Gene expression in ovarian cancer reflects both morphology and biological behavior, distinguishing clear cell from other poor-prognosis ovarian carcinomas. *Cancer research*. **62**(16), 4722–9.

Schwarz, R.F., Trinh, A., Sipos, B., Brenton, J.D., Goldman, N., Markowetz, F. (2014) Phylogenetic quantification of intra-tumour heterogeneity. *PLoS Computational biology*. **10**(4), e1003535.

Scully, R., Livingston, D.M. (2000) In search of the tumour-suppressor functions of BRCA1 and BRCA2. *Nature*. **408**(6811), 429–432.

Seidman, J.D., Yemelyanova, A., Cosin, J.A., Smith, A., Kurman, R.J. (2012) survival rates for international federation of gynecology and obstetrics stage III ovarian carcinoma by cell type. *International journal of gynecological cancer*. **22**(3), 367–371.

Senapati, S., Mahanta, A.K., Kumar, S., Maiti, P. (2018) Controlled drug delivery vehicles for cancer treatment and their performance. *Signal transduction and targeted therapy*. **3**, 7.

Senshu, T., Akiyama, K., Kan, S., Asaga, H., Ishigami, A., Manabe, M. (1995) Detection of deiminated proteins in rat skin: probing with a monospecific antibody after modification of citrulline residues. *The journal of investigative dermatology*. **105**(2), 163–9.

Senshu, T., Kan, S., Ogawa, H., Manabe, M., Asaga, H. (1996) Preferential Deimination of Keratin K1 and filaggrin during the terminal differentiation of human epidermis. *Biochemical and biophysical research communications*. **225**(3), 712–719.

Sentmanat, M.F., Peters, S.T., Florian, C.P., Connelly, J.P., Pruett-Miller, S.M. (2018) A survey of validation strategies for CRISPR-Cas9 editing. *Scientific reports*. **8**(1), 888.

Sharma, P., Lioutas, A., Fernandez-Fuentes, N., Quilez, J., Carbonell-Caballero, J., Wright, R.H., Di Vona, C., Le Dily, F., Schüller, R., Eick, D., Oliva, B., Beato, M. (2019) Arginine citrullination at the C-terminal domain controls RNA polymerase II transcription. Molecular cell. **73**(1), 84-96.

Shih, I.M., Panuganti, P.K., Kuo, K.T., Mao, T.L., Kuhn, E., Jones, S., Velculescu, V.E., Kurman, R.J., Wang, T.L. (2011) Somatic mutations of PPP2R1A in ovarian and uterine carcinomas. *The american journal of pathology*. **178**(4), 1442–7.

Sidhu, H., Capalash, N. (2017) UHRF1: The key regulator of epigenetics and molecular target for cancer therapeutics. *Tumor biology*. **39**(2), 101042831769220.

Siliciano, J.D., Canman, C.E., Taya, Y., Sakaguchi, K., Appella, E., Kastan, M.B. (1997) DNA damage induces phosphorylation of the amino terminus of p53. *Genes & development*. **11**(24), 3471–81.

Singh, A.B., Sharma, A., Dhawan, P. (2010) Claudin family of proteins and cancer: an overview. *Journal of oncology*. **2010**, 541957.

Slack, J.L., Jones, L.E., Bhatia, M.M., Thompson, P.R., Thompson, P.R. (2011) Autodeimination of protein arginine deiminase 4 alters protein-protein interactions but not activity. *Biochemistry*. **50**(19), 3997–4010.

Slade, D.J., Fang, P., Dreyton, C.J., Zhang, Y., Fuhrmann, J., Rempel, D., Bax, B.D., Coonrod, S.A., Lewis, H.D., Guo, M., Gross, M.L., Thompson, P.R. (2015) Protein arginine deiminase 2 binds calcium in an ordered fashion: implications for inhibitor design. *ACS chemical biology*. **10**(4), 1043–53.

Slade, D.J., Horibata, S., Coonrod, S.A., Thompson, P.R. (2014) A novel role for protein arginine deiminase 4 in pluripotency: The emerging role of citrullinated histone H1 in cellular programming. *BioEssays*. **36**(8), 736.

Smith, J.B., Stashwick, C., Powell, D.J. (2014) B7-H4 as a potential target for immunotherapy for gynecologic cancers: a closer look. *Gynecologic oncology*. **134**(1), 181–189.

Smolle, E., Taucher, V., Pichler, M., Petru, E., Lax, S., Haybaeck, J. (2013) Targeting signaling pathways in epithelial ovarian cancer. *International journal of molecular sciences*. **14**(5), 9536–9555.

Sol, A., Fujihashi, H., Amoros, D., Nussinov, R. (2006a) Residue centrality, functionally important residues, and active site shape: analysis of enzyme and non-enzyme families. *The protein society*. **15**(9), 2120–8.

Soldevilla, M.M., Pastor, F. (2018) Decoy-based, targeted inhibition of STAT3: a new step forward for b cell lymphoma immunotherapy. *Molecular therapy : the journal of the american society of gene therapy*. **26**(3), 675–677.

Somigliana, E., Vigano', P., Parazzini, F., Stoppelli, S., Giambattista, E., Vercellini, P. (2006) Association between endometriosis and cancer: A comprehensive review and a critical analysis of clinical and epidemiological evidence. *Gynecologic Oncology*. **101**(2), 331–341.

Song, S., Yu, Y. (2019) Progression on citrullination of proteins in gastrointestinal cancers. *Frontiers in oncology*. **9**, 15.

Soslow, R.A., Han, G., Park, K.J., Garg, K., Olvera, N., Spriggs, D.R., Kauff, N.D., Levine, D.A. (2012) Morphologic patterns associated with BRCA1 and BRCA2 genotype in ovarian carcinoma. *Modern pathology*. **25**(4), 625–636.

Soto-Reyes, E., González-Barrios, R., Cisneros-Soberanis, F., Herrera-Goepfert, R., Pérez, V., Cantú, D., Prada, D., Castro, C., Recillas-Targa, F., Herrera, L.A. (2012) Disruption of CTCF at the miR-125b1 locus in gynecological cancers. *BMC Cancer*. **12**(1), 40.

Splettstoesser, F., Florea, A.M., Büsselberg, D. (2007) IP(3) receptor antagonist, 2-APB, attenuates cisplatin induced Ca2+-influx in HeLa-S3 cells and prevents activation of calpain and induction of apoptosis. *British journal of pharmacology*. **151**(8), 1176–86.

Stadler, S.C., Vincent, C.T., Fedorov, V.D., Patsialou, A., Cherrington, B.D., Wakshlag, J.J., Mohanan, S., Zee, B.M., Zhang, X., Garcia, B.A., Condeelis, J.S., Brown, A.M.C., Coonrod, S.A., Allis, C.D. (2013) Dysregulation of PAD4-mediated citrullination of nuclear GSK3 activates TGF- signaling and induces epithelial-to-mesenchymal transition in breast cancer cells. *Proceedings of the national academy of sciences*. **110**(29), 11851–11856.

Stapf, M., Pömpner, N., Teichgräber, U., Hilger, I. (2016) Heterogeneous response of different tumor cell lines to methotrexate-coupled nanoparticles in presence of hyperthermia. *International journal of nanomedicine*. **11**, 485–500.

Stoffberg, S., Jacobs, D.S., Miller-Butterworth, C.M. (2004) Field identification of two morphologically similar bats, *Miniopterus schreibersii natalensis* and *Miniopterus fraterculus* (Chiroptera: Vespertilionidae). *African zoology*. **39**(1), 47–53.

Storey, D.J., Rush, R., Stewart, M., Rye, T., Al-Nafussi, A., Williams, A.R., Smyth, J.F., Gabra, H. (2008) Endometrioid epithelial ovarian cancer. *Cancer*. **112**(10), 2211–2220.

Strickland, K.C., Howitt, B.E., Shukla, S.A., Rodig, S., Ritterhouse, L.L., Liu, J.F., Garber, J.E., Chowdhury, D., Wu, C.J., D'Andrea, A.D., Matulonis, U.A., Konstantinopoulos, P.A. (2016) Association and prognostic significance of BRCA1/2-mutation status with neoantigen load, number of tumor-infiltrating lymphocytes and expression of PD-1/PD-L1 in high grade serous ovarian cancer. *Oncotarget*. **7**(12), 13587–98.

Stronach, E.A., Alfraidi, A., Rama, N., Datler, C., Studd, J.B., Agarwal, R., Guney, T.G., Gourley, C., Hennessy, B.T., Mills, G.B., Mai, A., Brown, R., Dina, R., Gabra, H. (2011) HDAC4-regulated STAT1 activation mediates platinum resistance in ovarian Cancer. *Cancer research*. **71**(13), 4412–4422.

Sugiyama, T., Kamura, T., Kigawa, J., Terakawa, N., Kikuchi, Y., Kita, T., Suzuki, M., Sato, I., Taguchi, K. (2000) Clinical characteristics of clear cell carcinoma of the ovary: a distinct histologic type with poor prognosis and resistance to platinum-based chemotherapy. *Cancer*. **88**(11), 2584–9.

Sun, F., Xu, X., Wang, X., Zhang, B. (2016) Regulation of autophagy by Ca2. *Tumour biology : the journal of the international society for oncodevelopmental biology and medicine*. **37**(12), 15467.

Takahara, H., Okamoto, H., Sugawara, K. (2014) Calcium-dependent properties of peptidylarginine deiminase from rabbit skeletal muscle. Agricultural and biological chemistry. **50** (11),2899-2904.

Tamir, A., Jag, U., Sarojini, S., Schindewolf, C., Tanaka, T., Gharbaran, R., Patel, H., Sood, A., Hu, W., Patwa, R., Blake, P., Chirina, P., Oh Jeong, J., Lim, H., Goy, A., Pecora, A., Suh, K.S. (2014) Kallikrein family proteases KLK6 and KLK7 are potential early detection and diagnostic biomarkers for serous and papillary serous ovarian cancer subtypes. *Journal of ovarian research*. **7**(1), 109.

Tan, S.H., Sapari, N.S., Miao, H., Hartman, M., Loh, M., Chng, W.J., Iau, P., Buhari, S.A., Soong, R., Lee, S.C. (2015) High-throughput mutation profiling changes before and 3 weeks after chemotherapy in newly diagnosed breast cancer patients. *PLOS one*. **10**(12), e0142466.

Tanaka, Y., Terai, Y., Tanabe, A., Sasaki, H., Sekijima, T., Fujiwara, S., Yamashita, Y., Kanemura, M., Ueda, M., Sugita, M., Franklin, W.A., Ohmichi, M. (2011) Prognostic effect of epidermal growth factor receptor gene mutations and the aberrant phosphorylation of Akt and ERK in ovarian cancer. *Cancer biology & therapy*. **11**(1), 50–7.

Tanday, S. (2016) Targeting PADI2 could stop the progression of myeloma. *The Lancet oncology*. **17**(8), e325.

Tanikawa, C., Ueda, K., Nakagawa, H., Yoshida, N., Nakamura, Y., Matsuda, K. (2009) Regulation of Protein Citrullination through p53/PADI4 Network in DNA Damage Response. *Cancer research*. **69**(22), 8761–8769.

Tarcsa, E., Marekov, L.N., Mei, G., Melino, G., Lee, S.C., Steinert, P.M. (1996) Protein unfolding by peptidylarginine deiminase. Substrate specificity and structural relationships of the natural substrates trichohyalin and filaggrin. *The journal of biological chemistry*. **271**(48), 30709–16.

Taylor, Martin S., Ponting, C.P., Copley, R.R. (2004) Occurrence and consequences of coding sequence insertions and deletions in mammalian genomes. *Genome research*. **14**(4), 555–566.

Terakawa, H., Takahara, H., Sugawara, K. (1991) Three types of mouse peptidylarginine deiminase: characterization and tissue distribution. *Journal of biochemistry*. **110**(4), 661–6.

Testa, U., Petrucci, E., Pasquini, L., Castelli, G., Pelosi, E., Testa, U., Petrucci, E., Pasquini, L., Castelli, G., Pelosi, E. (2018) Ovarian cancers: genetic abnormalities, tumor heterogeneity and progression, clonal evolution and cancer stem cells. *Medicines*. **5**(1), 16.

Thinnes, F.P. (2009) Human type-1 VDAC, a cisplatin target involved in either apoptotic pathway. *Molecular genetics and metabolism*. **97**(2), 163.

Tomaszewski, A., Büsselberg, D. (2007) Cisplatin modulates voltage gated channel currents of dorsal root ganglion neurons of rats. *Neurotoxicology*. **28**(1), 49–58.

Torchiaro, E., Lorenzato, A., Olivero, M., Valdembri, D., Gagliardi, P.A., Gai, M., Erriquez, J., Serini, G., Di Renzo, M.F. (2016) Peritoneal and hematogenous metastases of ovarian cancer cells are both controlled by the p90RSK through a self-reinforcing cell autonomous mechanism. *Oncotarget*. **7**(1).

Torre, L.A., Trabert, B., DeSantis, C.E., Miller, K.D., Samimi, G., Runowicz, C.D., Gaudet, M.M., Jemal, A., Siegel, R.L. (2018) Ovarian cancer statistics, 2018. *A cancer journal for clinicians*. **68**(4), 284–296.

Toss, A., Cristofanilli, M. (2015) Molecular characterization and targeted therapeutic approaches in breast cancer. *Breast cancer research*. **17**(1), 60.

Toss, A., Venturelli, M., Peterle, C., Piacentini, F., Cascinu, S., Cortesi, L. (2017) Molecular biomarkers for prediction of targeted therapy response in metastatic breast cancer: trick or treat? *International journal of molecular sciences*. **18**(1), 85.

Tothill, R.W., Tinker, A. V., George, J., Brown, R., Fox, S.B., Lade, S., Johnson, D.S., Trivett, M.K., Etemadmoghadam, D., Locandro, B., Traficante, N., Fereday, S., Hung, J.A., Chiew, Y.E., Haviv, I., Gertig, D., deFazio, A., Bowtell, D. D.L., Bowtell, David D L (2008) Novel molecular subtypes of serous and endometrioid ovarian cancer linked to clinical outcome. *Clinical cancer research*. **14**(16), 5198–5208.

Tsai, S.Q., Wyvekens, N., Khayter, C., Foden, J.A., Thapar, V., Reyon, D., Goodwin, M.J., Aryee, M.J., Joung, J.K. (2014) Dimeric CRISPR RNA-guided FokI nucleases for highly specific genome editing. *Nature biotechnology*. **32**(6), 569–576.

Tsuji-Hosokawa, A., Kashimada, K., Kato, T., Ogawa, Y., Nomura, R., Takasawa, K., Lavery, R., Coschiera, A., Schlessinger, D., Harley, Vincent R, Takada, S., Morio, T. (2018)

Peptidyl arginine deiminase 2 (Padi2) is expressed in Sertoli cells in a specific manner and regulated by SOX9 during testicular development. *Scientific reports*. **8**(1), 13263.

Turajlic, S., Litchfield, K., Xu, H., Rosenthal, R., McGranahan, N., Reading, J.L., Wong, Y.N.S., Rowan, A., Kanu, N., Al Bakir, M., Chambers, T., Salgado, R., Savas, P., Loi, S., Birkbak, N.J., Sansregret, L., Gore, M., Larkin, J., Quezada, S.A., Swanton, C. (2017) Insertion-and-deletion-derived tumour-specific neoantigens and the immunogenic phenotype: a pan-cancer analysis. *The lancet oncology*. **18**(8), 1009–1021.

Turel, K., Rao, S.G. (1998) Expression of the cell adhesion molecule e-cadherin by the human bone marrow stromal cells and its probable role in CD34+stem cell adhesion. *Cell biology international*. **22**(9–10), 641–648.

Tycko, J., Myer, V.E., Hsu, P.D. (2016) Methods for Optimizing CRISPR-Cas9 Genome Editing Specificity. *Molecular cell*. **63**(3), 355–70.

U, K.P., Subramanian, V., Nicholas, A.P., Thompson, P.R., Ferretti, P. (2014) Modulation of calcium-induced cell death in human neural stem cells by the novel peptidylarginine deiminase–AIF pathway. *Biochimica et biophysica acta (BBA) - molecular cell research*. **1843**(6), 1162–1171.

Vaidya, A.P., Parnes, A.D., Seiden, M. V (2005) Rationale and clinical experience with epidermal growth factor receptor inhibitors in gynecologic malignancies. *Current treatment options in oncology*. **6**(2), 103–14.

Valesini, G., Gerardi, M.C., Iannuccelli, C., Pacucci, V.A., Pendolino, M., Shoenfeld, Y. (2015) Citrullination and autoimmunity. *Autoimmunity reviews*. **14**(6), 490–497.

Vega, F.M., Ridley, A.J. (2008) Rho GTPases in cancer cell biology. *FEBS Letters*. **582**(14), 2093–2101.

Verardo, R., Piazza, S., Klaric, E., Ciani, Y., Bussadori, G., Marzinotto, S., Mariuzzi, L., Cesselli, D., Beltrami, A.P., Mano, M., Itoh, M., Kawaji, H., Lassmann, T., Carninci, P., Hayashizaki, Y., Forrest, A.R.R., Beltrami, C.A., Schneider, C., Schneider, C. (2014) Specific mesothelial signature marks the heterogeneity of mesenchymal stem cells from high-grade serous ovarian cancer. *Stem cells*. **32**(11), 2998–3011.

Vogelstein, B., Papadopoulos, N., Velculescu, V.E., Zhou, S., Diaz, L.A., Kinzler, K.W., Kinzler, K.W. (2013) Cancer genome landscapes. *Science*. **339**(6127), 1546–58.

Vossenaar, ER., Zendman, A.J.W., van Venrooij, W.J., Pruijn, G.J.M. (2003) PAD, a growing family of citrullinating enzymes: genes, features and involvement in disease. *Bioessays*. **25**(11), 1106–1118.

Vossenaar, E.R. (2004) Expression and activity of citrullinating peptidylarginine deiminase enzymes in monocytes and macrophages. *Annals of the rheumatic diseases*. **63**(4), 373–381.

Vossenaar, Erik R., Zendman, A.J.W., van Venrooij, W.J., Pruijn, G.J.M. (2003) PAD, a growing family of citrullinating enzymes: genes, features and involvement in disease. *BioEssays*. **25**(11), 1106–1118.

Walrath, J.C., Hawes, J.J., Van Dyke, T., Reilly, K.M. (2010) Genetically engineered mouse models in cancer research. *Advances in cancer research*.

Walsh, T., Casadei, S., Lee, M.K., Pennil, C.C., Nord, A.S., Thornton, A.M., Roeb, W., Agnew, K.J., Stray, S.M., Wickramanayake, A., Norquist, B., Pennington, K.P., Garcia, R.L., King, M.C., Swisher, E.M. (2011) Mutations in 12 genes for inherited ovarian, fallopian tube, and peritoneal carcinoma identified by massively parallel sequencing. *Proceedings of the national academy of sciences of the united states of america*. **108**(44), 18032–7.

Walton, J., Blagih, J., Ennis, D., Leung, E., Dowson, S., Farquharson, M., Tookman, L.A., Orange, C., Athineos, D., Mason, S., Stevenson, D., Blyth, K., Strathdee, D., Balkwill, F.R., Vousden, K., Lockley, M., McNeish, I.A. (2016) CRISPR/Cas9-Mediated Trp53 and Brca2 Knockout to Generate Improved Murine Models of Ovarian High-Grade Serous Carcinoma. *Cancer research*. **76**(20), 6118–6129.

Walton, J.B., Farquharson, M., Mason, S., Port, J., Kruspig, B., Dowson, S., Stevenson, D., Murphy, D., Matzuk, M., Kim, J., Coffelt, S., Blyth, K., McNeish, I.A. (2017) CRISPR/Cas9-derived models of ovarian high grade serous carcinoma targeting Brca1, Pten and Nf1, and correlation with platinum sensitivity. *Scientific reports*. **7**(1), 16827.

Wang, Haifeng, La Russa, M., Qi, L.S. (2016) CRISPR/Cas9 in Genome Editing and Beyond. *Annual review of biochemistry*. **85**(1), 227–264.

Wang, Huifeng, Xu, B., Zhang, X., Zheng, Y., Zhao, Y., Chang, X. (2016) PADI2 gene confers susceptibility to breast cancer and plays tumorigenic role via ACSL4, BINC3 and CA9 signaling. *Cancer cell international*. **16**(1), 61.

Wang, Lin, Song, G., Zhang, X., Feng, T., Pan, J., Chen, W., Yang, M., Bai, X., Pang, Y., Yu, J., Han, J., Han, B. (2017) PADI2-mediated citrullination promotes prostate cancer progression. *Cancer research*. **77**(21), 5755–5768.

Wang, S., Wang, Y. (2013) Peptidylarginine deiminases in citrullination, gene regulation, health and pathogenesis. *Biochimica et biophysica acta*. **1829**(10), 1126–35.

Wang, S.J., Bourguignon, L.Y.W. (2006) Hyaluronan-CD44 promotes phospholipase C–mediated Ca2+ signaling and cisplatin resistance in head and neck cancer. *Archives of otolaryngology–head & neck surgery*. **132**(1), 19.

Wang, T., Wei, J.J., Sabatini, D.M., Lander, E.S. (2014) Genetic Screens in Human Cells Using the CRISPR-Cas9 System. *Science*. **343**(6166), 80–84.

Weeraratna, A.T., Jiang, Y., Hostetter, G., Rosenblatt, K., Duray, P., Bittner, M., Trent, J.M. (2002) Wnt5a signaling directly affects cell motility and invasion of metastatic melanoma. *Cancer cell*. **1**(3), 279–88.

Weissenbach, J. (2016) The rise of genomics. *Comptes rendus biologies*. **339**(7–8), 231–239.

Weiswald, L.-B., Bellet, D., Dangles-Marie, V. (2015) Spherical cancer models in tumor biology. *Neoplasia*. **17**(1), 1–15.

Wiegand, K.C., Shah, S.P., Al-Agha, O.M., Zhao, Y., Tse, K., Zeng, T., Senz, J., McConechy, M.K., Anglesio, M.S., Kalloger, S.E., Yang, W., Heravi-Moussavi, A., Giuliany, R., Chow, C., Fee, J., Zayed, A., Prentice, L., Melnyk, N., Turashvili, G., Delaney, A.D., Madore, J., Yip, S., McPherson, A.W., Ha, G., Bell, L., Fereday, S., Tam, A., Galletta, L., Tonin, P.N., Provencher, D., Miller, D., Jones, S.J.M., Moore, R.A., Morin, G.B., Oloumi, A., Boyd, N., Aparicio, S.A., Shih, I.M., Mes-Masson, A.M., Bowtell, D.D., Hirst, M.,

Gilks, B., Marra, M.A., Huntsman, D.G. (2010) *ARID1A* Mutations in endometriosis-associated ovarian carcinomas. *New england journal of medicine*. **363**(16), 1532–1543.

Wilson, Laurence O W, O'Brien, A.R., Bauer, D.C. (2018) The current state and future of CRISPR-Cas9 gRNA design tools. *Frontiers in pharmacology*. **9**, 749.

Winkler, S., Mohl, M., Wieland, T., Lutz, S. (2005) GrinchGEF--a novel Rho-specific guanine nucleotide exchange factor. *Biochemical and biophysical research communications*. **335**(4), 1280–6.

Witalison, E., Thompson, P., Hofseth, L. (2015) Protein arginine deiminases and associated citrullination: physiological functions and diseases associated with dysregulation. *Current drug targets*. **16**(7), 700–710.

Wright, J.D., Chen, L., Tergas, A.I., Patankar, S., Burke, W.M., Hou, J.Y., Neugut, A.I., Ananth, C. V., Hershman, D.L. (2015) Trends in relative survival for ovarian cancer from 1975 to 2011. *Obstetrics & gynecology*. **125**(6), 1345–1352.

Wu, H., Cao, C. (2019) The application of CRISPR-Cas9 genome editing tool in cancer immunotherapy. *Briefings in functional genomics*. **18**(2), 129–132.

Wu, X., Kriz, A.J., Sharp, P.A. (2014) Target specificity of the CRISPR-Cas9 system. *Quantitative biology*. **2**(2), 59–70.

Xiao, Z., Wan, J., Nur, A.A., Dou, P., Mankin, H., Liu, T., Ouyang, Z. (2018) Targeting CD44 by CRISPR-Cas9 in multi-drug resistant osteosarcoma cells. *Cellular physiology and biochemistry*. **51**(4), 1879–1893.

Xu, L., Pathak, P.S., Fukumura, D. (2004) Hypoxia-induced activation of p38 mitogen-activated protein kinase and phosphatidylinositol 3'-kinase signaling pathways contributes to expression of interleukin 8 in human ovarian carcinoma cells. *Clinical cancer research : an official journal of the american association for cancer research*. **10**(2), 701–7.

Xue, J.Y., Huang, C., Wang, W., Li, H.B., Sun, M., Xie, M. (2018) HOXA11-AS: a novel regulator in human cancer proliferation and metastasis. *Oncotargets and therapy*. **11**, 4387–4393.

Yamaguchi, H., Wyckoff, J., Condeelis, J. (2005) Cell migration in tumors. *Current Opinion in Cell Biology*. **17**(5), 559–564.

Yamaguchi, K., Huang, Z., Matsumura, N., Mandai, M., Okamoto, T., Baba, T., Konishi, I., Berchuck, A., Murphy, S.K. (2014) Epigenetic determinants of ovarian clear cell carcinoma biology. *International journal of cancer*. **135**(3), 585–597.

Yang, G., Rosen, D.G., Liu, G., Yang, F., Guo, X., Xiao, X., Xue, F., Mercado-Uribe, I., Huang, J., Lin, S.H., Mills, G.B., Liu, J. (2010) CXCR2 Promotes ovarian cancer growth through dysregulated cell cycle, diminished apoptosis, and enhanced angiogenesis. *Clinical Cancer research*. **16**(15), 3875–3886.

Yang, Z. (2007) PAML 4: Phylogenetic analysis by maximum likelihood. *Molecular biology and evolution*. **24**(8), 1586–1591.

Yao, T., Asayama, Y. (2017) Animal-cell culture media: History, characteristics, and current issues. *Reproductive medicine and biology*. **16**(2), 99–117.

Ye, R.X., Xia, Y.H., Xue, T.C., Zhang, H., Ye, S.L. (2011) Down-regulation of osteopontin inhibits metastasis of hepatocellular carcinoma cells via a mechanism involving MMP-2 and uPA. *Oncology reports*. **25**(3), 803–8.

Yemelyanova, A., Vang, R., Kshirsagar, M., Lu, D., Marks, M.A., Shih, I.M., Kurman, R.J. (2011) Immunohistochemical staining patterns of p53 can serve as a surrogate marker for TP53 mutations in ovarian carcinoma: an immunohistochemical and nucleotide sequencing analysis. *Modern pathology*. **24**(9), 1248–1253.

Ying, S., Dong, S., Kawada, A., Kojima, T., Chavanas, S., Méchin, M.C., Adoue, V., Serre, G., Simon, M., Takahara, H. (2009a) Transcriptional regulation of peptidylarginine deiminase expression in human keratinocytes. *Journal of dermatological science*. **53**(1), 2–9.

Ying, S., Simon, M., Serre, G., Takahar, H. (2012) Peptidylarginine deiminases and protein deimination in skin physiopathology. In *psoriasis - a systemic disease*.

Yokoi, A., Matsuzaki, J., Yamamoto, Y., Yoneoka, Y., Takahashi, K., Shimizu, H., Uehara, T., Ishikawa, M., Ikeda, S., Sonoda, T., Kawauchi, J., Takizawa, S., Aoki, Y., Niida, S., Sakamoto, H., Kato, K., Kato, T., Ochiya, T. (2018) Integrated extracellular microRNA profiling for ovarian cancer screening. *Nature communications*. **9**(1), 4319.

Yoshihara, K., Tsunoda, T., Shigemizu, D., Fujiwara, Hiroyuki, Hatae, M., Fujiwara, Hisaya, Masuzaki, H., Katabuchi, H., Kawakami, Y., Okamoto, A., Nogawa, T., Matsumura, N., Udagawa, Y., Saito, T., Itamochi, H., Takano, M., Miyagi, E., Sudo, T., Ushijima, K., Iwase, H., Seki, H., Terao, Y., Enomoto, T., Mikami, M., Akazawa, K., Tsuda, H., Moriya, T., Tajima, A., Inoue, I., Tanaka, K., Japanese Serous Ovarian Cancer Study Group (2012) High-risk ovarian cancer based on 126-gene expression signature is uniquely characterized by downregulation of antigen presentation pathway. *Clinical cancer research*. **18**(5), 1374–1385.

Yoshioka, S., King, M.L., Ran, S., Okuda, H., MacLean, J.A., McAsey, M.E., Sugino, N., Brard, L., Watabe, K., Hayashi, K. (2012) WNT7A Regulates tumor growth and progression in ovarian cancer through the WNT/ -Catenin pathway. *Molecular cancer research*. **10**(3), 469–482.

Yuan, J., Zhu, Q., Liu, B. (2014) Phylogenetic and biological significance of evolutionary elements from metazoan mitochondrial genomes. *PloS one*. **9**(1), e84330.

Yurchenco, P.D., Schittny, J.C. (1990) Molecular architecture of basement membranes. *FASEB journal : official publication of the federation of american societies for experimental biology*. **4**(6), 1577–90.

Yurkovetsky, Z., Skates, S., Lomakin, A., Nolen, B., Pulsipher, T., Modugno, F., Marks, J., Godwin, A., Gorelik, E., Jacobs, I., Menon, U., Lu, K., Badgwell, D., Bast, R.C., Lokshin, A.E. (2010) Development of a multimarker assay for early detection of ovarian cancer. *Journal of clinical oncology*. **28**(13), 2159–2166.

Yuzhalin, A.E. (2019) Citrullination in cancer. *Cancer research*. **79**(7), 1274–1284.

Yuzhalin, A.E., Gordon-Weeks, A.N., Tognoli, M.L., Jones, K., Markelc, B., Konietzny, R., Fischer, R., Muth, A., O'Neill, E., Thompson, P.R., Venables, P.J., Kessler, B.M., Lim, S.Y., Muschel, R.J. (2018) Colorectal cancer liver metastatic growth depends on PAD4-driven citrullination of the extracellular matrix. *Nature communications*. **9**(1),

4783.

Zaino, R.J., Brady, M.F., Lele, S.M., Michael, H., Greer, B., Bookman, M.A. (2011) Advanced stage mucinous adenocarcinoma of the ovary is both rare and highly lethal: a gynecologic oncology group study. *Cancer*. **117**(3), 554–62.

Zamanian-Daryoush, M., Lindner, D., Tallant, T.C., Wang, Z., Buffa, J., Klipfell, E., Parker, Y., Hatala, D., Parsons-Wingerter, P., Rayman, P., Yusufishaq, M.S.S., Fisher, E.A., Smith, J.D., Finke, J., DiDonato, J.A., Hazen, S.L. (2013) The cardioprotective protein apolipoprotein a1 promotes potent anti-tumorigenic effects. *Journal of biological chemistry*. **288**(29), 21237–21252.

Zapardiel, I., Peiretti, M., Zanagnolo, V., Biffi, R., Bocciolone, L., Landoni, F., Aletti, G., Colombo, N., Maggioni, A. (2011) Diaphragmatic surgery during primary cytoreduction for advanced ovarian cancer. *International journal of gynecological cancer*. **21**(9), 1698–1703.

Zhan, L., Zhang, Y., Wang, W., Song, E., Fan, Y., Li, J., Wei, B. (2016) Autophagy as an emerging therapy target for ovarian carcinoma. *Oncotarget*. **7**(50), 83476–83487.

Zhan, T., Rindtorff, N., Betge, J., Ebert, M.P., Boutros, M. (2019) CRISPR/Cas9 for cancer research and therapy. *Seminars in cancer biology*. **55**, 106–119.

Zhang, G., Vemulapalli, T.H., Yang, J.Y. (2013a) Phylooncogenomics: Examining the cancer genome in the context of vertebrate evolution. *Applied & translational genomics*. **2**, 48–54.

Zhang, L., Conejo-Garcia, J.R., Katsaros, D., Gimotty, P.A., Massobrio, M., Regnani, G., Makrigiannakis, A., Gray, H., Schlienger, K., Liebman, M.N., Rubin, S.C., Coukos, G. (2003) Intratumoral T Cells, Recurrence, and survival in epithelial ovarian cancer. *New england journal of medicine*. **348**(3), 203–213.

Zhang, L., Yang, N., Katsaros, D., Huang, W., Park, J.W., Fracchioli, S., Vezzani, C., Rigault de la Longrais, I.A., Yao, W., Rubin, S.C., Coukos, G. (2003) The oncogene phosphatidylinositol 3'-kinase catalytic subunit alpha promotes angiogenesis via vascular endothelial growth factor in ovarian carcinoma. *Cancer research*. **63**(14), 4225–31.

Zhang, S., Balch, C., Chan, M.W., Lai, H.C., Matei, D., Schilder, J.M., Yan, P.S., Huang, T.H.M., Nephew, K.P. (2008) Identification and characterization of ovarian cancer-initiating cells from primary human tumors. *Cancer research*. **68**(11), 4311–4320.

Zhang, X., Bolt, M., Guertin, M.J., Chen, W., Zhang, S., Cherrington, B.D., Slade, D.J., Dreyton, C.J., Subramanian, V., Bicker, K.L., Thompson, P.R., Mancini, M.A., Lis, J.T., Coonrod, S.A. (2012) Peptidylarginine deiminase 2-catalyzed histone H3 arginine 26 citrullination facilitates estrogen receptor target gene activation. *Proceedings of the national academy of sciences*. **109**(33), 13331–13336.

Zhang, Y., Cao, L., Nguyen, D., Lu, H. (2016) TP53 mutations in epithelial ovarian cancer. *Translational cancer research*. **5**(6), 650–663.

Zhang, Z., Bast, R.C., Yu, Y., Li, J., Sokoll, L.J., Rai, A.J., Rosenzweig, J.M., Cameron, B., Wang, Y.Y., Meng, X.Y., Berchuck, A., van Haaften-Day, C., Hacker, N.F., de Bruijn, H.W.A., van der Zee, A.G.J., Jacobs, I.J., Fung, E.T., Chan, D.W. (2004) Three biomarkers identified from serum proteomic analysis for the detection of early stage ovarian

Cancer. *Cancer research*. **64**(16), 5882–5890.

Zhao, J., Xu, H., He, M., Wang, Z., Wu, Y. (2014) Rho GTPase-activating protein 35 rs1052667 polymorphism and osteosarcoma risk and prognosis. *Biomed research international*. **2014**, 396947.

Zhao, X., Guan, J.L. (2011) Focal adhesion kinase and its signaling pathways in cell migration and angiogenesis. *Advanced drug delivery reviews*. **63**(8), 610–615.

Zheng, Q., Cai, X., Tan, M.H., Schaffert, S., Arnold, C.P., Gong, X., Chen, C.Z., Huang, S. (2014) Precise gene deletion and replacement using the CRISPR/Cas9 system in human cells. *Biotechniques*. **57**(3), 115–24.

Zhong, X., Rescorla, F.J. (2012) Cell surface adhesion molecules and adhesion-initiated signaling: Understanding of anoikis resistance mechanisms and therapeutic opportunities. *Cellular signalling*. **24**(2), 393–401.

Zhou, J., Liu, Y., Zhang, W., Popov, V.M., Wang, M., Pattabiraman, N., Suñé, C., Cvekl, A., Wu, K., Jiang, J., Wang, C., Pestell, R.G. (2010) Transcription elongation regulator 1 is a co-integrator of the cell fate determination factor Dachshund homolog 1. *The journal of biological chemistry*. **285**(51), 40342–50.

Zhou, Y., Mittereder, N., Sims, G.P. (2018) Perspective on protein arginine deiminase activity-bicarbonate is a PH-independent regulator of citrullination. *Frontiers in immunology*. **9**, 34.

Zhu, H., Wang, Yuji, Wang, Yaonan, Zhao, S., Zhao, M., Gui, L., Xu, W., Chen, X.A., Wang, Yanming, Peng, S. (2013) Folded conformation, cyclic pentamer, nanostructure, and PAD4 binding mode of YW3-56. *The journal of physical chemistry*. **117**(19), 10070–10078.

Zischewski, J., Fischer, R., Bortesi, L. (2017) Detection of on-target and off-target mutations generated by CRISPR/Cas9 and other sequence-specific nucleases. *Biotechnology advances*. **35**(1), 95–104.

Zorn, K.K., Bonome, T., Gangi, L., Chandramouli, G.V.R., Awtrey, C.S., Gardner, G.J., Barrett, J.C., Boyd, J., Birrer, M.J. (2005) Gene Expression profiles of serous, endometrioid, and clear cell subtypes of ovarian and endometrial cancer. *Clinical cancer research*. **11**(18), 6422–6430.

APPENDIX

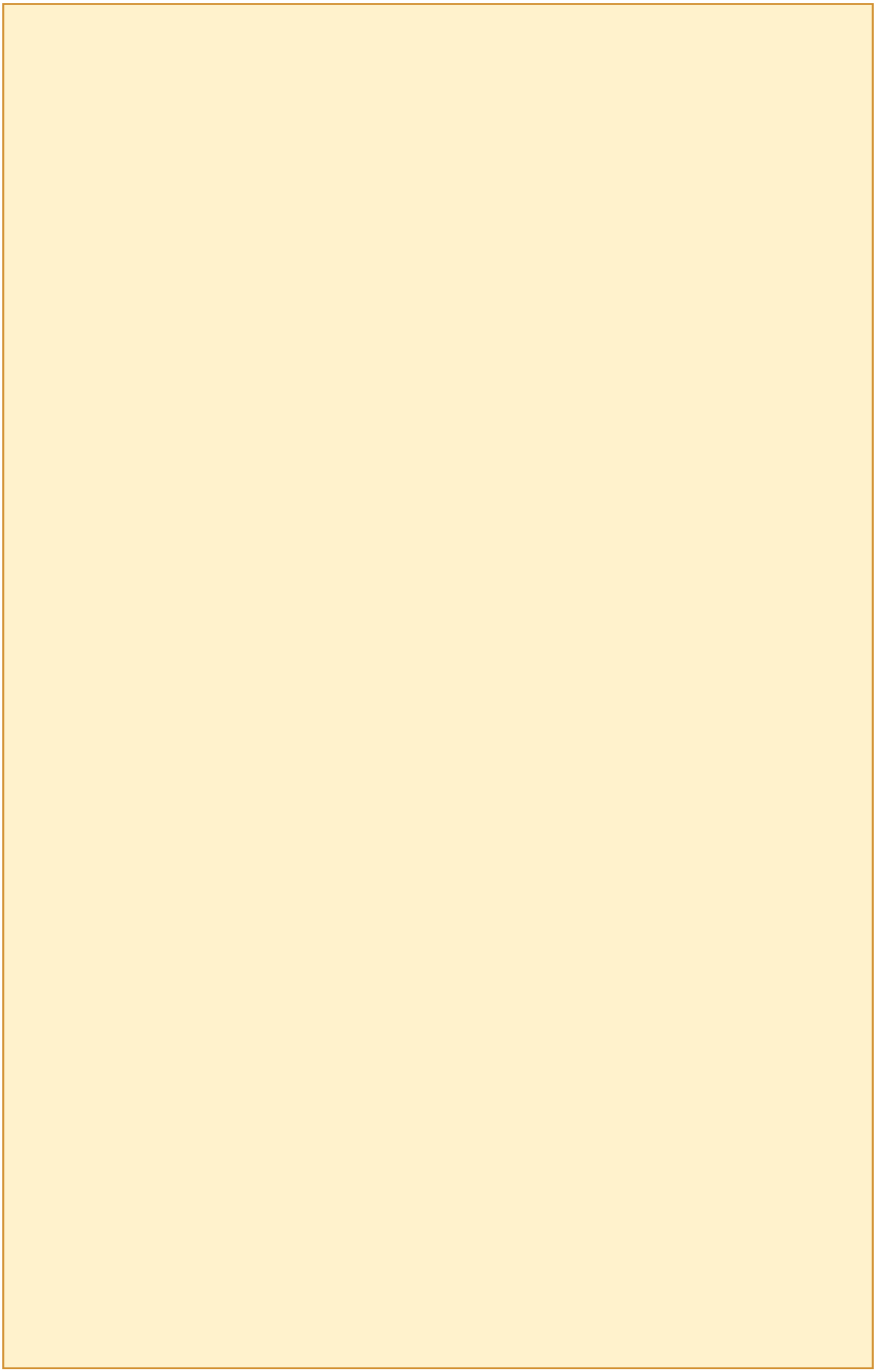

Figure S.1. EMBL-EMBOSS Matcher output between Human and Mouse *PADI2* DNA sequence

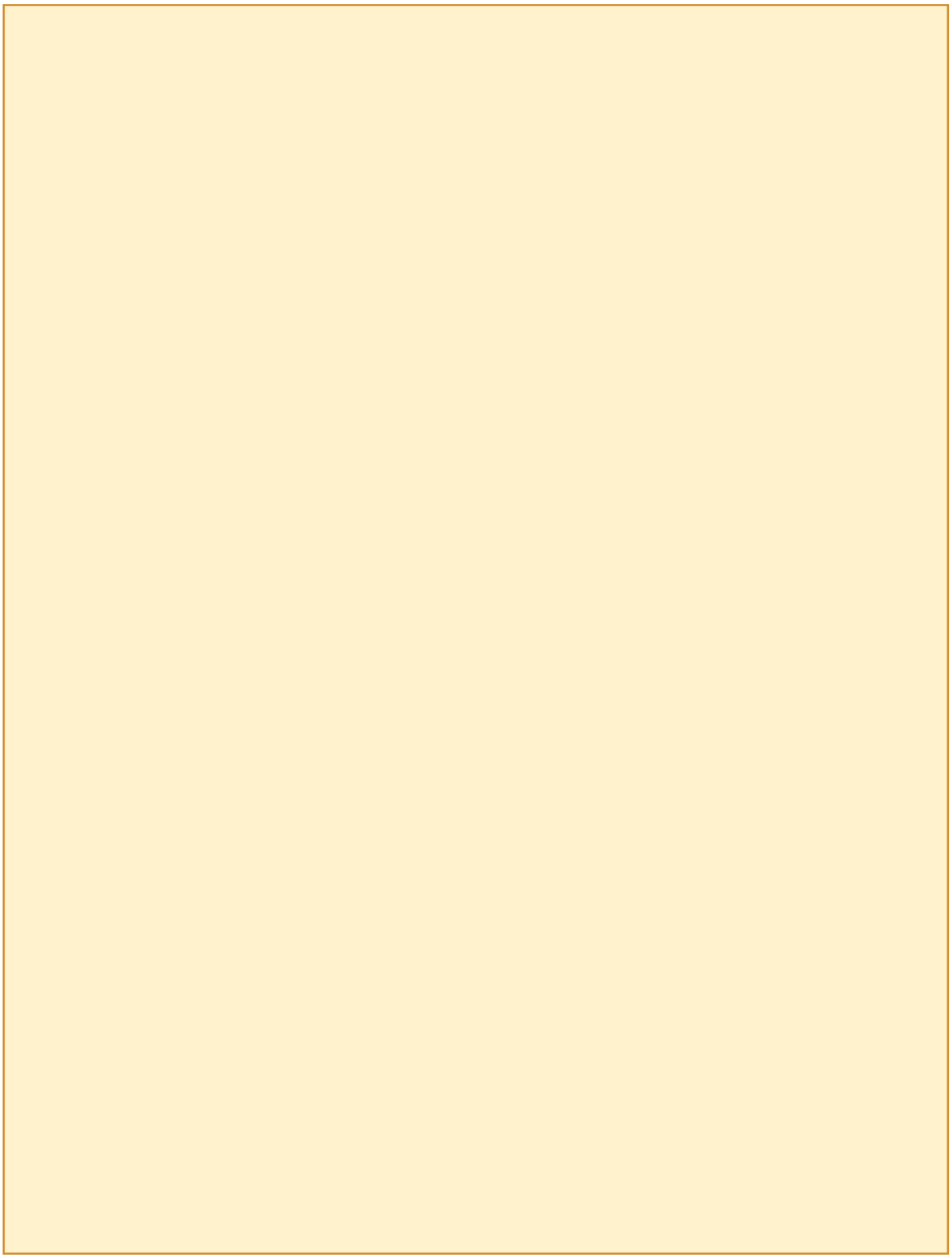

Figure S.2. EMBL-EMBOSS Matcher output between Human and Mouse PADI2 protein sequence

Table S.1. Species names and database IDs

Species name	Latin name	Database ID
Human	*Homo sapiens*	XM_017000148.2
Rhesus Monkey	*Macaca mulatta*	XM_015122520.1
Chimpanzee	*Pan troglodytes*	XM_513113.7
Olive Baboon	*Papio anubis,*	XM_003891202.4
Mouse	*Mus musculus*	XM_006538632.3
Rat	*Rattus norvegicus*	XM_008764215.2
Alpine Marmot	*Marmota marmota*	XM_015485640.1
Molerat	*Nannospalax galili,*	XM_008822632.1
Rousette	*Rousettus aegyptiacus*	XM_016128392.1
Flying Fox	*Pteropus alecto*	XM_006914312.1
Opterus Natalensis	*Miniopterus natalensis*	XM_016219459.1
Wild Camel	*Camelus ferus*	XM_014562260.1
Horse	*Equus caballus*	NM_001163822.2
Ass	*Equus asinus,*	XM_014836181.1
Dog	*Canis lupus familiaris*	XM_022414183.1
Giant Panda	*Ailuropoda melanoleuca*	XM_019804628.1
Canary	*Serinus canaria*	XM_009095754.2
Ruff	*Calidris pugnax*	XM_014959888.1
Eagle	*Haliaeetus leucocephalus*	XM_010577500.1
Chicken	*Gallus gallus*	NM_001319019.1
Bony Tongue	*Scleropages formosus*	XM_018725780.1
Piranha	*Pygocentrus nattereri*	XM_017697840.1
Catfish	*Ictalurus punctatus*	XM_017479674.1
Molly	*Poecilia Formosa*	XM_007546957.2
Vulus	*Kryptolebias marmoratus*	XM_017408778.2
Rhinocerous	*Sinocyclocheilus rhinocerous*	XM_016512332.1
Barramundi Perch	*Lates calcarifer*	XM_018683884.1
Poecilia Mexicana	*Poecilia Mexicana*	XM_014968042.1
Japonicus	*Gekko japonicus*	XM_015412620.1
Frog	*Xenopus laevis*	NM_001086900.1

Table S.2. The correlation between PADI2 expression and other co-expressed genes in EOC.

Gene abbreviation	Gene name	Gene function	Gene accession number	Gene fold change	
				Pearson's	Spearman's
ARHGEF10L	Rho guanine nucleotide exchange factor (GEF) 10-Like	Member of Rho GEF family of guanine nucleotide exchange factors (GEFs) that activate Rho GTPases (Winkler *et al.*, 2005).	NC_000001.11 NT_032977.10 NC_018912.2	0.37 0.42	0.36 0.42
BMPR1B (bone)	Bone morphogenetic protein receptor, type IB	Member of the bone morphogenetic protein (BMP); involved in endochondral bone formation and embryogenesis and produced in ovaries, receptor family of transmembrane serine/threonine kinases (Inman et al., 2002).	NC_000004.12 NT_016354.20 NC_018915.2	-0.26 -0.28	-0.23 -0.20
DACH1	Dachshund family transcription factor 1	Encodes a chromatin-associated protein that associates with other DNA-binding transcription factors to regulate gene expression and cell fate determination during development. Expression of this gene is lost in some forms of metastatic cancer, and is correlated with poor prognosis (Zhou *et al.*, 2010).	NC_000013.11 NT_024524.15 NC_018924.2	-0.23 -0.25	-0.25 -0.21
EPB41L1	Erythrocyte membrane protein band 4.1-like1	Multifunctional protein that mediates interactions between the erythrocyte cytoskeleton and the overlying plasma membrane. The encoded protein binds and stabilizes D2 and D3 dopamine receptors at the neuronal plasma membrane.	NC_000020.11 NT_011362.11 NC_018931.2	0.35 0.42	0.37 0.36
FUS	FUS RNA binding protein (nucleus,	Member of FET family of RNA-binding proteins which have been implicated in cellular processes that include regulation of gene expression, maintenance of genomic integrity and mRNA/microRNA processing. Functions in transcription dysregulation in cancer, *nucleic acid*	NC_000016.10 NT_187260.1 NC_018927.2	-0.23 -0.3	-0.20 -0.25

		binding and identical protein binding (Haile et al., 2011).			
FUT8	Fructosyltransferase 8 (alpha (1,6) fructosyltransferase)	Member of fructosyltransferases family. The product of this gene catalyses the transfer of fucose from GDP-fucose to N-linked type complex glycol-peptides. The expression of this gene may contribute to the malignancy of cancer cells and to their invasive and metastatic capabilities. Alternative splicing results in multiple transcript variants (pancreatic acinar cell adenocarcinoma) (Roos et al., 2002).	NC_000014.9 NT_026437.13 NC_018925.2	-0.24 -0.26	-0.26 -0.24
FZD5	Frizzled class receptor 5	Encode 7-transmembrane domain proteins that are receptors for Wnt signalling proteins. The FZD5 protein is a receptor for Wnt5A ligand. Involved in transduction and intercellular transmission of polarity information during tissue morphogenesis and/or in differentiated tissues (Kubo *et al.*, 2003).	NC_000002.12 NC_018913.2 NT_005403.18	-0.31 -0.37	-0.3 -0.21
KRT7	Keratin 7, type II	Encoded by this gene is a member of the keratin gene family. Expressed in epithelia lining the cavities of the internal organs and in the gland ducts and blood vessels. Blocks interferon-dependent interphase and stimulates DNA synthesis in cells. Diseases associated with include clear cell basal cell carcinoma and renal pelvis transitional cell carcinoma (Lin et al., 2001).	NC_000012.12 NT_029419.13 NC_018923.2	0.42 0.43	0.41 0.36
LDLRAP1	Low density lipoprotein receptor adaptor protein 1	Encoded by this gene is a cytosolic protein which contains a phosphoserine binding (PTD) domain. The PTD domain has been found to interact with the cytoplasmic tail of the LDL receptor (Michaely *et al.*, 2004; Mishra *et al.*, 2002).	NC_000001.11 NT_032977.10 NC_018912.2	0.36 0.35	0.36 0.32

NPTXR	Neuronal pentraxin receptor	Involved in mediating uptake of synaptic material during synapse remodelling.	NC_000022.11 NC_018933.2 NT_011520.13	0.40 0.33	0.40 0.41
PFKM	Phosphofructokinase, muscle	Catalyses the phosphorylation of D-fructose 6-phosphate to fructose 1,6-bisphosphate by ATP, the first committing step of glycolysis (Durante *et al.*, 1996).	NC_000012.12 NT_029419.13 NC_018923.2	-0.26 -0.28	-0.22 -0.21
RPS6KA1	Ribosomal protein s6 kinase, 90kda, polypeptide 1	Ribosomal S6 protein kinases (RSKs) are a family of protein serine/threonine kinases that regulate diverse cellular processes, such as cellular growth, motility, survival and proliferation (Shimamura et al., 2000).	NC_000001.11 NT_032977.10 NC_018912.2	0.38 0.42	0.42 0.44
SNRPE	Small Nuclear Ribonucleoprotein Polypeptide E	Plays an important role in the splicing of cellular pre-mRNAs (Fury *et al.*, 1997).		-0.27 -0.35	-0.27 -0.22
ZNF22	Zinc finger protein 22	Involved in transcriptional regulation and may play a role in tooth formation (Bray et al., 1991).	NC_000010.11 NC_018921.2 NT_030059.14	-0.24 -0.27	-0.24 -0.24
ZSCAN12	Zinc finger and scan domain containing 12	Involved in transcriptional regulation, *transcription factor activity, sequence-specific DNA binding.*	NC_000006.12 NT_007592.16 NC_018917.2	-0.21 -0.29	-0.23 -0.27

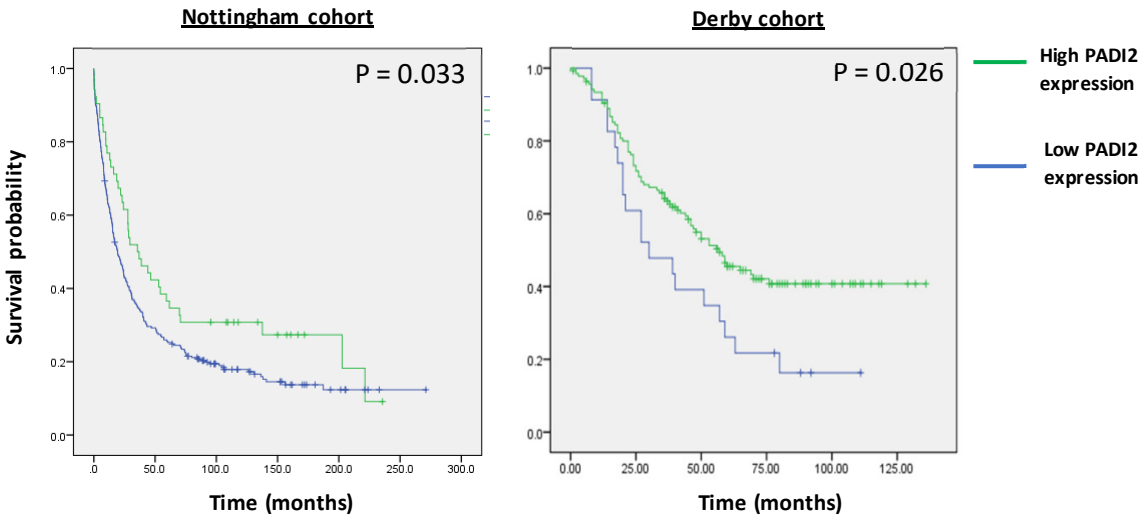

Figure S.3. Kaplan Meier curves showing OS in EOC patients. (a) The Nottingham cohort and **(b)** The larger Derby cohort**.** Unpublished TMA data collected and analysed by Dr Lee Machado.

PADI2 whole amino

RERTVRLQYGSRVEAVYVLGTYLWTDVYSAAPAGAQTFSLKHSEHVWVEVVRDGEAEEVATN
GKQRWLLSPSTTLRVTMSQASTEASSDKVTVNYYDEEGSIPIDQAGLFLTAIEISLDVDADR
DGVVEKNNPKKASWTWGPEGQGAILLVNCDRETPWLPKEDCRDEKVYSKEDLKDMSQMILRT
KGPDRLPAGYEIVLYISMSDSDKVGVFYVENPFFGQRYIHILGRRKLYHVVKYTGGSAELLF
FVEGLCFPDEGFSGLVSIHVSLLEYMAQDIPLTPIFTDTVIFRIFRIAMTPNILPPVSVFVC
CMKDNYLFLKEVKNLVEKTNCELKVCFQYLNRGDRWIQDEIEFGYIEAPHKGFPVVLDSPRD
GNLKDFPVKELLGPDFGYVTREPLFESVTSLDSFGNLEVSPPVTVNGKTYPLGRILIGSSFP
LSGGRRMTKVVRDFLKAQQVQAPVELYSDWLTVGHVDEFMSFVPIPGTKKFLLLMASTSACY
KLFREKQKDGHGEAIMFKGLGGMSSKRITINKILSNESLVQENLYFQRCLDWNRDILKKELG
LTEQDIIDLPALFKMDEDHRARAFFPNMVNMIVLDKDLGIPKPFGPQVEEECCLEMHVRGLL
EPLGLECTFIDDISAYHKFLGEVHCGTNVRRKPFTFKWWHMVPSRRS

PAD domain PAD_M domain PAD_N domain

Figure S.4. The whole protein sequence of PADI2 (without sequence alignment)

Search results from domains: Manual domain Provisional domain Automatic domain

Domain ID	PDB Range	X Group Name	H Group Name	T Group Name	F Group Name	Protein Name
e4n2kA3	A:3-115	Cupredoxin-like	Cupredoxin-related	Cupredoxin-related	PAD_N	Protein-arginine deiminase type-2
e4n2kA1	A:116-294	Immunoglobulin-like beta-sandwich	Immunoglobulin-related	Common fold of diphtheria toxin/transcription factors/cytochrome f	PAD_M	Protein-arginine deiminase type-2
e4n2kA2	A:295-668	Pentein	Pentein	Pentein	PAD	Protein-arginine deiminase type-2

4n2k chain A [A:-20-0,A:666-669] (*Protein-arginine deiminase type-2*) is considered as a **expression_tag** .

Figure S.5. PADI2 different domains

Table S.3. PADI2 ligands

Ligand	Ligand Name	Residue N/ Chain ID	Number of atoms	CATH Superfamily	Function
MPD	(4S)-2-METHYL-2,4-PENTANEDIOL	701A 702A 703A	8	-	Transport/binding protein, hydrolase, cell adhesion
CA	Calcium Ion	705A 706A	1	2.60.40.1700	Hydrolase, serine protease, transport/ metal binding protein, cell adhesion and oxidoreductase
ACT	Acetate Ion	704A	4	2.40.128.20	Hydrolase, cell cycle, transcription, oxidoreductase and transferase

Ligand-Protein Contacts (LPC) in PADI2 derived from the LPC software and analysed by CATH and PDBeMotif tools

Ligands pattern names, size of the clusters, the number of atoms in the pattern, the protein fold classifications according to CATH, the annotated function

Table S.4. List of public resources and databases relevant to domain analysis